

Aspects of Weber Electrodynamics

PhD Thesis

Thesis submitted in accordance with the requirements of the University of Liverpool for
the degree of Doctor in Philosophy by

Christof Baumgärtel

Science is not about having the right answers.
Science is about asking the right questions.



Department of Electrical Engineering and Electronics
University of Liverpool

Supervisor: Simon Maher

Internal Examiner: Stephen Taylor

Initial Submission: May 2022

External Examiner: Neal Graneau

Revised Manuscript: September 2022

Abstract

Aspects of Weber Electrodynamics, by Christof Baumgärtel

This study investigates certain aspects of the direct-action electrodynamic theory of Wilhelm Eduard Weber with a special focus on selected experimental topics. Weber electrodynamics is an alternative to electromagnetic field theory and Maxwell's equations that can describe a wide range of electric and magnetic phenomena and in addition provides a basis for other branches of physics by explaining phenomena beyond the scope of electromagnetism. It is of interest to investigate the validity of the theory and if it can be a viable alternative to existing approaches, exploring its modelling capabilities and determining boundaries of its applicability. Further, it is sought what experimental evidence can be obtained in support of either theory and if there are associated benefits and drawbacks to the respective theories.

The literature analysis gives a brief introduction to both the standard theory of fields and that of Weber. It then continues to review the capabilities of Weber's electrodynamics and shows how it has been used in the literature as an explanation for several phenomena, including, but not limited to, electricity and magnetism. In addition, limitations that exist in Weber's electrodynamics are also addressed and criticism the theory has faced historically re-explored.

Experiments have been performed encompassing electron beam deflection and unipolar induction, which also investigates the movement of a rotating magnetic field. The experimental results are used to juxtapose predicted results from Weber as well as a standard field model to measured data, enabling the validity of the theories to be assessed within the constraints of the experiments.

The results of this work show that, in the low velocity limit, Weber's theory and Maxwell's are similar, if not the same. For the experiments performed with electron beam deflection and unipolar induction, both theories are found to arrive at the same results, qualitatively as well as quantitatively. Further to good agreement between experimentally observed quantities and predictions from the theoretical models, open questions about unipolar induction could be answered and new insight was gained regarding the working mechanism of the unipolar induction phenomenon.

Although agreement is found between Weber's theory and these specific experiments, the theory is not without limitations and still needs further development. The similarity between Weber's and Maxwell's theories are discussed and extended to fundamental concepts such as the ether, particles and fields; Weber's theory as a particle-based theory is considered as a promising approach to gain new insight into some of the fundamental concepts of physics.

Acknowledgment

The author wishes to express his gratitude to the continued help and support to all the people involved directly or indirectly in this project. I wish to thank my supervisor, Simon Maher, for continued guidance and support over these years of research, and my senior academic advisor, Ray T. Smith, for guidance, wisdom, support and scientific nurture. I am also especially grateful to the mechanics and electronics workshop of the department, without whose assistance this work would have not been possible. Further, the School of Electrical Engineering, Electronics and Computer Science of the University of Liverpool has granted financial support in the form of a stipend, which I am very grateful for. I have been lucky to receive further assistance, inspiration, academic discussion, motivation and all the small things from a number of different and very dear people. My special thanks go to Mark Burnley, Gareth Blacoe, Cedric Boisdon, John Gillmore, Mark Norman, Jill Anson, Barry Smith, my parents, family and friends, Imo Emah, André Assis and Martin Tajmar.

Contents

List of Symbols and Abbreviations	iii
1 Introduction	1
2 Literature Review	8
2.1 Different Theories of Electrodynamics	9
2.1.1 Maxwell's Equations and Field Theory	9
2.1.2 Alternative Theories	13
2.2 Weber Electrodynamics in the Literature	19
2.2.1 Electromagnetic Phenomena	20
2.2.2 Relevance of Weber's Force Beyond Electromagnetism	28
2.2.3 Cosmology and Breakthrough Physics	33
2.3 Criticism of Weber's Theory	40
3 Fundamentals of Weber's Theory	51
4 Weber Applied to Electron Beam Deflection	56
4.1 Deflection Perpendicular to Solenoid Axis	57
4.1.1 Mathematical Modelling	58
4.1.2 Experiment	68
4.1.3 Results	72
4.2 Further Analysis of the Magnetic Field	77
4.3 Deflection Parallel to Solenoid Axis	80
4.3.1 Modelling	81
4.3.2 Experiments	87
4.3.3 Results	89
4.4 Toroids	91
4.4.1 Modelling	92
4.4.2 Results	97
5 Unipolar Induction with Weber Electrodynamics	98
5.1 Stationary Detector	104
5.1.1 Mathematical Modelling	105
5.1.2 Experiment With a Standard Faraday Generator	111
5.1.3 Results of Standard Faraday Generator Experiment	112
5.2 Rotating Detector	114
5.2.1 Influence of the Closing Wire	114
5.2.2 Experiment to Test the Influence of the Closing Wire	117
5.2.3 Results From Rotating Detector Experiments	122
5.3 Discussion of Unipolar Induction Experiments	126
6 Discussion	133
6.1 Similarities of Weber and Field Theory: Can They Be Distinguished? . . .	133
6.2 The Ether Concept	137
6.2.1 Historical Role of Ether in Field Theories	137
6.2.2 Change of Ether Terminology and its Replacement by the Electro- magnetic Field	139

6.2.3	Re-introducing Ether in Modern Theories	141
6.3	The Fundamentality of Fields and Particles	143
6.3.1	The Size of the Electron	144
6.3.2	Ontological and Philosophical Aspects of Models	145
6.4	Language, Philosophy of Science and Basic Assumptions in Specific Theories	147
6.5	Additional Remarks	152
7	Conclusion and Future Work	155
7.1	Review: Contrasting Weber and Field Approaches	156
7.2	Revision: Can the Theories be Distinguished?	157
7.3	Reflection: Limitations and Advantages	159
7.4	Future Work and Speculation	161
7.4.1	Future Work	161
7.4.2	Speculation	163
7.5	Closing Remarks	167
	References	169
	Appendix	196
A	Circular and Helical Motion	196
A.1	Circular Motion	196
A.2	Helical Motion	197
B	Toroid Parametrisation	198
C	Matlab Codes and CPO Databuilder File	199

List of Symbols and Abbreviations

Abbreviations

AB	Aharonov-Bohm
AC	Alternatic Current
BEM	Boundary Element Method
CRT	Cathode Ray Tube
CCW	Counter-Colockwise
CDM	Cold Dark Matter
CPO	Charged Particle Optics
CW	Clockwise
DC	Direct Current
EMF	Electromotive Force
FD	Finite Difference
FE	Finite Element
GRT	General Relativity Theory
ID	Innner Diameter
IP	Inverted Polarity
LED	Light Emitter Diode
MFH	Moving Field Hypothesis
MOND	Modified Newtonian Dynamics
NP	Normal Polarity
OD	Outer Diameter
PCB	Printed Circuit Board
SFH	Stationary Field Hypothesis
SRT	Special Relativity Theory
QED	Quantum Electrodynamics
QFT	Quantum Field Theory

Latin Symbols

a	Acceleration
\vec{A}	Vector potential
\vec{B}	Magnetic field
c	Speed of light (in vacuum)
D	Diameter
d	Distance
e	Elementary charge
\vec{E}	Electric field
\mathcal{E}	Complete elliptic integral of the second kind
F, \vec{F}	Force
G	Gravitational constant
\vec{G}	Vector potential
\hbar	Planck constant
I	Current
\vec{J}	Current density

$\mathcal{J}, \vec{\mathcal{J}}$	Impulse
k	Free parameter
\mathcal{K}	Complete elliptic integral of the first kind
l, L	Length
m, M	Mass
N, n	Number of windings in a coil
p	Pitch of a coil
q	Point Charge
Q	Charge
R	Radius or separation of constant magnitude
\vec{r}	Radius or position as a variable
t	Time
T	Kinetic energy
U	Potential energy
v	Velocity
V	Electric Potential
x, y, z	Coordinates in Cartesian coordinate system

Greek Symbols

α, β, γ	Numerical constants
Γ	Scalar potential
ε_0	Vacuum permittivity
θ	Polar coordinate
λ	Line charge density, wavelength
μ	Constant parameter
μ_0	Vacuum permeability
ξ	Geometrical parameter
χ	Geometrical parameter
ζ	Geometrical parameter
π	Mathematical constant
φ	Polar coordinate
Φ	Scalar potential
Ψ	Magnetic flux
Π	Complete elliptic integral of the third kind
ρ	Volume charge density, radial coordinate
σ	Charge density
ω	Angular velocity, geometrical parameter
Ω	Angular velocity

1 Introduction

The drive of the human mind to understand the world it experiences and resides in can be found throughout human history. Early philosophy, for example in ancient Greece, attempted to explain the world with the simpler concepts it had at the time, such as Empedocles' four elements, fire, earth, wind and water, that have some resemblance to the states of matter; or the idea that everything strives to move towards the natural centre is an early attempt to describe gravitational attraction. A shift in perspective and the development of instrumentation has allowed us to explore previously hidden parts of the physical world, bringing new understanding and driving our knowledge, moving worldviews from a geocentric to a heliocentric model and even beyond, as our solar system is only a tiny component of a larger galactic structure and an even larger universe. In the same way we can look back at ancient philosophers who were aware of only a very limited range of the electromagnetic spectrum, the same may well be true for our current understanding. In perhaps a thousand years from now, people may well look back at our understanding of the world and smile at our limited perspective of the universe as we continue to uncover some of the mysteries governing our universe.

Throughout the history of science there have been many competing theories in research of all disciplines, for example theories of micro and macro sociology, a nature vs nurture debate, competing personality theories in psychology (Behaviourism vs Cognitive Psychology), distinct evolutionary theories (Punctuated Equilibrium vs Gradualism), different theories about mass extinctions of species throughout the Earth's history or the movement of people and how certain continents and regions were populated. There are also medical debates such as the possibility of low-power, non-ionising electromagnetic radiation from cell phones and other electrical devices to be carcinogenic. Every scientific field is alive with discussion about differing theories, which is an important process of discourse to allow a consensus to be reached. Particularly within the context of scientific research, open debate and free exploration is necessary, as is expressed within the very roots of the word "research" itself.

The same applies to physics and its subsidiary disciplines which engage in scientific

discussion. For example, we currently find General Relativity and Quantum Mechanics irreconcilable with each other, leading to competing theories such as Superstring theory and Loop Quantum Gravity, the Big Bang vs eternal inflation vs oscillating universe theory, stationary vs co-rotating field in electrodynamics concerning the rotation of a bar magnet and the associated magnetic field around its cylindrical axis (often discussed with flux linking and flux cutting) or the many-worlds interpretation vs the Copenhagen interpretation, which are only two of the many existing rationalisations of quantum mechanics.

Modern physics and our understanding of the universe hinges on the very important scientific concepts of the late 19th and early 20th century. The development of electrodynamic field theory by James Clerk Maxwell [1], the inception of quantum mechanics with contributions from Heisenberg, Planck, Born, Sommerfeld, Schrödinger and others [2] and of course Albert Einstein who developed the theory of Special Relativity (SRT) [3] and later General Relativity (GRT) [4], which leads to cosmology models based on dark matter and dark energy. In the same way, Quantum Electrodynamics (QED) and Quantum Field Theory (QFT) are based on the principles of electromagnetism and SRT, and our understanding of the structure of atoms and magnetism involves quantum mechanical as well as relativistic considerations.

These theories have proven to be very successful models in describing the universe and are backed by many observations; however, there are still some unresolved problems in the standard model suggesting that the theories are incomplete. This is not unexpected as no theory is intrinsically perfect nor can it be, and every theory undergoes a number of development stages, being amended over time to better account for new observations, which may then lead to new theories, superseding their predecessors, where experiments must always be the final arbiter. One such problem, for example, is the contradictory nature of GRT and quantum mechanics, also called the unitarity crisis [5], which scientists try to resolve with the help of quantum gravity theories and Superstring theory. Or for instance in cosmology, where recent data in dark matter mapping [6] leads scientists to suggest that the concordance model of cosmology based on GRT might need amendments [7], it becomes clearer that there is more research needed as the theory seems to be

incomplete and the debate about different models is still ongoing.

Others have championed Modified Newtonian Dynamics (MOND) over dark matter cosmology [8] and despite its empirical nature it seems to be rather successful in explaining many observations [9]. Nevertheless, the theory of MOND has problems, i.e. with energy and momentum conservation [10] and other recent data suggests counter-evidence [11, 12] to the theory, and MOND itself has seen modifications such as TeVeS [13] or the recent relativistic MOND [14]. Further there is observational data that suggests that dark matter is not needed everywhere in the universe, some exotic ultra diffuse galaxies disagree with both cold dark matter cosmology and MOND [15]. There also exist other cosmology models in early stages [16–18] and the approach by Das [16] based on Mach’s principle coincides well with available data of galactic rotation speeds. There even exists a claim based on observed data that the cosmological speed limit is $v + c$ rather than just the speed of light c [19], but with some of the measurements suggesting problems with the standard model, only time will tell if those are statistical outliers or not, and there is still a large quantity of evidence in support of the established theories in cosmology, particle physics and electrodynamics.

Aside from cosmology, there are still some critics who have raised various concerns about SRT [20–41] since its inception. Especially the clock paradox has been much debated in the literature and McDonald has compiled an interesting analysis of the paradox with an extensive list of over 300 references [42]. But even a theory as successful as SRT [43, 44] sees modifications, for example so called “Deformed Special Relativity”, which itself has limitations [45].

The snapshot of examples given here serves to emphasise the point that no theory is perfect and all research is incremental towards a description of reality. With the debate about different theories in mind, the present study is motivated to further explore the premise of electrodynamics that underpin many such models describing the observable universe. The motivation is thus to investigate the foundation and expand the point of view beyond the Maxwell-Lorentz field based approach and examine alternative theories, one in particular, Weber’s electrodynamics. Due to the imperfect nature inherent to all

theories it is useful to investigate alternative yet promising theories. Conceptual problems with classical electrodynamics have been discussed by Pietsch [46] and Lazarovici [47], which will be further discussed in section 2.1.1. As an alternative, Pietsch suggests action-at-a-distance theories to resolve the existing problems and argues further that they are not that different from the established view of particle-field theories in modern physics when locality and energy conservation criteria are regarded in action-at-a-distance theories.

As one of those candidates for describing electromagnetic phenomena, this work gives specific focus to Weber's theory of electrodynamics [48]. It is an alternative description of electrodynamic interaction to the Maxwell-Lorentz field equations and based on direct-action of particles instead of contact-action requiring a medium in field theory. It has been argued by Lentze [49] that direct-action between charges can provide deeper insight into explaining the origin of electromagnetic forces and the light speed principle, thus improving our understanding of nature. As these theories have not been developed to the same degree as classical theories, it appears beneficial to develop this approach and expand the research. In particular, magnetic forces form a key component of applications investigated in later sections of this work.

This line of enquiry can lead to new insights, as it can allow for interesting possibilities to extend the boundaries of known physics and the development of breakthrough applications. Researchers have suggested that, based on the idea of manipulating inertial mass and Weber-like theories, technologies such as cold nuclear fusion, advanced space propulsion systems (e.g. warp drives for interstellar space travel) and even anti-gravity are conceivable [50–52].

Eventually, in order to judge the validity of any alternative approach, experimental evidence is a key factor to determine boundaries of applicability and distinguish between them. In an interesting review about Maxwell's equations and the field approach Tran [53] concludes that there are only few experiments supporting the Maxwell-Ampère and Maxwell-Faraday equation, at least not to the same degree of accuracy that the continuity equation and the magnetic law are supported. Further, the question is raised if fields exist independently from forces and what electromagnetic fields are in terms of their modern

definition. This quickly leads to a discussion about the physical nature of fields, for example, the field as immaterial space as opposed to the field as a solely mathematical description. At this point an experimental distinction seems rather difficult and can also involve considerations about unipolar induction phenomena or Feynman's paradox – this is discussed at length in section 5. A purely mathematical description cannot rotate with its source, so experiments involving rotating magnets can provide insight regarding the physical reality of fields, and direct evidence of a rotating field would be an important step. By extension, this can further inform the limitations of direct-action approaches since the field is not necessarily conceived as a real medium in these theories.

These types of experiments are considered necessary, especially in view of Hossenfelder's comments [54] that in recent years an overproduction of theories in physics has occurred, some of which lack supporting experimental evidence. Thus, this work is an attempt to subject Weber's theory to greater experimental scrutiny, comparing it to the field approach and observational data from experiments, making the experimentation a core aspect. Based on this, some key questions driving this work are formulated. For example: can Weber electrodynamics be considered as a viable alternative to describe electromagnetic phenomena? What, if any, experimental evidence can be found for or against Weber's theory? Can the theory be proved or disproved? Can limits be put on the validity of the theory? Does the direct-action approach provide certain advantages or disadvantages? Could it even be beneficial to use both theories in conjunction within the right set of constraints?

In trying to address such questions, the experimentation and data collection will be significant, but first the thesis will focus on several theoretical aspects. In section 2, the literature review, an overview is given about the Maxwell-Lorentz field theory and Weber's theory, introducing both approaches as an initial comparison. Then the focus is specifically on Weber's electrodynamics and how the theory has been used in the literature by different authors to explain and model electromagnetism as well as other phenomena (e.g. gravity or the strong force). This is followed by a subsection about criticism of Weber's electrodynamics that historically led to the theory being superseded by the field

approach and a review thereof. The question is asked whether Weber's theory has been refuted and after analysing all points of criticism, if Weber can provide a suitable alternative to the field model. In section 3 a general theoretical and mathematical introduction to Weber's theory is given, to lay the foundation of how the theory can later be used to build mathematical models and apply it to different phenomena.

Once these fundamental topics have been addressed, Weber's theory can then be utilised to investigate specific problems, which provide predictions to compare with real data obtained from experiments. Therefore the thesis is structured into sections that focus on applied subtopics within the field of electrodynamics, in particular electron beam deflection (sec. 4) and unipolar induction (sec. 5) are investigated. The reader is first introduced to the subtopic and then predictions of outcomes are made based on both field theory and Weber's theory. Moreover, the experimental apparatus and procedures are presented, and finally the resulting data compared with prediction and conclusions drawn.

Electron beam deflection (sec. 4) is chosen for mainly two reasons: i) it is part of charged particle optics, which is a widely applied technology throughout different disciplines, incorporating particle accelerators, mass spectrometry, electron microscopy and medical instrumentation. As Weber's force is a microscopic force law applicable to point charges which are particles, it is certainly of interest to investigate its relations to topics such as charged particles and particle accelerators, traditionally built on field theory; ii) electron beams are commonly deflected by employing solenoids, which are used in turn for the controlled generation of magnetic fields through supplying a defined current. This allows to examine two-fold, how magnetic fields, respectively magnetic interaction, arises with Weber's electrodynamics and also a direct comparison of the Lorentz force and Weber force through the deflection of electrons in the generated magnetic field.

Another chosen topic for investigation is the unipolar induction phenomenon (sec. 5), which is among the more lively discussed topics in electrodynamics. It has been described as paradoxical; science is divided over the different proposed explanations of the observed effect and debate is ongoing about the possibility of the magnetic field co-rotating with

a spinning magnet or remaining stationary. As this informs the discussion about the reality of macroscopic magnetic fields an investigation seems well-suited in the context of this work. It is explored how unipolar induction can be modelled with Weber's theory, what predictions we can make based on it and, in conclusion, how the theory can offer an explanation that resolves associated paradoxes. After the experimental findings have been presented and analysed, the thesis will engage in a wider discussion (sec. 6) of Weber's theory informed by the newly obtained data and eventually come to a conclusion (sec. 7) based on the present investigation.

2 Literature Review

The history of electrodynamics is interesting and has fascinated humanity and scientists since ancient times. There are reports about the amber effect and lodestones (the first naturally discovered magnetic materials) by the Greeks and other ancient civilisations. Important advancements were made during the 18th century with electrostatic experiments and the first capacitors in the form of Leyden jars by researchers like Gray, du Fay, Benjamin Franklin and their contemporaries; also the invention of the first battery by Volta in 1791 based on findings by Galvani. Further important experiments and the early forms of the theory known today were advanced in the early 19th century by Ohm, Coulomb, Ampère, Faraday and many more, eventually leading to Maxwell's *Treatise*, which forms the basis of modern physics and electrical engineering. This is only a very brief overview and the history of electricity and the development of associated electromagnetic theories has been documented in several excellent books such as [55–59], among others.

Many scientists have therefore contributed to the development of our modern understanding of electrodynamics and it is only natural that those scientists have formulated their own hypotheses and theories throughout the centuries. Amongst the various historical viewpoints, there are a few theories of particular note that have attempted to describe the observed phenomena of electricity and magnetism. First some of the different theories are examined in the following section 2.1 to provide a brief introduction to electrodynamics and then attention is directed to Weber's theory as the specific focus of this thesis. It is shown how it is used in the literature and how it offers a range of connections throughout different disciplines of physical science and engineering (see sec. 2.2) and yet still offers much potential to be developed further. But since Weber's theory has been historically superseded by Maxwell-Lorentz field theory, it is necessary to discuss the criticism and reasons that eventually led to the wide-spread abandonment of the idea in the late 19th century (sec. 2.3).

2.1 Different Theories of Electrodynamics

In this section, brief comments will be given regarding some of the different theories of electrodynamics that have been of note historically, starting with the established theory of fields and ether by Maxwell. The latter forms the foundation of modern science and technological inventions, from particle accelerators to modern medical instrumentation (e.g. various imaging and treatment devices). Following this, Weber's force law is introduced and some other historic and existing theories of note are commented on, along with the possibility of further modifications especially to Weber's formula.

2.1.1 Maxwell's Equations and Field Theory

When James Clerk Maxwell presented his *magnum opus* on electromagnetic theory [1] in 1873, he formulated his ideas about the action of electric and magnetic fields partly in prose and partly as mathematical descriptions and equations he introduced. These can be summarised in the concise form of only four equations as widely disseminated in modern times [60]. The differential forms of Maxwell's equations in a vacuum and in SI-units are commonly given as:

$$\nabla \cdot \vec{E} = \frac{\rho}{\varepsilon_0}, \quad (2.1)$$

$$\nabla \cdot \vec{B} = 0, \quad (2.2)$$

$$\nabla \times \vec{E} = -\frac{\partial \vec{B}}{\partial t}, \quad (2.3)$$

$$\nabla \times \vec{B} = \mu_0 \left(\vec{J} + \varepsilon_0 \frac{\partial \vec{E}}{\partial t} \right). \quad (2.4)$$

Here, ρ is the local charge density, ε_0 and μ_0 are the vacuum permittivity and permeability and \vec{J} is the current density. \vec{E} and \vec{B} are the electric and magnetic field respectively, through which charged particles interact, meaning contact-action where a particle always interacts with the field as a medium and the fields themselves can interact, as for example in the transmission of electromagnetic waves.

Equation (2.1) is Gauss's law, which relates the electric field with the charge density, (2.2) is the law of non-existence of magnetic monopoles, (2.3) is the Maxwell-Faraday equation that expresses induction, and (2.4) is the Maxwell-Ampère equation that correlates currents and time-varying electric fields to magnetic fields, which is also a form of induction. Due to the time-dependent nature of (2.3) and (2.4) electromagnetic waves can be predicted. While Maxwell's approach was originally based on the ether through which electromotive forces and waves would propagate, from today's point of view the fields themselves have effectively replaced the ether as the dominant medium and are now considered to be responsible for interaction transmission. The ether as an original construct is largely and effectively ignored (which is further addressed in section 6.2).

Further to the field equations, the Biot-Savart law is formulated to obtain the magnetic field for a current element integrated along a closed circuit path

$$\vec{B}_{BS} = \frac{\mu_0}{4\pi} \int \frac{Id\vec{l} \times \hat{r}}{r^2}, \quad (2.5)$$

where $Id\vec{l}$ is a current element and r is the distance from $d\vec{l}$ to the point where the field is evaluated and \hat{r} is the corresponding unit vector. For forces between two current elements, Grassmann's force is normally utilised based on the Biot-Savart law,

$$\begin{aligned} d^2 F_{Grassmann} &= I_1 d\vec{l}_1 \times d\vec{B}_{BS} = I_1 d\vec{l}_1 \times \left(\frac{\mu_0}{4\pi} \frac{I_2 d\vec{l}_2 \times \hat{r}}{r^2} \right) \\ &= -\frac{\mu_0}{4\pi} \frac{I_1 I_2}{r^2} \left[(d\vec{l}_1 \cdot d\vec{l}_2) \hat{r} - (d\vec{l}_1 \cdot \hat{r}) d\vec{l}_2 \right]. \end{aligned} \quad (2.6)$$

For any charged particle q in more general situations moving in the presence of electric and magnetic fields the interaction is usually given by the Lorentz force:

$$\vec{F}_L = q \left(\vec{E} + \vec{v} \times \vec{B} \right). \quad (2.7)$$

In general, field theory and Maxwell's equations are a 'macroscopic' approach as they were developed from a continuous medium model (the ether). But as we will see in the following section, Weber's force is 'microscopic' in that sense as it describes the interaction between two charged particles in its standard form. For a better comparison between Maxwell's and Weber's theory, Assis shows the derived force between two point charges

from field theory [61] up to second order in v/c based on the work of Liénard, Wiechert and Schwarzschild, which was first obtained by O’Rahilly [62] as

$$\begin{aligned} \vec{F}_{21} = & q_1 \vec{E}_2(\vec{r}_1) + q_1 \vec{v}_1 \times \vec{B}_2(\vec{r}_1) = q_1 \left\{ \frac{q_2}{4\pi\epsilon_0} \frac{1}{r^2} \left[\hat{r} \left(1 + \frac{\vec{v}_2 \cdot \vec{v}_2}{2c^2} \right. \right. \right. \\ & \left. \left. - \frac{3(\hat{r} \cdot \vec{v}_2)^2}{c^2} - \frac{\vec{r} \cdot \vec{a}_2}{2c^2} \right) - \frac{r\vec{a}_2}{2c^2} \right] \right\} + q_1 \vec{v}_1 \times \left\{ \frac{q_2}{4\pi\epsilon_0} \frac{1}{r^2} \frac{\vec{v}_2 \times \hat{r}}{c^2} \right\}. \end{aligned} \quad (2.8)$$

In this formula q_1 is the test charge and q_2 is the source charge generating the fields \vec{E}_2 and \vec{B}_2 , where according to Assis time retardation, radiation and relativistic effects have been included. The constant c is the speed of light and \vec{a}_2 denotes the acceleration of the point charge. It is apparent that the expression depends on the square of the source charge velocity and on its acceleration, whereas Weber’s force depends on the relative velocity and acceleration, as will be seen in section 2.1.2.1. Assis also shows how this expression can be obtained from the Darwin Lagrangian [63, sec. 6.8], as the Darwin Lagrangian is more widely used in the literature to describe systems of point charges [64–66]. Both the Schwarzschild force (2.8) and Lorentz force (2.7) have been criticised as violating conservation of linear and angular momentum. To restore conservation it is usually argued that the energy is lost or gained by the electromagnetic field generated by the charges or that self force needs to be taken into account [67, 68]. However, a system of two point charges seems extremely difficult to test. The general applicability (or non-applicability) of Newton’s third law to the Lorentz force and generally in electrodynamics has been discussed in [69–71]. Cornille [70] also claims that if the electrodynamic force laws indeed violate Newton’s third law, then it inevitably leads to the conclusion that energy can be extracted from the ether, as the ether exerts a force that is responsible for the violation. Possible macroscopic experiments that are claimed by Cornille to show this effect are summarised in [70].

It has further been criticised that the velocity \vec{v} in the Lorentz force formula (2.7) is not clearly defined, that is what it is defined with respect to, was not even given by Lorentz himself [63, 72]. It thus remains ambiguous if the definition is w.r.t a coordinate system or a source charge, which might itself be moving, although there seems to be support to

the idea that Lorentz viewed the velocity as relative to the ether [63, 72]. However in relativistic treatments this is usually resolved by a chosen inertial frame of reference and regarding the velocity relative to the measuring device or observer.

There is further discussion about conceptual problems in classic electromagnetism and modern particle-field theories in the literature [46, 47]. This mainly focuses on the problem of point charges and their diverging self-energy, as the calculated energy of an electron with its own field tends to infinity based on classic electromagnetism. One solution is the renormalisation approach in the quantum theory of Dirac where the point charge is treated as a singularity and the infinite energy is subtracted as a constant from the problem to renormalise the energy content. The other solution is the extended particle model, where elementary charges are not treated as point-like anymore and consequently the divergence in the singularity disappears. Pietsch [46] discusses both approaches and the associated cost of the proposed solutions, and for an interesting discussion of these approaches including a mathematical perspective, see [73], on which Pietsch bases his arguments. Pietsch then argues that both approaches are incompatible at a fundamental level and a better solution is needed, in which direct-action theories are proposed. Lazarovici [47] also discusses the self-energy problem and the Lorentz-Dirac as well as the extended particle solutions as unsatisfactory, but also involves free fields, among other philosophical, mathematical and physical arguments, and proposes the Wheeler-Feynman direct-action theory in particular as a solution to those problems. The renormalisation approach has also been criticised by other authors [74], including Feynman [75] and Dirac [76]. A similar argument has been made by Kastner about the Wheeler-Feynman direct-action theory, not only does it avoid self-energy problems, it is also not subject to Haag's theorem and the consequent problems of free and interacting fields in QFT [77]. (Briefly summarised and oversimplified, Haag's Theorem is a mathematical argument, stating that in any relativistic QFT interacting and free fields cannot be brought into a consistent mathematical framework, hence the problem.)

This concludes the brief overview of field theory and Maxwell's equations and further reading where fields, waves, radiation and relativity are treated can be found in the works

of other authors [64, 78–81]. Attention will now be given to alternative formulations of electrodynamics with a special focus on Weber-type theories.

2.1.2 Alternative Theories

Historically, many scientists have worked on electrodynamics and electromagnetic phenomena, performing a wide range of experiments to investigate the nature of electricity and magnetism. From these experiments researchers have developed a multitude of hypotheses, laws and eventually attempted to merge them into cohesive theories, leading to several attempts to explain electrodynamics, some of them more successful than others. Many alternative theories have been proposed over the years with important contributions from several scientists. Some examples include Gauss, Neumann, Lorentz, Riemann, Weber, Ritz, Warburton, Moon & Spencer, Wesley and Wheeler-Feynman direct-action theory, amongst others. Of these, the most relevant to the present investigation are briefly outlined below (sec. 2.1.2.1 and 2.1.2.2).

2.1.2.1 Weber’s Theory of Electrodynamics Wilhelm Eduard Weber first published his force law to describe the interaction of charged particles in 1846, only 15 years before Maxwell published his first work on electromagnetism, ‘On physical lines of force’ [82], a concept which would only tangentially relate to the field concept later introduced in Maxwell’s *Treatise* [60]. Maxwell as a contemporary of Weber was well aware of his work and Maxwell positively mentions Weber in his *Treatise*, expressing admiration for Weber’s work. As a 19th century scientist, Weber engaged with several physical disciplines, but a collection of his original work on electrodynamics can be found in [48, 83] and English translations of his eight major memoirs on electromagnetism can be found in [84–91].

The main difference between Weber’s theory and Maxwell’s field equations is that Weber’s is a direct-action-at-a-distance theory, such as Newton’s law of gravity or Coulomb’s force of electrostatic attraction, **and the fields themselves are not conceptualised as a primary part of the mathematical description**. Instead, Weber’s force depends on the direct interaction and force transmission between microscopic charges themselves,

as opposed to contact action in field theory, where the charges give rise to fields so a source charge and a test charge only interact with the field of the other. Some aspects of how fields can still be conceived with Weber will be discussed later in section 2.2.

In modern vector notation and SI units, Weber's force can be expressed as

$$\vec{F}_{21} = \frac{q_1 q_2}{4\pi\epsilon_0} \frac{\hat{r}_{12}}{r_{12}^2} \left(1 - \frac{\dot{r}_{12}^2}{2c^2} + \frac{r_{12}\ddot{r}_{12}}{c^2} \right). \quad (2.9)$$

When Weber developed his force, his aim was to connect Coulomb's force and Ampère's force, arriving at a more general interaction law. Weber's force acts along the line joining two interacting point charges, following Newton's third law in the strong form with equal action and reaction, conserving linear and angular momentum. It depends only on the relative distance, relative velocity and relative acceleration of the interacting charges.

As this force is electrodynamic in nature, it contains electrostatic (i.e. Coulomb's force) and magnetic (i.e. Ampère's force) interactions, which is comparable with the Lorentz force (2.7) where a static (i.e. the electric field term) and a moving component (i.e. the magnetic field term) of the force are considered. The speed of light c in (2.9) was introduced as the ratio between electrostatic and electromagnetic units of charge, whose value was first determined experimentally in 1856 (10 years later) by Weber and Kohlrausch based on Weber's force. In 1848, two years after the presentation of the force law, Weber also showed that the force can be derived from a velocity dependent potential, which will be further addressed in section 3.

A further analysis of the capabilities of Weber's theory will follow in section 2.2 and the theory has undergone more development in recent decades. It is noteworthy that predominantly in the low velocity limit, Weber and Maxwell theory predict very similar results, if not the same results for a given phenomenon. Weber has also been shown to be consistent with field equations by a number of authors and the matter will be further addressed in section 2.2.1.

However, it must be stressed, Weber's electrodynamic theory has not yet been developed to anywhere near the same degree that other theories have, which includes the high velocity regime near the speed of light. When quantum interactions are considered,

the Wheeler-Feynmann approach to direct-action has undergone development by Davies who introduced a quantum theory based on Wheeler-Feynman electrodynamics [92]. In the case of Weber, only some initial connections between Weber's theory and quantum mechanics have been made, as will be seen in section 2.2.2, however, a rigorous treatment is yet to be developed. This is considered a work in progress and more research is needed before any conclusions can be drawn about Weber's theory in the quantum realm.

2.1.2.2 Ritz's Emission Theory of Light Walter Ritz was a contemporary of Einstein working on electrodynamics and spectroscopy and suggested his force formula in 1908. His formulation is an emission theory of light and takes the opposite approach to Einstein's theory of relativity – instead of keeping the laws of electrodynamics and altering the laws of mechanics, Ritz kept the laws of mechanics and modified the laws of electrodynamics. In fact, Ritz was opposed to Einstein's views at the time and would engage in discussions with his colleague, being of the opinion that Galilean relativity should be retained instead of adopting Einstein's SRT [93]. Although Ritz regarded his work as unfinished and met an untimely death in 1909, at 31 years of age, he formulated the following force law of electromagnetics and optics:

$$\vec{F}_{Ritz} = \frac{q_1 q_2}{4\pi\epsilon_0 r^2} \left\{ \left[1 + \frac{3-k}{4} \left(\frac{v}{c} \right)^2 - \frac{3(1-k)}{4} \left(\frac{\vec{v} \cdot \vec{r}}{c^2} \right)^2 - \frac{r}{2c^2} (\vec{a} \cdot \vec{r}) \right] \frac{\vec{r}}{r} - \frac{k+1}{2c^2} (\vec{v} \cdot \vec{r}) \vec{v} - \frac{r}{c^2} (\vec{a}) \right\}, \quad (2.10)$$

where k is a parameter to be determined experimentally. As an electrodynamic force law, Ritz's formula is rather successful, as Ritz explained electrostatics, induction phenomena, the action of magnets and closed circuits on charged particles, and even Hertzian oscillators with his theory [93]. A further treatment of Ritz's force can be found in O'Rahilly [62], where it is compared to the Lorentz force and shown to be able to explain a variety of electromagnetic phenomena such as radiation pressure and electromagnetic waves. It was further related to gravitational attraction, with Ritz's formula leading to a modification of Newton's law of gravitation where gravitation is a residual statistical force between groups of moving charges. Furthermore, it can be seen that Weber's force can be obtained from

Ritz's when $k = -1$ and the last term in the direction of acceleration is omitted, also for $k = 3$ it predicts the behaviour of high speed electrons similar to SRT [94].

Yet, from today's point of view, Ritz's theory as an emission theory of light is regarded as disproven. A re-evaluation of the theory and experimental evidence supporting the independence of the velocity of light from its source in the 1960s [95–101], provided further evidence against the ballistic theory of light. It is, however, remarkable how successful Ritz's theory seems to be from an electromagnetic perspective despite its optical notions being mistaken. Ritz had a strong opinion about electromagnetic phenomena and criticised Maxwell-Lorentz theory quite heavily in his lifetime [102]. However, since his theory has been refuted, his criticisms did not prevail and from today's point of view the arguments by Pietsch [46] and Kastner [77] are considered more substantial. For an extensive and thorough review of Ritz's scientific endeavours and reception in the scientific community, the reading of Martínez [93] is recommended. Lastly it is noteworthy that Brown [103] has used a retarded action-at-a-distance Ritz-type force and applied it not only to circuits, radiation and induction but also to stellar aberration, gravitation, inertia, Mercury's perihelion precession, gravitational red-shift and high speed particles, and even beyond to optics [104] and diffraction [105], which emphasises the versatility Ritz's approach offers.

2.1.2.3 Other Theories and Modifications of Theories There are a number of other interesting contributions, theories and concepts by different researchers working in the field of electrodynamics which shall be briefly mentioned here so that the reader can gain some appreciation of the sheer scale of the scientific effort that has been made over the years.

Gauss worked on a velocity dependent force law, however, he never published his formula officially as it did not satisfy his own criteria and it is also inconsistent with energy conservation, even though it followed Newton's third law, rendering it unlikely as a possible theory. However, Weber worked closely with Gauss in Göttingen and Weber's theory was also influenced by Gauss's work to a degree, especially with regard to Weber's attempt to generalise Coulomb's force to a velocity dependent form. Additionally, Riemann

and Clausius also proposed force laws that depend on velocity and acceleration terms of the charges involved. While Riemann's force conserves energy and follows Newton's third law, it does not conserve angular momentum. Clausius's force, however, neither conserves linear nor angular momentum. The forces of Gauss, Riemann and Clausius can all be found in appendix B of [63], where the force laws are shown and a brief summary of each is given.

Furthermore, Neumann made important contributions to electromagnetic theory, such as the concept of the vector potential \vec{A} and with it the field \vec{B} as a derivation of the former by use of the gradient operator, or the Neumann formula to calculate the inductance of circuits. For an interesting analysis of contributions by Gauss, Neumann and Hertz, see Moon and Spencer's review [106].

Another common concept in research is the modification of theories, e.g. SRT can be regarded as a modification of Maxwell's field theory allowing for the transformation of fields between reference frames and including relativistic effects at high speeds of movement close to that of light. In the same way the electron theory suggested by Lorentz is also a modification to field theory that was being developed in the late 1900s. The agenda of the Lorentz electron theory [107, 108], was a reintroduction of particles of atomistic nature into Maxwell's field view. However, it did not prevail against the success of relativity theory and thus was superseded.

Other important contributions have been made by Helmholtz, who had developed an expression that combined potential functions of Neumann and Weber with a free parameter in an attempt to arrive at a more general expression, and even includes Maxwell's theory as a special case. Otherwise his works helped in advancing Maxwell's theory among continental physicists and they were a key factor for Hertz to pursue the experiments giving support to Maxwell's views [109].

In a way, Ritz's theory can also be seen as a modification of Weber's force, but there exist more suggestions to possible modification of Weber's electrodynamics in the literature. Wesley has suggested a force law based on Weber's force that incorporates fields, slowly varying effects and also agrees with relativistic electron beam deflection of the

Kaufmann-Bucherer and Bertozzi type experiment, so long as a relativistic modification of mass is assumed [110].

Other modifications have been proposed, such as Phipps' modification to Weber's potential [111], which was further investigated by Caluzi and Assis [112] and found to lead to unphysical behaviour in certain situations when particles are moving at high speeds. Further, Montes' investigated different modifications to Weber's potential and analysed their behaviour close to the speed of light [113], while Assis modified Weber's potential and force based on Phipps' idea and finds a possible connection to gravitational forces from his model (see sec. 2.2.2). In the early 20th century, Tisserand [114], Gerber [115] and Schrödinger [116] have modified the Weber potential and investigated the precession of mercury's perihelion on that basis. Since research in Weber electrodynamics is still developing, it is possible that the theory will see suitable modifications in the future and some interesting features of existing modifications will also be discussed in the following section 2.2.

Lastly, other modern approaches include new electrodynamics by Moon & Spencer and the Wheeler-Feynman direct action electrodynamics. Moon & Spencer utilise a modified force law which is especially successful in the treatment of time varying charges like antenna theory, and they have further analysed the subject for many topics in electromagnetic research [117–121]. The Wheeler-Feynman approach to direct-action electrodynamics [122, 123] has seen a quantum development [92] and cosmological considerations based on the theory [124–126]. Thus both theories can claim successes as electrodynamic theories, the Wheeler-Feynman theory even beyond, and represent interesting approaches to electrodynamics. This concludes the brief overview about alternative theories in electromagnetism and some of the notable modifications that have been suggested. Now, an in depth review of Weber's theory will follow and the many facets of the theory in the literature are shown.

2.2 Weber Electrodynamics in the Literature

This chapter will focus on Weber's electrodynamics and its appearance in the scientific literature. After Maxwell's success in the late 19th and early 20th century it has not received a lot of attention except from a few, with important contributions from O'Rahilly [62], Wesley [127–129], Assis [63] and others. Over the years, many connections have been made from Weber's theory of electrodynamics to different topics within physics. While Weber's force is electromagnetic in nature and has been used to describe phenomena in that field, it is also shown to interconnect with mechanics, the structure of the atom, gravity, quantum mechanics and even some effects of general relativity and topics that are usually referred to as "breakthrough physics". A visual overview of the relations Weber has with electromagnetics and other disciplines can be seen in Fig. 2.1.

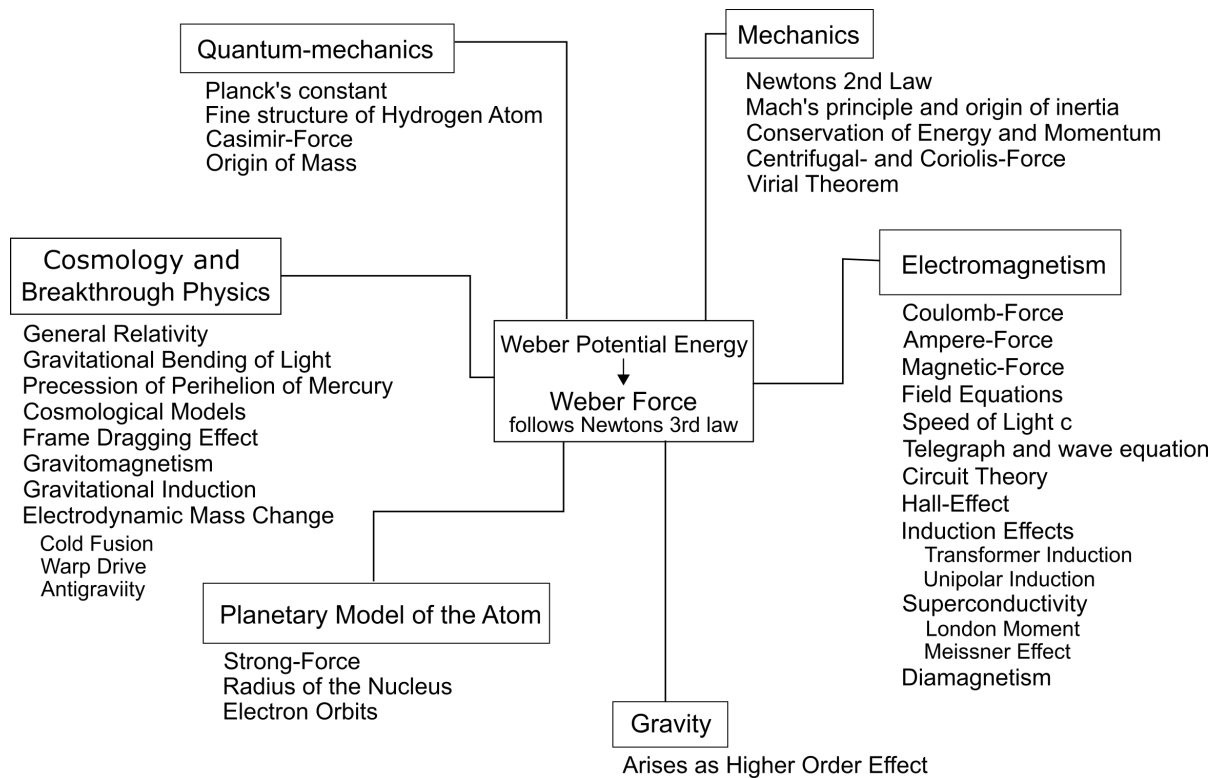


Figure 2.1: A visual map providing an overview of the different subsidiary fields and phenomena that Weber's theory has been shown to provide a basis for and connects with throughout the branches of physics and engineering.

2.2.1 Electromagnetic Phenomena

As Weber is essentially a theory of electrodynamics, it has been shown to explain many pure and applied phenomena in electricity and magnetism. From its basic form (2.9), it is easy to see that Weber's force reduces to the Coulomb force for stationary charges. That means for static charges where their velocities are zero, the formula can be simplified to

$$F_{Coulomb} = \frac{q_1 q_2}{4\pi\epsilon_0} \frac{\hat{r}_{12}}{r_{12}^2}. \quad (2.11)$$

Thus, Weber can be readily seen to describe purely electrostatic interactions. When interacting charges start moving, the force then changes, and for two current elements in a circuit Ampère's force can be derived from Weber's force as shown by Assis [130]. For two steady current elements $I_1 d\vec{l}_1$ and $I_2 d\vec{l}_2$ this takes the form:

$$d^2 F_{Ampere} = -\frac{\mu_0}{4\pi} I_1 I_2 \frac{\hat{r}}{r^2} \left[2(d\vec{l}_1 \cdot d\vec{l}_2) - 3(\hat{r} d\vec{l}_1 \cdot \hat{r} d\vec{l}_2) \right] \quad (2.12)$$

Grassman's force (2.6) from section 2.1.1, for comparison, is slightly different in its interaction. Assis' extensive analysis indicates the similarities and differences between Ampère's and Grassmann's forces [63] and most notably shows, that Grassmann's force violates Newton's third law. However, it has been claimed that, when the respective force expressions are applied to any closed circuit, they are equivalent and lead to the same result [131]. There has been a discussion in the literature about which force is the correct one. For example a paper by Cavalleri [132] claims that Grassmann's force gives the correct result for any given circuit and Ampère's does not; but as Assis commented in response [133], they did not consider all contributions of Ampère's force in their deductions and when carried out, both models predict the same force values [131, 134]. This inevitably leads to the conclusion that it is impossible to distinguish between the two forces for any closed circuit, which has been verified for several configurations [135, 136].

In this context, it seems adequate to briefly discuss the Ampère force and note its importance, as even Maxwell himself stated that it must remain the cornerstone of electrodynamics. The divide in the literature between Ampère's vs Grassmann's force seems to stem from the nature of the Ampère force, which includes a longitudinal force compo-

ment along the wire in the direction of movement of the current elements. This feature complies with Newton's third law but appears to be incompatible with the Lorentz force, whereas Grassmann's force for current elements does not include a longitudinal component and is in turn compatible with the Lorentz force, but violates Newton's third law. When Ampère conducted his original experiments, investigating the force between two wires [137–140], he found his force law as a result of these experiments and included the longitudinal component according to his observations. Further to the discussions about the general applicability of Newton's third law in electrodynamics [69, 70], Chaib and Lima [141] have re-iterated that Ampère did not find any evidence in his experiments that would contradict Newton's third law and that it remains applicable in electrodynamics. They also clarify that Ampère regarded the third law as a consequence of his experiments, rather than an assumption he tried to conform to, and explain his philosophical reasoning in arriving at that conclusion. The authors of [141] also give a review of some of Ampère's main work in the manuscript and show that Ampère was the first to obtain an expression similar to the Biot-Savart law from his experiments.

This special quality of the Ampère force to incorporate longitudinal forces has sparked the interest of researchers and in modern times more experiments have been performed to investigate it, where the force has also been connected to a variety of effects and applications. In particular, Graneau *et al.* have extensively investigated Ampère's force [142–151] where the force has been associated with water jet propulsion, exploding wires, fusion and railguns, as well as the electromagnetic impulse pendulum, liquid mercury experiments (e.g. Ampère's bridge) and homopolar motors [152–161]. Even though the exploding wire phenomenon has been investigated further [162, 163] and the longitudinal Ampère force component does not seem responsible for the bursting of wires, it is still important in other situations. For example, the importance of Ampère's force to induction in general has been discussed along with the ability of the force to explain EM-waves in the near field [164]. A classical approach to derive longitudinal forces has been taken by Rambaut and Vigier [165], where they find longitudinal forces as an average effect of conduction electrons and lattice charges of a current element. In a follow-up paper [166] the authors

then derive longitudinal forces with a different approach based on the Liénard-Wiechert potentials and discuss their influence on conductors in all phases, including plasmas and fusion applications. Recently Moyssides also succeeded in deriving longitudinal forces with the help of the Biot-Savart-Grassmann-Lorentz force law acting on a submarine projectile in mercury, showing that both forces are equivalent and both agree with experimental results presented in the paper [167]. Further experiments to detect longitudinal forces have been performed by Saumont [168], where difficulties in measurements of these forces due to thermal effects and rapid spurious forces are also addressed and the compatibility of longitudinal tensile forces with relativity theory and the Lorentz force is considered. An experiment by Graneau *et al.* [169] has investigated longitudinal forces utilising spark gaps in a circuit and found them consistent with Ampère’s force, which has been interpreted as a direct proof of the existence of longitudinal forces. A new experiment has recently investigated how the charges in a neon glow lamp are influenced in the near field of a capacitor dependent on the signal frequency [170]. It was found that there is a longitudinal force component on the charges moving in the plasma that agrees with predictions of a Weber-Ampère model calculated in the paper. We can deduce from this brief analysis that longitudinal forces appear in both classic and Weber approaches which shows the similarity of the two theories.

As an interesting side note, some authors speak of the re-discovery of longitudinal forces [166] through Graneau’s work, however, this is a peculiar phrasing as it implies that the longitudinal forces have been forgotten at some point, and that of course raises the question how and why this was the case. The author of the present thesis is in possession of at least one textbook [171] where Ampère’s force is explicitly taught at university level and the “neglecting” of longitudinal forces might be an artefact that can be attributed to the method of teaching undergraduate classes on electromagnetism in modern physics and engineering, where neither Grassmann’s nor Ampère’s force are necessarily taught. This however, is a didactic discussion beyond the scope of this thesis.

Moving on from current elements, Weber’s force in the general form, Eq. (2.9) is a force between point charges and depends on the relative velocity between them, it

is intrinsically electromagnetic in nature and so incorporates magnetic interaction by design. The magnetic force naturally arises from the movement of the charges, whereas the Lorentz-force (2.7) is usually derived by considering SRT or Lorentz transformation of the Coulomb Force or electric field [3, 81, 172, 173] and magnetism is considered to arise as a relativistic effect in this context. But recently it has also been suggested that it may not be necessary to treat magnetism as a consequence of SRT and instead Maxwell's equations can be derived from Coulomb's force and time retardation without any further assumptions [174]. In Weber electrodynamics however, the intrinsic velocity dependence of the force can be used in combination with the concept of current elements to calculate magnetic interaction forces, such as has been applied to the fields of solenoids [94, 175–177] and will be shown in more detail in section 4.1. Specifically in the case of the magnetic field of a long straight wire [94] the Lorentz and Weber force on a charged particle have been found to be identical in the low velocity limit.

Further to the similarities between Ampère's and Grassmann's force as well as the Weber and the Lorentz force, Weber has been shown to be consistent with Maxwell's field equations by a number of authors [63, 127, 178–181], even though it does not conceptually depend on them. For example, Wesley [127] derives field equations from Weber by introducing charge densities and current densities into Weber's equation and integrates over a fixed volume. He arrives at the form

$$\begin{aligned} \frac{d^3 F}{d^3 r} = & -\rho \nabla \Phi + \vec{J} \times (\nabla \times \vec{A}) \frac{1}{c} - \rho \frac{\partial \vec{A}}{\partial t c} - \vec{J} \nabla \cdot \vec{A} \frac{1}{c} \\ & + \frac{\partial \vec{J}}{\partial t} \frac{\Phi}{c^2} + (\vec{J} \cdot \nabla) \nabla \Gamma \frac{1}{c} + \rho \nabla \frac{\partial \Gamma}{\partial t c} - \left(\frac{\partial \vec{J}}{\partial t} \cdot \nabla \right) \vec{G} \frac{1}{c^2}, \end{aligned} \quad (2.13)$$

with

$$\Phi = \int d^3 r' \rho'(\vec{r}', t) \frac{1}{R}, \quad (2.14)$$

$$\vec{A} = \int d^3 r' \vec{J}'(\vec{r}', t) \frac{1}{cR}, \quad (2.15)$$

$$\Gamma = \int d^3 r' \vec{R} \cdot \vec{J}'(\vec{r}', t) \frac{1}{cR}, \quad (2.16)$$

$$\vec{G} = \int d^3 r' \vec{R} \rho'(\vec{r}', t) \frac{1}{R}. \quad (2.17)$$

The primed quantities in this formula are sources acting on the unprimed test currents and charges separated by distance R . It is especially interesting that in addition to the usual electric potential Φ and magnetic potential \vec{A} two new potentials, Γ and \vec{G} appear and Wesley points out that the Lorentz force and Maxwell's equations are a special case where only the first three terms on the left hand side of (2.13) appear. Wesley further argues that the representations through a force equation and field expression are mathematically isomorphic as long as the fields are intermediate without time retardation. But when time retardation is introduced into (2.13), the field expressions then contain wave equations with velocity c .

While Assis [63] and Kinzer [178] have taken a similar approach to Wesley, starting from Weber's formula and deriving the field equations from it, the opposite approach, starting from Maxwell's equation and arriving at a Weber-type formulation, does also exist [179]. With extensive mathematical work the author of [179] shows that there are two implicit restrictions in Maxwell's field equations and without these restrictions a set of Weber equations can be re-obtained from Maxwell's. One limitation is the condition that the charge density function ρ is a constant in time and the other is that the test charge velocity is required to be zero for mathematical consistency according to the author of [179]. The procedure of removing the restrictions from Maxwell's field theory is then to allow for moving test charges and time varying charge densities, which emphasises Wesley's argument that Maxwell's equations are a special case of Weber's law. Another important opposite approach has also been discussed where Weber's and Ampère's forces are obtained as a non-relativistic limit from the Liénard-Wichert potentials [166] and from a Fermi distribution of accelerated charges [182]. In the recent approach of Li [180] a field representation of Weber's force is developed with the help of Einstein notation, where the velocity and acceleration dependent terms in Weber's force can then each be identified with a respective tensor field. Li states that this approach has the advantage in simplifying the necessary calculations in systems of many particles, reducing the number of required force calculations.

One of the strengths that is usually ascribed to Maxwell's field equations is that the

velocity of light appears from the wave equations as does the relation between permittivity ε and μ . However, it was not Maxwell who first discovered the relation between the speed of light c and electromagnetic waves, in fact it was Weber and Kohlrausch who first predicted the value of c from Weber's equation and confirmed it experimentally [183,184]. Following this, Weber and Kirchhoff derived the telegraphy equation for the propagation of electromagnetic signals through a wire independently of each other, and Assis has provided a modern derivation and analysis of the equation [185–187]. This equation also reduces to a regular wave equation when the resistance of the wire goes to zero. Fukai [188] has further argued that modern views of the vacuum can be assumed, where the vacuum behaves as a medium with inductance and capacitance, similar to a coaxial cable or transmission line problem, Weber's theory predicts a signal propagation at light velocity in vacuum and thus should be able to predict radiation as well.

In relation to circuit theory, Assis [189] has analysed the self inductance of circuits with the help of Weber's force and Newton's second law and compared them to similar derivations based on the Lorentz force and the Liénard-Schwarzschild force for circuits. He manages to derive the self inductance from Weber's force by examining the acceleration that conductor charges will be subjected to. The result can be interpreted as an effective mass of the conduction electrons in the circuit, with the positive lattice ions opposing the motion of the accelerated electrons. In a further study [190] Assis and Bueno also show that the self inductance formulae for a single circuit of Weber and Maxwell are equivalent. This has added to the previously known fact that the mutual inductance formulae were the same, however when a single circuit is considered, the equivalence can be obtained by considering surface charge or volume charge elements instead of line charge elements. Weber himself also worked on circuit resistances [83], conducting many experiments to investigate their resistive behaviour and considered the derivation of an absolute unit of resistance based on his force law.

A possible derivation of the Hall effect from Weber's force has been investigated by McDonald [191] and it is deduced that, under the condition that only negative charges are assumed to be charge carriers in Weber's theory, and disregarding the original Fechner

hypothesis, Weber does predict the Hall effect consistent with the Lorentz force derivation. Based on this assumption the Hall effect cannot distinguish between the two forces, as they are equivalent in this particular case. The Fechner hypothesis itself will be further discussed in section 2.3.

In addition to self inductance and the generation of a Hall voltage, Weber's theory has also been applied to voltages arising through induction. Smith *et al.* [192, 193] have developed a model for transformer induction with the assumption of conduction electrons following accelerated motion. They arrive at an expression identical to Faraday's law and predict voltages in receiver coils correctly. Maxwell pointed out in his *Treatise* [1] that it is possible to derive Faraday's law from Weber's law, as Weber derived it himself from his force, and Wesley has also indicated the connection between Faraday's law and Weber's, besides consideration of induction in general [127, 128].

Unipolar induction (also called homopolar induction), as another example, has been analysed by Assis [194] on the basis of Weber electrodynamics. He arrives at the conclusion, that the phenomenon can only be predicted correctly if the closing wire is included in the analysis, thus considering the whole circuit that is influenced by the presence of a magnet in a Faraday generator setup. How an electromotive force is induced in homopolar machines and general considerations about spinning magnets are further explored in section 5 of this thesis. There are also recent claims in the literature [195] that not all observed induction effects can be explained by Faraday's law or the flux cutting rule, mentioning Weber as a possible fuller explanation. Assis has even presented an analysis [196] where he explores beyond the regular scope of unipolar induction and describes a situation where an additional voltage is induced due to the presence of an electrostatic potential, calling it Weberian induction. In this scenario a spinning disk is placed inside a charged spherical shell, with or without the magnet. From the perspective of field theory and the Lorentz force, the charge on the shell cannot induce a voltage in the disk due to the absence of a field inside the shell, but according to Assis' analysis, in Weber's electrodynamics the charge on the shell would still exert a force on the disk charges and an additional voltage should be induced. However, such an effect would be many orders

of magnitude smaller than regular unipolar induction. This field-free electrostatic force is closely related to a criticism of Weber's theory and will be further discussed in sections 2.2.3 and 2.3.

Related to unipolar induction is the so-called Feynman disk paradox [197], where metal spheres are mounted on a plastic disk free to rotate and a current carrying coil is situated on the same axis. Initially, the apparatus is at rest, but when the current is switched off, the paradox arises. Analysing the problem in terms of the change in magnetic flux would expect the disk to rotate as an electric field is induced and seen by the spheres, however, analysing from the perspective of angular momentum would mean that the disk does not start to rotate, as the momentum is initially zero and since it must be conserved, the disk should remain stationary. The apparent contradiction in field theory is resolved by taking into account the electromagnetic angular momentum stored in the fields, so that initially the angular momentum was not zero [198]. Fukai argues that the problem is equally well explained by Weber's theory [188] and considers the force on the sphere exerted by the change of current in the solenoid, which turns out to be non-zero, so the disk will move accordingly.

It was also shown recently that superconductivity can be derived from Weber's theory according to two independent authors in two different ways. One approach by Prytz [199] considers a magnet or solenoid with a DC current at rest and the centripetal acceleration of the conductor charges. This acceleration causes the Meissner effect to appear in conduction materials according to his deductions. Assis and Tajmar [200] instead follow a more general treatment where AC currents are considered, and in turn the acceleration of the charges causes the Meissner effect and the London moment to appear from Weber's force.

The so called Aharonov-Bohm effect (AB-effect) that describes a phase shift experienced by electrons when they are scattered around a finite solenoid is usually explained through the quantum mechanical influence of the vector potential \vec{A} . Wesley [201] managed to establish a connection between Weber's force and the existence of the AB-effect. First, he takes a more classical approach and considers the force due to motional induction

on the electron beam, which leads him to find a phase shift depending on the electron path due to this force component. Then, he shows that the same force is present when considering Weber's potential and force, causing the appearance of the phase shift and thus the AB-effect. Unfortunately in the digital version there seems to be a misprint and large parts of the paper are missing, but his essential deductions can still be found in the first and last sections of the manuscript [201].

An initial connection between Weber's force and antenna theory has been made by Prytz [202]. In this approach the concept of retarded time is considered to account for far distance effects and utilised with the acceleration dependent induction of Weber's force. This can describe loop antennae by itself and also contributes to dipole antennae, and simultaneously relates back to the transmission of radio waves. This is, of course, similar to the approach taken by Moon and Spencer [118] who had derived the behaviour of the loop and dipole antenna about 60 years prior, and also arrived at Neumann's inductance formula for circuits based on the acceleration dependent force in the process.

Weber also considered early forms of diamagnetism in his work, based on the molecular currents introduced by Ampère, where diamagnetism occurs when molecular currents are induced by an external field in a diamagnetic material that has otherwise no molecular currents. While the general idea of molecular currents remains to this day, present explanations necessitate quantum mechanical considerations to fully account for the existence of diamagnetism, due to the Bohr-Van Leeuwen theorem.

This overview shows the electromagnetic versatility Weber's theory possesses as an alternative to Maxwell's equations, but it is not the only area in which Weber's force has been utilised. Weber's theory will now be explored beyond the realm of electromagnetic phenomena and how it can be used in other areas of physics.

2.2.2 Relevance of Weber's Force Beyond Electromagnetism

There are several aspects of Weber's force that are not immediately obvious when just regarding it as an electrodynamic force law between charged particles. It holds wider consequences in its action and has been connected to a variety of topics in the literature.

The first connection of note is the structure of the atom. Weber himself used his theory to devise a planetary model of the atom [203,204], where negative charges orbit around a positively charged centre, even before the electron was discovered. He realised a special feature of his force law by which an atomic structure emerges as a consequence, that is, a certain critical distance exists in his force law. It is most remarkable that below this critical distance like charges will start to attract instead of repel and opposite charges will still attract regardless. Furthermore, when two or more charges interact with only each other (no external forces are present in that scenario) they cannot transition to the inside or outside of that critical distance. If the interaction started below the critical radius, it would remain inside the radius, and if it began outside it would remain outside. Interestingly, the critical distance can be calculated to be of the order of the known diameter of the atomic nucleus when electron or positron interaction is considered. Thus, it seems possible to interpret Weber's force as relating to the strong nuclear force that is responsible for the attraction inside the nucleus, even though it is not yet known how it would work for protons. Additionally, for two charges of opposite sign orbiting each other in this model, a confinement to elliptical orbits is found which would experience a precession of the elliptical axis [203–206] and remain within an upper and lower bound of the orbit radius [203, 205, 207–209].

Weber also speculated based on his model of the atom on the mechanism of heat conduction and a possible connection between light and electricity. He related the orbital frequency of charged particles in his model to the wavelength of excited heat- and light-waves. Zöllner [210] even considered that from Weber's model it would be possible to derive the spectral lines of chemical elements. Upon considering the possibility of multiple orbits in a molecule and that each orbit could be populated with a number of charges, Weber also deduced a classification system characterising the possible combinations of positive and negative charges in a table that has similarities to the periodic table of elements. He further concluded that these molecular configurations could attract other molecules and combine to form stable systems. Eventually he was led to the hypothesis that chemical bonds might have an electrical origin and arrived at a bond that is similar

to a covalent bond between two atoms sharing an electron pair [203].

Unfortunately, Weber passed away before he could finish his planetary model of the atom, nevertheless it shows some very interesting properties. While Weber speculated about spectral lines emerging from his model, the fine structure of the atom was still in an early stage of discovery. There are relatively recent works in the literature [211, 212] analysing the connections between Weber's theory and quantised energy levels, they generally tend to show slightly different splittings for the fine structure of the atom. In 2015, Torres-Silva *et al.* [211] used the Hamiltonian formalism of Weber's theory and also considered spin-orbit corrections, whereas Frauenfelder and J. Weber [212] used a Bohr-Sommerfeld quantisation on Weber's Hamiltonian for a hydrogen atom. Wesley obtained a similar result in [213] where he considered the perturbation energy on the electron orbit in the hydrogen atom by utilising the Schrödinger perturbation method, which leads to energy levels different from the experimentally known splittings. It is also reviewed by Post [214] that Phipps' modification to Weber's potential leads to twice the number of observed splittings. As the experimental determinations of QED, such as the fine structure, lamb shift, Rydberg constant and anomalous dipole moments are among the most well tested predictions derived from field theory, this will remain the greatest challenge for Weber-type theories as it seems that it cannot make the necessary predictions in its current form. However, it seems worth noting that Feynman has directly utilised ideas of direct-action and retarded time in his approach to develop QED [75].

The Weber force has also been shown to be similar to velocity dependent forces in nuclear physics, such as nucleon-nucleon forces [215]. These are central forces and obey Newton's third law, and in [215] the authors show that the momentum dependent inter-nucleon forces in the interaction potential and Hamiltonian are generalised Weber forces, pointing out that Weber's force can be considered a special case of the forces appearing in nuclear physics. They state further that a similarity to Ampère's force exists in nuclear physics as well for scattering processes of spinless projectiles and that it cannot be understood on the basis of only the Lorentz force analogy, but is consistent with a Weber force analogy.

Another interesting similarity with the forces of nature exists between Weber's force and gravity, and Weber had already speculated about such a connection based on his atomic model. One of the underlying ideas is that the attractive force between charged particle assemblies is slightly larger than the repulsive force. Based on this idea, Assis [216,217] has developed a model to derive gravitational effects as a fourth order effect from the electromagnetic interaction through an extension of Weber's formula. He considers a series expansion of Weber's force law:

$$\vec{F}_{21} = \frac{q_1 q_2}{4\pi\epsilon_0} \frac{\hat{r}_{12}}{r_{12}^2} \left(1 - \frac{\alpha}{c^2} (\dot{r}_{12}^2 - 2r_{12}\ddot{r}_{12}) - \frac{\beta}{c^4} (\dot{r}_{12}^4 - 4\dot{r}_{12}^2 r_{12}\ddot{r}_{12}) - \frac{\gamma}{c^6} (\dot{r}_{12}^6 - 6\dot{r}_{12}^4 r_{12}\ddot{r}_{12}) \right), \quad (2.18)$$

with numerical constants α, β and γ and omitting any higher order terms of the series expansion. Equation (2.18) is then used to study the interaction of two neutral dipoles that consist of a positive charge in the centre and an oscillating negative charge. After an extensive analysis, Assis arrives at a non-zero force of attraction between the two dipoles which he proceeds to interpret as a gravitational interaction force. These derivations later led Tajmar [218] to analyse a minimum energy requirement between two neutral dipoles that is similar in nature to Planck's constant. The approach used by Assis is then further investigated by Baumgärtel and Tajmar [219] and it is found that there is not only a gravitationally interactive term as a higher order effect from Weber's electrodynamics. The result obtained in [219] is slightly different to the one originally obtained by Assis, but the authors of [219] interpret the resulting force to contain the Casimir force and inertial effects as well. Further analysis of this result in regards to a minimum energy requirement is pursued and the study finds a connection to Planck's constant and the origin of mass. So far, Planck's constant was derived to within 93% from this approach, which still leaves a 7% discrepancy, but a general relation between Weber's theory and Planck's constant can be established solely on electrodynamic properties of particles. One can generally see with the appearance of the Casimir force, Planck's constant and the fine structure of the atom that Weber's theory ties to certain quantum mechanical effects, however it requires significant development on quantum theoretical aspects in the future.

There are other considerations about Weber's force and gravitational interaction. A

common approach in the literature is to utilise a gravitational force of the Weber type, such as has been investigated by Tisserand [114], Gerber [115], Schrödinger [116] and others. Utilising such a gravitational form of Weber's law, Assis and Wesley [129, 220] have shown that it is also possible to arrive at the origin of inertia in combination with Mach's principle. Their derivations generally follow the form

$$F = -Gm_1m_2\frac{\hat{r}_{12}}{r_{12}^2}\left[1 + \frac{1}{c^2}\left(\vec{v}_{12}\cdot\vec{v}_{12} - \frac{3}{2}(\hat{r}_{12}\cdot\vec{v}_{12})^2 + \vec{r}_{12}\cdot\vec{a}_{12}\right)\right], \quad (2.19)$$

where it is easy to see that the usual charges q_1 and q_2 have been replaced by masses m_1 , m_2 and gravitational constant G . As a consequence of this approach however, Newton's second law, $F = ma$, follows naturally from this formulation, so that the interaction with the distant masses is responsible for the existence of inertia. In essence, Assis calculates the force on a body by investigating its interaction with what is more or less a celestial sphere and the cosmic microwave background, while Wesley uses a gravitational field in his derivations. Additionally, in Assis' model the resulting force contains terms that represent centrifugal and Coriolis forces.

Because there are many possible variations of Weber-type gravitational forces of similar nature, e.g. [114–116, 129, 221], their form has been further generalised by Bunchaft and Carneiro [222] as

$$F = k\frac{\hat{r}_{12}}{r_{12}^2}\left(1 - \mu\dot{r}_{12}^2 + \gamma r_{12}\ddot{r}_{12}\right). \quad (2.20)$$

Here, k is a parameter depending on the nature of the interacting bodies (like charges or masses) and the parameters μ and γ are positive constants of the velocity and acceleration terms usually of the order $1/c^2$. Further aspects of these approaches, with regards to cosmology and conservation of energy, will be discussed in the next section.

In its basic form (2.9) as a microscopic force law, the theory obeys certain general principles of mechanics. Weber's force law intrinsically follows Newton's third law of action and reaction. Any action arising from Weber's force has an opposing force of equal magnitude and inverse sign, making it consistent with linear momentum conservation. It can also be shown that Weber's theory follows energy and angular momentum conservation

[63, 179], and Weber himself only succeeded in 1871 to show that conservation of energy is obeyed.

It is even possible to derive a virial theorem from Weber's force as has been shown by Mendes and Assis [223]. The virial theorem states that the time average of kinetic energy in a system of discrete particles is related to the potential energy of the particles. For Weber's formula this takes the form

$$2\langle T \rangle = -\langle U_w \rangle, \quad (2.21)$$

with the potential energy U_w being Weber's potential (see sec. 3). As a consequence, this offers the possibility for statistical treatments of problems with Weber, such as the formations of galaxies on an astronomical scale or plasma physics, although limitations have been indicated regarding the applicability to cold plasmas [224].

Weber's force has also been used with a modified version of mechanics [225]. The idea is based on the relational nature of Weber's force, making mechanics relational as well. In essence, Newton's mechanical principles are extended with Mach's principle and a Weber-type force for interacting masses is implemented. This has consequences for cosmology, affecting the interpretation of Hubble's law and the cosmological redshift as light interacting on its journey. The cosmic microwave radiation background would then indicate an equilibrium state and the precession of mercury's perihelion is due to the interaction with distant fixed stars. Although the idea is intricate and intriguing, this would of course not be compatible with the standard cosmological interpretation of an expanding universe.

Nonetheless, we have seen in this chapter that Weber has ties to other forces of nature, like nuclear forces and gravity, which also makes it possible to consider consequences for cosmology as an extension. It will be discussed in the following section how certain cosmological aspects emerge from Weber's force.

2.2.3 Cosmology and Breakthrough Physics

From the previous section it was shown that Weber has ties to other forces of nature, like nuclear forces and gravity, and it was suggested that Weber's force has significant

links to cosmological theories and phenomena. Based on the possibility of gravitational modifications to Weber's force, there have been many investigations about planetary motion and in particular the precession of mercury's perihelion [114–116, 226–232]. In addition, some of these also investigate the bending of light in a gravitational field and the two effects are usually explained from GRT. From these investigations it can be seen that Weber generally offers a possible explanation for both observations, but the applicability has been shown to have limits.

The general form of Weber-type forces of the order $1/c^2$ (2.20), is further investigated by Bunchaft and Carneiro [222] with specific attention to energy conservation. The authors of [222] show that such a force is only conservative under a special condition when the parameters μ and γ of (2.20) obey the form $2\mu = \gamma$. They deduce from this analysis that a Weber-type gravitational force cannot predict the correct values for the precession of mercury's perihelion and the gravitational bending of light at the same time under the condition of being conservative. However, more generalised formulations of higher order might still be able to predict both effects whilst remaining conservative, and it is still evident from this that Weber's force offers an alternative approach to phenomena that are usually attributed to GRT.

A somewhat more general discussion about how general relativity and Weber-type theories are related on a fundamental level can be found by Giné [233], although that approach has been challenged [234] in not having a proper Einsteinian approach and thus may well have flaws. A further analysis by Tiandho [235] came to the conclusion that Weber-type gravitational forces are a weak field approximation of GRT and thus a special case, nonetheless, it shows the similarity and connection between the two theories once again.

Recently, Weber-like gravitational interactions in combination with Mach's principle have been investigated with regards to their implications in cosmology [236]. The advantage of such an approach is that inertia arises naturally from the interaction with a celestial sphere and avoids the incompatibility of inertia in GRT with Mach's principle; and additionally maintains the equivalence of gravitational and inertial mass and the

equivalence of kinematic and dynamic rotation rates of the Earth. On the other hand, the resulting universe is non-expanding and the redshift arises from energy loss of light on its journey. Another cosmology model based on Mach's principle has recently been developed and investigated by Das [16], where the universe is governed by Machian Gravity. According to Das it is able to explain rotational curves and mass distribution of galaxies without dark matter or dark energy and when comparing the model to observed cosmological data it fits well with the measurements. Previous to these approaches, the general idea of a Machian cosmology had been suggested in the literature [225, 237–240], where P. and N. Graneau [240] have even found a connection to the expanding universe, but Das seems to be the first to apply the concept to available data of galactic rotation curves.

Beyond the general connection of Weber's theory and GRT, some works have analysed more specific effects arising from gravitational perturbations, for example spacecraft flyby anomalies [221, 241]. These approaches also utilise gravitational formulations of Weber's force, similar to the previously discussed modifications. The first of such gravitationally-influenced effects is called frame dragging, also known as the Lense-Thirring-effect, which has its usual explanation in GRT. This effect adds a precession to a gyroscope or orbiting satellite in the presence of a large rotating mass. It is possible to arrive at a similar effect by utilising Weber's theory [241] for gravitational interactions. The authors of [241] present the formula for the action of a large spinning shell with mass M , radius R and angular velocity $\vec{\Omega}$ on a test body, mass m , at position \vec{r} , velocity \vec{v} and acceleration \vec{a} to be

$$\vec{F} = -\frac{2GmM}{Rc^2} \left[\vec{a} + \vec{\Omega} \times (\vec{\Omega} \times \vec{r}) + 2\vec{v} \times \vec{\Omega} + \vec{r} \times \frac{d\vec{\Omega}}{dt} \right], \quad (2.22)$$

where G and c are the gravitational constant and speed of light, respectively. As can be seen it is similar to the previously presented gravitational-type Weber forces, with terms resulting from the rotation and acceleration, for example the second and third term in square brackets of (2.22) represent centrifugal and Coriolis' force, which appear due to the implementation of Mach's principle. After analysing the problem with the help of

Newton's second law, they arrive at a gravitationally induced azimuthal acceleration that will be experienced by the test body, similar to a frame dragging effect.

The gravitomagnetism arising from this principle has also led Tajmar and Assis to investigate flyby anomalies with a similar implementation of gravity-like Weber forces [221]. They found that flyby anomalies due to Weber-based interactions are several magnitudes smaller than currently measurable. They relate this to data of Rosetta flyby manoeuvres where expected anomalies have not been measured, even though the standard approach would have predicted them. But if the effect is, according to the Weber-interaction, below the threshold of current detectability, this result would not be surprising.

Apart from the general and specific connections to GRT, an interesting possibility seems to exist in Weber's theory that pushes the boundaries of known physics. A situation can be created according to Assis, where the mass of charged particles can be manipulated under the influence of a field-free electrostatic force [63, 242]. If it is indeed possible to change the inertial mass of a charged particle through electrodynamic means, it can possibly be applied to breakthrough propulsion physics technologies, such as the warp drive, anti-gravity or even cold fusion [50–52] which could revolutionise space travel, energy production and transportation in general.

The approach taken by Assis shows the influence of a charged spherical shell on a point charge according to Weber's force, whereby the force on the point charge can be interpreted as an inertial mass change of the particle. Assis considers a hollow spherical shell made of a dielectric with charge Q of radius R , with an angular velocity $\vec{\omega}$. This approach is similar in nature to the gravitational model of gravitomagnetism with Weber for a massive spherical shell producing a frame dragging effect. Here, the charged sphere acts on a point charge q at position \vec{r} , velocity \vec{v} and acceleration \vec{a} . For the point charge inside of the spherical shell, he arrives at the expression

$$\vec{F} = \frac{\mu_0 q Q}{12\pi R} \left[\vec{a} + \vec{\omega} \times (\vec{\omega} \times \vec{r}) + 2\vec{v} \times \vec{\omega} + \vec{r} \times \frac{d\vec{\omega}}{dt} \right], \quad (2.23)$$

which can further be simplified with the restriction $\vec{\omega} = 0$, the sphere being stationary, to:

$$\vec{F} = \frac{\mu_0 q Q}{12\pi R} \vec{a}. \quad (2.24)$$

With the help of Newton's second law this is interpreted by Assis as a change in effective inertial mass of the particle due to the potential on the surrounding shell.

This is an especially interesting prediction of Weber's theory, because in standard theory, the field inside a charged spherical shell is zero and such an effect is not intuitively expected. Assis also estimates an order of magnitude for the effect, which entails a sphere of radius 0.5 m and a potential on the shell of 1.5 MV to double the mass of an electron, which is generally in the realm of the possible to obtain in the laboratory. However, from these values compared with the size and charge of the electron it can be seen that the effect is still considerably small in nature. But as a logical conclusion, in theory a particle can be made to have an effective negative mass through the influence of an electrostatic potential at the cost of sufficient energy expenditure. This behaviour could then be applied to breakthrough propulsion applications with sufficient technological ingenuity and is thus of interest for these applications.

As this is an interesting prediction and experiment to determine boundaries of the validity of Weber's force law, several experimental efforts have tried to investigate this predicted phenomenon, with recent evidence suggesting the non-existence of this effect. Mikhailov had first reported an experiment in 1999 [243] where he claims to have successfully observed the effect in question, with two follow-up experiments in 2001 and 2003 [244, 245], which he reported to be equally successful. However, the attempts of independent researchers to repeat and respectively improve his experiments have not yielded positive results [246–248]. For example, the original experiment by Mikhailov [243] which included a neon glow lamp flashing in a charged spherical shell was repeated and modified by Junginger et al. [246] to utilise optical coupling instead of capacitive coupling. With the application of an optical fibre and a photodiode they found no influence of the electrostatic potential on the flashing frequency, contrary to the expected and reported change of Mikhailov. Additionally, the modifications to the original experiment by Lörincz and Tajmar also showed negative results [247]. They tried various configurations, but also

employed optical coupling to remove any stray effects from circuit coupling and tried different types of enclosures, one of which was a configuration with electrets to avoid the generation of mirror charges and an additional Faraday cage to prevent electric field influence. Up to -15 kV no effect was observed.

Mikhailov's second experiment [244] featured an electron tube that was electrically excited to perform a Barkhausen-Kurz-oscillation. An ammeter was used to measure a current that was supposedly coupled to the generated frequency by an antenna, which showed a change in the oscillation frequency of the electrons dependent on the mass when the potential on the surrounding sphere was applied. According to Mikhailov a general trend of the current was observed that correlated with the potential in the expected way, leading to his conclusion that the effect in question was found. When Weikert and Tajmar repeated this experiment [248], they used a spectrum analyser to observe the received frequency of the antenna and the exciting circuit was placed outside of the shell, so that only the tube itself was enclosed. Even though their test eventually reached a Barkhausen-Kurz-oscillation, the measured frequency did not show a dependence on the applied voltage on the shell in this experiment.

This brief overview shows that all the experiments that Mikhailov [243–245] conducted were claimed to yield positive results, while the replications [246–248] could not validate these outcomes. Since all of the re-evaluated experiments feature a refined methodology and uncover flaws in the settings of Mikhailov, one must conclude that he did not measure the effect in question. An important point is discussed by Lörincz and Tajmar [247] as to what degree a glow discharge is suited to produce and measure a possible mass change of charge carriers, because the discharge is always made up of a neutral plasma and hence probably not suited to show the effect, and Weikert and Tajmar also speculated that the oscillatory motion of electrons in a Barkhausen-Kurz configuration could mask the effect in question [248].

There is new evidence [249] that the sought after mass change effect does not seem to exist. Tajmar and Weikert tested electron beam deflections in a Perrin tube where under a certain magnetic field the beam would be deflected precisely into a Faraday cup

measuring the beam current. The arrangement was located in an aluminium sphere that was charged up to ± 20 kV and they simultaneously observed the current feeding a set of Helmholtz coils generating the magnetic field and the measured beam current of the Faraday cup. By observing the necessary current to keep the beam consistently in the Faraday cup they concluded that the sought after effect can be ruled out by two orders of magnitude. This makes this topic a valid point of criticism against Weber electrodynamics and it will be discussed further in the following section 2.3.

These many investigations of Weber's force in the literature demonstrate the strength of the theory and how it links to many fields across physics, and therefore it is an interesting alternative model to standard electrodynamics. Weber's force law has even been suggested in the literature as a unified theory of nature [216,250], especially as it includes the electromagnetic force, a form of nuclear or strong force, a gravitational-type force and additionally an explanation of the origin of inertia. It can be seen from this that Weber offers an elegant path towards the unification of theories and, to quote O'Rahilly [62, Vol. II, p. 535]: 'If any one man deserves credit for the synthetic idea which unifies the various branches of magnetic and electrical science, that man is Wilhelm Weber.' Weber's theory connecting so many disciplines is of course not an accident, since it is an electromagnetic theory. Field theory and relativity which the standard model of modern physics is based on also show these properties and strive for a unified theory of physics. It is well known that three out of the four forces of nature can be unified in the standard model (magnetic force, strong nuclear force and electroweak force) and attempts are made through quantum gravity to connect the remaining force to those three. So in general, any theory attempting to explain the natural phenomena on a larger scale is likely to show the characteristics of a unified theory. However, Weber's theory, despite the time that has elapsed since its inception, is still very much in an early stage of development and has not been researched to the same degree as conventional models. Nevertheless this should not be taken as discouraging, quite the opposite in fact, it gives motivation for further investigation of Weber's force to explore its capabilities to describe and predict the universe, especially if it has an intrinsic unifying character. Although now that the mostly positive

aspects of Weber's force have been presented, certain limitations of a Weber-type theory need to be examined and aspects of Weber's theory open to criticism confronted.

2.3 Criticism of Weber's Theory

In the previous section some of the positive aspects of Weber's theory have been discussed and how it can be applied in a range of physics sub-disciplines. However, Weber's force was not pursued by mainstream physics as it was superseded by Maxwell's theory of fields and ether, and so it must be questioned just why the theory was largely abandoned in favour of another. Historically there were three main points of criticism leading to the neglect of Weber's theory and a fourth factor of experimental nature. The points of criticism of Weber's force were: i) it is based on the Fechner hypothesis, i.e. currents being comprised of equal amounts of moving positive and negative charges, ii) Helmholtz first criticised Weber's force as violating energy conservation, and iii) then criticised the theory for exhibiting unphysical behaviour in the form of negative mass and infinite acceleration. Finally, what was claimed as decisive evidence in favour of the field model were the successful experiments of Hertz, demonstrating electromagnetic waves and therefore taken as direct proof supporting Maxwell's theory as opposed to Weber's. These historical factors will now be re-investigated to see how they have aged and after that more modern criticisms or limitations of the theory are looked at. Another review of historic criticisms from a philosophical perspective of action-at-a-distance theories in general can be found in [251] with a strong focus on epistemological aspects.

First, the criticism that Weber's force is originally based on Fechner's hypothesis will be considered. In the middle of the 19th century it was assumed that a current in a circuit consisted of equal amounts of positive and negative charge (or electric "fluidae") moving in opposite directions. While it is true that Weber designed his force based on this assumption to derive Ampère's force, he himself moved away from the idea of a double current consisting of moving positive and negative charges towards a simple current where the positive charges remain fixed in the lattice and only the negative charges move in his later works. Despite this change in perspective, he did not alter the formulation of his force

law because it would still remain valid in predicting observable effects. Assis showed [130] that it is possible to derive Ampère's force regardless of the Fechner hypothesis from Weber's force. The only assumptions made are the charge neutrality of current elements and the independence of velocities of positive and negative charge carriers therein. This means that it holds true for moving electrons and stationary lattice charges as well as oppositely moving positive and negative charges as, for example, in plasma states. It was noted in the previous section that the Hall effect can be explained with Weber's theory when the Fechner hypothesis is abandoned. In later chapters Weber's force will be applied only with the assumption of moving electrons and stationary lattice charges and it will be shown how different phenomena can be predicted without the double current requirement.

When discussing this matter it should be mentioned that Clausius was the first to claim in 1877 that Weber's force would lead to unphysical situations when only one kind of charge is moving and the other kind is fixed in a conductor [252]. This criticism seems to have been taken as a critical argument against the theory as reviewed by Woodruff [253] and persisted in the more recent literature when Pearson and Kilambi analysed the similarity with nuclear forces [215]. The argument is that in the situation where Weber's force is not balanced by oppositely moving charge carriers so called electrostatic induction occurs outside of a conductor and this has been considered an exclusion criterion of Weber's theory as an explanation for electrodynamics in [215]. However, it must be said that an early extensive refutation of this argument has been given by Zöllner as early as 1877 [254] in response to Clausius, arguing that these electrostatic effects have been known since 1801 through experiments by Erman [255] and others and Weber's theory is erroneously criticised. Assis and Hernandez [256–258] have given a modern review of electrostatic induction effects in theory and experiment, showing that these effects do indeed exist on different orders of magnitude and that it is too early to dismiss Weber's force law on such a basis. In fact, the existence of such effects could even provide experimental support for Weber's theory. In conclusion it can be said that at present there is no requirement for Fechner's hypothesis in Weber's theory and the criticism is not valid.

Helmholtz originally criticised the theory by saying it did not obey conservation of energy. He considered the potential and kinetic energy, especially with particles in circular motion and came to the conclusion that there are possible situations in Weber's theory where energy can be lost or gained and thus objected to the theory. At the time, Maxwell was familiar with Weber's theory and knew of Helmholtz's argument, supporting the objection stated by him. It was only in 1869 and 1871 that Weber succeeded in showing that energy is conserved in his force law. After this proof Maxwell even acknowledged in his *Treatise* that Weber's theory was mistakenly criticised in that regard [1] and reconsidered it as a possible theory of electrodynamics. Helmholtz erroneously came to the conclusion that energy conservation is violated as he only included the velocities between interacting charges and did not consider the complete form of Weber's force which also depends on the acceleration of charges, leading him to an incomplete deduction [61].

Furthermore, Helmholtz issued a second major criticism of Weber's theory, where he describes a situation that leads a particle to exert behaviour of negative mass and upon movement it could accelerate infinitely in the presence of an external force, such as friction, and an infinite amount of work would be done. He describes a particle inside a charged spherical shell that experiences friction from a fluid and as it is infinitely accelerating, it would continue to heat the fluid due to friction and thus perform an infinite amount of work. An argument ensued between the two parties with Weber trying to defend against the criticism, but Helmholtz again countered his arguments and the criticism prevailed [253] and to this day remains an open question in Weber electrodynamics.

This is indeed a similar situation to the suggested inertial mass change of Assis due to a field-free electrostatic force and the criticism has been further analysed by Assis and Caluzi [259]. They have suggested three possible ways to resolve the problem: 1) If instead of using Weber's force and Newton's mechanics, a modification of mechanics to a relativistic type kinetic energy is assumed, then the particle will not accelerate *ad infinitum*. The modified expression for mechanics has also been obtained by Schrödinger [116] and Wesley [129] by considering Weber-type forces. 2) It is also possible to avoid the problem by a modification of Weber's potential energy, e.g. Phipps [111], which leads

to a force expression where infinite acceleration does not occur. 3) It is still possible that nature behaves this way, it just has not been sufficiently tested.

However, with the new experiment of Tajmar and Weikert [249] it seems very unlikely that nature behaves in a way where this change of mass or energy is involved. Especially when according to Helmholtz an infinite amount of work can be gained if a particle experiencing friction forces from a fluid would continue to increase the fluid's temperature due to the friction. By implication this would violate the first law of thermodynamics and allow for a perpetual motion machine under the condition that the energy can be extracted from the closed system formed by the charged shell, fluid and point charge. It could theoretically still be possible that in order for the effect to manifest, a friction force is needed, as this is what Helmholtz originally considered and was also included in the analysis of Assis and Caluzi [259]. But this seems unlikely as Assis also made the prediction for a mass change without the consideration of friction forces at first [242] and further a situation like this seems very unlikely to manifest in practice. As far as we know, a similar system has never been observed in nature and the described phenomenon seems unlikely to occur naturally. If mankind attempted to create such a situation, it would likely need ingenious engineering to build, assemble and operate such a system in a stable configuration. So even if the rules of physics supposedly allowed for it, the realisation might be impossible for practical reasons.

If one now considers resolutions 1) and 2) suggested by Assis and Caluzi, it can be said for point 1) that the infinite acceleration of a particle can be avoided through the assumption of modified mechanics, but this would change the behaviour mainly for velocities near the speed of light, as pointed out by Weikert and Tajmar [249]. Also in this case Assis and Caluzi still speak of an effective inertial mass influenced by the electrodynamics, so an apparent mass change would still occur in this instance. As for point 2), the modification of Weber's potential energy to Phipp's potential, this can generally present a solution to the problem, however Phipp's potential turns out to have other shortcomings [112]. Nevertheless, there might still be a more fundamental, more general Weber-type potential where the change in mass is avoided and the problem is

resolved, such as suggested by Li [260]. So this criticism is a valid point, however, there might well be other ways not yet known to avoid the problem like a more general potential and here more research is needed. It must also be added to this discussion that due to the self-energy divergence in field theory, the Lorentz-Dirac renormalisation solution also leads to runaway behaviour with infinite self-acceleration of a particle [47]. Albeit a different situation where the particle interacts with its own field, as opposed to Weber's theory where the particle interacts with a field-free charge distribution, this shows that we can find the same unphysical behaviour through infinite acceleration exhibited in the framework of field theory as well. It would seem inadequate to use this singular behaviour as a decisive argument against Weber's theory when field theory is not rid of such a problem itself.

The fourth factor that was historically held against Weber's theory are Hertz's experiments which showed a finite propagation velocity of electromagnetic signals, and were taken as a direct verification of Maxwell's field theory. However, it was seen in the previous sections that Weber's theory has been shown to be consistent with fields and can indeed predict wave equations propagating with the speed of light and related to radiation phenomena when the right physical methods and constraints are applied. So it remains questionable if Hertz's experiments should only be taken as a direct proof of Maxwell's equations. For example, the experiments are also consistent with Ritz's theory, and it would be premature to exclude Weber's theory on that basis.

Also it should be mentioned that Weber believed in a form of ether, i.e. the luminiferous ether, which nowadays has been effectively replaced by the electromagnetic field model. So one could argue that his theory is based on the same ethereal premise as Maxwell's, as he tried to model the interactions of charges within the fluid of ether that was general scientific belief at the time. Although it should be said that Weber's force does not conceptually depend on the ether due to only involving relative velocities. A further discussion of the ether will be found in section 6.2. Furthermore when invoking the principle of Ockham's razor, that is, entities should not be multiplied beyond necessity, it becomes apparent that Weber's theory is considered to be preferable over Maxwell's as it

makes fewer assumptions. Weber being based only on the interaction of charges without invoking the concept of field entities conforms to minimal assumptions as only the charges and their motion is relevant. Also there is an argument in the literature, when discussing contact-action through fields or emitted virtual particles, that entities like the ether or the field which cannot be observed directly should be avoided [261].

At its core this issue relates to a more general criticism of Weber's theory being a direct-action-at-a-distance theory with apparent instantaneous transmission unlike a field theory. The instantaneous nature of force laws like this is usually argued to be a problem since it violates causality and since the propagation of electromagnetic effects are clearly of finite velocity, hence there is an apparent problem with the theory. Take, for example, Newton's gravitational force law: if one body experiences a change in position, body two will immediately feel this change in force, no matter the distance between them. However, there exists a claim in the literature that Newtonian gravity actually propagates at the speed of light [262]. Although the analysis is based on dimensional, empirical and observational arguments, this is a remarkable postulate, and even though Newtonian gravity is formulated mathematically as instantaneous-action-at-a-distance, a finite propagation speed is implicitly contained within the formula, suggesting that the same could be true for other so called "instantaneous" force laws.

So the real question is how propagation velocities behave in Weber's theory or how they can be limited. There are multiple factors to consider here. First, Weber's force itself models a delay in propagation intrinsically with the constant c in the formula, as argued by Brown [103], c should be viewed as a retardation constant at which cause and effect occur. Related to this Sokol'skii and Sadovnikov [232] have studied planetary orbits with a gravitational form of Weber and find that gravitational interaction propagates at the speed of light c in their model. In the previous section 2.2.1 we have seen different considerations showing how Weber is able to predict wave propagation of electromagnetic signals at the speed of light, for example in combination with the principle of retarded time applied by Moon and Spencer, and Wesley who derived wave equations based on this premise. Also Weber and Kohlrausch first obtained experimentally the value of

c with Weber's force and Kirchhoff and Weber both arrived at the telegraph equation for propagation of signals in a circuit independently from each other based on Weber's force. From these considerations, it can be seen that Weber indeed expresses a delay in propagation and a finite propagation velocity despite its action-at-a-distance origin, meaning causality is not violated.

The overall concept of action-at-a-distance theories on a more philosophical basis has been discussed by Pietsch [46]. The discussion is on a more general level about energy conservation, necessity of contact for transmission of energy, locality criteria and metaphysical considerations and does not favour Weber's theory over the Wheeler-Feynman type or other action-at-a-distance theories [123]. First the problem of divergent self energy of a point charge in classic electromagnetism is discussed, with the existing resolutions of renormalisation versus extension approach. It is argued that both solutions come at a cost and that action-at-a-distance can offer an alternative to resolve either problem that arises in one approach or the other. Similarities of pure particle action and pure field theories are explored in the analysis and then continues to point out similarities of action-at-a-distance theories with modern particle-field theories of electrodynamics widely established today. In conclusion direct-action theories remain valid options to consider in physics, as it helps to overcome the arising conceptual issues in the standard approaches. Further discussion of direct-action theories, also more focussed on the quantum version of the Wheeler-Feynman approach with respect to Haag's inconsistency theorem and how direct-action can overcome the mathematical inconsistencies and problems arising from QED and QFT can be found in [77], but are beyond the scope of this work.

From a modern perspective, Weber's force has been critiqued as it does not account for relativistic corrections of deflected electron beams, such as the Kaufmann-Bucherer or Bertozzi experiments [110, 263] in its basic form. Also Weber's force does not impose the same relativistic speed limit of c on a particle [264] as is expected from SRT, and it does not seem to be compatible with SRT and the Lorentz transformation based on these shortcomings. In its standard form Weber is only an approximation in v^2/c^2 for high speed particles compared with relativistic corrections, as shown by [94, 263]. There are,

however, some approaches in the literature to address and solve these inconsistencies of Weber's force. For example, this could suggest that the regular form of Weber's force (2.9) might still be an incomplete theory and only modified forms may be able to overcome this problem. Attempts on limiting the velocity have been made by Montes [113], Wesley [110] and Phipps [111] which manage to include relativistic corrections to varying degrees. Assis [265] investigated Phipp's potential and the inclusion of higher order terms similar to [216,217] in relation to their relativistic compatibility. He finds that this type of Weber theories either holds the speed limit c for an individual charge or their relative speed, but not both at the same time. In general these approaches consider some form of modification of Weber's theory, which might involve other costs as analysed for the gravitational type forces and their energy conservation [222], and even if a suitable modification is discovered, its properties should be studied further on this basis. In a recent study [260], Li utilises an extension of Weber's potential and the additional assumption of modified mechanics and arrives at high velocity particle behaviour that is identical to the predictions made from SRT. This has certain similarities to Wesley's approach [213] of modified mechanics in conjunction with a Weber-type force and could indicate that further research is necessary in relation to the high velocity regime.

Another interesting approach to potentially resolve the problem was suggested by Bush [205]. Bush investigated a direct-action force of the Weber-Ampère type and instead of a variation of mass with velocity assumes a variation of charge with velocity. He deduces from these investigations that the e/m ratio obtained with his approach is consistent with the Kaufmann-Bucherer experiments. Further, with this approach it is the force which tends to zero for a relative velocity between charges close or equal to the speed of light, rather than the mass tending to infinity. The reason why no superluminal particles are observed experimentally is then the lack of force transmission at the speed of light. From these different suggestions to reconcile Weber's force with relativistic corrections it can thus be concluded that the theory has not been fully developed for high speed interactions yet, and more research is needed if Weber can be correctly used in that sense.

Recently, a new study by Kühn found that it is also possible to resolve the problem

with wave equations derived from Weber electrodynamics [181], where the wave solutions are obtained in the reference frame of the receiver. The article first shows how Maxwell's equations lead to Weber's force within the low velocity limit and then further investigates how the wave propagation in the far field can be limited to the velocity of light. Interestingly, the Lorentz transformation is not a necessity in that approach and rather than viewing the propagation velocity as constant w.r.t. the transmitter, it is perceived as constant by the receiver. The physical mechanism responsible for this behaviour is discussed with regard to a newly developed emission theory by Kühn [41] and its implications for electrodynamics and SRT. Concluding from these different approaches, while in its standard form Weber's force seems incompatible with SRT, it can be seen that solutions have been suggested and further research is needed to investigate how Weber's theory and relativistic physics are related.

Other modern criticisms have been issued where Weber's force was shown to lead to unphysical results [224, 266]. In the case of the investigation carried out by Clemente *et al.* Weber's force is applied to cold plasmas and analysed for the resulting propagation of waves in the plasma oscillations. The authors of [224] find that Weber predicts a type of longitudinal wave propagation that is unphysical and contradicts the well established experimental evidence [267] about dispersion relations in cold plasmas. On this basis it is also concluded that only the existence of electromagnetic fields can account for this effect and that Weber's force leads to erroneous results in this case because it strictly follows Newton's third law. This is, of course, an important point of criticism and it shows that Weber's theory has not yet been developed in relation to plasma physics at all. It might be interesting to see if Weber still leads to unphysical results if retarded action is taken into account (as it was discussed in sec. 2.2.1 that Weber is consistent with fields in that case). It might be possible to arrive at the correct result by modification of Weber's equation or potentially Ritz's formula could account for the discrepancy. While this is a shortcoming of Weber's force it would be of interest to further develop a plasma physics approach based on Weber's force and it might not be impossible to resolve the problem on that basis.

An analysis by Sherwin [266] compares the transmission and detection of an idealised radar system between Weber's force and the Liénard-Wiechert force in the standard theory. While the magnitude is found to be the same for both approaches, the angular dependence, direction of signal transmission and propagation delay is different between the two. Sherwin states that the standard results through the Liénard-Wiechert equation is well supported by experiments in radar technology and disagrees with the Weber prediction. On the other hand, the field model result cannot easily account for longitudinal forces, which the Weber force can (for a discussion of longitudinal forces see earlier sec. 2.2.1), and at least the propagation delay can be introduced through a retarded time approach, such as Wesley's [127, 268]. From this, Sherwin concludes that neither theory agrees sufficiently well with observable phenomena yet. This seems to be a peculiar situation and neither theory fully agrees with expectations yet, as it is likely that the inclusion of longitudinal forces in the Liénard-Wiechert model would also change the angular dependence and transmission direction closer towards the Weber force result. Certainly, more research is needed to arrive at an answer to the problem and it would be advantageous to give Weber's theory a further rigorous development for signal transmission and radar applications, also on the basis of the approaches reviewed herein [118, 127, 202, 268].

It has been outlined how Weber's theory offers particular value in explaining phenomena arising in various areas of physics. Most of the original objections to the theory have been answered and the criticisms that remain are not yet completely resolved. Neither the Maxwellian field approach nor Weber's electrodynamics are free of criticism and problems, each theory has its own advantages and disadvantages and unreconciled inconsistencies. In the same way that established theories are continually researched and developed further and eventually amended, the author would like to make the argument that the same is necessary for action-at-a-distance theories, especially considering that there are significant parallels between both theories and many connections have been established between the two. Several authors have presented the view point that direct-action-at-a-distance theories are a valid alternative to be considered in physics and can help overcome problems associated with field theory. None of the theories are perfect, so it is not wise to dismiss

direct-action too early and it should be further developed to inform research and to investigate what explanations it can offer. Another useful approach might be to regard the two theories as complementary, and depending on the application to employ whichever theory is most suitable.

3 Fundamentals of Weber's Theory

In the previous chapter Weber's electrodynamics have been introduced, including a review of different phenomena analysed from a Weber-perspective. In this chapter a mathematical overview is now provided to familiarise the reader with Weber's direct-action approach which will be used for modelling and simulation in later chapters of the thesis.

Weber's force describes the interaction of two point charges and was postulated before the electron was even discovered. Hence, it is originally based on Fechner's hypothesis that a current consists of equal amounts of positive and negative charges moving in opposite directions, which was the conventional wisdom at the time, as scientists imagined so called "electrical fluidae" moving through wires and circuits when subjected to electromotive forces. Fechner's hypothesis has been addressed previously (see sec. 2.3) and it was indicated that Weber's theory can still be used when it is assumed that only electrons are charge carriers in motion responsible for conduction currents in circuits. With this restriction lifted the general workings of Weber's theory can now be explained.

First, let us consider two charged particles, q_1 and q_2 , in a Cartesian coordinate system (x, y, z) , at their respective positions \vec{r}_1 and \vec{r}_2 (see Fig. 3.1). The position of these particles, which are time dependent spatial coordinates, can be expressed by

$$\vec{r}_1 = x_1(t)\hat{x} + y_1(t)\hat{y} + z_1(t)\hat{z}, \quad \vec{r}_2 = x_2(t)\hat{x} + y_2(t)\hat{y} + z_2(t)\hat{z}, \quad (3.1)$$

where the unit vectors are

$$\hat{x} = \begin{pmatrix} 1 \\ 0 \\ 0 \end{pmatrix}, \quad \hat{y} = \begin{pmatrix} 0 \\ 1 \\ 0 \end{pmatrix}, \quad \hat{z} = \begin{pmatrix} 0 \\ 0 \\ 1 \end{pmatrix}. \quad (3.2)$$

Their relative position is the difference between \vec{r}_1 and \vec{r}_2 :

$$\vec{r}_{12} = \vec{r}_1 - \vec{r}_2 \quad (3.3)$$

and a distance r_{12} given by the magnitude of \vec{r}_{12}

$$r_{12} = |\vec{r}_1 - \vec{r}_2| = \sqrt{(x_1(t) - x_2(t))^2 + (y_1(t) - y_2(t))^2 + (z_1(t) - z_2(t))^2}. \quad (3.4)$$

With this the unit vector along \vec{r}_{12} can be defined as

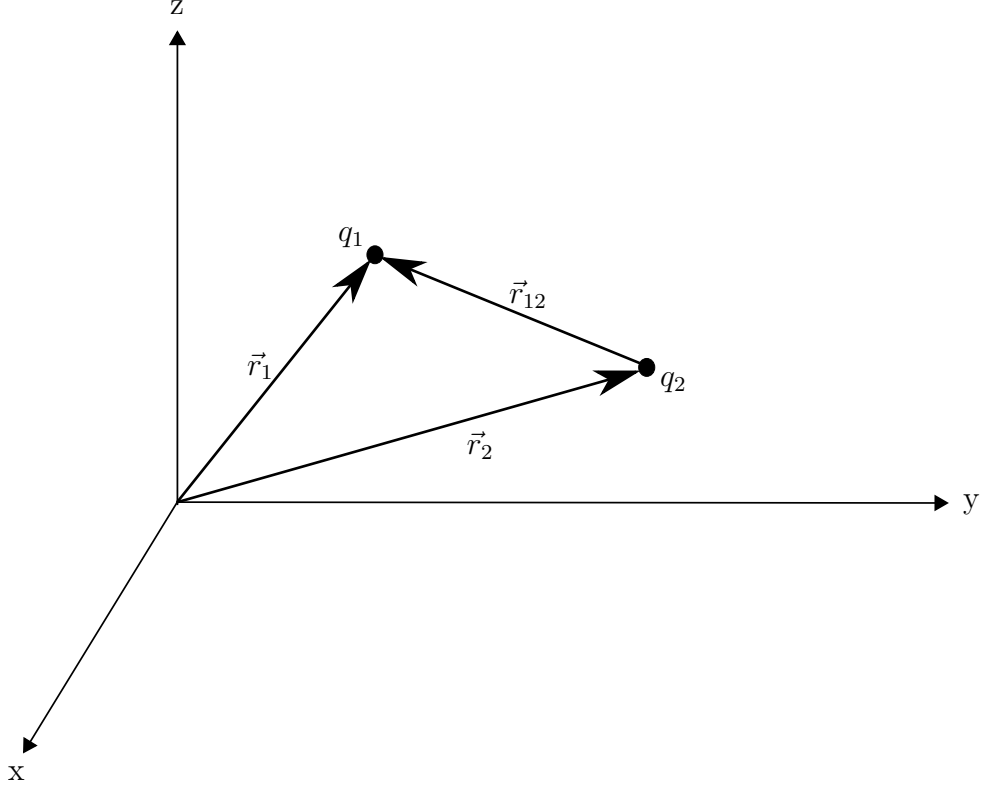


Figure 3.1: Two charged particles q_1 and q_2 in a cartesian coordinate system (x, y, z) at positions \vec{r}_1 and \vec{r}_2 . Their relative position \vec{r}_{12} is a vector pointing from q_2 to q_1 .

$$\hat{r}_{12} = \frac{\vec{r}_{12}}{r_{12}} \quad (3.5)$$

and both \vec{r}_{12} as well as \hat{r}_{12} are pointing from q_2 to q_1 . The relative velocity \vec{v}_{12} and relative acceleration \vec{a}_{12} between the two charges can be calculated as first and second time derivatives of the relative position, (3.6) and (3.7) respectively:

$$\frac{d\vec{r}_{12}}{dt} = \vec{v}_{12}, \quad (3.6)$$

$$\frac{d^2\vec{r}_{12}}{dt^2} = \frac{d\vec{v}_{12}}{dt} = \vec{a}_{12}. \quad (3.7)$$

To arrive at the time derivative \dot{r}_{12} of r_{12} the chain rule is utilised:

$$\begin{aligned}
\dot{r}_{12} &= \frac{dr_{12}}{dt} = \frac{d}{dt} [(x_1(t) - x_2(t))^2 + (y_1(t) - y_2(t))^2 + (z_1(t) - z_2(t))^2]^{\frac{1}{2}} \\
&= [2x_1(t)\dot{x}_1 - 2(\dot{x}_1x_2(t) + \dot{x}_2x_1(t)) + 2x_2(t)\dot{x}_2 + 2y_1(t)\dot{y}_1 - 2(\dot{y}_1y_2(t) + \dot{y}_2y_1(t)) + 2y_2(t)\dot{y}_2 \\
&\quad + 2z_1(t)\dot{z}_1 - 2(\dot{z}_1z_2(t) + \dot{z}_2z_1(t)) + 2z_2(t)\dot{z}_2] \\
&\quad \cdot \frac{1}{2\sqrt{(x_1(t) - x_2(t))^2 + (y_1(t) - y_2(t))^2 + (z_1(t) - z_2(t))^2}} \\
&= \hat{r}_{12} \cdot \vec{v}_{12}.
\end{aligned} \tag{3.8}$$

By analogy, the same procedure can be applied to arrive at the second time derivative, or the quotient and product rule along with the substitutions $u = \vec{r}_{12}$, $v = \vec{v}_{12}$, $w = r_{12}$ can be used:

$$\left(\frac{u \cdot v}{w} \right)' = \frac{(u'v + v'u)w - w'uv}{w^2}, \tag{3.9}$$

$$\ddot{r}_{12} = \frac{d^2 r_{12}}{dt^2} = \frac{d\dot{r}_{12}}{dt} = \frac{[\vec{v}_{12} \cdot \vec{v}_{12} - (\hat{r}_{12} \cdot \vec{v}_{12})^2 + \vec{r}_{12} \cdot \vec{a}_{12}]}{r_{12}}. \tag{3.10}$$

With the help of these definitions, Weber's potential between the charges in question can now be examined, which will eventually lead to Weber's force. It was two years after Weber introduced his force law that he succeeded in showing that it could be derived from a potential, and this takes the form:

$$U = \frac{q_1 q_2}{4\pi\epsilon_0} \frac{1}{r_{12}} \left(1 - \frac{\dot{r}_{12}^2}{2c^2} \right). \tag{3.11}$$

To arrive at the force, the principle of virtual work is invoked which states

$$\begin{aligned}
\vec{F}_{21} &= -\hat{r}_{12} \frac{dU}{dr_{12}} \\
\text{or} \quad \vec{v}_{12} \cdot \vec{F}_{21} &= -\frac{dU}{dt}.
\end{aligned} \tag{3.12}$$

Now applying (3.12) to (3.11) gives Weber's force law in the following way:

$$\begin{aligned}
\vec{F}_{21} &= -\hat{r}_{12} \frac{dU}{dr_{12}} \\
&= \frac{q_1 q_2}{4\pi\epsilon_0} \frac{\hat{r}_{12}}{r_{12}^2} \left(1 - \frac{\dot{r}_{12}^2}{2c^2} + \frac{2r_{12}\ddot{r}_{12}}{2c^2} \right) \\
&= \frac{q_1 q_2}{4\pi\epsilon_0} \frac{\hat{r}_{12}}{r_{12}^2} \left(1 - \frac{\dot{r}_{12}^2}{2c^2} + \frac{r_{12}\ddot{r}_{12}}{c^2} \right) \\
&= \frac{q_1 q_2}{4\pi\epsilon_0} \frac{\hat{r}_{12}}{r_{12}^2} \left[1 + \frac{1}{c^2} \left(\vec{v}_{12} \cdot \vec{v}_{12} - \frac{3}{2}(\hat{r}_{12} \cdot \vec{v}_{12})^2 + \vec{r}_{12} \cdot \vec{a}_{12} \right) \right],
\end{aligned} \tag{3.13}$$

where again the chain rule is necessary to derive the expression $\frac{d\dot{r}^2}{dr}$ correctly,

$$\frac{d\dot{r}^2}{dr} = \frac{d(\dot{r}(t))^2}{dt} \frac{dt}{dr} = 2\dot{r} \frac{d\dot{r}}{dt} \frac{dt}{dr} = 2\ddot{r}. \tag{3.14}$$

It can be seen in (3.13) that the familiar form of Weber's force (2.9) from section 2.1.2.1 is contained within, repeated here for convenience.

$$\vec{F}_{21} = \frac{q_1 q_2}{4\pi\epsilon_0} \frac{\hat{r}_{12}}{r_{12}^2} \left(1 - \frac{\dot{r}_{12}^2}{2c^2} + \frac{r_{12}\ddot{r}_{12}}{c^2} \right). \tag{2.9 revisited}$$

In later chapters, the form of Eq. (3.15) will often be utilised and applied to specifically investigate the interaction between charge carriers for a given experiment or apparatus.

$$\vec{F}_{21} = \frac{q_1 q_2}{4\pi\epsilon_0} \frac{\vec{r}_{12}}{r_{12}^3} \left(1 - \frac{3}{2c^2} \left[\frac{\vec{r}_{12} \cdot \vec{v}_{12}}{r_{12}} \right]^2 + \frac{1}{c^2} (\vec{v}_{12} \cdot \vec{v}_{12} + \vec{r}_{12} \cdot \vec{a}_{12}) \right). \tag{3.15}$$

It can be seen from these derivations that the force depends on the relative position, velocity and acceleration of the particles involved. The force is along the line joining them and follows Newton's third law in the strong form, that is every action has an equal and opposite reaction. Furthermore, conservation of energy as well as conservation of linear and angular momentum are followed by this law. Additionally the principle of superposition applies to this force law, similar to the superposition principle with electric and magnetic fields of Maxwellian field theory.

Other formulations of Weber's force formula exist in the literature, as in the previous section 2.2.1 it has been shown that Weber can be formulated to incorporate electromagnetic fields [63, 127, 178, 179, 269] and especially in [179] the field-based Weber force is formulated with focus on the relation between source and test charges and how they

define current elements and densities. Further, Hamiltonian and Lagrangian formulations of the force law have been obtained [63, 270] and expressions like this have occasionally been used in the literature [211, 212, 232].

4 Weber Applied to Electron Beam Deflection

In this chapter we will apply Weber electrodynamics specifically to electron beams and investigate their behaviour when travelling in the presence of electric and magnetic fields produced by electromagnets, such as coils, solenoids or toroids. In general, charged particle dynamics or charged particle optics considers the deflection of charged particles (like electrons, protons or ions) in electromagnetic fields. Understanding the interaction between particles and electromagnetic fields or forces is of great importance in physical sciences, engineering and life sciences, and has led to a wide range of applied technologies, such as particle accelerators [271–274], decelerators (e.g., storage rings) [275, 276], electron microscopes [277, 278], electronics [279], nuclear fusion reactors [280, 281] and magnetrons [282, 283], through to medical diagnostics (e.g., radiation therapy) [284, 285], mass spectrometry [286] and electron beam welding [287, 288], amongst many others.

For design purposes it is advantageous to predict the trajectories of particle beams with the help of simulation as it is costly and time consuming to test experimentally the influence of disturbing effects on different designs. Perturbations commonly arise from space charge effects and fringe fields, especially in low energy beams within the low velocity limit, where they can lead to sudden shifts in position, tune and chromaticity shifts [289] which are undesired effects introducing beam instabilities. It is thus of interest for cost-effectiveness and securing functionality to obtain accurate simulations before constructing apparatus to manipulate charged species.

The influence of electromagnetic fields is often solved with the help of numerical methods, such as finite element (FE) [290], finite difference (FD) [291] or boundary element (BE) methods [292]. These methods have proved very successful in the past and each have benefits and drawbacks, broadly relating to accuracy, resolution, computational time and memory requirements [293]. As they are all solving the field equations based on Maxwell-Lorentz, this chapter is motivated to test the fidelity of a Weber force approach to the deflection of electron beams.

Therefore, the influence of coils, solenoids and toroids on an electron beam will be investigated in this chapter. These are long established and fundamental charge optical

elements used to control and manipulate charged species, e.g. through focussing and beam guiding. Especially solenoids are commonly employed for controlled magnetic field generation but they can subject charged particles to non-linear effects in the vicinity of the ends (i.e. the fringe field region) which can impact the trajectory significantly and are difficult to accurately predict [294–297]. To this end, different models will be derived to predict the motion of the beam, both with Weber’s force and with standard field theory. Not only are the predictions compared to each other, but further experiments are carried out to evaluate the performance of the models against observed electron deflection data.

4.1 Deflection Perpendicular to Solenoid Axis

The first line of investigation focuses on the generation of a magnetic field with solenoids to deflect an electron beam travelling past the electromagnet, where the beam is perpendicular to the axis of the solenoid. The deflection of the beam will be modelled with the help of Weber’s force and with conventional field models in order to compare both approaches. Furthermore, an experiment with a Cathode-Ray-Tube (CRT) is conducted to evaluate the validity and accuracy of the predictions.

A previous investigation by Smith et al. [175], utilising a similar setup, has reported minor discrepancies between a Weber and a field based approach. Hence it seems worthy to re-investigate the approach and obtain more experimental data to compare predictions with and advance the Weber-based modelling in this area, so that full three dimensional models can be used (as opposed to a reduced order model as used by Smith *et al.*). In the current context with the relatively slow electron speeds achieved in the CRT, the modelling could be especially relevant for low energy decelerators. It is a further incentive to test the increasingly fringing regions of the field as these are known to cause disturbances in the beam and its trajectory, and to check the fidelity of the modelling. The author has previously published insights from the research in this section [176], however this chapter can be considered more refined and provides additional insight to the initial publication.

4.1.1 Mathematical Modelling

To predict the deflections of an electron beam caused by the magnetic field generated with the solenoid, where the beam can pass any field region, three different models are used. These are: i) Weber-model, where a direct force between the charges in the solenoid and the electron beam is calculated. ii) Field-based model, where Maxwellian electrodynamics are employed to calculate the magnetic field \vec{B} with which the charges in the beam interact. iii) The software package Charged Particle Optics (CPO) [292] where the Boundary-Element-Method (BEM) is used with field-theory to numerically calculate the field and beam deflections. In the following subsections these approaches will be described in detail.

4.1.1.1 Weber Model In the work of Smith *et al.* [175] a Weber-based approach has been developed where electrons are deflected across a single current loop as a two dimensional (2D) model and later a summation performed to account for an elongated solenoid consisting of multiple loops, where the beam was also limited to only pass the solenoid across its centre. In order to properly apply Weber's force to the fringing field region, the simplified two dimensional (2D) model has been refined significantly in [176], expanding it to three dimensions (3D) to apply any arbitrary solenoid geometry and allow for different initial positions of the beam. However, in order to transition to a 3D model, it is still useful to assume a single current loop in a 2D plane as a first simplified step. As shown in Fig. 4.1a, with a current loop in the xy-plane an electron beam traverses across the loop in positive x-direction at a fixed height h with velocity \vec{v}_1 , giving it position \vec{r}_1 .

A current I passes through the coil in positive mathematical sense, with velocity \vec{v}_2 at radius R so that it has position \vec{r}_2 and can be represented by a current element, $I d\theta$. Here, θ is the polar coordinate as shown in Fig. 4.1a and $d\theta$ the associated differential. In this definition we follow the physical direction of current flow, the physical motion of electrons in the current element is regarded as the direction of the current, opposite to the conventional flow of current which is often considered in engineering. When a real solenoid geometry is considered, the model can be expanded to 3D space. The solenoid axis elongates from $-\frac{l}{2}$ to $\frac{l}{2}$ and the coordinate system is centred in the solenoid

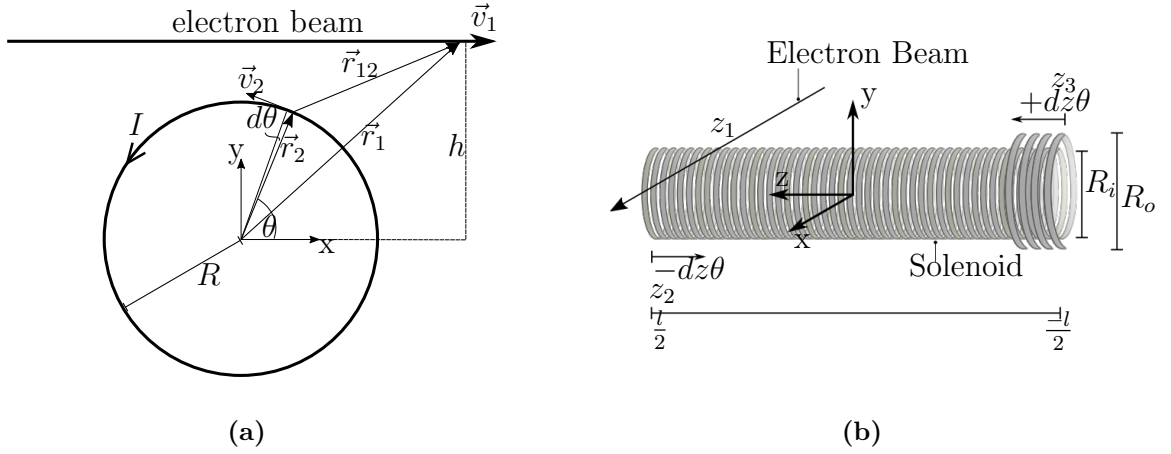


Figure 4.1: Geometry and system of coordinates to model the electron beam and solenoid: a) Simplified 2D geometry for a single current carrying loop and an electron beam travelling parallel to the x -axis; b) Expanded 3D geometry with the coordinate origin at the centre of the double wound solenoid with the beam at a position, z_1 , travelling parallel to the x -axis.

as depicted in Fig. 4.1b. The solenoids used in practice for the experiments in the next section are all double wound, where the wire is wound once down the length of the solenoid and then returns on top of the first layer, retaining the same handedness of helicity. Each layer has a number of windings N per layer, where in this case both layers have the same number of windings. This means that the current will travel from one end of the solenoid through one layer and then back the opposite way through the other layer, as indicated in Fig. 4.1b. The inner layer has a coil radius R_i and the outer layer radius R_o , with corresponding forces, due to the current, F_i and F_o , respectively. For a densely wound solenoid we can further approximate $R_i \approx R_o$ to simplify the calculations, and assume the electron-current is fed to the solenoid at $z_2 = \frac{l}{2}$ into the inner layer of windings, travelling towards $z_3 = -\frac{l}{2}$ and returning through the outer layer towards z_2 .

The path the current travels can be modelled two-fold. Option one is helical motion, where the current follows the pitch of the windings, progressively moving along the z -axis while exercising circular motion. Option two is a summation model, where the individual windings are assumed as single current loops, each at a fixed position, and the sum of the force is found by superimposing the total number of individual loops. A brief mathematical overview about circular and helical motion can be found in appendix A. In the helical model the current travels along the axis depending on the pitch with an

infinitesimal element $dz \cdot \theta$, either in a positive or negative sense according to the layer it is fed to or returning from, as indicated in Fig. 4.1b. Due to this motion a given current element has a velocity component in z-direction as $\frac{v_2}{R}dz$, where now its relational position, \vec{r}_{12} , and velocity, \vec{v}_{12} , for inner and outer layers respectively, are defined as:

$$\vec{r}_1 = \begin{pmatrix} x_1 \\ h \\ z_1 \end{pmatrix}, \quad \vec{r}_{2i} = \begin{pmatrix} R \cos(\theta) \\ R \sin(\theta) \\ z_2 - dz\theta \end{pmatrix}, \quad \vec{r}_{2o} = \begin{pmatrix} R \cos(\theta) \\ R \sin(\theta) \\ z_3 + dz\theta \end{pmatrix}, \quad (4.1)$$

$$\vec{r}_{12i} = \begin{pmatrix} x_1 - R \cos(\theta) \\ h - R \sin(\theta) \\ z_1 - z_2 + dz\theta \end{pmatrix}, \quad \vec{r}_{12o} = \begin{pmatrix} x_1 - R \cos(\theta) \\ h - R \sin(\theta) \\ z_1 - z_3 - dz\theta \end{pmatrix}, \quad (4.2)$$

$$r_{12i} = \sqrt{(x_1 - R \cos(\theta))^2 + (h - R \sin(\theta))^2 + (z_1 - z_2 + dz\theta)^2}, \quad (4.3)$$

$$r_{12o} = \sqrt{(x_1 - R \cos(\theta))^2 + (h - R \sin(\theta))^2 + (z_1 - z_3 - dz\theta)^2}, \quad (4.4)$$

$$\vec{v}_1 = \begin{pmatrix} v_1 \\ 0 \\ 0 \end{pmatrix}, \quad \vec{v}_{2i} = \begin{pmatrix} -v_2 \sin(\theta) \\ v_2 \cos(\theta) \\ -\frac{v_2}{R}dz \end{pmatrix}, \quad \vec{v}_{2o} = \begin{pmatrix} -v_2 \sin(\theta) \\ v_2 \cos(\theta) \\ \frac{v_2}{R}dz \end{pmatrix}, \quad \vec{v}_{12i,o} = \begin{pmatrix} v_1 + v_2 \sin(\theta) \\ -v_2 \cos(\theta) \\ \pm \frac{v_2}{R}dz \end{pmatrix}. \quad (4.5)$$

Acceleration terms in this scenario are negligibly small, since the current elements move with a constant velocity, and even if the centripetal acceleration due to circular motion, respectively helical motion, was considered in the calculations, they would be several magnitudes smaller than the current velocity, $v_2 \gg a_2 R$ and would not have any influence on the result. The electron beam is moving at constant speed after passing the final anode of the electron gun and continues to travel undisturbed and is not subject to further acceleration.

To calculate the resulting Weber force between beam and solenoid we must now consider the interaction of all the charges involved and perform a superposition of the individual forces in between the charges. Specifically, there will be a force \vec{F}_{2-1-} between the electrons of the beam and the electrons in the current element and also a force \vec{F}_{2+1-} between beam electrons and the static metallic lattice charges of the solenoid. With the additional assumptions $q_{1-} = -q_{1+}$ and $q_{2-} = -q_{2+}$, as well as $v_1 \gg v_2$, we arrive at a force $\vec{F}_{i_{helix}}$ for the inner windings and $\vec{F}_{o_{helix}}$ for the outer windings of the solenoid with the helical motion model:

$$\begin{aligned}
\vec{F}_{helix} &= \vec{F}_{i2-1-} + \vec{F}_{i2+1-} \\
&= \frac{q_1+q_2}{4\pi\epsilon_0} \frac{v_1 v_2}{c^2} \frac{\vec{r}_{12i}}{r_{12i}^3} \left\{ 2 \sin \theta - 3 \sin \theta \frac{(x - R \cos \theta)^2}{r_{12i}^2} \right. \\
&\quad \left. + 3 \cos \theta \frac{(x - R \cos \theta)(h - R \sin \theta)}{r_{12i}^2} \right. \\
&\quad \left. - 3 \frac{dz}{R} \frac{(x - R \cos \theta)(z_1 - z_2 + dz\theta)}{r_{12i}^2} \right\}, \tag{4.6}
\end{aligned}$$

$$\begin{aligned}
\vec{F}_{ohelix} &= \vec{F}_{o2-1-} + \vec{F}_{o2+1-} \\
&= \frac{q_1+q_2}{4\pi\epsilon_0} \frac{v_1 v_2}{c^2} \frac{\vec{r}_{12o}}{r_{12o}^3} \left\{ 2 \sin \theta - 3 \sin \theta \frac{(x - R \cos \theta)^2}{r_{12o}^2} \right. \\
&\quad \left. + 3 \cos \theta \frac{(x - R \cos \theta)(h - R \sin \theta)}{r_{12o}^2} \right. \\
&\quad \left. + 3 \frac{dz}{R} \frac{(x - R \cos \theta)(z_1 - z_3 - dz\theta)}{r_{12o}^2} \right\}. \tag{4.7}
\end{aligned}$$

Similarly, for the summation model, an inner and outer force can be determined. But now the motion of the current in z-direction is omitted, so that only the circular motion remains:

$$\vec{v}_{2i} = \vec{v}_{2o} = \begin{pmatrix} -v_2 \sin(\theta) \\ v_2 \cos(\theta) \\ 0 \end{pmatrix}. \tag{4.8}$$

Instead of the axial velocity component, each single loop is now assumed to be positioned at one distinct point on the solenoid axis $p \cdot (n - 1)$. With the total number of turns N in one layer, the integer index $n = 1 \dots N$ moves each following loop by the amount p , which is the pitch of the coil. The inner and outer winding forces are then found to be:

$$\begin{aligned}
\vec{F}_{isummation} &= \vec{F}_{i2-1-} + \vec{F}_{i2+1-} \\
&= \frac{q_1+q_2}{4\pi\epsilon_0} \frac{v_1 v_2}{c^2} \frac{\vec{r}_{12i}}{r_{12i}^3} \left\{ 2 \sin \theta - 3 \sin \theta \frac{(x - R \cos \theta)^2}{r_{12i}^2} \right. \\
&\quad \left. + 3 \cos \theta \frac{(x - R \cos \theta)(h - R \sin \theta)}{r_{12i}^2} \right\}, \tag{4.9}
\end{aligned}$$

$$\begin{aligned}
\vec{F}_{o_{summation}} &= \vec{F}_{o_{2-1-}} + \vec{F}_{o_{2+1-}} \\
&= \frac{q_1+q_2}{4\pi\epsilon_0} \frac{v_1 v_2}{c^2} \frac{\vec{r}_{12o}}{r_{12o}^3} \left\{ 2 \sin \theta - 3 \sin \theta \frac{(x - R \cos \theta)^2}{r_{12o}^2} \right. \\
&\quad \left. + 3 \cos \theta \frac{(x - R \cos \theta)(h - R \sin \theta)}{r_{12o}^2} \right\}.
\end{aligned} \tag{4.10}$$

In order to transition from the discrete current sources $q_{1,2}$ to linear current elements, the following assumption is considered: while a continuous current is flowing through the solenoid, each current element (consisting of a moving electron and a stationary lattice charge) is immediately replaced with the next. This holds a linear charge density λ and the transformation $qv \rightarrow \lambda v d\vec{l} \rightarrow IR d\theta$ can be applied to replace $q_2 v_2$. When this is integrated over the entire solenoid the total force exerted on the beam can be evaluated, yielding the forces

$$\begin{aligned}
\vec{F}_{W_{helix}} &= \frac{q_1+v_1 I}{4\pi\epsilon_0 c^2} \int_0^{N \cdot 2\pi} \left\{ \frac{\vec{r}_{12i}}{r_{12i}^3} \left[2 \sin \theta - 3 \sin \theta \frac{(x - R \cos \theta)^2}{r_{12i}^2} + 3 \cos \theta \frac{(x - R \cos \theta)(h - R \sin \theta)}{r_{12i}^2} \right. \right. \\
&\quad \left. \left. - 3 \frac{dz}{R} \frac{(x - R \cos \theta)(z_1 - z_2 + dz\theta)}{r_{12i}^2} \right] + \frac{\vec{r}_{12o}}{r_{12o}^3} \left[2 \sin \theta - 3 \sin \theta \frac{(x - R \cos \theta)^2}{r_{12o}^2} \right. \right. \\
&\quad \left. \left. + 3 \cos \theta \frac{(x - R \cos \theta)(h - R \sin \theta)}{r_{12o}^2} + 3 \frac{dz}{R} \frac{(x - R \cos \theta)(z_1 - z_3 - dz\theta)}{r_{12o}^2} \right] \right\} R d\theta,
\end{aligned} \tag{4.11}$$

$$\begin{aligned}
\vec{F}_{W_{sum}} &= \frac{q_1+v_1 I}{4\pi\epsilon_0 c^2} \sum_{n=1}^N \int_0^{2\pi} \left\{ \frac{\vec{r}_{12i}}{r_{12i}^3} \left[2 \sin \theta - 3 \sin \theta \frac{(x - R \cos \theta)^2}{r_{12i}^2} + 3 \cos \theta \frac{(x - R \cos \theta)(h - R \sin \theta)}{r_{12i}^2} \right] \right. \\
&\quad \left. + \frac{\vec{r}_{12o}}{r_{12o}^3} \left[2 \sin \theta - 3 \sin \theta \frac{(x - R \cos \theta)^2}{r_{12o}^2} + 3 \cos \theta \frac{(x - R \cos \theta)(h - R \sin \theta)}{r_{12o}^2} \right] \right\} R d\theta.
\end{aligned} \tag{4.12}$$

As both forces are vector quantities with components in x-, y- and z-direction it is apparent that three kinds of forces will act on the beam: a longitudinal force, a vertically transversal force and a horizontally transversal force. This means the beam will be deflected “vertically” due to a transverse force acting in y-direction and deflected “horizontally” due to a transverse force acting in z-direction. These two deflections are calculated with help of the impulse a force exerts on the beam with time t , which is the duration the beam takes to travel from the anode to a fluorescent screen (that is excited upon electron

collision) on which the deflection is recorded. Generally, the impulse can be expressed as:

$$\vec{\mathcal{J}} = \int_0^t \vec{F}_W dt. \quad (4.13)$$

Due to the vertical and horizontal forces, there will be an accompanying change of vertical and horizontal momentum, which is equal to the vertical and horizontal impulse

$$\mathcal{J}_v = m_e v_v, \quad \mathcal{J}_h = m_e v_h, \quad (4.14)$$

where m_e is the electron mass and v_h , v_v are the horizontal and vertical velocities gained from the deflection force. With this, the total deflections in y- and z-direction can be calculated as,

$$y_d = \frac{1}{2} a_v t^2 = \frac{1}{2} v_v t = \frac{1}{2} \frac{\mathcal{J}_v}{m_e} t, \quad z_d = \frac{1}{2} a_h t^2 = \frac{1}{2} v_h t = \frac{1}{2} \frac{\mathcal{J}_h}{m_e} t. \quad (4.15)$$

These deflections can be accurately predicted with the help of numerical integration in *MATLAB* (MathWorks, MA, USA). The beam trajectory is simulated as a straight path across the solenoid at constant electron speed v_e with a step size of 0.1 mm that is translated to a step in the time domain by dividing by the velocity the electrons travel with. The force is then integrated with the trapezium rule twice, first for the angle θ with a step size of 0.5° and then for the time taken to travel from cathode to detector screen. The resulting impulse from the force is then used in eq. (4.15) to obtain the deflections, an example code can be found in appendix C. For both helical and summation approach the simulations show the same force for a respective deflection in y- or z-direction, which is expected, as both models should give the same result. For the longitudinal force acting along the propagation direction of the beam a zero value is found, which agrees with the Lorentz force vector. From the vector cross product $\vec{v} \times \vec{B}$ in the Lorentz force (2.7) we only expect transversal beam deflections to occur, which will become clear in the next section where the field-based model is discussed. With the Weber model here it can be deduced that the rotational direction of the current affects the direction the beam is deflected in, which is similar to the magnetic field direction that determines the deflection direction in the standard model. For mathematically positive rotating electrons we find a deflection in positive y-direction and negative z-direction and the opposite, negative

y-direction and positive z-direction for negative rotation. This is consistent for the expected vertical deflection direction from the right-hand-rule, respectively left-hand-rule in the standard field based approach, which will be examined next.

4.1.1.2 Field Model To calculate the deflections of the beam due to the magnetic field, one needs to obtain the Lorentz force (2.7) acting on the beam electrons due to the magnetic field \vec{B} generated by the solenoid. To calculate the magnetic field itself, a useful tool in the form of a *MATLAB* code by D. Cébron is utilised [298]. This code incorporates the work of Derby and Olbert [299] and Callaghan and Maslen [300] who derived the magnetic field expressions inside and outside of any finite solenoid with help of the Biot-Savart law (2.5).

This field model has been the foundation for further work on finite solenoids that has been further investigated and applied to solenoids with a permeable core [301], internal magnetic fields of off-axis solenoids [302], parallel finite solenoids [303] and axis alignment measurements of solenoids [304–306]. In their model [299], Derby and Olbert obtained formulations for the radial component B_ρ as well as the axial component B_z , where the residual field $B_{res} = \mu_0 n_{unit} I$ is extracted as a factor. (Here, n_{unit} is the number of turns per unit length, giving B_{res} as the idealised uniform field inside a long solenoid.) This expression is modified for radial and axial components through complete elliptic integrals depending on the geometry of the solenoid, and solving these gives numerical values for the field for any given position around the solenoid. They are calculated as follows:

$$B_\rho = \frac{B_{res}}{\pi} \sqrt{\frac{R}{\rho}} \left[\frac{\omega_\pm^2 - 2}{2\omega_\pm} \mathcal{K}(\omega_\pm) + \frac{\mathcal{E}(\omega_\pm)}{\omega_\pm} \right]_{-}^{+}, \quad (4.16)$$

where \mathcal{K} and \mathcal{E} are the complete elliptic integrals of the first and second kind and

$$\omega_\pm = \sqrt{\frac{4R\rho}{(R+\rho)^2 + \xi_\pm^2}}, \quad (4.17)$$

with $\xi_\pm = z \pm L/2$. Then the following definitions are made for the axial magnetic field,

$$\gamma = (R - \rho)/(R + \rho), \quad (4.18)$$

$$\zeta_{\pm} = \sqrt{\frac{(R - \rho)^2 + \xi_{\pm}^2}{(R + \rho)^2 + \xi_{\pm}^2}}, \quad (4.19)$$

$$\chi_{\pm} = \frac{\xi_{\pm}}{\sqrt{(R + \rho)^2 + \xi_{\pm}^2}}. \quad (4.20)$$

The axial field is then for $\zeta_+ < 1$

$$B_z = \frac{B_r}{\pi} \frac{R}{R + \rho} \frac{1}{\gamma + 1} \left[\chi_{\pm} \left(\mathcal{K} \left(\sqrt{1 - \zeta_{\pm}^2} \right) + \gamma \Pi \left(1 - \gamma, \sqrt{1 - \zeta_{\pm}^2} \right) \right) \right]_{-}^{+} \quad (4.21)$$

and for $\zeta_{\pm} \geq 1$

$$B_z = \frac{B_r}{\pi} \frac{R}{R + \rho} \frac{1}{\gamma(\gamma + 1)} \left[\frac{\chi_{\pm}}{\zeta_{\pm}} \left(\gamma \mathcal{K} \left(\sqrt{1 - \frac{1}{\zeta_{\pm}^2}} \right) + \Pi \left(1 - \frac{1}{\gamma^2}, \sqrt{1 - \frac{1}{\zeta_{\pm}^2}} \right) \right) \right]_{-}^{+}, \quad (4.22)$$

with Π being the complete elliptic integral of the third kind and ρ the radial coordinate. The total magnetic field at any point can be expressed as $B = \sqrt{B_{\rho}^2 + B_z^2}$ and is shown in Fig. 4.2, simulated with the same accuracy as in the previous section. The white lines in the Figure are situated at $\rho = \pm R$ and their value is undefined. This is due to the definition of γ (4.18), which will inevitably lead to a division by zero problem and the algorithm did not converge in this case.

Previously in [176], these field values were used to obtain the Lorentz force and then the deflection was calculated by considering the Larmor radius. This approach has been refined based on an impulse calculation considering the entire path of the beam, similar to the Weber model in the previous subsection. In order to exemplify the difference, the method of calculation in [176] is repeated and then elaborated with the improved calculations.

To find the Larmor radius it is considered that the electric field \vec{E} of a solenoid is negligibly small, so that the Lorentz force reduces to

$$\vec{F}_L = q(\vec{v}_1 \times \vec{B}), \quad (4.23)$$

giving the deflecting force on the electrons. Next, in order to obtain the y- and z-deflections resulting from the Larmor radius due to this Lorentz force, the Larmor radius

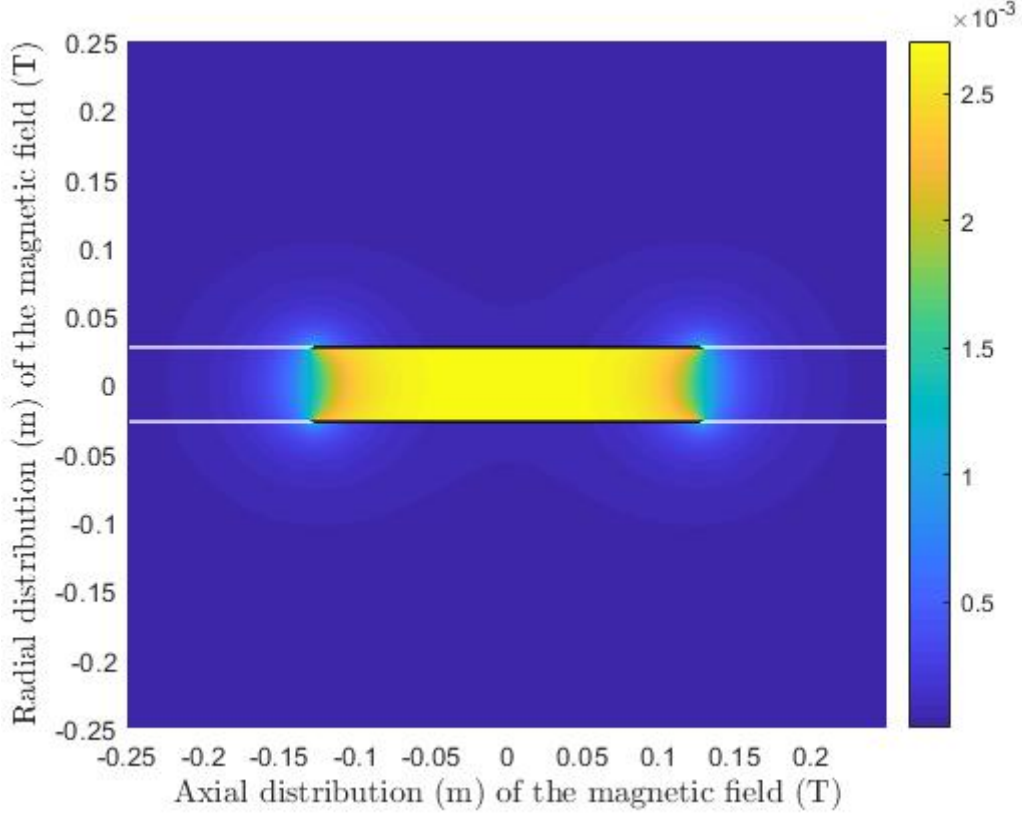


Figure 4.2: Field of solenoid S2 generated with the field calculations from [298]. The field strength (T) is shown around the solenoid, except for the white lines at the radial position $\rho = R$, as the algorithm did not converge at these points. N.B., Solenoid S2 is defined in Table 4.1 (sec. 4.1.2).

itself has to be considered to originate from a certain point around the solenoid from where the beam is forced onto its circular path by the Lorentz force. To this end the point $(0, -h, z_1)$ is chosen, as the beam passes below the solenoid at $-h$ and the field is transformed from cylindrical to Cartesian coordinates at that point. As this point corresponds with an angle of $\theta = \frac{3}{2}\pi$ the Cartesian expression for the field is found as:

$$\vec{B} = \begin{pmatrix} 0 \\ -B_\rho \\ B_z \end{pmatrix}. \quad (4.24)$$

This approach gives the field values only at the point of evaluation $(0, -h, z_1)$, which can then be used to obtain the Larmor radius according to the formula

$$r_L = \frac{m_e v_e^2}{F_L}, \quad (4.25)$$

with which deflections can be calculated as

$$y_{dL} = r_L \pm \sqrt{r_L^2 - d^2}, \quad (4.26)$$

where d is the distance from the centre of the solenoid to the fluorescent screen. As a means of double checking the Larmor radius based deflection results, an impulse approach was used in [176] as well to calculate the deflections with the field values, but only over the distance d . Over this shorter distance d , which is not the entire beam path, the impulse and Larmor radius deflections predict the same results.

Both of these approaches incorporate the assumption that the beam is deflected at the point $(0, -h, z)$ directly below the centre of the solenoid, since this is where the full circle of the circular Larmor radius path would eventually be completed, and is a good approximation. However, this assumption is limited as it assumes a shorter path upon which the deflection acts. Hence, a refined impulse based calculation that includes the entire beam trajectory is utilised here, which leads to improved predictive accuracy compared to the Larmor radius approach.

To calculate the impulse acting on the beam, the electrons are again simulated to travel along a straight path with constant speed and transformed into the time domain as in the Weber model. At each time step the field values of B_ρ and B_z are calculated, and B_ρ transformed to Cartesian coordinates through the relations

$$B_x = B_\rho \cdot \frac{x_1}{\rho}, \quad (4.27)$$

$$B_y = B_\rho \cdot \frac{-h}{\rho}. \quad (4.28)$$

With these the vector cross product can be performed to obtain the Lorentz force, and since only an x-component in the velocity vector \vec{v}_1 is assumed, there will only be resulting deflection forces in y- and z-direction as the x-component of the force amounts to zero. The force values obtained along the beam path are then integrated with the trapezium rule and the time taken for the beam to travel from cathode to detector screen. Again, an example code is shown in appendix C. The resulting vertical and horizontal impulses are then used to calculate y- and z-deflections according to (4.15). The results of the field model and Weber model can both be seen in section 4.1.3 where they are further

compared with observations from experiments.

4.1.1.3 Modelling with CPO The third approach chosen to model deflections across the solenoid is a state-of-the-art commercially available software package CPO [292]. With this software the solenoid is modelled as a stack of current loops set along the z -axis following the geometry of the solenoid. As in the software conventional current is considered, a current of 1.00 A is supplied to rotate in the mathematically negative sense, which represents positive rotation of the electrons moving through the solenoid. As in the previous models, the solenoid is centred on the origin and the beam starts at a distance of $-h$ on the y -axis. The beam across the solenoid is then set to be treated as individual rays of electrons and the direct method is chosen for tracing of the beam, where the beam is travelling over the whole distance from emission to screen at fixed velocity in direction of the x -axis. A plane is set to intercept the beam after it travelled from its origin across the solenoid, where it is deflected, so that the deflection values can be read from the software after subtracting the initial values $-h$ and z_1 . A databuilder file used with the software can be found in appendix C. Additionally, the field generated by the solenoid with this method can be seen in Fig. 4.3 for visual representation, where field values have been extracted from the software in steps of 2mm on the positive ρ - and z -axis respectively.

The resulting deflections from the Weber model, field model and CPO software package are summarised in Table 4.2 showing values for both vertical and horizontal deflection. In order to compare them with experimental data, it will now be explained how the data is obtained with a CRT setup.

4.1.2 Experiment

The experimental setup is shown as a sketch in Fig. 4.4, where a current carrying solenoid is deflecting an electron beam emitted from an electron gun, which then strikes a fluorescent screen. A CRT from a Hameg 203-6 oscilloscope is adapted for this experiment, comprising the electron gun and the fluorescent screen in a glass body. An external solenoid is placed across the glass body of the CRT, so that it sits perpendicular to the electron beam's trajectory. The electron gun can be controlled through modified circuitry

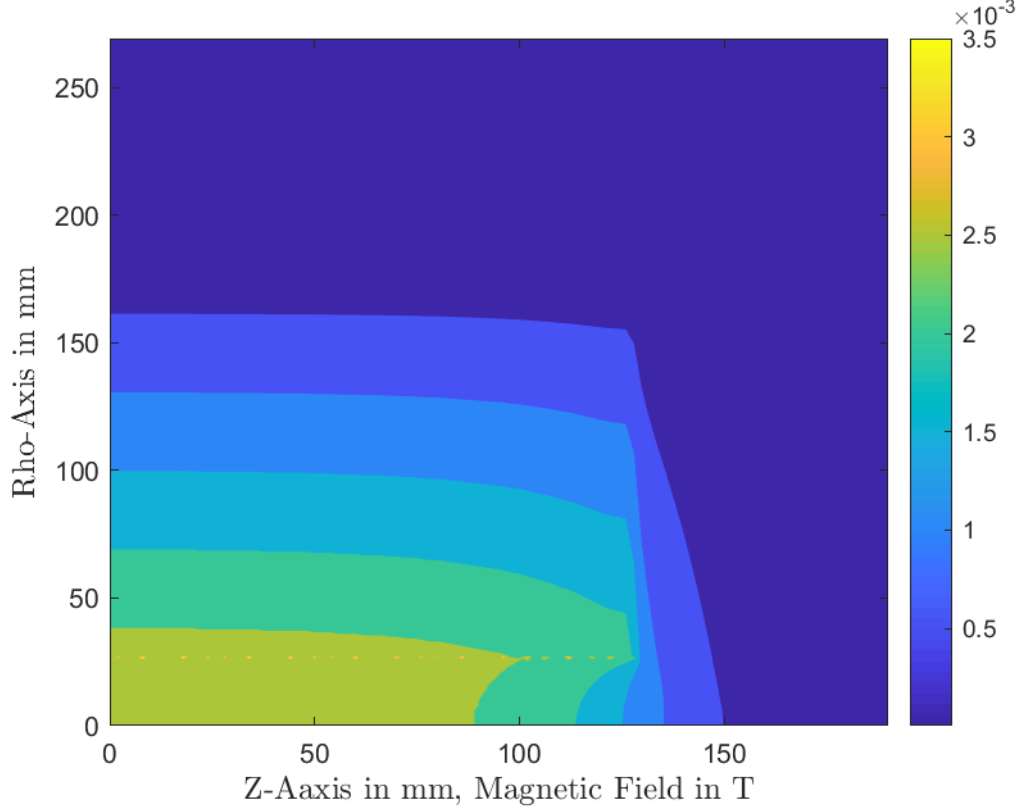


Figure 4.3: Magnetic field of solenoid S2 that is generated by CPO, extracted with a 2 mm granularity. Due to the symmetry of the field only positive ρ - and z -axis are shown. N.B., Solenoid S2 is defined in Table 4.1 (sec. 4.1.2).

of the oscilloscope, where an external cable connects the electron gun and the control circuit.

With the electron gun operating at an acceleration voltage of 2000 V between cathode and anode, the electrons reach a terminal velocity of

$$v_e = \sqrt{\frac{2eV}{m_e}} \approx 2.65 \times 10^7 \text{ m s}^{-1}. \quad (4.29)$$

From the point of emission the electrons pass the last anode at a distance of 6.5 cm, after an arrangement of focussing and accelerating anodes. When propagating in a straight line the fluorescent screen is intercepted after travelling another 21 cm, amounting to a total distance of 27.5 cm of beam travel. The evacuated glass tube enclosing the electron gun has a diameter of 50 mm, with the solenoid sitting directly on top of the glass and a distance from the last anode of 3 cm. For the choice of coordinates with the origin in the centre of the solenoid, the beam propagates at a height of $h = -(25 + R)$ mm and the

fluorescent screen sits at a distance of 18 cm from the coordinate origin.

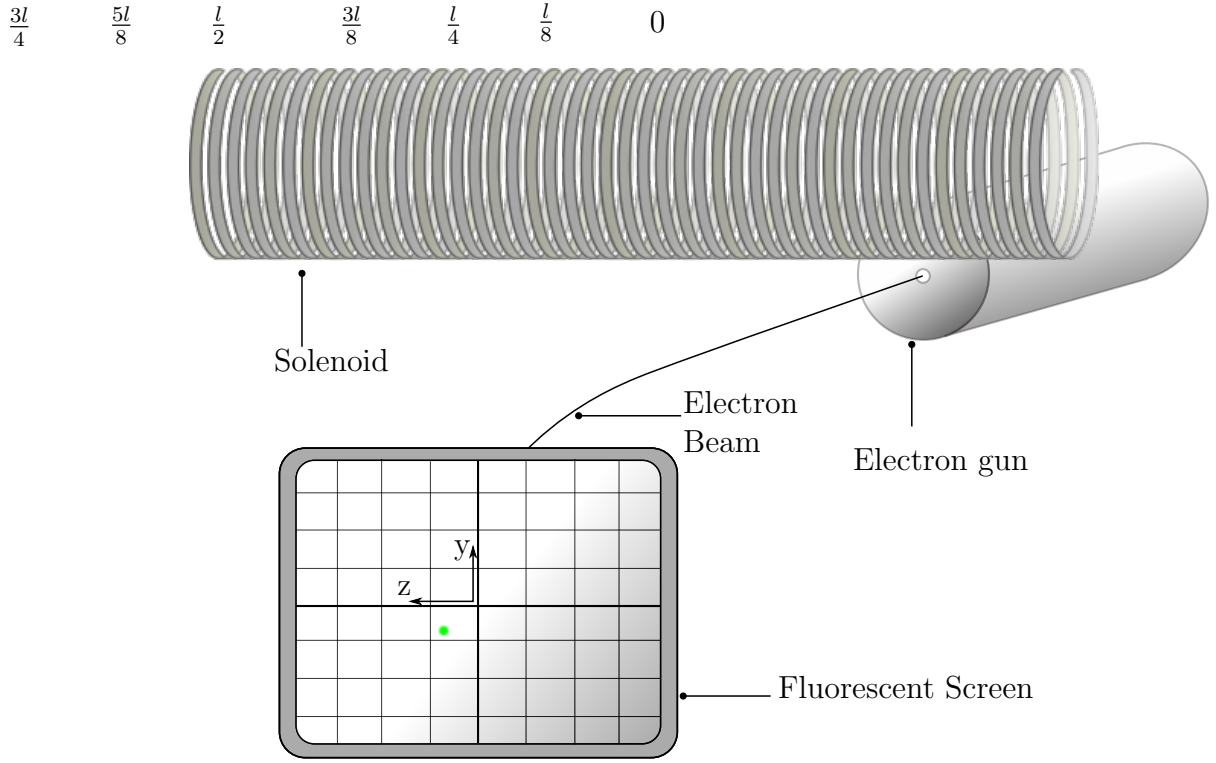


Figure 4.4: Solenoid positioned across the electron beam from the electron gun at $z_1 = 0$ where the electrons are deflected and intercepted by the fluorescent screen with an indicated beam spot (green). Also depicted are the positions $\frac{l}{8}$ to $\frac{3l}{4}$ where the beam can also be positioned with reference to the centre of the solenoid.

The fluorescent screen is factory-equipped with a graticule divided in 10 mm steps and subdivisions of 2 mm, which can give a rough indication of where the beam is intercepted after it has been deflected by the solenoid. With the control circuit the size of the beam spot can be focused to roughly 1 mm diameter, and the beam spot is indicated in Fig. 4.4 as the green coloured dot. Three different solenoids are used to deflect the beam to various degrees, they are labelled S1, S2 and S3, with different lengths, radii and numbers of windings, all of which are documented in Table 4.1. Although the shortest solenoid with a length of 25 mm is by definition considered a coil, it will further be referred to as solenoid S1 for labelling consistency. The solenoids are driven by a benchtop power supply that is supplying a continuous DC-current of 1.00 A.

To investigate the behaviour of the beam in the fringe field region, the solenoids are

Table 4.1: Properties of the three Solenoids S1, S2 and S3 that are used in the experiments, showing radius, length, number of windings and supplied DC current

Solenoid	Radius (mm)	Length (mm)	Absolute number of windings and $[n_{unit}]$	Current (A)
S1	20	25	61 [2440]	1.00
S2	27	255	560 [2200]	1.00
S3	30	500	1300 [2600]	1.00

placed so that the beam can cross through different regions of the field. Relative to the coordinate origin in the centre of the solenoid where the field is relatively homogeneous, the field becomes increasingly fringing closer to the solenoid ends. In this way the solenoids are set so that the beam passes at different positions z_1 from the origin. For example, when the beam crosses at position $z_1 = 0$, which is above the coordinate origin, it passes the per se ‘middle’ of the solenoid. The solenoid can then be moved for the beam to cross a different point, which is done in fractions of the solenoid lengths. For S1 the beam also passes at $z_1 = \frac{l}{4}$, $z_1 = \frac{l}{2}$ where it is aligned with the end of the solenoid on the z-axis, and then further to $z_1 = \frac{3l}{4}$ and $z_1 = l$. For the two longer solenoids, S2 and S3, the positions are shifted in $\frac{1}{8}$ steps of the solenoid length, up to the point $z_1 = \frac{3l}{4}$. For a graphic representation, these positions are indicated in Fig. 4.4, showing where the beam will cross through the field and travel across in relation to the solenoid’s centre and coordinate origin.

Especially at the positions around $z_1 = \frac{l}{2}$, it is said that the field is fringing and strongly deviates from the ideal homogeneous field associated with an infinite solenoid. Furthermore, the shortest coil, S1, will have a very inhomogeneous field according to theory due to its length and radius being nearly identical, with a relatively small number of windings, which is ideal to investigate the behaviour of the beam in fringing fields.

The following procedure is adopted to obtain measurements of the beam deflection. First, the solenoid is set so that the electron beam crosses at a desired point z_1 , then the beam is focussed and centred in the middle of the fluorescent screen with the help of the control circuit. Next, the power supply is switched on and adjusted to provide a current of 1.00 A magnitude to the solenoid, so that the beam is deflected. The deflected position is acquired with the help of a plastic vernier and the graticule on the screen and lastly

the power supply is switched off again. This procedure is repeated 3 times, giving a mean deflection of the beam, for each position z_1 with the three solenoids.

4.1.3 Results

As the deflections of the beam are measured in vertical and horizontal directions, they can be represented as points on the yz -plane. The Figures 4.5-4.7 summarise the deflections across each of the three solenoids, where the axis of ordinates shows vertical deflection and the axis of abscissae shows horizontal deflection. Fig. 4.5 shows the measured vertical and horizontal deflections at each position z_1 across S1 on the yz -plane, as well as the predicted values from the simulations. Similarly, Fig. 4.6 shows the data for S2 and Fig. 4.7 shows data for S3. In these bubble charts the blue squares represent the experimental data, with the size indicating the position z_1 where the beam crossed the solenoid. Paired to the experimental data are the predictions from the Weber model (red x), the field based model (yellow triangle) and numerical field model using CPO (purple circle), where each pair of predictions has the same data point size as the experimental data at a given position z_1 . To identify the positions the solenoid was crossed on the z -axis, labels have been added to the measurement data points to uniquely identify where the beam travelled.

The general trend of the observed deflections across S1 in Fig. 4.5 show that the beam is increasingly deflected horizontally as it moves into the fringing field region, however the vertical deflection is greatest across the centre of the coil and reduces in magnitude the further away the beam moves from the centre. It can be seen from the simulation results that all three models follow the general trend. Both field and Weber model predict similar deflection values and agree well with the experimental data for $z_1 = 0$ to $l/2$. In these cases CPO seems to underestimate the deflection values, a pattern which continues for positions $z_1 = 3l/4$ and l , but similarly the Weber and field based predictions are now further off from the observed value.

For S2 (see Fig. 4.6) the deflections first show an increase in both horizontal and vertical direction up to $z_1 = 3l/8$, but when the beam is crossing over the end of the solenoid at $l/2$ there is almost negligible vertical deflection, however the horizontal deflection reaches

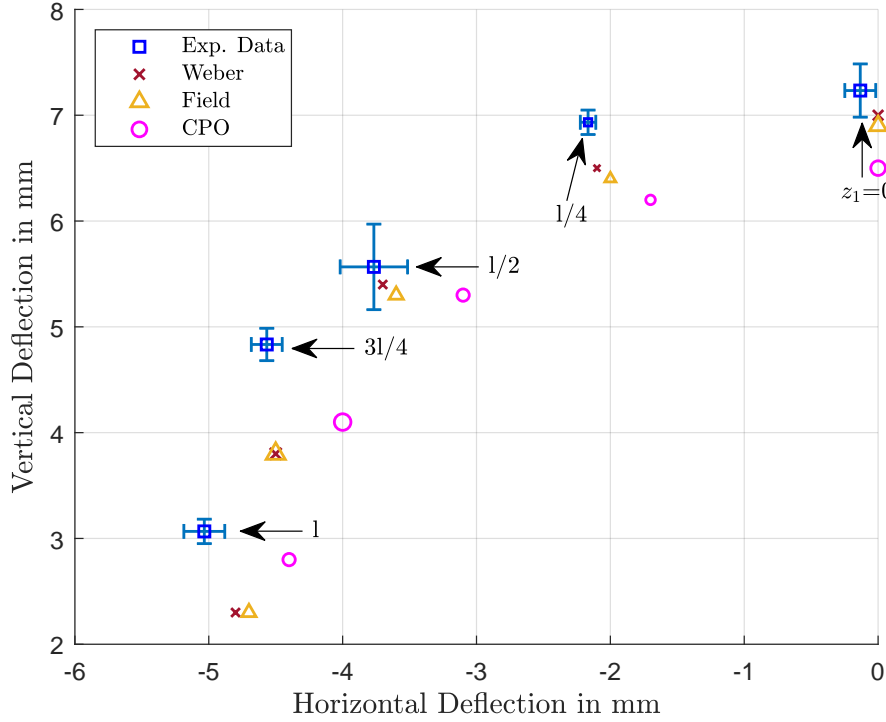


Figure 4.5: Measured and predicted deflections of the electron beam across S1 for both vertical and horizontal directions. In the bubble chart, the blue squares show the experimental data and are labelled with the beam position relative to the solenoid centre, i.e. the axial or “z”-position (as illustrated in Figure 4.4). For each given beam position, the size of the data points relating to that position are uniquely the same size, so that predictions from the Weber model (red x), Field model (yellow triangle) and CPO (purple circle) all have the same size marker (as the corresponding blue square/experimental measurement) for each given “z”-position.

its maximum. Beyond this point the direction of vertical deflection is inverted, with the magnitude falling off as the beam moves further away from the solenoid while simultaneously the horizontal deflection also decreases. This trend is again followed by the three modelling approaches, where generally the Weber and field model predict similar deflection values that tend to underestimate the deflection slightly while CPO is inclined to overestimate the displacement values.

In Fig. 4.7 the data for the longest solenoid S3 is shown, where the observed values show the same behaviour as they did for S2, with both deflections first growing as the beam moves towards the edge of the solenoid, then the horizontal deflection peaks at $l/2$ and after that the vertical deflection direction is inverted. It can also be noticed that the positions $3l/8$ and $5l/8$, as well as $l/4$ and $3l/4$ are almost symmetric to the horizontal

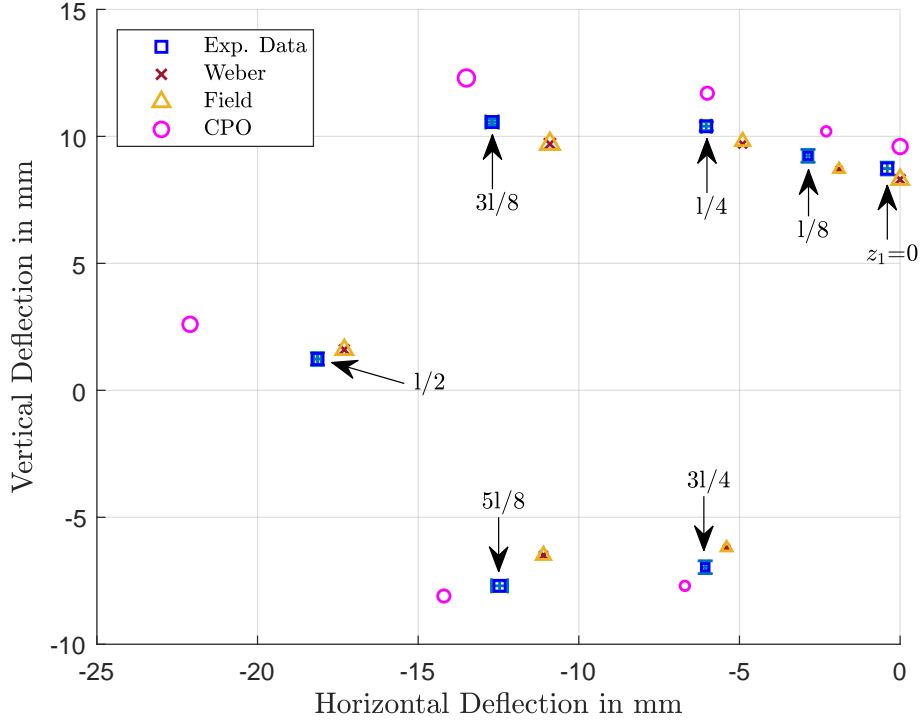


Figure 4.6: Measured and predicted deflections of the electron beam across S2 for both vertical and horizontal directions. The blue squares show the experimental data, the red x (Weber model), yellow triangle (Field Model) and purple circle (CPO) show the predictions of the various models whereby all data points of the same, unique size relate to a given axial (i.e., “z”) beam position.

axis, it is likely that this behaviour would become increasingly visible with even longer solenoids where the field becomes even more homogeneous. It can further be seen that the Weber and field model are both in close agreement with the measured deflections while CPO visibly overestimates the fringing region, but all predictions follow the same general trend, including the change of sign in vertical deflection.

Overall, Weber and field model show reasonable agreement with measurement, closely followed by CPO which has a few outliers but also makes reasonable predictions, although especially with the longer S2 and S3 it has a tendency to overestimate deflections. In the non-fringing region $z_1 = 0$ to $l/4$ the three models perform equally well. It is possible that CPO uses a different derivation method of the field values next to the BEM characteristic alone and this could be the reason why it tends to differ from the other two models especially in the fringing region. For a complete comparison of the observed and predicted values, Table 4.2 shows the mean deflection values of the experimental data with the

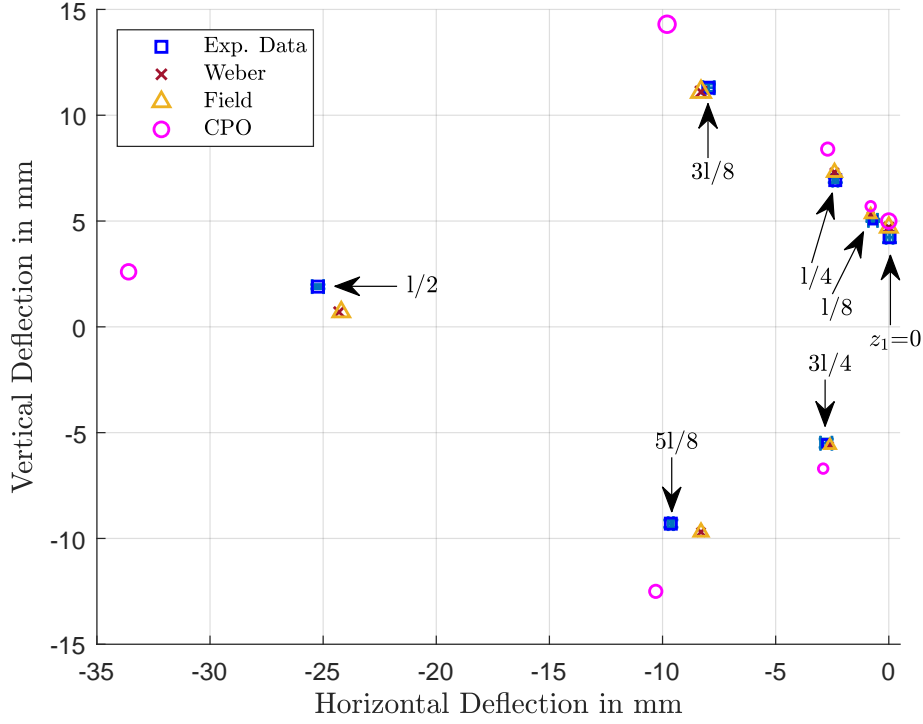


Figure 4.7: Measured and predicted deflections of the electron beam across S3 for both vertical and horizontal directions. The blue squares show the experimental data, the red x (Weber model), yellow triangle (Field model) and purple circle (CPO) show the predictions of the various models whereby all data points of the same, unique size relate to a given axial (i.e., “z”) beam position.

corresponding standard deviation, next to the simulation results for each of the models.

From this table it appears clear that both field and Weber model predict very similar deflection values, which is expected, as in the near field and for the low velocity limit both theories are nearly identical, as reviewed in section 2, so both theories predicting the same deflection is a sensible result. From the previous research [175,176] the models performed similarly in terms of their predictive accuracy, given the experimental limitations and modelling assumptions. With the improvements in modelling (especially the assumptions made for the field model) it is further apparent that both theories perform equally well for this experimental setup.

Upon further consideration of the simulations it was found that the Weber model can be simplified from a double wound treatment with both R_i and R_o to instead using just the total number of windings and a single radius. It was first not clear if this simplification is justified with Weber’s force, but the simulations that were tested arrived at similar results.

Table 4.2: Measured and predicted values for the vertical deflection y_d and horizontal deflection z_d across all three solenoids

Solenoid	z_1	Vertical Deflection y_d				Horizontal Deflection z_d			
		Experiment	Weber	Field	CPO	Experiment	Weber	Field	CPO
S1	0	7.2 (± 0.25)	7.0	6.9	6.5	-0.1 (± 0.12)	0	0	0
	$l/4$	6.9 (± 0.12)	6.5	6.4	6.2	-2.2 (± 0.06)	-2.1	-2.0	-1.7
	$l/2$	5.6 (± 0.40)	5.4	5.3	5.3	-3.8 (± 0.25)	-3.7	-3.6	-3.1
	$3l/4$	4.8 (± 0.15)	3.8	3.8	4.1	-4.6 (± 0.12)	-4.5	-4.5	-4.0
	l	3.1 (± 0.12)	2.3	2.3	2.8	-5.0 (± 0.15)	-4.8	-4.7	-4.4
S2	0	8.7 (± 0.25)	8.3	8.3	9.6	-0.4 (± 0.17)	0	0	0
	$l/8$	9.2 (± 0.25)	8.7	8.7	10.2	-2.9 (± 0.15)	-1.9	-1.9	-2.3
	$l/4$	10.4 (± 0.17)	9.7	9.8	11.7	-6.0 (± 0.25)	-4.9	-4.9	-6.0
	$3l/8$	10.6 (± 0.12)	9.7	9.7	12.3	-12.7 (± 0.20)	-10.9	-10.9	-13.5
	$l/2$	1.2 (± 0.25)	1.6	1.6	2.6	-18.1 (± 0.12)	-17.3	-17.3	-22.1
	$5l/8$	-7.7 (± 0.20)	-6.5	-6.5	-8.1	-12.5 (± 0.25)	-11.1	-11.1	-14.2
	$3l/4$	-7.0 (± 0.25)	-6.2	-6.2	-7.7	-6.1 (± 0.12)	-5.4	-5.4	-6.7
S3	0	4.2 (± 0.25)	4.7	4.7	5.0	0.0 (± 0.15)	0	0	0
	$l/8$	5.0 (± 0.06)	5.3	5.3	5.7	-0.7 (± 0.20)	-0.8	-0.8	-0.8
	$l/4$	6.9 (± 0.12)	7.3	7.3	8.4	-2.4 (± 0.12)	-2.4	-2.4	-2.7
	$3l/8$	11.3 (± 0.17)	11.1	11.1	14.3	-8.0 (± 0.25)	-8.3	-8.3	-9.8
	$l/2$	1.9 (± 0.10)	0.7	0.7	2.6	-25.2 (± 0.25)	-24.3	-24.2	-33.6
	$5l/8$	-9.3 (± 0.17)	-9.7	-9.7	-12.5	-9.6 (± 0.12)	-8.3	-8.3	-10.3
	$3l/4$	-5.5 (± 0.20)	-5.6	-5.6	-6.7	-2.8 (± 0.25)	-2.6	-2.6	-2.9

This is similar to the field approach where usually only the total number of windings on a coil is considered for field calculation along with a mean radius, regardless of it being double or triple wound or having several more layers of windings. It seems logical that this approximation will be justified for any number of windings as long as $R_{min} \approx R_{max}$.

Further it can be noted that in the field-based model there is a slight conceptual difference regarding the deflections. For vertical deflection it is the axial component B_z that is responsible for the deviation of the beam, whereas for horizontal deflection it is the radial component B_ρ . This is of course due to the cross product in the Lorentz force that defines the force as acting orthogonally to the field vector itself at any point in space when the force is calculated from the magnetic field. In the Weber model the respective force component in either z- or y-direction is calculated directly and responsible for the deflection in the corresponding direction, but this shows that there is a general connection between the two forces and the two have previously been related to each other [94].

Given the slight discrepancy between the model considering the entire path of beam

travel and the Larmor radius approach, it could indicate that the Larmor radius itself is a special case of beam deflection not manifest until the field is strong enough to force the beam on a circular path. If it is true that the Larmor radius itself is an exception rather than the rule this could also have consequences for experiments of the Kaufmann-Bucherer or Bertozzi type, but further research is needed. Nonetheless, the general similarity of Weber's and field theory can be seen from these experiments and simulations and we will now proceed to analyse the magnetic field further in the next section and see how Weber and field model compare in principle for a solenoid.

4.2 Further Analysis of the Magnetic Field

Upon demonstrating the similarity of the electron deflection results with Weber's force and field theory alike, it appears feasible to analyse the field itself further in this chapter. Previously, the field predicted by the model of Derby & Olbert [299] has been shown in Fig. 4.2, where the total field $B = \sqrt{B_\rho^2 + B_z^2}$ is shown. It has been argued by Slepian [307] that lines of force do not need to be continuous, individual or closed curves and that it is enough to know only the local vectorial value of the field in direction and magnitude to predict observable phenomena. In this sense, the field can be thought of as a vectorial map that indicates how much interaction of charged particles is possible in which direction at any point in space. It is possible to compare this with Weber's theory directly if we obtain a similar map of the force values like the map of the field values.

With the electron energy at 2000 eV, the force values in the yz-plane can be calculated, where $x = 0$ and $\rho = y$ with the electrons moving in x-direction. The values have been obtained for both y- and z- axis in steps of 1mm, similar to the simulated field values before. In order to compare this with the total field values B , the total force is similarly obtained as

$$F_w = \sqrt{F_x^2 + F_y^2 + F_z^2} \quad (4.30)$$

and can then be scaled by the electron velocity to the total field values according to

$$B_w = \frac{F_w}{qv_e}. \quad (4.31)$$

Here, B_w can be interpreted as the magnitude of total “force-field” values based on Weber’s force. It must be noted that this is not a strict equivalence since only the magnitudes have been manipulated and this does not apply in the same way to the vectorial values themselves, which should be clear from the previous comparison with the Lorentz force based on the cross product. Nevertheless, for the magnitudes it can be seen that B_w is also in units of T and a comparison of the field and the Weber force becomes possible. In Fig. 4.8a we can again see the total field from the Derby & Olbert model for easier comparison (the same as in Fig. 4.2) and in Fig. 4.8b the values for B_w are shown next to it.

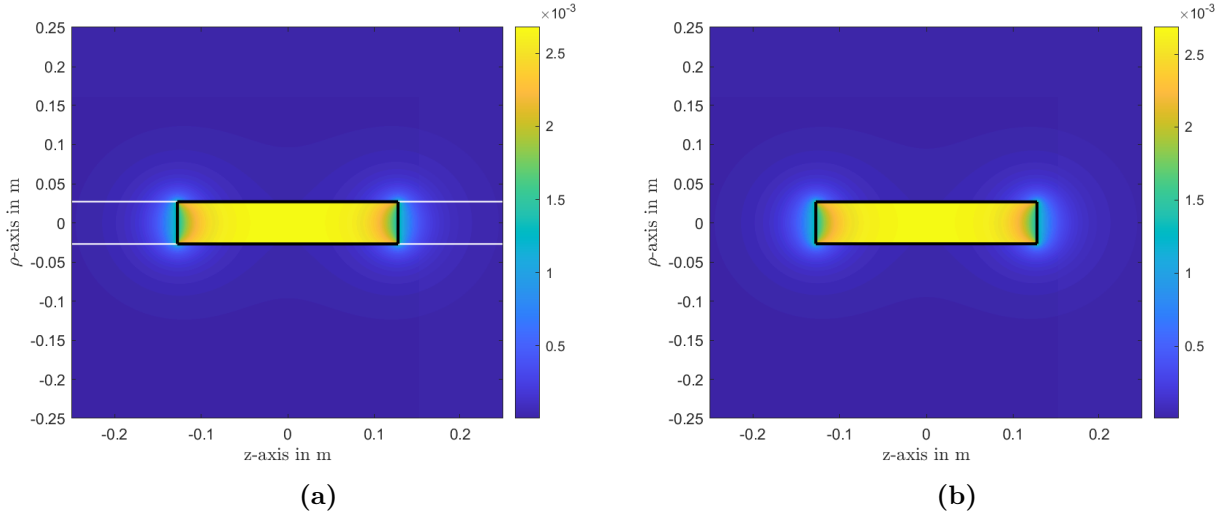


Figure 4.8: A comparison of the magnitude of field \vec{B} as produced by solenoid S2 in the ρz -plane with the magnitude of Weber force scaled to a ‘force field’ representation \vec{B}_w ; a) field magnitudes calculated with the model by Derby & Olbert, similar to figure 4.2; b) representation of the Weber force as a field magnitude scaled by charge q and electron velocity v_e according to equation (4.31) in units of T.

As can be seen from this juxtaposition, both field and Weber force represented by these magnitudes are exactly the same, qualitatively as well as quantitatively. The black lines represent the dimension of the solenoid and it can be seen that most interaction is possible inside of the solenoid, where the field is strongest. Anywhere outside of the solenoid (except very close to the ends) the field values are much smaller than inside. It can also be seen that the field outside has a tendency to concentrate closer to the poles

and falls off with increasing distance, which seems consistent with the notion that an ideal, infinitely long solenoid only produces a field inside of itself and does not have a field outside. (Note: Since the field values outside the solenoid are one or two orders of magnitude smaller than the strong values inside the solenoid, the shades of blue might be difficult to distinguish in the print version. However, their structure can be better seen in the digital version.)

Further to the comparison of the total field values, the individual components of the field and the force can be analysed respectively. Since the values for both field and force have been obtained in the yz -plane, it is found that $F_x = 0$, $B_x = 0$ and of course $B_\rho = B_y$. This allows to compare the axial field values B_z (Fig. 4.9a) with the vertical force values F_y (Fig. 4.9b) and the radial field values B_ρ (Fig. 4.10a) to the horizontal force values F_z (Fig. 4.10b). However, in this case, a scaling factor for the vectorial values cannot be applied, so only a qualitative comparison is possible. Nonetheless, it is instructive to look at the magnitudes of the respective field and force components. (Since the direction of the field, respectively force, changes inside and outside of the solenoid, it is advantageous to look at just the magnitudes again, as it allows for easier comparison of the values.)

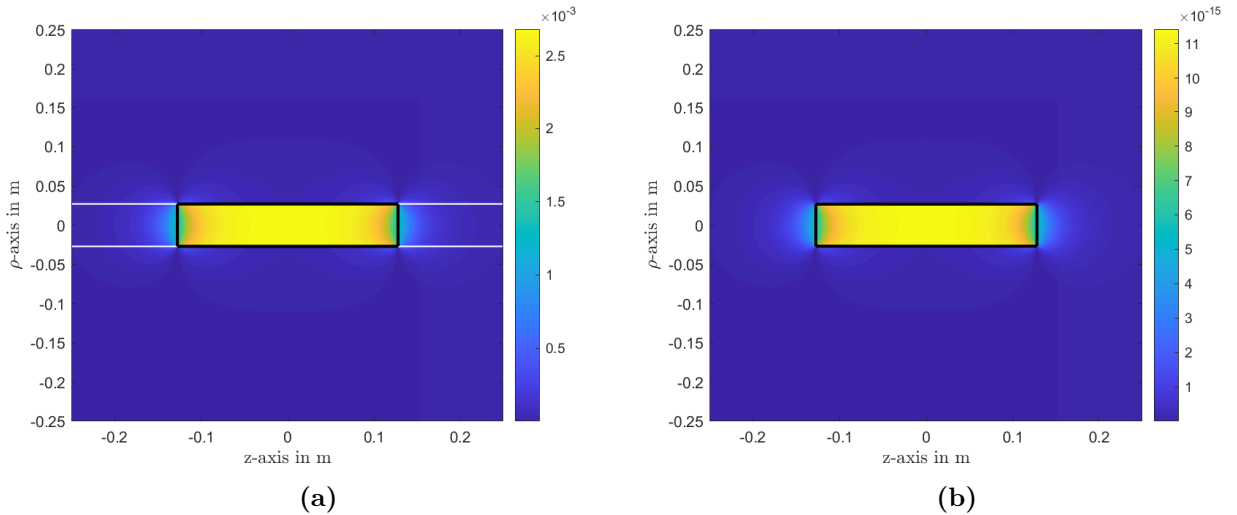


Figure 4.9: Direct comparison of individual components of field and force values, represented by their magnitude in the ρz -plane; a) axial field component B_z ; b) vertical Weber force component F_y .

Even though the magnitude of the force is much smaller compared to the field value (as the field is in units of T while the force is in N, of course,) it is easy to see that they are

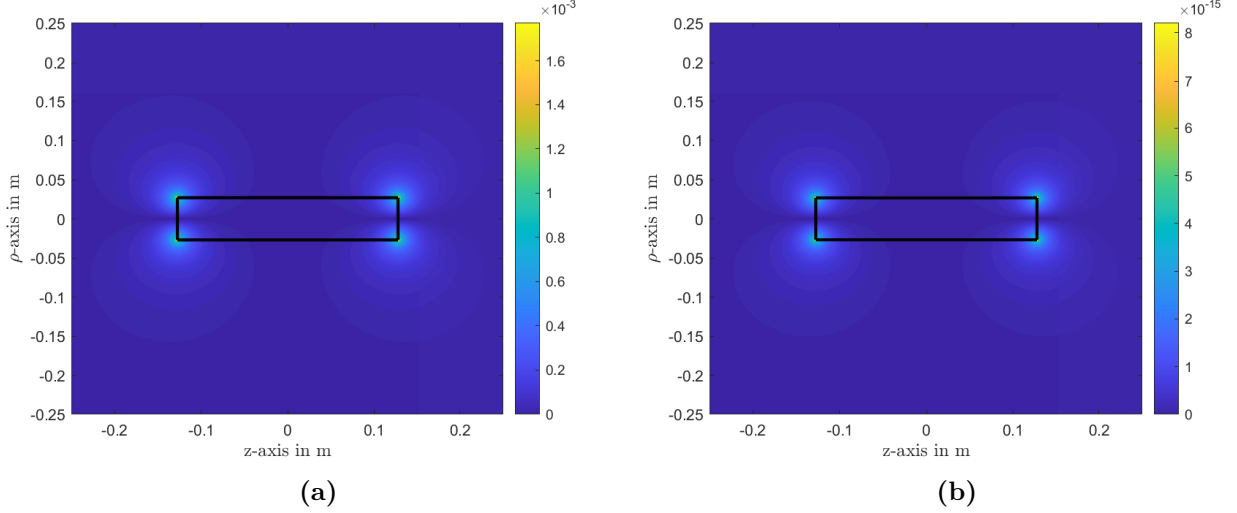


Figure 4.10: Direct comparison of individual components of field and force values, represented by their magnitude in the ρz -plane; a) radial field component B_ρ ; b) horizontal Weber force component F_z .

qualitatively the same, i.e. B_z and F_y are similar and so are B_ρ and F_z . These relations are hardly surprising as it was seen in the previous section that the deflection values are similar, so the field and force values must be similar too. Furthermore, it can be seen that the axial field is primarily responsible for the strong field inside of the solenoid and also contributes to the field outside of the solenoid and close to the poles. The radial field is mostly only contributing to field values around the poles themselves which relates to the bigger horizontal deflection values close to the ends of the solenoids that were visible in the experiments.

4.3 Deflection Parallel to Solenoid Axis

The next investigation will examine the behaviour of the beam in the magnetic field when it is travelling through the solenoid, i.e. it will propagate through the fringe field region, entering into the inside of the solenoid where the field is strongest, and exit at the other end through the other fringe field region. This can happen by having the beam travel parallel to the axis of the solenoid or at an angle to the axis, the latter of which will be investigated experimentally with a CRT subsequently. It should be noted that by definition, the electromagnet used for experiments in this section is by definition a coil, as it does not meet the formal definition of a solenoid, where the length of the coil is at least

twice its radius. However, for labelling consistency, it will be referred to as a solenoid in the following.

4.3.1 Modelling

Similar to the modelling applied in section 4.1.1, a Weber force model, a field based model and the software package CPO will again be used to predict the deflections caused by the beam travelling through the solenoid. Additionally, both Weber and field model will receive some modification in this section to extend the modelling approach, so that equations of motion are included. The predictions obtained from the three models will then be compared with experimental data obtained with a longer 290 turn solenoid and further compared with each other for a shorter 20 turn solenoid.

4.3.1.1 Weber Model Similar to the previous model in section 4.1.1.1 where the beam was travelling past the solenoid, a 3D model is constructed based on Weber's force. First, we can assume the positions of the electrons in the beam and the current in the solenoid w.r.t. the coordinate origin, set in the very centre of the solenoid and obtain the position vectors \vec{r}_1 , \vec{r}_2 and \vec{r}_{12} (see Fig. 4.11):

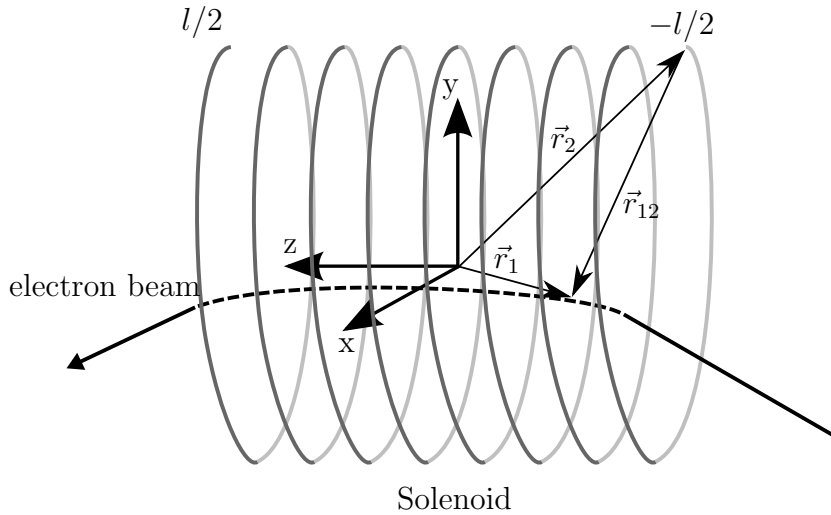


Figure 4.11: Coordinate system situated in the centre of a solenoid with an electron beam entering at one end and exiting the other. The positions \vec{r}_1 , \vec{r}_2 and \vec{r}_{12} are used to calculate the force on the beam exerted by the current in the solenoid, elongating from $-l/2$ to $l/2$.

$$\vec{r}_1 = \begin{pmatrix} x_1 \\ y_1 \\ z_1 \end{pmatrix}, \quad \vec{r}_2 = \begin{pmatrix} R \cos(\theta) \\ R \sin(\theta) \\ z_2 + dz\theta \end{pmatrix}, \quad (4.32)$$

$$\vec{r}_{12} = \begin{pmatrix} x_1 - R \cos(\theta) \\ y_1 - R \sin(\theta) \\ z_1 - z_2 - dz\theta \end{pmatrix}, \quad (4.33)$$

$$r_{12} = \sqrt{(x_1 - R \cos(\theta))^2 + (y_1 - R \sin(\theta))^2 + (z_1 - z_2 - dz\theta)^2}. \quad (4.34)$$

Here, the initial position of the electron beam is kept arbitrary with the general variables x_1, y_1, z_1 to allow for any desired point of emission. The current through the solenoid I is considered as the movement of the electrons as helical motion along the windings, entering the solenoid at $z_2 = -l/2$ and moving towards the opposite end with infinitesimal steps of $dz\theta$. The motion of the electron beam itself is also kept as general velocity variables v_{1x}, v_{1y}, v_{1z} , which leads to the velocities

$$\vec{v}_1 = \begin{pmatrix} v_{1x} \\ v_{1y} \\ v_{1z} \end{pmatrix}, \quad \vec{v}_2 = \begin{pmatrix} -v_2 \sin(\theta) \\ v_2 \cos(\theta) \\ \frac{v_2}{R} dz \end{pmatrix}, \quad \vec{v}_{12} = \begin{pmatrix} v_{1x} + v_2 \sin(\theta) \\ v_{1y} - v_2 \cos(\theta) \\ v_{1z} - \frac{v_2}{R} dz \end{pmatrix}. \quad (4.35)$$

The beam is then set to travel parallel to the axis of the solenoid by setting the initial value of v_{1z} equal to the electron velocity v_e and can then enter the solenoid at an angle by setting initial values for v_{1x} or v_{1y} . The initial values are set by an electrostatic offset and will further be explained in section 4.3.2.

These velocities and positions can now be substituted into the Weber force (3.15) to formulate a force \vec{F}_{2-1-} between the electrons in the beam q_{1-} and the electrons in the solenoid q_{2-} and respectively a force \vec{F}_{2+1-} between q_{1-} and the lattice charges q_{2+} . It will again be assumed that $q_{1-} = -q_{1+}$ and $q_{2-} = -q_{2+}$.

$$\begin{aligned}
 \vec{F}_{2-1-} &= \frac{q_1+q_2}{4\pi\epsilon_0} \frac{\vec{r}_{12}}{r_{12}^3} \left\{ 1 - \frac{3}{2c^2} \frac{1}{r_{12}^2} \left[\begin{pmatrix} x_1 - R \cos(\theta) \\ y_1 - R \sin(\theta) \\ z_1 - z_2 - dz\theta \end{pmatrix} \cdot \begin{pmatrix} v_{1x} + v_2 \sin(\theta) \\ v_{1y} - v_2 \cos(\theta) \\ v_{1z} - \frac{v_2}{R} dz \end{pmatrix} \right]^2 \right. \\
 &\quad \left. + \frac{1}{c^2} \left(\begin{pmatrix} v_{1x} + v_2 \sin(\theta) \\ v_{1y} - v_2 \cos(\theta) \\ v_{1z} - \frac{v_2}{R} dz \end{pmatrix}^2 + \begin{pmatrix} x_1 - R \cos(\theta) \\ y_1 - R \sin(\theta) \\ z_1 - z_2 - dz\theta \end{pmatrix} \cdot \begin{pmatrix} a_{1x} - a_{2x} \\ a_{1y} - a_{2y} \\ a_{1z} - a_{2z} \end{pmatrix} \right) \right\} \\
 &= \frac{q_1+q_2}{4\pi\epsilon_0} \frac{\vec{r}_{12}}{r_{12}^3} \left\{ 1 - \frac{3}{2c^2} \frac{1}{r_{12}^2} [(v_{1x} + v_2 \sin(\theta))(x_1 - R \cos(\theta)) + (v_{1y} - v_2 \cos(\theta))(y_1 - R \sin(\theta)) \right. \\
 &\quad + (v_{1z} - \frac{v_2}{R} dz)(z_1 - z_2 - dz\theta)]^2 + \frac{1}{c^2} ((v_{1x}^2 + 2v_{1x}v_2 \sin(\theta) + v_2^2 \sin^2(\theta) \\
 &\quad + v_{1y}^2 - 2v_{1y}v_2 \cos(\theta) + v_2^2 \cos^2(\theta) + v_{1z}^2 - 2\frac{v_{1z}v_2}{R} dz + (\frac{v_2}{R} dz)^2) \\
 &\quad + (a_{1x} - a_{2x})(x_1 - R \cos(\theta)) + (a_{1y} - a_{2y})(y_1 - R \sin(\theta)) \\
 &\quad \left. + (a_{1z} - a_{2z})(z_1 - z_2 - dz\theta)) \right\}
 \end{aligned} \tag{4.36}$$

$$\begin{aligned}
 \vec{F}_{2+1-} &= -\frac{q_1+q_2}{4\pi\epsilon_0} \frac{\vec{r}_{12}}{r_{12}^3} \left\{ 1 - \frac{3}{2c^2} \frac{1}{r_{12}^2} \left[\begin{pmatrix} x_1 - R \cos(\theta) \\ y_1 - R \sin(\theta) \\ z_1 - z_2 - dz\theta \end{pmatrix} \cdot \begin{pmatrix} v_{1x} - 0 \\ v_{1y} - 0 \\ v_{1z} - 0 \end{pmatrix} \right]^2 \right. \\
 &\quad \left. + \frac{1}{c^2} \left(\begin{pmatrix} v_{1x} - 0 \\ v_{1y} - 0 \\ v_{1z} - 0 \end{pmatrix}^2 + \begin{pmatrix} x_1 - R \cos(\theta) \\ y_1 - R \sin(\theta) \\ z_1 - z_2 - dz\theta \end{pmatrix} \cdot \begin{pmatrix} a_{1x} - 0 \\ a_{1y} - 0 \\ a_{1z} - 0 \end{pmatrix} \right) \right\} \\
 &= -\frac{q_1+q_2}{4\pi\epsilon_0} \frac{\vec{r}_{12}}{r_{12}^3} \left\{ 1 - \frac{3}{2c^2} \frac{1}{r_{12}^2} [(v_{1x})(x_1 - R \cos(\theta)) + (v_{1y})(y_1 - R \sin(\theta)) \right. \\
 &\quad + (v_{1z})(z_1 - z_2 - dz\theta)]^2 + \frac{1}{c^2} ((v_{1x}^2 + v_{1y}^2 + v_{1z}^2) \\
 &\quad \left. + (a_{1x})(x_1 - R \cos(\theta)) + (a_{1y})(y_1 - R \sin(\theta)) + (a_{1z})(z_1 - z_2 - dz\theta)) \right\}
 \end{aligned} \tag{4.37}$$

It can be seen that acceleration terms \vec{a}_1 of the beam cancel out and with the additional assumptions of $v_1 \gg v_2$ and a_2 being negligibly small, the two forces can be summed as

$$\begin{aligned}
 \vec{F}_w &= \vec{F}_{2-1-} + \vec{F}_{2+1-} \\
 &= \frac{q_1+q_2}{4\pi\epsilon_0} \frac{v_2}{c^2} \frac{\vec{r}_{12}}{r_{12}^3} \left\{ -\frac{3}{r_{12}^2} [(v_{1x} \sin(\theta))(x_1 - R \cos(\theta))^2 \right. \\
 &\quad + (v_{1y} \sin(\theta) - v_{1x} \cos(\theta))(x_1 - R \cos(\theta))(y_1 - R \sin(\theta)) \\
 &\quad - (v_{1y} \cos(\theta))(y_1 - R \sin(\theta))^2 + (v_{1z} \sin(\theta) - v_{1x} \frac{dz}{R})(x_1 - R \cos(\theta))(z_1 - z_2 - dz\theta) \\
 &\quad + (-v_{1z} \cos(\theta) - v_{1y} \frac{dz}{R})(y_1 - R \sin(\theta))(z_1 - z_2 - dz\theta) \\
 &\quad \left. + (-v_{1z} \frac{dz}{R})(z_1 - z_2 - dz\theta)^2] + [v_{1x} \sin(\theta) - v_{1y} \cos(\theta) - \frac{v_{1z}}{R} dz] \right\}.
 \end{aligned} \tag{4.38}$$

To transition from discrete sources to continuous currents it will again be integrated over the entire solenoid as a helical path through $qv \rightarrow \lambda v d\vec{l} \rightarrow IR d\theta$, replacing $q_2 v_2$, which leads to

$$\vec{F}_{w_{helix}} = \frac{q_1+IR}{4\pi\epsilon_0 c^2} \int_0^{N2\pi} \left\{ \frac{\vec{r}_{12}}{r_{12}^3} \dots \right\} d\theta. \tag{4.39}$$

As in the previous Weber model, N is the total number of windings of the solenoid. Next to just the helical model, it can again be assumed that the solenoid consists of individual stacked loops and their action on the beam can be superposed to arrive at a summation approach. In this case $v_{1z} = 0$ and the infinitesimal dz is replaced with a position for each loop determined by the pitch of the coil $p \cdot (n - 1)$, with $n = 1 \dots N$, so that we have

$$\vec{r}_2 = \begin{pmatrix} R \cos(\theta) \\ R \sin(\theta) \\ z_2 + p \cdot (n - 1) \end{pmatrix}, \quad \vec{v}_2 = \begin{pmatrix} -v_2 \sin(\theta) \\ v_2 \cos(\theta) \\ 0 \end{pmatrix}. \tag{4.40}$$

This can be again substituted into the Weber force with the usual assumptions, which then leads to the summation of all individual loops as

$$\begin{aligned}
 \vec{F}_{w_{sum}} &= \frac{q_1+q_2}{4\pi\epsilon_0} \frac{v_2}{c^2} \frac{\vec{r}_{12}}{r_{12}^3} \left\{ -\frac{3}{r_{12}^2} [(v_{1x} \sin(\theta))(x_1 - R \cos(\theta))^2 \right. \\
 &\quad + (v_{1y} \sin(\theta) - v_{1x} \cos(\theta))(x_1 - R \cos(\theta))(y_1 - R \sin(\theta)) \\
 &\quad - (v_{1y} \cos(\theta))(y_1 - R \sin(\theta))^2 + v_{1z} \sin(\theta)(x_1 - R \cos(\theta))(z_1 - z_2 - p(n - 1)) \\
 &\quad \left. - v_{1z} \cos(\theta)(y_1 - R \sin(\theta))(z_1 - z_2 - p(n - 1))] + [v_{1x} \sin(\theta) - v_{1y} \cos(\theta)] \right\},
 \end{aligned} \tag{4.41}$$

$$\vec{F}_{w_{sum}} = \frac{q_{1+}IR}{4\pi\epsilon_0c^2} \sum_{n=1}^N \int_0^{2\pi} \left\{ \frac{\vec{r}_{12i}}{r_{12i}^3} \dots \right\} d\theta. \quad (4.42)$$

Both (4.39) and (4.42) can be used to simulate the behaviour of the beam travelling through the solenoid. The simulation first defines the initial values for \vec{v}_1 and \vec{r}_1 and then utilises equations of motion to update the positions and velocities for each step. To this end, the propagation of the beam is transitioned from the spatial to the time dimension. The time step is set to be the total distance travelled by an undeflected beam (from emission to detector screen) over the initial electron velocity, so that

$$\Delta t = \frac{\Delta z_1}{v_e}, \quad (4.43)$$

with $t_0 = 0$ and $t_{last} = z_{1_{last}}/v_e$.

At every time step the force (4.39) (respectively (4.42)) is then calculated and this force will subject the beam to a certain acceleration \vec{a}_f . Within the low velocity limit, we can assume the electron mass m_e as constant and obtain \vec{a}_f through the Weber force acting on the beam:

$$\vec{a}_f = \frac{1}{m_e} \vec{F}_w. \quad (4.44)$$

With this the positions and velocities for the following time step can be calculated according to the equations of motion

$$x_{1_{k+1}} = x_{1_k} + v_{1_{x_k}} \Delta t + \frac{1}{2} a_{fx} \Delta t^2, \quad (4.45)$$

$$y_{1_{k+1}} = y_{1_k} + v_{1_{y_k}} \Delta t + \frac{1}{2} a_{fy} \Delta t^2, \quad (4.46)$$

$$z_{1_{k+1}} = z_{1_k} + v_{1_{z_k}} \Delta t + \frac{1}{2} a_{fz} \Delta t^2, \quad (4.47)$$

$$v_{1_{x_{k+1}}} = v_{1_{x_k}} + a_{fx} \Delta t, \quad (4.48)$$

$$v_{1_{y_{k+1}}} = v_{1_{y_k}} + a_{fy} \Delta t, \quad (4.49)$$

$$v_{1_{z_{k+1}}} = v_{1_{z_k}} + a_{fz} \Delta t, \quad (4.50)$$

where k is an index value denoting the current time step and $k + 1$ the following time step. The simulation itself is carried out in *MATLAB* where the trapezium rule is used to integrate for θ at each time step with a step size of 0.5° . The beam position \vec{r}_1 can then be

read at the penultimate time step to obtain the horizontal and vertical deflections x_d and y_d respectively, where they are intercepted by the detector screen. Here too, an example code of the simulation can be found in appendix C. Both the helical and summation approach Weber force predict the same deflection values for a given solenoid, as expected, and the simulation results are further compared with experiments and the other models in section 4.3.3. Further, it is again found that the force component acting longitudinal to the beam (F_{w_z} in this case) is again zero, similar to the previous model where the beam travelled across the solenoid, which is in agreement with the Lorentz force.

4.3.1.2 Field Model The beam deflections based on the magnetic field will again be obtained with the Lorentz force (2.7) and the field inside and outside of the solenoid is calculated with the help of the model by Derby & Olbert [299] and the corresponding *MATLAB* script by Cébron [298]. As this model and how the axial field B_z and radial field values B_ρ are obtained has been explained previously in section 4.1.1.2, it will not be repeated here.

The beam is simulated to travel from source to detector screen in the time domain, with the same time step, distance of travel and initial beam position and velocity as the Weber model in the previous section. The field values are then obtained at every time step and substituted into the Lorentz force, with which the acceleration values can be obtained similar to (4.44), as

$$\vec{a}_f = \frac{1}{m_e} \vec{F}_L. \quad (4.51)$$

Through this the same equations of motion (4.45) can be applied to calculate beam position and velocity for every time step. Horizontal deflection x_d and vertical deflection y_d are thus obtained at the positions of the penultimate time step of the simulation, an example code of which can be seen in appendix C.

4.3.1.3 Modelling with CPO Lastly, beam deflections through the solenoid are also predicted with the software package CPO [292]. As in the previous CPO model in section 4.1.1.3 the solenoid is modelled as a set of stacked hoops which are fed with conventional

current. The solenoid is again centred on the origin and the initial parameters, such as position and velocity of the beam, are defined in the software. After travelling from source through the inside of the solenoid, the beam is intercepted by a test plane where the detector screen would be, so that the horizontal and vertical deflections x_d and y_d can be read. Here, the beam is also set to be treated as individual rays of electrons and traced with the direct method in the software, and this time it is travelling parallel to or at an angle to the z-axis.

4.3.2 Experiments

An experiment has been performed to obtain deflection values from the magnetic action exerted on the beam by a solenoid. The beam is emitted by an electron gun in a CRT (similar to previous sec. 4.1.2) and its position recorded on the fluorescent screen of the CRT. A single wound solenoid with 290 windings has been placed around the glass body of the CRT, with a radius of $R = 159.5$ mm and a length of $l = 170$ mm, which is supplied with a current of 1 A. A sketch of the cross section of this setup can be seen in Fig. 4.12.

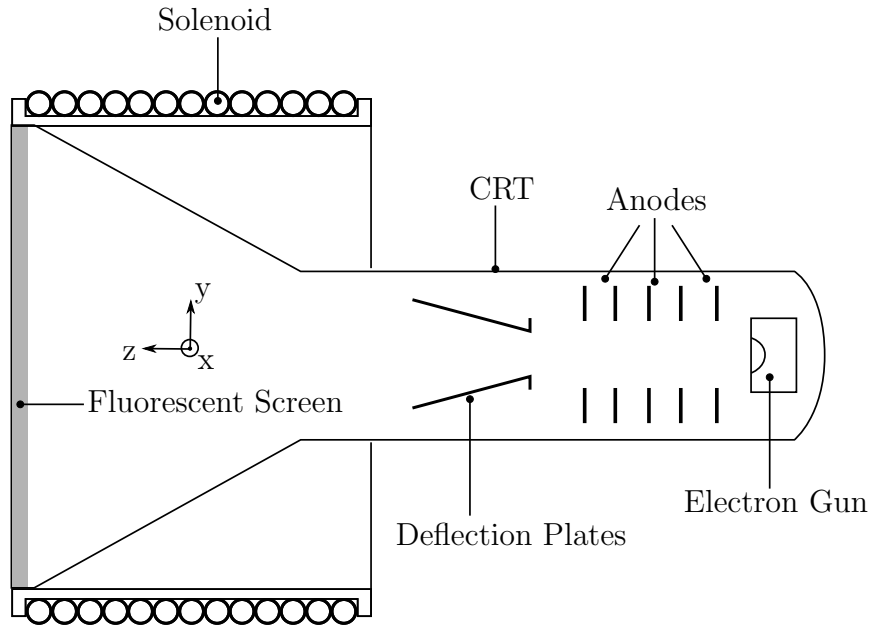


Figure 4.12: Cross section of the experimental setup comprising a CRT with fluorescent detector screen, surrounded by a solenoid through which an electron beam is deflected. The electron gun emits the beam, it is accelerated by a set of anodes and then imposed with an initial deflection by the deflection plates to enter the solenoid at an angle.

With the present setup the screen is located at the end of the solenoid after the beam

has travelled a total distance of 27.5 cm from the point of emission at terminal velocity v_e (4.29). The electrons are accelerated over a distance of 2.5 cm until they pass the anode and from there travel another 25 cm to the detector screen. As the centre of the solenoid aligns vertically with the point of beam emission (see Fig. 4.12), the beam is given an initial deflection with the electrostatic deflection plates of the CRT so that it will enter the solenoid at an angle to the z-axis, which allows to investigate different magnitudes of deflection. The beam that is initially travelling in a straight line is off-set on the y-axis in steps of 5 mm, which gives the beam an additional velocity component v_{1y} . Due to the beam travelling a distance of 250 mm after the anode where the vertical deflection plates sit, the ratio of v_y/v_e is obtained in steps of 1/50, reaching from the least initial deflection of 5 mm as 1/50 to 40 mm as 8/50.

These initial deflections however, necessitate a slight simplification in the simulations so that the deflections can be included through the velocity component v_{1y} accordingly. It must be assumed here that the beam travels in a straight line from the cathode for the first 25 mm up to the anode and is only deflected by the deflection plates from this point onwards, and respectively not noticeably affected by the magnetic field of the solenoid up to this point. The closer end of the solenoid is 80 mm away from the anode and the assumed deflected path of 250 mm is ten times the assumed straight path. It will be seen from the results (in the following section) that this assumption appears reasonable for the present setup and the beam is not significantly deflected by the field for the initial acceleration phase up to the anode.

With this consideration experimental values can be obtained with the following procedure. First the beam is focused and centred in the middle of the graticule on the fluorescent screen. Then it is offset vertically through the deflection plates by the desired amount and lastly the power supply is turned on to deflect the beam with the magnetic field. The vertical and horizontal deflection are both read from the screen with the help of a plastic vernier and the power supply is switched off. This process is repeated five times for each initial deflection value on the y-axis, which allows for obtaining mean values and standard deviations of the experimental data.

4.3.3 Results

The observed and predicted deflections in horizontal and vertical direction can be shown as points on the xy-plane and are depicted together in Fig. 4.13 as a bubble chart. Here horizontal deflection is represented on the axis of abscissae and vertical deflection on the axis of ordinates. The observed data from the experiments is shown as a blue square and they are directly contrasted with the simulation values in the figure. Results from the Weber model are shown as a red x, field-based values as a yellow triangle and deflections obtained with CPO as a purple circle. Additionally, the data points have different sizes for each of the initial offsets and have been labelled with the ratio of v_y/v_e that initially deflected the beam so it would enter the solenoid at different angles, resulting in different deflection values.

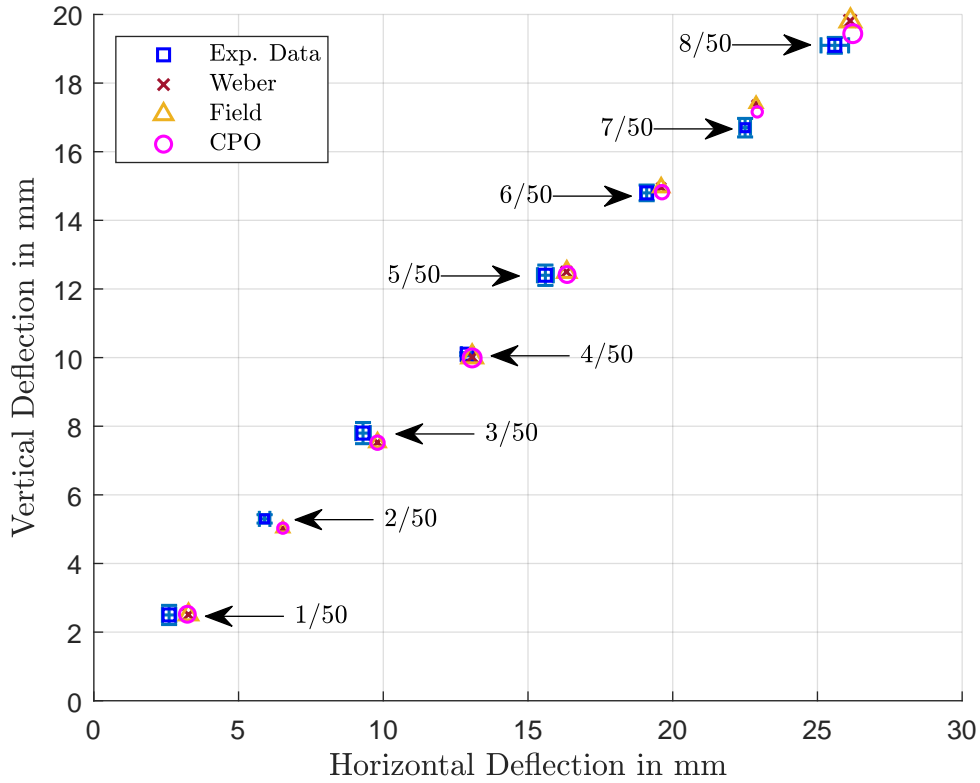


Figure 4.13: Horizontal and vertical deflections of the beam travelling through a solenoid with 290 windings. The blue squares represent experimental data, while the red x shows predicted values from the simulations with the Weber force, the yellow triangle predictions with field theory and the purple circle simulation results from CPO. Each data point is labelled with the respective ratio of v_y/v_e .

From this figure it can be seen that the deflection values follow a trend of increasing

vertical and horizontal deflection that seems to grow linearly for stronger initial offset values. The deflection through the magnetic field is minimal for a vertical velocity of $1/50$ of the electron velocity, but greatest for the maximum offset value of $8/50$ utilised in this experiment. Further, the vertical deflection value y_d can be seen to be nearly half of the initial offset value in mm. The predictions of the three models all follow the overall trend equally well and they are additionally presented in Table 4.3, where numerical values from the simulations can be compared with the observed experimental data readily.

Table 4.3: Deflection results for an electron beam traversing through the 290 turn solenoid showing simulation results for Weber, field and CPO model next to the observed data acquired from experiment.

v_y/v_e	Weber		Field		CPO		Observed	
	x_d	y_d	x_d	y_d	x_d	y_d	x_d	y_d
1/50	3.27	2.51	3.27	2.51	3.23	2.52	2.6(± 0.28)	2.5(± 0.23)
2/50	6.53	5.02	6.53	5.02	6.53	5.03	5.9(± 0.12)	5.3(± 0.18)
3/50	9.80	7.53	9.80	7.53	9.80	7.52	9.3(± 0.31)	7.8(± 0.25)
4/50	13.07	10.02	13.07	10.02	13.07	9.99	12.9(± 0.04)	10.1(± 0.20)
5/50	16.33	12.50	16.34	12.49	16.35	12.42	15.6(± 0.30)	12.4(± 0.27)
6/50	19.60	14.96	19.60	14.96	19.63	14.82	19.1(± 0.23)	14.8(± 0.18)
7/50	22.86	17.40	22.88	17.39	22.92	17.16	22.5(± 0.27)	16.7(± 0.19)
8/50	26.13	19.81	26.14	19.81	26.22	19.44	25.6(± 0.23)	19.1(± 0.48)

From this table and Fig. 4.13 it is clear that all three models, CPO, field and Weber approach give the same deflection results and agree well with measurements for this setup. For the biggest offsets $7/50$ and $8/50$ Weber and field model seem to marginally overestimate the deflection compared to CPO which is very slightly closer to experimental values in these two cases, but with a difference of only about half a millimetre the values are still almost virtually the same. This also indicates that CPO has a slightly better performance for predicting deflections of beams that are deflected or focused inside of solenoids rather than crossing over the outside, as seen earlier in section 4.1.3. But with Weber and field-based model predicting identical deflection results we find agreement with the earlier outcome in section 4.1.3 that field and Weber theory are the same within the low velocity limit, which is a reasonable result.

Further to the 290 turn solenoid where experimental values have been obtained, a short coil with 20 turns was additionally simulated to check the behaviour of the beam

when travelling through an inhomogeneous field. The hypothetical coil has a radius of 52 mm , length 10 mm and is sitting 100 mm away from the emitting electron gun and 75 mm from the anode respectively, with the coordinate system still considered in the centre of the electromagnet. With a current of 1 A and the same offset values for v_y/v_e simulation results are obtained in exactly the same way as described in chapter 4.3.1, the results of which are presented in the following table 4.4.

Table 4.4: Predicted vertical and horizontal deflections for an electron beam traversing through a 20 turn coil where only simulation results are presented for Weber, field and CPO model.

v_y/v_e	Weber		Field		CPO	
	x_d	y_d	x_d	y_d	x_d	y_d
1/50	0.39	4.87	0.39	4.87	0.39	4.87
2/50	0.78	9.73	0.78	9.73	0.78	9.73
3/50	1.17	14.60	1.17	14.60	1.17	14.60
4/50	1.56	19.46	1.56	19.46	1.57	19.46
5/50	1.95	24.33	1.95	24.33	1.96	24.32
6/50	2.34	29.19	2.34	29.19	2.35	29.19
7/50	2.72	34.05	2.73	34.05	2.75	34.05
8/50	3.11	38.91	3.11	38.91	3.15	38.90

It appears from these results that, even though the coil is relatively short with only 20 windings and producing a rather inhomogeneous field, there is barely any noticeable deflection on the beam. As the v_y/v_e ratios correspond to initial offsets in 5 mm steps, the beam is almost not shifted from the vertical y-offset at all. Further, only a slight displacement is predicted for the position on the x-axis, so overall the electron beam is barely moved. Nevertheless, all three models predict very similar deflection values and are in good agreement with each other, which serves to further confirm the similarity of Weber force and field theory.

4.4 Toroids

A Toroid is a coil that is wound on a ring instead of a cylinder, this makes it similar to a solenoid where both of its ends are connected, effectively emulating an infinite solenoid. Due to this property, toroids have little to no magnetic field outside and the field is entirely confined on the inside and they respectively have little to no leakage fields [308].

This characteristic of toroidal transformers is beneficial in applications where leakage flux is undesired, e.g. in audio systems, as compared to other transformers with rectangular cross sections. However, this can also be disadvantageous for high-power applications where a larger leakage inductance is desired, and applications and design are discussed in [309].

This chapter will investigate the influence of toroids on electron beams travelling outside of the electromagnet, with the limitation that the field is produced by a steady DC-current. Initially the expectation is that there is no significant influence on the beam due to the magnetic field being confined inside of the toroid. Nevertheless, it has been considered by Hernandez *et al.* [310] that a steady poloidal current still produces an electric field around the toroid and this can potentially have an effect on the electron beam passing by the toroid.

4.4.1 Modelling

In order to predict how an electron beam will behave due to a toroid, a Weber and field-based model have been derived for this situation. The models share some similarities with the previous modelling approaches and use equations of motions again to describe the beam, but they have of course also been modified to fit the toroid geometry. To this end the parametrisation of a toroid in Cartesian coordinates is a valuable tool and will be explained in the following section and another mathematical summary thereof can be found in appendix B.

4.4.1.1 Weber Model To calculate the interactions of the current in the toroid with the electrons in the beam we first have to define positions and velocities for the particles. The toroid itself has a radius R_1 that defines the size of the individual turns and a radius R_2 that defines the size of the ring the individual turns follow. Therefore, a Cartesian coordinate system is placed in the centre of the toroid, where the angle θ is locally defined to describe the smaller radius R_1 and the angle φ is chosen between the x- and the z-axis, with which the bigger circle of radius R_2 can be described. This geometry can be seen in Fig. 4.14.

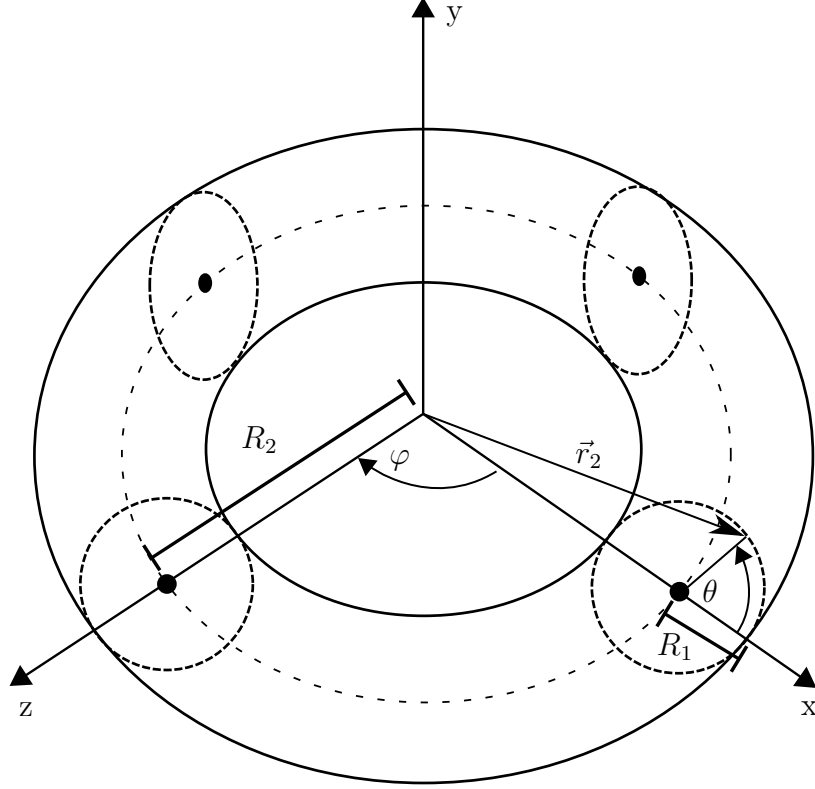


Figure 4.14: A toroid centred on a Cartesian coordinate system, it can be parametrised with the help of radii R_1 and R_2 . Here, θ is defined as the local angle within the smaller circle of size R_1 , and ϕ is defined as an azimuthal angle between x - and z -axes.

The beam is then allowed to have any arbitrary initial position \vec{r}_1 and can define the position of a current element \vec{r}_2 within the toroid wire through the parametrisation of the toroid, with the chosen geometry this leads to

$$\vec{r}_1 = \begin{pmatrix} x_1 \\ y_1 \\ z_1 \end{pmatrix} \quad \vec{r}_2 = \begin{pmatrix} (R_2 + R_1 \cos(\theta)) \cos(\phi) \\ R_1 \sin(\theta) \\ (R_2 + R_1 \cos(\theta)) \sin(\phi) \end{pmatrix}, \quad (4.52)$$

$$\vec{r}_{12} = \begin{pmatrix} x_1 - (R_2 + R_1 \cos(\theta)) \cos(\phi) \\ y_1 - R_1 \sin(\theta) \\ z_1 - (R_2 + R_1 \cos(\theta)) \sin(\phi) \end{pmatrix}, \quad (4.53)$$

$$r_{12} = \sqrt{(x_1 - (R_2 + R_1 \cos(\theta)) \cos(\phi))^2 + (y_1 - R_1 \sin(\theta))^2 + (z_1 - (R_2 + R_1 \cos(\theta)) \sin(\phi))^2}. \quad (4.54)$$

Further to the arbitrary initial position of the beam, it will also be allowed to have any desired velocity \vec{v}_1 . For this particular model, we will follow a summation approach so that the toroid is considered as a stack of individual loops that follow along the radius R_2 . This means that we can find the velocity components for the electrons in a current element as \vec{v}_2 , giving

$$\vec{v}_1 = \begin{pmatrix} v_{1x} \\ v_{1y} \\ v_{1z} \end{pmatrix}, \quad \vec{v}_2 = \begin{pmatrix} -(v_2 \sin(\theta)) \cos(\varphi) \\ v_2 \cos(\theta) \\ -(v_2 \sin(\theta)) \sin(\varphi) \end{pmatrix}, \quad \vec{v}_{12} = \begin{pmatrix} v_{1x} + (v_2 \sin(\theta)) \cos(\varphi) \\ v_{1y} - v_2 \cos(\theta) \\ v_{1z} + (v_2 \sin(\theta)) \sin(\varphi) \end{pmatrix}. \quad (4.55)$$

These positions and velocities can now be used to calculate the forces \vec{F}_{2-1-} , between beam electrons and current electrons, and \vec{F}_{2+1-} , between beam electrons and lattice charges, where the lattice charges have a velocity of zero, as they are stationary. This allows us to calculate the Weber force on the electron beam due to the current similar to the previous models, utilising the same assumptions of $v_1 \gg v_2$, negligible acceleration terms and transitioning to continuous current elements:

$$\begin{aligned} \vec{F}_w = \frac{q_1 + R_1 I}{4\pi\epsilon_0 c^2} \int_0^{2\pi} \frac{\vec{r}_{12}}{r_{12}^3} \left\{ -\frac{3}{r_{12}^2} [(v_{1x} \sin(\theta) \cos(\varphi))(x_1 - (R_2 + R_1 \cos(\theta)) \cos(\varphi))^2 \right. \\ + (v_{1y} \sin(\theta) \cos(\varphi) - v_{1x} \cos(\theta))(x_1 - (R_2 + R_1 \cos(\theta)) \cos(\varphi))(y_1 - R_1 \sin(\theta)) \\ - (v_{1y} \cos(\theta))(y_1 - R_1 \sin(\theta))^2 + (v_{1z} \sin(\theta) \cos(\varphi) + v_{1x} \sin(\theta) \sin(\varphi)) \\ \cdot (x_1 - (R_2 + R_1 \cos(\theta)) \cos(\varphi))(z_1 - (R_2 + R_1 \cos(\theta)) \sin(\varphi)) \\ + (-v_{1z} \cos(\theta) + v_{1y} \sin(\theta) \sin(\varphi))(y_1 - R_1 \sin(\theta))(z_1 - (R_2 + R_1 \cos(\theta)) \sin(\varphi)) \\ \left. + (v_{1z} \sin(\theta) \sin(\varphi))(z_1 - (R_2 + R_1 \cos(\theta)) \sin(\varphi))^2 \right] \\ + [v_{1x} \sin(\theta) \cos(\varphi) - v_{1y} \cos(\theta) + v_{1z} \sin(\theta) \sin(\varphi)] \Big\} d\theta. \end{aligned} \quad (4.56)$$

The integration along θ from 0 to 2π gives the force for an individual loop and is carried out in the *MATLAB* simulation with the trapezium rule and 0.5° step size. This force is calculated for each individual loop at its respective position along the toroid, where the position is given through the azimuthal angle $\varphi = [0, 2\pi]$. Through this angle the positions of the individual loops are set in discrete steps of $\frac{2\pi}{N}$, where N is the number of turns in the toroid, which allows to calculate the sum of the individual forces on the electron beam as

$$\vec{F}_{sum} = \sum_{\varphi=0}^{2\pi} \vec{F}_w. \quad (4.57)$$

This gives the total force of the toroid on the beam and is consequently obtained at every time step of the simulation to predict the trajectory of the beam. Similar to the previous model where the beam was traversing through the solenoid, the simulation is again transformed into the time domain to calculate the acceleration on the beam electrons and

update the positions and velocities with the same equations of motion for each following time step. This way the deflection of the beam at the detector screen can be obtained.

Next to the summation model, a simulation model based on helical motion of the current has been tested, but this approach predicted extremely large deflections in the vicinity of the toroid, which is presumably due to artificial asymmetries introduced into the model by the helical motion for the toroid. As this is in contradiction with the expected zero deflection, this unphysical result is a shortcoming of that particular model, but could be overcome by using the summation model.

4.4.1.2 Field Model A field model has been derived to predict the influence of the toroid on the electron beam that follows in parts the approach taken in [311]. The Biot-Savart law will be used to derive an expression for the magnetic field of the toroid that is then used with the Lorentz force to calculate the action on the beam. As the toroid is supplied with a steady DC current of fixed magnitude, the current can be taken outside of the integrand and the Biot-Savart law can be written as

$$\vec{B}_{Toroid} = \frac{\mu_0 I}{4\pi} \int \frac{d\vec{l} \times \vec{r}_{12}}{|\vec{r}_{12}|^3}. \quad (4.58)$$

Here, \vec{r}_1 is the position of the electrons in the beam and \vec{r}_2 is the position of the current element in the toroid, so that we have, with the same coordinate system as in Fig. 4.14,

$$\vec{r}_1 = \begin{pmatrix} x_1 \\ y_1 \\ z_1 \end{pmatrix}, \quad \vec{r}_2 = \begin{pmatrix} (R_2 + R_1 \cos(\theta)) \cos(\varphi) \\ R_1 \sin(\theta) \\ (R_2 + R_1 \cos(\theta)) \sin(\varphi) \end{pmatrix}. \quad (4.59)$$

We can then find $d\vec{l}$ as the derivation of the position of the current element:

$$d\vec{l} = \begin{pmatrix} \frac{\partial x_2}{\partial \theta} \\ \frac{\partial y_2}{\partial \theta} \\ \frac{\partial z_2}{\partial \theta} \end{pmatrix} = \begin{pmatrix} \frac{\partial x_2}{\partial \theta} + \frac{\partial x_2}{\partial \varphi} + \frac{\partial x_2}{\partial \rho} \\ \frac{\partial y_2}{\partial \theta} + \frac{\partial y_2}{\partial \varphi} + \frac{\partial y_2}{\partial \rho} \\ \frac{\partial z_2}{\partial \theta} + \frac{\partial z_2}{\partial \varphi} + \frac{\partial z_2}{\partial \rho} \end{pmatrix}, \quad (4.60)$$

where ρ is the radial coordinate defined by the magnitude $\rho = \sqrt{x^2 + y^2 + z^2}$. That leaves the differential line element as

$$d\vec{l} = \begin{pmatrix} -R_1 \sin(\theta) \cos(\varphi) d\theta - \sin(\varphi) (R_2 + R_1 \cos(\theta)) d\varphi \\ R_1 \cos(\theta) d\theta \\ -R_1 \sin(\theta) \sin(\varphi) d\theta + \cos(\varphi) (R_2 + R_1 \cos(\theta)) d\varphi \end{pmatrix}. \quad (4.61)$$

We can then extract $d\theta$ from the brackets and find with the help of the winding ratio the relation between the angles θ and φ

$$\varphi = \frac{\theta}{N} \quad \rightarrow \quad \frac{d\varphi}{d\theta} = \frac{1}{N}, \quad (4.62)$$

where N is the number of windings on a single wound toroid. This relation (4.62) is substituted into (4.61) and only an integration along θ is left. Following this, $d\vec{l}$ is substituted back into the Biot-Savart-law (4.58) and the cross product can be calculated to obtain the magnetic field:

$$\vec{B}_{Toroid} = \frac{\mu_0 I}{4\pi} \int_0^{N2\pi} \frac{1}{|\vec{r}_{12}|^3} \begin{pmatrix} X_T \\ Y_T \\ Z_T \end{pmatrix} d\theta, \quad (4.63)$$

where

$$\begin{aligned} X_T = & R_1 \cos(\theta)(z_1 - (R_2 + R_1 \cos(\theta)) \sin(\varphi)) \\ & - (-R_1 \sin(\theta) \sin(\varphi) + \cos(\varphi)(R_2 + R_1 \cos(\theta)) \frac{1}{N})(y_1 - R_1 \sin(\theta)) \end{aligned} \quad (4.64)$$

$$\begin{aligned} Y_T = & (-R_1 \sin(\theta) \sin(\varphi) + \cos(\varphi)(R_2 + R_1 \cos(\theta)) \frac{1}{N})(x_1 - (R_2 + R_1 \cos(\theta)) \cos(\varphi)) \\ & - (-R_1 \sin(\theta) \cos(\varphi) - \sin(\varphi)(R_2 + R_1 \cos(\theta)) \frac{1}{N})(z_1 - (R_2 + R_1 \cos(\theta)) \sin(\varphi)) \end{aligned} \quad (4.65)$$

$$\begin{aligned} Z_T = & (-R_1 \sin(\theta) \cos(\varphi) - \sin(\varphi)(R_2 + R_1 \cos(\theta)) \frac{1}{N})(y_1 - R_1 \sin(\theta)) \\ & - R_1 \cos(\theta)(x_1 - (R_2 + R_1 \cos(\theta)) \cos(\varphi)) \end{aligned} \quad (4.66)$$

The integration for θ is carried out from 0 to $N2\pi$ to account for the total number of windings of the toroid and φ is replaced with $\frac{\theta}{N}$ according to (4.62). After the magnetic field is obtained it is respectively used to calculate the Lorentz force, where the simulation is transformed to the time domain as in previous models and the field and force calculated at every time step. With this the positions of the beam can be updated for the next time step up to the beam being intercepted by the detector screen.

4.4.2 Results

The simulations were carried out with electrons at 2000 eV, similar to all previous calculations. Both the summation based Weber model and the field model predict an effective zero deflection for a beam passing through a given toroid, or at most on the order of 1×10^{-5} m. As the field is confined mostly to the inside of the toroid and near zero outside, this is consistent with the expectation of negligible deflection of the beam.

A test was carried out to examine the influence of the toroid on the beam experimentally, where a toroid was placed around the glass body of the CRT described in previous chapters, so that the beam would pass through the central hole of the toroid. No significant beam deflection could be observed upon supplying current to the toroid, although a minimal displacement of the beam was noted, which is suspected to originate from an electric field influence. However, with the current setup, the given number of windings, the magnitude of current and slow electrons, the deflection due to the electric field was barely quantifiable and no useful results could be obtained. It could also not be clarified in experiment if the electric field was the intrinsic field caused due to the current (which is strongest close to the origin of current supply according to Hernandez *et al.* [310]) or due to winding inconsistencies in the toroid itself. While the author of the present work believes that the observed disturbance of the beam was caused by an electric field in nature, the influence was small in this case and future research is needed to quantify the influence of the electric field in a charged particle scenario. Still, no magnetic influence on the beam outside the toroid was found, which agrees well with expectations and simulations.

5 Unipolar Induction with Weber Electrodynamics

The phenomenon of unipolar induction was first discovered by Michael Faraday [312] after his prior discovery of the general principle of electromagnetic rotation [313]. This was, of course, one of the most important discoveries during the early 19th century as it would lead to the development of the electromagnetic motor and generator. Faraday continued to investigate a generator configuration comprising a conducting disk rotating around its cylindrical axis in the magnetic field of one pole of a bar magnet. As only one magnetic pole is involved in the induction of a voltage, the term unipolar induction (or sometimes homopolar induction) was coined by Weber [314] and the apparatus is also often referred to as a Faraday generator or homopolar generator. Figure 5.1 depicts a typical configuration for a unipolar induction machine, with either a magnet (usually a permanent bar magnet) or electromagnet (e.g. a solenoid or coil), a disk and a measurement device, a voltmeter in this case, forming the circuit ABCDA.

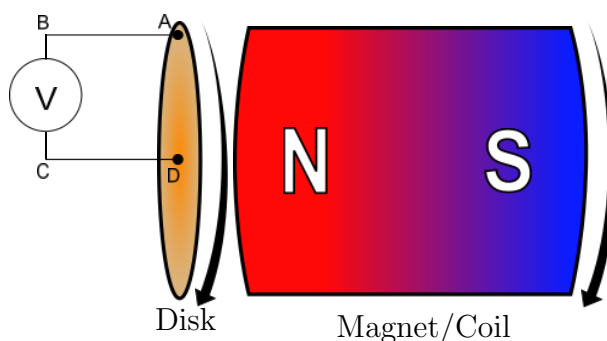


Figure 5.1: Sketch of a unipolar induction machine (also known as a Faraday generator), comprising a permanent magnet, a conducting metal disk and a measurement device (in this case a voltmeter).

The phenomenon of unipolar induction is also titled “Faraday’s paradox” and is debated among scientists and engineers even to this day with no clear consensus as to how the observed voltage is physically caused and what the underlying mechanism of induction is. In this regard, physicists are divided about the seat of induction, if the magnetic field co-rotates with the magnet or if it remains stationary upon the magnet’s rotation, and about the applicability of Faraday’s flux rule. This chapter aims to investigate the phenomenon further, based on theoretical aspects of Weber’s direct-action theory and conducting experiments to test the theory, and addressing the questions about the seat

of induction and rotation of the magnetic field.

First, we will have to recall the phenomenon and the usually discussed situations that involve disk and magnet spinning around their axes, these are categorised as:

- (i) The disk is rotating and the magnet remains stationary. A voltage can be measured across the radius of the disk.
- (ii) The disk remains stationary and the magnet rotates. No voltage can be measured across the disk.
- (iii) Both disk and magnet rotate at the same speed and direction, and again a voltage is observed across the disk.

Originally, Faraday imagined the field lines of the magnet remaining stationary when the magnet rotates and it is the disk (DA) cutting the field lines that is responsible for the appearance of an Electromotive Force (EMF). At a later point he changed his mind and instead considered the field lines as co-rotating with the magnet. In this case it is the cutting of the external part of the circuit, the closing wire and measurement device (BC), that results in an induced voltage. It seems like a logical deduction on Faraday's part to regard the field lines as co-rotating when one considers rectilinear motion of a magnet, where the field must clearly follow the magnet's movement. Or similarly, one could consider a horseshoe magnet rotating or a bar magnet rotating around any other axis apart from its cylindrical one – it seems only logical that the field lines would follow the movement of the poles. However, if that is the case, then it also appears odd that a voltage is not induced in case (ii) where the magnet is rotating on its own. On the other hand the one-piece Faraday generator (where the disk and magnet always rotate in unison, e.g. as a conducting magnet) has been interpreted as the field remaining stationary upon rotation and the magnet cutting its own field lines, as researched by Crooks *et al.* [315]. This creates an apparent paradox: unipolar induction seems better explained with the field remaining stationary upon the magnet's rotation, but there are obvious other situations where the magnetic field must follow the magnet's movement.

Additionally, a contradiction with Faraday's flux rule is often discussed, with the flux rule stating

$$V = -\frac{d\Psi}{dt} \quad (5.1)$$

meaning that a varying magnetic field induces a voltage, V , with Ψ being the magnetic flux. Since the field of the bar magnet is rotationally symmetric, there is no obvious change in magnetic flux, yet a voltage is induced across the disk despite the lack of change, which seems to violate the flux rule. However, much of this confusion can be avoided when the (5.1) is restated as the general case

$$V = \oint_C \vec{E} \cdot d\vec{l} = \oint_C (\vec{v} \times \vec{B}) \cdot d\vec{l} - \frac{\partial}{\partial t} \oint_S \vec{B} \cdot d\vec{S} \quad (5.2)$$

as reviewed in [316]. Due to the relationship (5.1), Feynman went as far as to label unipolar induction as an exception to the flux rule [197]. There also exist a number of other paradoxes that fall into the same category of violating the flux rule, e.g. Hering's paradox [317,318] and Cullwick's experiment [79,319], but it seems particularly interesting that the paradox surrounding unipolar induction is linked to the rotation around the symmetry axis. If we consider the example of the horseshoe magnet again, spinning its poles in succession, there would be no doubt that the field moves and follows accordingly with the position of the poles. This is further exemplified by an investigation of Leus and Taylor [316] where a quadrupole magnet was rotated and it was concluded that the field rotates with the magnet. So unipolar induction seems to be a special case of rotation that creates a paradox because the rotation happens around the field's symmetry axis. But even further than this peculiarity, there is a fundamental underlying question related to these paradoxes, that is whether the electromagnetic field is physically real or not? If the field is not a tangible physical entity then a discussion about its movement with the magnet cannot be had, as it is not real and discussing its movement is meaningless. Instead, if it is only a mathematical tool then it is rather the motion of charges that give rise to the hypothetical field responsible for the observed phenomenon. It seems therefore feasible to investigate unipolar induction, as a typical low velocity application involving

rotating magnetic fields, from a Weber-perspective, and probe what deductions can be made about the phenomenon, the seat of induction and the magnetic field from this point of view.

As unipolar induction is roughly 190 years old by now, the phenomenon has been repeatedly treated in the literature, theoretically as well as experimentally. Different explanations have been proposed and discussed, but between both experimentalists and theorists there largely seem to be two popular view points: (i) the Moving Field Hypothesis (MFH), which regards the field lines as co-rotating with the magnet and (ii) the Stationary Field Hypothesis (SFH), which maintains the field lines as stationary upon the magnet's rotation. SFH has support [55, 66, 197, 320–327] as well as has MFH [316, 328–332]. But other discussions exist about the applicability of Faraday's law, especially with Feynman taking the position that it is not applicable [197, 333, 334], as well as others taking the contrary stance that it is applicable [322, 335, 336]. It has been further argued that SRT explains the phenomenon [79, 337–340] with the counter-argument that SRT cannot be used in rotating frames of reference [341] and instead GRT must be used [322, 342], and even quantum mechanical approaches exist [343–345]. For a further discussion of explanations for unipolar induction based on SRT, a review by Bordoni [346] is recommended. Special focus is given to the Wilson experiments [347, 348] on induction in a rotating dielectric in a magnetic field, and the Einstein-Laub paper [349]. On this matter the views of Laue, Föppl and Becker are summarised, which are in support of a special relativistic explanation of unipolar induction.

The problem has also been analysed mathematically by different authors, showing that the EMF and induced voltage can be obtained in several ways [350–354]. Especially the review by McDonald focuses on the correct formulation of Faraday's law and restates its applicability [354]. Among the theoretical explanations, an approach exists by Montgomery [355, 356] where instead of the magnetic field, the motion of the conductor charges and energy conservation are considered in order to predict the EMF. Further to this charge based approach, unipolar induction has of course seen treatment with Weber electrodynamics [48, 63, 128, 357, 358] and Weber himself derived Faraday's law from

his force formula [48, 63, 357] as was acknowledged by Maxwell in his *Treatise* [1, article 856, p. 486]. Wesley has also shown how Weber’s force can predict unipolar induction in general [128], and more recently, Weber’s force has been successfully applied specifically to a spinning disk and stationary electromagnet setup by the author [358], which will be further explained in section 5.1.

Next to the extensive theoretical treatments, several experimental studies have tried to investigate the phenomenon of unipolar induction, Faraday’s law, rotating magnetic fields and related topics [312, 315, 316, 330, 333, 338, 339, 341, 359–373] and an even more extensive list of references regarding the phenomenon can be found in McDonald’s review [354]. Despite these many studies and great efforts the results are still inconclusive as to whether MFH or SFH is correct. Supporting evidence for MFH has been reported from recent investigations [316, 330], whereas other recent results support SFH [371–373] and the debate is still ongoing.

Kelly [330] has tested unipolar induction with special focus on the return wire, the wire was arranged in such a way that it would run partially parallel to the disk and form what he called a “zig-zag” pattern. He reports a reduction of magnitude in observed EMF and claims this can only be explained with the magnetic field lines cutting the multiple wire segments upon their rotation. This leads to locally opposing EMFs from one wire segment to the next, resulting in an overall effective reduction of the magnitude as the flow of current is reduced by the segments that are polarised in the same direction by the magnetic field.

However, Macleod [371] has challenged these findings and reports that different wire routing configurations have been tested in an attempt to repeat Kelly’s experiments, but are found to be not reproducible and no form of wire routing had any influence on the measurement results. Even so, Macleod did not report exactly how and what configurations of wire routing were tested and if Kelly’s setup was recreated or if the routing was tested with Macleod’s original setup. The original setup of Macleod was a twin-disk assembly where a ring magnet was attached to each disk so that they would be in opposite polarity. With this the voltages induced in the disks could be measured

individually and combined. From the results of these measurements, Macleod concluded that the observations agreed with the field remaining stationary.

In the experiments of Leus and Taylor [316] a ring magnet and annular iron yoke with an air gap were rotated in unison to measure induced voltages. A stationary probe through the air gap connected a voltmeter outside to a copper cylinder sitting inside the ring magnet, but isolated from the same. The cylinder was connected inside of the assembly to a brass ring sitting at the opposite end of the magnet and the brass ring was in turn connected to the voltmeter. Additionally, they rotated a quadrupole ring magnet and used a current loop to observe the induction. From the results obtained they conclude that the field is spinning with the magnet.

Müller [372] has experimented with an assembly where conducting magnets would perform oscillatory motions – instead of a full rotation, they would only rotate back and forth on a short circular arc. The magnets were situated in a yoke confining the magnetic field, so that the external part of the circuit was effectively shielded from the field. The external part was then connected to an amplifier circuit and measurements of the induced voltages taken. From the results Müller concluded that the field remains stationary upon the magnet’s rotation.

The same conclusion was reached by Chen *et al.* [373], after investigating a twin-disk setup. Each disk was sitting next to a ring magnet and could rotate in opposite directions, either independently with the magnets remaining stationary or rotating together with the magnets in unison. They measured the induced voltages for individual and combined rotations and found that their results agreed with the field remaining stationary.

Further, from a slightly older investigation, Valone [374] has devised a one-piece Faraday generator where he allowed the measurement device to rotate with the conducting magnets. He utilised a circuit with an indicator LED for threshold voltage detection. The circuit was designed so that the LED would be powered continuously by a battery, only when a voltage over an arbitrarily chosen threshold of 15 mV in his apparatus was exceeded would the LED turn off, signalling the presence of a potential difference. First the detection circuit was kept stationary and upon connecting it to the spinning magnets,

a voltage was detected. Next he attached the detector to the magnets so that they would spin in unison and no voltage was detected. Although Valone does not comment on this result in regards to the motion of the field itself, he still states his opinion that the field remains stationary upon rotation in the introduction of the same work.

But from only the recent experiments summarised here, it can be seen that there exists supporting evidence for MFH and SFH in the literature and no clear conclusion can be drawn about which hypothesis is correct and the debate remains ongoing. But instead of only focussing on the field, Assis and Thober [194] have further analysed unipolar induction from the perspective of Weber's theory and they have put emphasis on a part that is often overlooked in the discussions surrounding the field: the closing wire (BC) of the circuit. They state that when the entire circuit ABCDA is taken into account, the appearance of an EMF will be determined solely by relative motion between the disk (DA) and the closing wire (respectively measurement device (BC)). As this can correctly predict the typically discussed cases i), ii) and iii) this seems a promising approach and the influence of the closing wire will be researched further in this work.

To investigate unipolar induction using Weber electrodynamics, this chapter is divided into two main parts for better presentation and to investigate specific aspects of the phenomenon. First, in section 5.1, we will assume the measurement device (BC) to be always stationary, where mathematical models are derived and quantitative measurements are carried out to compare predicted induction values with experiments. Following, in section 5.2, the measurement device (BC) will be allowed to rotate to investigate qualitatively the influence of the closing wire and a novel experimental design is devised to test the claims of Assis and Thober. Finally, after reporting those results it will be discussed what insights have been gained and what implications can be derived for the general phenomenon of unipolar induction.

5.1 Stationary Detector

First we will focus on unipolar induction with the restriction of the measurement device (BC) always being stationary in the laboratory reference frame. With this we will consider

unipolar induction with the help of Weber electrodynamics and see how Weber's force can mathematically model the induced voltage. Similarly, a field based model is derived and subsequently experiments carried out with a Faraday generator to obtain data against which the predictions will be compared.

5.1.1 Mathematical Modelling

This section will focus on the modelling used to predict the induced voltages in a Faraday generator where the magnet and measurement device are kept stationary and only the disk is allowed to rotate. We will first show the direct-action approach based on Weber electrodynamics, which is then followed by the calculations employing field theory and the respective magnetic field \vec{B} of the magnet.

5.1.1.1 Weber Model Unipolar induction has previously been related to and analysed with Weber electrodynamics in the literature [48, 63, 128, 357, 358], and Weber himself derived Faraday's law from his force formula [48, 63, 357], which was acknowledged by Maxwell in his *Treatise* [1, article 856, p. 486]. Wesley has also shown in a more general fashion how Weber's force can predict unipolar induction [128], but without applying it to any specific case or setup. However, the present author believes that such considerations are necessary since the distribution of charges is paramount to the Weber force and might also be especially important when trying to predict other types of induction phenomena. The Weber model in this chapter and associated experiment as well as results have previously been published in [358], and the derivations will follow the same structure.

For a stationary coil and spinning disk, we consider the charges both in the disk and the coil. For any arbitrary coil centred on the origin of a Cartesian coordinate system we can use the Weber force in the laboratory reference frame and determine the usual vectorial quantities according to Figure 5.2.

As in the previous sections modelling solenoids (sec. 4.1.1.1), a continuous current I flows through a coil with radius R_1 , length L and number of windings N in helical motion, with the negative charge of the current q_{1-} moving and the positive lattice charge q_{1+} stationary. The disk next to the coil has a radius R_2 and the charges are equally

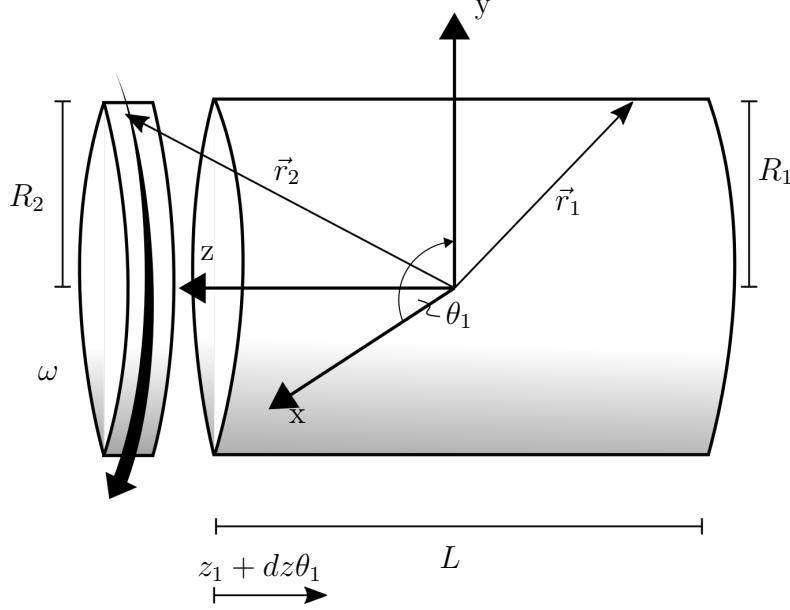


Figure 5.2: Diagram of coil geometry with radius R_1 and length L centred on a Cartesian coordinate system. A disk with radius R_2 is spinning with angular velocity ω and positioned on the z -axis at z_2 . Vectors \vec{r}_1 and \vec{r}_2 describe the position of charges in the coil or disk with the help of polar angles θ_1 and θ_2 , where θ_2 is the polar angle in the plane of the disk.

distributed, and we can designate the positions:

$$\vec{r}_1 = \begin{pmatrix} R_1 \cos(\theta_1) \\ R_1 \sin(\theta_1) \\ z_1 - dz\theta_1 \end{pmatrix}, \quad \vec{r}_2 = \begin{pmatrix} R_2 \cos(\theta_2) \\ R_2 \sin(\theta_2) \\ z_2 \end{pmatrix}, \quad (5.3)$$

$$\vec{r}_{12} = \vec{r}_1 - \vec{r}_2 = \begin{pmatrix} R_1 \cos(\theta_1) - R_2 \cos(\theta_2) \\ R_1 \sin(\theta_1) - R_2 \sin(\theta_2) \\ z_1 - z_2 - dz\theta_1 \end{pmatrix}, \quad (5.4)$$

$$r_{12} = |\vec{r}_1 - \vec{r}_2|. \quad (5.5)$$

Due to the disk's rotation its charges q_{2+} and q_{2-} will move with angular velocity ω ; and the negative charge of a current element q_{1-} travelling through the coil will move with velocity \vec{v}_1 , so that we obtain:

$$\vec{v}_1 = \begin{pmatrix} -v_1 \sin(\theta_1) \\ v_1 \cos(\theta_1) \\ -v_1 dz/R_1 \end{pmatrix}, \quad \vec{v}_2 = \begin{pmatrix} -\omega R_2 \sin(\theta_2) \\ \omega R_2 \cos(\theta_2) \\ 0 \end{pmatrix}, \quad (5.6)$$

$$\vec{v}_{12} = \begin{pmatrix} -v_1 \sin(\theta_1) + \omega R_2 \sin(\theta_2) \\ v_1 \cos(\theta_1) - \omega R_2 \cos(\theta_2) \\ -v_1 dz/R_1 \end{pmatrix}, \quad (5.7)$$

while the lattice charges q_{1+} in the coil remain at rest, so their velocity is zero.

For the acceleration terms in this case we can find that \vec{a}_1 -terms, seen by the current element's negative charges due to the helical motion, are negligibly small, since $R_1\vec{a}_1 \ll \omega R_2$ and any acceleration terms \vec{a}_2 of charges in the disk cancel out in the calculations.

Based on the distribution of the charges q_{1+} , q_{1-} , q_{2+} and q_{2-} in the coil and in the disk we can formulate the four interaction forces \vec{F}_{2-1-} , \vec{F}_{2+1-} , \vec{F}_{2-1+} , \vec{F}_{2+1+} to predict the induced voltage. Of these, the forces \vec{F}_{2+1-} , \vec{F}_{2+1+} are acting on the lattice charges of the disk and thus they will be counteracted by the lattice itself. However, the electrons in the disk are free to move and so the forces \vec{F}_{2-1-} , \vec{F}_{2-1+} will act on them accordingly:

$$\begin{aligned} \vec{F}_{2-1-} = & \frac{q_1 q_2}{4\pi\epsilon_0} \frac{\vec{r}_{12}}{r_{12}^3} \left\{ 1 - \frac{3}{2c^2} \frac{1}{r_{12}^2} \left[\begin{pmatrix} R_1 \cos(\theta_1) - R_2 \cos(\theta_2) \\ R_1 \sin(\theta_1) - R_2 \sin(\theta_2) \\ z_1 - z_2 - dz\theta_1 \end{pmatrix} \begin{pmatrix} -v_1 \sin(\theta_1) + \omega R_2 \sin(\theta_2) \\ v_1 \cos(\theta_1) - \omega R_2 \cos(\theta_2) \\ -v_1 dz/R_1 \end{pmatrix} \right]^2 \right. \\ & + \frac{1}{c^2} \left(\begin{pmatrix} -v_1 \sin(\theta_1) + \omega R_2 \sin(\theta_2) \\ v_1 \cos(\theta_1) - \omega R_2 \cos(\theta_2) \\ -v_1 dz/R_1 \end{pmatrix} \begin{pmatrix} -v_1 \sin(\theta_1) + \omega R_2 \sin(\theta_2) \\ v_1 \cos(\theta_1) - \omega R_2 \cos(\theta_2) \\ -v_1 dz/R_1 \end{pmatrix} \right) \\ & \left. + \begin{pmatrix} R_1 \cos(\theta_1) - R_2 \cos(\theta_2) \\ R_1 \sin(\theta_1) - R_2 \sin(\theta_2) \\ z_1 - z_2 - dz\theta_1 \end{pmatrix} \begin{pmatrix} a_{1x} - a_{2x} \\ a_{1y} - a_{2y} \\ a_{1z} - a_{2z} \end{pmatrix} \right\}, \end{aligned} \quad (5.8)$$

$$\begin{aligned} \vec{F}_{2-1+} = & -\frac{q_1 q_2}{4\pi\epsilon_0} \frac{\vec{r}_{12}}{r_{12}^3} \left\{ 1 - \frac{3}{2c^2} \frac{1}{r_{12}^2} \left[\begin{pmatrix} R_1 \cos(\theta_1) - R_2 \cos(\theta_2) \\ R_1 \sin(\theta_1) - R_2 \sin(\theta_2) \\ z_1 - z_2 - dz\theta_1 \end{pmatrix} \begin{pmatrix} \omega R_2 \sin(\theta_2) \\ -\omega R_2 \cos(\theta_2) \\ 0 \end{pmatrix} \right]^2 \right. \\ & + \frac{1}{c^2} \left(\begin{pmatrix} \omega R_2 \sin(\theta_2) \\ -\omega R_2 \cos(\theta_2) \\ 0 \end{pmatrix} \begin{pmatrix} \omega R_2 \sin(\theta_2) \\ -\omega R_2 \cos(\theta_2) \\ 0 \end{pmatrix} \right) \\ & \left. + \begin{pmatrix} R_1 \cos(\theta_1) - R_2 \cos(\theta_2) \\ R_1 \sin(\theta_1) - R_2 \sin(\theta_2) \\ z_1 - z_2 - dz\theta_1 \end{pmatrix} \begin{pmatrix} -a_{2x} \\ -a_{2y} \\ -a_{2z} \end{pmatrix} \right\}. \end{aligned} \quad (5.9)$$

The total force on the electrons is then given as the sum:

$$F_{sum} = \vec{F}_{2-1-} + \vec{F}_{2-1+}. \quad (5.10)$$

We can once again transition from discrete charges $q_1 v_1$ to continuous current elements $IR_1 d\theta_1$ and utilise the assumption $\omega R_2 \gg v_1$, since the conduction electrons in the coil are much slower than the electrons moving with the disk, which holds

$$\begin{aligned}
 \vec{F}_w = \frac{Iq_2R_1}{4\pi\epsilon_0c^2} \frac{\vec{r}_{12}}{r_{12}^3} \left\{ -\frac{3}{2} \frac{1}{r_{12}^2} \left[-2\omega R_2 \sin(\theta_1) \sin(\theta_2) (R_1 \cos(\theta_1) - R_2 \cos(\theta_2))^2 \right. \right. \\
 + (2\omega R_2 \cos(\theta_1) \sin(\theta_2) + 2\omega R_2 \sin(\theta_1) \cos(\theta_2)) (R_1 \cos(\theta_1) - R_2 \cos(\theta_2)) (R_1 \sin(\theta_1) - R_2 \sin(\theta_2)) \\
 \left. \left. - 2\omega R_2 \cos(\theta_1) \cos(\theta_2) (R_1 \sin(\theta_1) - R_2 \sin(\theta_2))^2 \right] \right. \\
 \left. + [-2\omega R_2 \sin(\theta_1) \sin(\theta_2) - 2\omega R_2 \cos(\theta_1) \cos(\theta_2)] \right\} d\theta_1.
 \end{aligned} \tag{5.11}$$

From the force (5.11) acting on the electrons, the corresponding EMF can be obtained by dividing the equation by q_2 and integrating along the disk's radius R_2 , as this is the path along which the potential difference manifests and the voltage can be measured, giving

$$\begin{aligned}
 EMF = \int_0^{R_{disk}} \int_0^{N \cdot 2\pi} \frac{I\omega R_1 R_2}{4\pi\epsilon_0c^2} \frac{\vec{r}_{12}}{r_{12}^3} \left\{ -\frac{3}{2} \frac{1}{r_{12}^2} \left[-2\sin(\theta_1) \sin(\theta_2) (R_1 \cos(\theta_1) - R_2 \cos(\theta_2))^2 \right. \right. \\
 + (2\cos(\theta_1) \sin(\theta_2) + 2\sin(\theta_1) \cos(\theta_2)) (R_1 \cos(\theta_1) - R_2 \cos(\theta_2)) (R_1 \sin(\theta_1) - R_2 \sin(\theta_2)) \\
 \left. \left. - 2\cos(\theta_1) \cos(\theta_2) (R_1 \sin(\theta_1) - R_2 \sin(\theta_2))^2 \right] \right. \\
 \left. + [-2\sin(\theta_1) \sin(\theta_2) - 2\cos(\theta_1) \cos(\theta_2)] \right\} d\theta_1 dR_2.
 \end{aligned} \tag{5.12}$$

Formulation (5.12) predicts the induced voltage for any arbitrary stationary coil and rotating disk at any position \vec{r}_2 in a typical Faraday-generator (Fig. 5.1). With the help of *MATLAB* (release 2020a, Mathworks, MA, USA) (5.12) is numerically integrated by the in-built *integral2* function for the variable θ_1 in the bounds of 0 to $N \cdot 2\pi$ and the radius R_2 from 0 to R_{disk} . As the voltage measurement across the disk's radius is a one-dimensional line and the problem is rotationally symmetric, the angle θ_2 is a fixed value between 0 and 2π that can be chosen arbitrarily. For convenience the value $\pi/4$ has been chosen which regards the EMF along the y-axis. This means that the entirety of the EMF will be visible in the y-component of (5.12) and the x-component is zero. This means generally the EMF along the radius can then be found as

$$EMF_R = \sqrt{EMF_x^2 + EMF_y^2}, \tag{5.13}$$

which gives the expected value of induced voltage for any choice of θ_2 . An example code of this calculation is found in appendix C.

Further to this calculation based on the current through a coil, it is possible to approximate a permanent magnet when the integral in (5.12) is estimated as:

$$\int_0^{N2\pi} (\dots) \approx N \cdot \int_0^{2\pi} (\dots), \quad (5.14)$$

and including the definition of remanence B_r (the field of an ideal, long solenoid, similar to section 4.1.1.2):

$$B_r = \mu_0 I \frac{N}{L}, \quad (5.15)$$

which allows (5.12) to be expressed as

$$EMF \approx \frac{BL\omega R_1 R_2}{4\pi} \int_0^{R_{disk}} \int_0^{2\pi} \{\dots\} d\theta_1 dR_2. \quad (5.16)$$

However, this is only an approximation and there might be further modifications necessary before the equation can be fully applied to any permanent magnet setup.

5.1.1.2 Field Model With a field based approach, there is more than one possible way to calculate the induced voltage across the disk in the Faraday generator. The methods are usually based on Faraday’s flux rule, the Lorentz force or SRT and they have been reviewed in [350, 352–354] and especially McDonald emphasises using the “complete flux formula” in his review.

Here we will only show one possible way, utilising the Lorentz force acting on the charges in the disk to obtain numerical simulations in *MATLAB* to predict the induced voltages. The Lorentz force acting on the conduction electrons in the disk will be set up in such a way that there is an equilibrium between the radial electrostatic field $E(r)$ and the magnetic field the charges are subject to, such that the total force on the charge is zero. By virtue of the right-hand rule it can also be identified that it is only the axial field component B_z that is contributing to the radial EMF acting on the charges, thus giving:

$$F = -qE(r) - B_z(r)\omega R_2 q = 0 \quad (5.17)$$

and solving for the radial electric field

$$E(r) = -B_z(r)\omega R_2. \quad (5.18)$$

To obtain the EMF, once again we have to integrate between the centre and radial dis-

tance, R_2 , giving

$$EMF(R_2) = \omega \int_0^{R_{disk}} [B_z|_{R_2, z_2} \cdot R_2] dR_2. \quad (5.19)$$

To calculate the axial field component the same field model by Derby & Olbert [299] is employed as in the previous section 4.1.1.2, so that equations (4.21) and (4.22) can be used. Field values for B_z are evaluated with the corresponding *MATLAB* tool [298] along the radius R_2 of the disk and at distance z_2 . The radius is divided into 100 equally spaced points between 0 and desired value of $R_2 = R_{disk}$, giving 100 values for B_z at each point R_2, z_2 which are then used to numerically integrate (5.19) with the trapezium rule. It is found that a hundred points along the radius gives sufficient accuracy and no further increase in accuracy is found by using additional points. The code used for these calculations can again be found in appendix C.

The predictions for both field and Weber model are thus found with the help of numerical tools, although it can be seen that the value of B_z itself is independent of the variables R_2, z_2 and has a constant value at each individual point on the radius. Thus we can find for the integral of (5.19):

$$EMF(R_2) = \frac{\omega R_2^2}{2} (B_z|_{R_{max}, z_2} - B_z|_{R_{min}, z_2}) \quad (5.20)$$

where the values for B_z are found at the points on the radius R_{max}, R_{min} representing the inner and outer point between which the potential difference across the disk is obtained. With the common choice of $R_{min} = 0$ coinciding with the z-axis of the coil where $B_z = 0$, this simplifies the formula to

$$EMF = \frac{\omega B_z R_2^2}{2}. \quad (5.21)$$

This is the well known expression for the induced voltage where B_z is the value of field at the outer point of the disk where the potential difference is measured. With predictions ready for both models, experimental measurements have been performed as described in the subsequent section 5.1.2 to compare the predictions of both Weber and field model to observed values.

5.1.2 Experiment With a Standard Faraday Generator

In order to measure induced voltages across a disk a standard Faraday-generator configuration has been chosen. A DC motor is rotating a brass disk at 1100 RPM ($\omega \approx 115 \text{ rad s}^{-1}$). Voltage is measured from the centre of the disk to different radial distances R_2 (0.5, 1, 1.5, ..., up to the edge of the disk at 4 cm) and grooves have been cut into the disk at each distance. A short coil with mean radius $R_1 = 68 \text{ mm}$, length $L = 2 \text{ cm}$ and $N = 320$ windings is used to generate a magnetic field by being supplied with a continuous DC current of 3 A. The disk is positioned at two different locations w.r.t. the coil, so that voltages are measured across the disk sitting at $z_2 = 0$, in the centre of the coil and also at $z_2 = 1 \text{ cm}$, aligned with the end of the coil. A drawing of the apparatus can be seen in Figure 5.3. To measure the induced voltage at each radius for both locations of the disk a Rhode & Schwarz HMC8012 digital multimeter (accuracy $\approx 0.01 \text{ mV}$) is used with two copper wires that are pressed against the disk. Upon pressing the wires against the disk no reduction in rotation speed could be observed as the DC motor provided a sufficient torque to compensate the perturbation. The voltage measurement is repeated 20 times at each point to obtain a statistical average and standard deviation, with the readings showing good reproducibility. Further, the friction of the copper wires on the brass disk was not significant enough to produce any noticeable thermoelectric effects, within the given measurement accuracy and time frame no voltage was observed due to the copper wires making contact with the spinning disk. The control test in absence of the coil further revealed that no measurable voltage is induced in the rotating disk up to the range of measurement, which excludes potential sources of error such as the Earth's magnetic field or stray electromagnetic fields present in the laboratory. All reported values are obtained with the positive probe of the multimeter in the centre of the disk and the negative probe placed in the respective groove. This is due to the direction of the magnetic field forcing the electrons to the periphery of the disk and a positive sign can be obtained on the voltage readings this way. A control test revealed that changing the positioning of the probes (negative probe in centre, positive on periphery) changed the sign of the observed voltage, as expected.

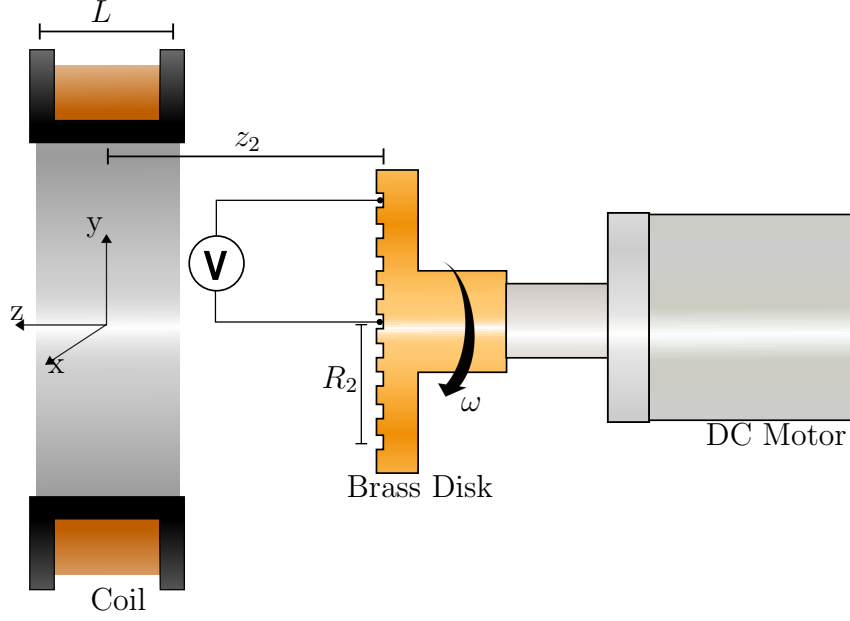


Figure 5.3: Experimental setup of a brass disk with grooves rotated by a DC motor and a short coil with 320 windings

5.1.3 Results of Standard Faraday Generator Experiment

The results of the measurements are shown in Table 5.1 and Table 5.2 where they are also compared to the predictions obtained from the Weber model and field model for the different radii along the brass disk. For the disk located in the centre of the coil ($z_2 = 0$), Table 5.1 shows observed and calculated values and Table 5.2 shows results for the disk located at $z_2 = 1$ cm, where the edge of the coil and the disk are aligned.

Table 5.1: Predicted and observed values of induced voltage in mV. Measurements were taken at the centre of the coil for different radii as indicated.

Radius in cm	Weber model EMF in mV	Field model EMF in mV	Measured EMF in mV
0.5	0.01	0.01	0.01(± 0.002)
1	0.05	0.05	0.05(± 0.008)
1.5	0.12	0.12	0.12(± 0.008)
2	0.21	0.21	0.23(± 0.009)
2.5	0.33	0.33	0.35(± 0.012)
3	0.49	0.49	0.49(± 0.011)
3.5	0.69	0.69	0.66(± 0.012)
4	0.94	0.94	0.92(± 0.018)

With the help of these tables we can compare the predicted values of the Weber model to the predictions of the field model. It appears immediately obvious that for any location

Table 5.2: Predicted and observed values of induced voltage in mV at the edge of the coil for different radii.

Radius in cm	Weber model EMF in mV	Field model EMF in mV	Measured EMF in mV
0.5	0.01	0.01	$0.01(\pm 0.003)$
1	0.05	0.05	$0.05(\pm 0.005)$
1.5	0.11	0.11	$0.14(\pm 0.007)$
2	0.2	0.2	$0.24(\pm 0.010)$
2.5	0.32	0.32	$0.36(\pm 0.009)$
3	0.47	0.47	$0.49(\pm 0.009)$
3.5	0.66	0.66	$0.67(\pm 0.010)$
4	0.89	0.89	$0.92(\pm 0.008)$

z_2 of the disk and any radial distance along the disk R_2 both approaches predict the same induced voltages. The predictions show further good agreement with the measurements obtained from experiment both in the centre of the coil and at the end of the coil. The observed voltages are shown as a function of radius R_2 for $z_2 = 0$ in Figure 5.4a and for $z_2 = 1$ cm in Figure 5.4b. The trend of the data points in both plots shows a clear R^2 dependence, as is expected from theory.

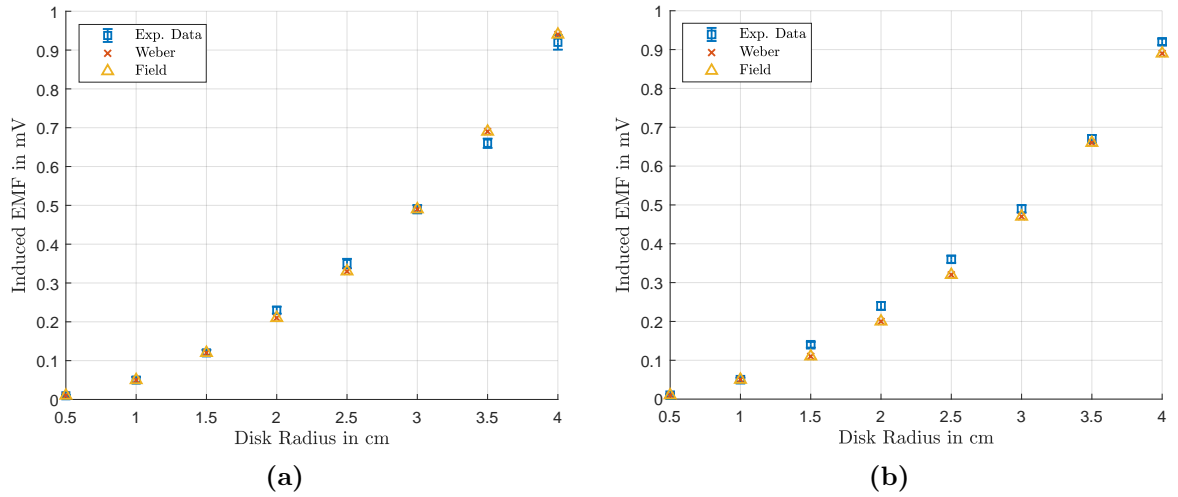


Figure 5.4: Predicted and observed values of induced voltage shown as a function of Radius R_2 . a) In the centre of the coil, b) at the edge of the coil

5.2 Rotating Detector

Now we will extend considerations by allowing the measurement device to be free to rotate in the laboratory reference frame as well, this allows for an analysis of the influence of the closing wire on the phenomenon (sec. 5.2.1) and this can be investigated experimentally (sec. 5.2.2) to check if there is an influence on the system as a whole.

5.2.1 Influence of the Closing Wire

In their analysis, Assis and Thober [194] consider each of the elements, disk (DA), magnet and closing wire (BC) to be free to rotate around a common axis and consider the full circuit ABCDA in the process. As there are now 3 components in 2 states of motion (stationary or rotating) they analyse all 8 possible cases of induction instead of just the usual 3. As they analyse these configurations only from a Weber-perspective, we would like to extend the analysis to include MFH and SFH and predict the possible inductions with these two approaches as well. Table 5.3 summarises the predictions, with ω indicating the rotation of a component and 1 (i.e., true) indicating an expected voltage induced in the circuit. The expected results can now be explained for each individual case:

Table 5.3: Predicted EMF in 8 possible cases for three different theoretical interpretations. BC and DA relate to the parts of the measurement circuit that can move, where BC is the closing wire and DA the disk, as illustrated in Fig. 5.1.

Case	DA	BC	Magnet	SFH	MFH	Weber
1	0	0	0	0	0	0
2	ω	0	0	1	1	1
3	ω	ω	0	0	0	0
4	ω	0	ω	1	1	1
5	0	ω	0	1	1	1
6	0	ω	ω	1	1	1
7	0	0	ω	0	0	0
8	ω	ω	ω	0	0	0

Case 1: None of the parts move, therefore no voltage can be induced.

Case 2: Only the disk (DA) is rotating. For both stationary and co-rotating field perspectives the disk cuts the field lines once, the disk gets polarised due to the magnetic force, whereas the closing wire (BC) stays neutral. Thus, a current can flow and

an induced voltage can be observed. In Weber's theory, the charges in the disk are moving and consequentially see an EMF from the magnet which polarises the disk while the closing wire stays neutral and a current can flow, so a voltage is observed.

Case 3: Disk (DA) and measurement circuit (BC) are rotating. The field lines are being cut twice in this case, once by the disk and once by the closing wires of the measurement device. This means that both parts of the circuit are polarised in the same way as they both see a magnetic force, however, current cannot flow in this case as the polarisation is in the same sense, so the circuit is never completed and the voltage cannot manifest. Similarly in a direct-action approach, both parts of the circuit are polarised in the same way and current cannot flow.

Case 4: Disk (DA) and magnet are rotating. Considering the field remaining stationary, the disk is cutting the field lines and in turn polarised while the closing wire (BC) remains neutral. So a current flows and the voltage is induced across the disk. If the field is regarded as co-rotating with the magnet, the field lines now cut the closing wire and polarise it while the disk remains neutral. But again, a current can flow and a voltage is induced. With Weber's force, the charges moving with the disk see an EMF, the disk is polarised, the closing wire stays neutral, a current can flow and the voltage appears.

Case 5: Only the measurement circuit (and its associated closing wire (BC)) is moving. Similar to case 2, the field lines are cut only once, this time by the closing wire, which gets polarised while the disk (DA) remains neutral, a current can flow and a voltage is induced. With a direct force approach, the force is acting on the moving charges in the closing wire and causing it to polarise. As the disk remains neutral, a current can flow and a voltage is observable.

Case 6: Measurement device (BC) and magnet are rotating. If the field remains stationary, then the closing wire is cutting the field lines and gets polarised, while the disk (DA) remains neutral and a voltage is induced. Vice versa, should the field be moving with the magnet, the field lines cut the disk, polarise it and induce a voltage. With

Weber's theory, it is the charges in the closing wire that experience a force due to their movement. The closing wire will then be polarised while the disk is neutral, a current can flow and a voltage is induced.

Case 7: Only the magnet rotates. For the field remaining stationary this is the same as case 1. For the field co-rotating this is similar to case 3 where the field lines cut the circuit twice and no voltage appears. Considering the Weber force, disk and closing wire will be polarised the same way, a current cannot flow and a voltage cannot appear.

Case 8: For each of the approaches, there is no relative motion and thus no EMF is expected.

As we can see from this analysis, even with the closing wire included in the deductions the three approaches MFH, SFH and Weber electrodynamics all predict the same results. However, they disagree on the physical reasons as to why an EMF is appearing in certain cases. This is especially apparent when case 4 and 6 are compared, both field approaches predict the appearance of an EMF but for opposite physical reasons. In case 4, from the perspective of SFH the voltage appears due to the disk (DA) cutting the stationary field lines, while with MFH the moving field lines cut the stationary closing wire (BC). In case 6, SFH predicts the moving closing wire (BC) cutting the stationary field lines, while MFH sees the moving field lines cutting the stationary disk (DA). Nonetheless, the three theories still agree on the fact that a voltage can only be observed when there is relative motion between the disk (DA) and closing wire (BC).

The specific influence of the closing wire has not been tested experimentally to a sufficient degree prior to this work. Some of the previously reviewed experiments, like those of Kelly [330], Müller [372] and Valone [374], are the closest known to the author of the present work to consider the influence on the results, but do still not rigorously investigate the relative motion between magnets, disk (DA) and closing wire/measurement device (BC). Kelly's results with different wire routings were contended by Macleod [371], however, neither allowed for rotation of the measurement device itself. Müller allowed an external portion of the circuit to rotate, but the measurement device was also still

stationary and the external portion was effectively shielded from the magnetic field. Valone allowed the entire measurement circuit to spin with the conducting magnets in the one-piece Faraday Generator, however this only examines cases 4 and 8 of the analysis above. Thus, a new experimental setup has been devised for this work to investigate whether the closing wire has an influence on unipolar induction and test all 8 possible configurations of relative motion in a Faraday generator. The apparatus is explained in the following section 5.2.2 and results from this investigation have also been published previously in [375].

5.2.2 Experiment to Test the Influence of the Closing Wire

In order to investigate the influence of the closing wire and where the induction occurs experimentally, a new setup has been used in [375]. It consists of a mini lathe with a brass shaft, two permanent ring magnets, a brass disk and a PCB with a measurement circuit. A sketch of the assembly is shown in Figure 5.5 and a photograph in Figure 5.6. The three major components, magnets, disk and PCB, are all situated on an individual aluminium sleeve each running on a bearing. This allows for a component to be held stationary with a stop screw or to rotate it with the shaft by tightening two grub screws in the sleeve. With this mechanism each part of the assembly can be held stationary or rotate independently so that the 8 possible cases of induction can be tested.

Two permanent neodymium ring magnets of type N42 (part number F2516-1) were acquired from Bunting eMagnets (Hertfordshire, UK). Their outer diameter is 25 mm and inner diameter 16 mm, with an individual thickness of 5 mm and a remanence $B_r=0.4$ T. They have been glued to the sleeve with the help of epoxy resin to secure their position. The brass disk has a similar thickness of 5 mm and an outer diameter of 42 mm. The PCB with the measurement circuit is likewise manufactured to be circular with an outer diameter of 43 mm. The measurement circuit utilises an LED as a visual indicator light to detect the presence of a voltage across the disk and is driven by an amplifier. Contact with the disk is made through two relay contacts that are soldered onto the PCB and then bent into a Z-shape, which spring loads the contacts and ensures a continuous connection

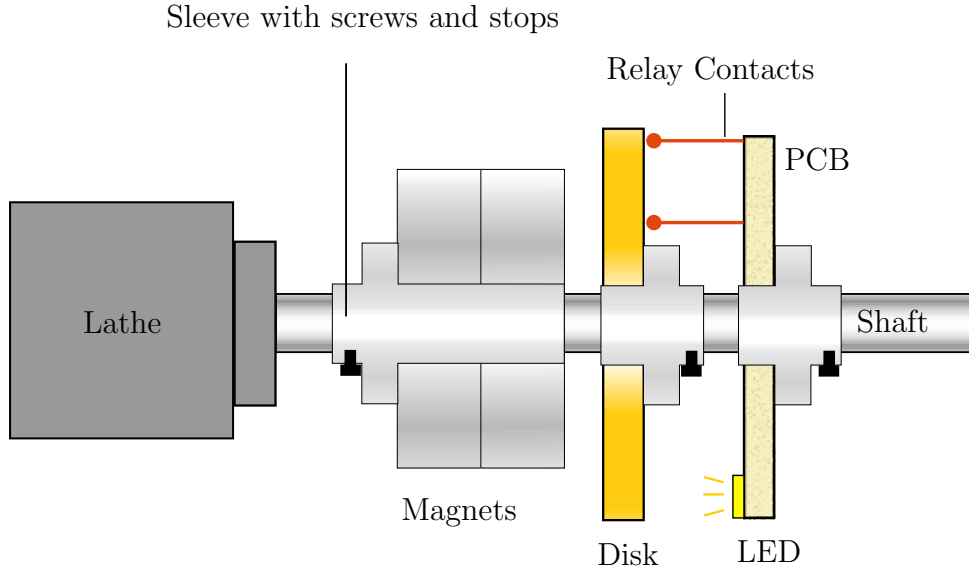


Figure 5.5: Sketch of the experimental setup to test the rotation of the three individual parts: magnet, disk and measurement circuit (respectively closing wire).

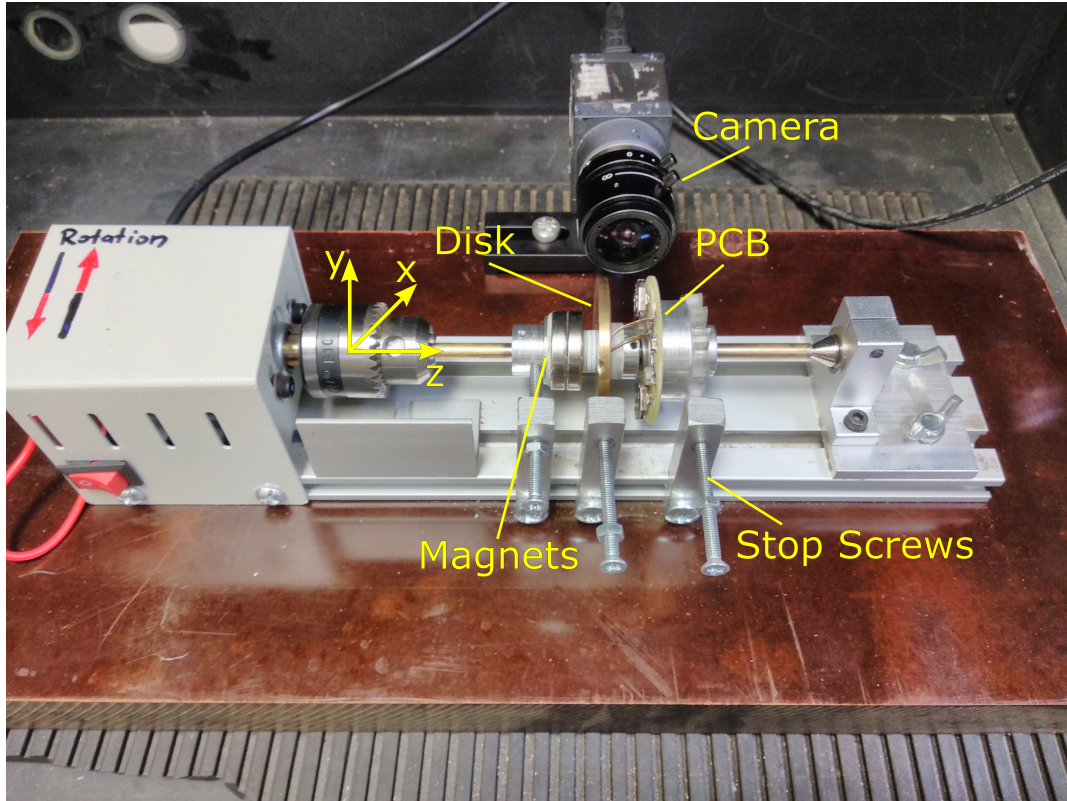


Figure 5.6: Photograph of the experimental setup. A right-handed system of coordinates is placed so that the brass shaft is coaxial with the z-axis. Neodymium magnets and brass disk are each glued to an aluminium sleeve, the measurement PCB is screwed to an aluminium sleeve with nylon screws. Each of the sleeves sits on bearings and can rotate with the shaft or be fixed with the help of dedicated stop screws as indicated in the photograph.

between the brass tip of the contact and the disk, even when either part is spinning. The contacts are separated by roughly 10 mm to 12 mm along the radius of the PCB and the

tracks they are soldered onto are 3 mm wide and connect to the inputs of the amplifier.

The PCB and circuit have been specifically designed to qualitatively test the existence of an EMF in the assembly, where the copper tracks connecting the relay contacts to the inputs of the amplifier form the closing wire. A differential In-Amp LTC2053 amplifies the input voltage induced in the circuit ABCDA and outputs it to a yellow high efficiency LED (ROHM SML-D11YWT86, 1.85 V, 2 mA) with a current limiting resistor, while two button batteries BR1225 power the amplifier. A schematic of the circuit is shown in Figure 5.7.

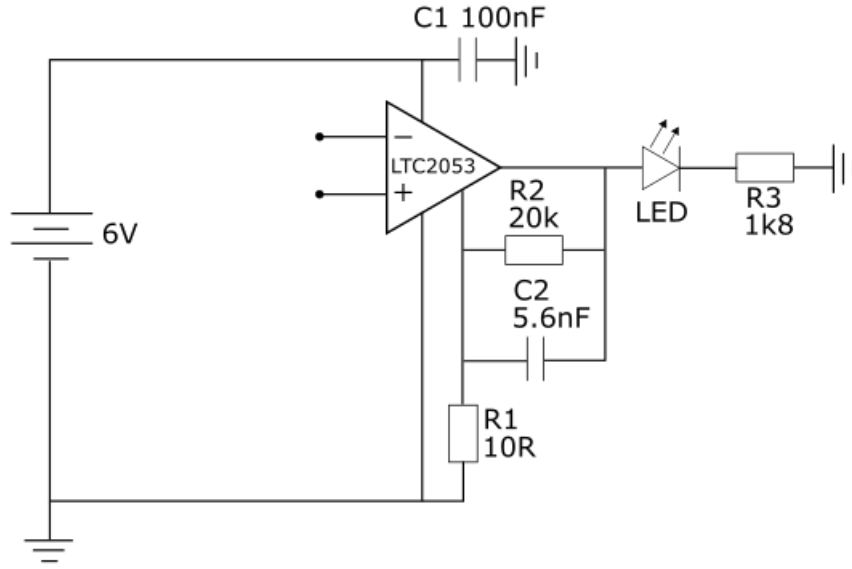


Figure 5.7: Circuit Diagram of the detector circuit with amplifier and LED

In order to determine the necessary amplifier gain, a first test was run with the disk rotating in the magnetic field and the induced voltage measured with a Rhode & Schwarz HMC8012 digital multimeter. Across the entire radial distance of 14 mm on the backside of the disk a maximum potential difference of about 2 mV was observed. But as the separation of the relay contacts is slightly less (10 mm to 12 mm) the voltage between the contacts is closer to ≈ 1.5 mV. The contacts are also subject to some slight positional inaccuracies as they can't be soldered onto the PCB at an exact 90° angle and when the PCB is rotating they will experience centrifugal forces. Due to these constraints the gain was chosen to be set at 2000, which ensures the operation of the LED even with slight fluctuations of the induced voltage due to slight positional shifts of the contacts.

The trade-off however, is that with this high gain factor the relay contacts pick up surrounding noise from the laboratory environment due to them acting like antennae, which results in the LED turning on weakly in its base state. However, when the contacts are touching the brass disk they are short-circuited and the LED turns off in consequence, giving an expected “0” base state of the circuit. As an additional means of controlling the noise picked up, a low pass filter was included in the circuit, attenuating 3 dB at 620 Hz, which gives roughly 5 to 10 times the bandwidth of a single rotation, depending on the speed of the lathe. However, no significant noise reduction could be achieved with the additional filter, only the spring loaded nature of the contacts achieved a continuous connection to the disk, even upon rotation, which guaranteed the turned off base state of the LED.

The rotational speed of the lathe could be varied by changing the magnitude of the supply voltage V_S and the included power supply comes factory-equipped with seven different settings. The rotational speeds of the lathe have been measured in the no-load configuration through two distinct methods. Method one measured the acoustic frequency emitted by the lathe in each setting with a microphone and spectrum analyser, and method two determined the rotational speed through a strobe light. The measured speeds are listed in Table 5.4.

Table 5.4: Measured rotational speeds of the lathe in no load condition, via the emitted acoustic frequency and with the aid of a strobe light.

V_S	$f_{acoustic}$	$RPM_{acoustic}$	$\omega_{acoustic}$	RPM_{strobe}
12 V	80 Hz	4800	$502.65 \text{ rad s}^{-1}$	4800
15 V	99 Hz	5940	622 rad s^{-1}	5960
16 V	106 Hz	6360	666 rad s^{-1}	6360
18 V	119 Hz	7140	747.7 rad s^{-1}	7180
19 V	125 Hz	7500	785.4 rad s^{-1}	7550
20 V	131 Hz	7860	823.1 rad s^{-1}	7960
24 V	156 Hz	9360	980.2 rad s^{-1}	9450

Before the main test of checking the 8 cases was conducted, the working condition of the apparatus was checked with several control tests. The polarity of the DC motor driving the lathe could be easily switched, which also reversed the rotational direction the shaft was spinning in. It was first determined how the disk would be polarised by

the magnetic field depending on the rotational direction. With the magnets glued to the sleeve, their orientation remained the same for all experiments throughout, making it possible to control the polarity (and thus the sign) of the EMF by means of the rotational direction only. Further, the two rotational directions are called clockwise (CW) and counter-clockwise (CCW) and are determined by the coordinate system indicated in Fig. 5.6. With the help of the HMC8012 multimeter the sign of induced voltage can be observed upon rotation of the disk which ascertained the polarisation. For CCW rotation the disk polarises with the negative charges on the perimeter and the positive charges in the centre. When rotated CW, the opposite occurs with the negative charges now in the centre of the disk and the positive charges on the periphery.

With the knowledge of polarisation direction, two PCBs were manufactured with a detector circuit each but in opposite polarities. For the first circuit the relay contacts are connected to the In-Amp so that the outer contact is connected to the inverting input of the amplifier, while the non-inverting input is connected to the relay contact closer to the centre of the PCB, further called “Normal Polarity” (NP). In the second configuration, called “Inverted Polarity” (IP), the outer contact connects to the non-inverting input and the central contact connects to the inverting input. Photographs of the two PCBs manufactured in NP and IP configuration can be seen in Figure 5.8.

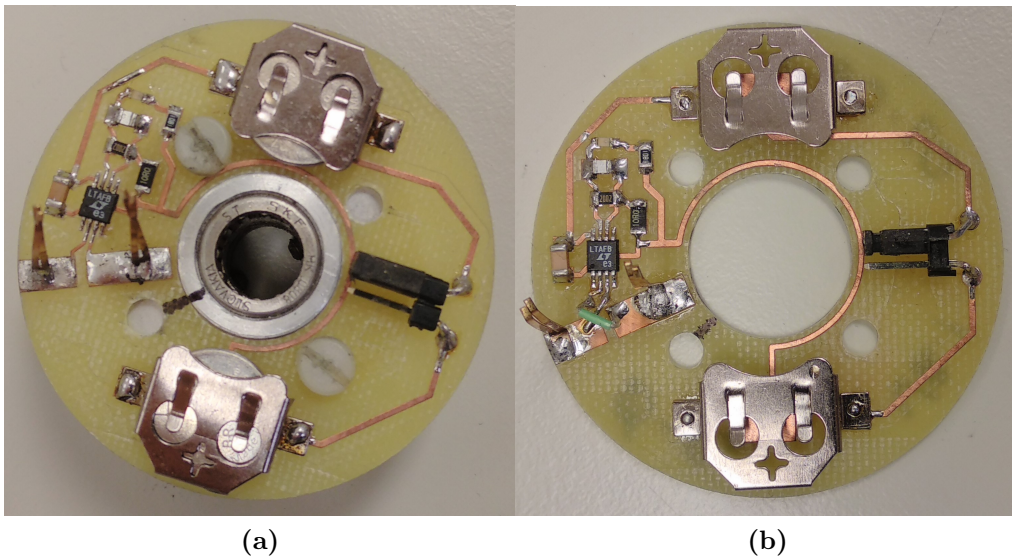


Figure 5.8: Photograph of the circuit board with LED and amplifier circuit a) Normal Polarity (NP), b) Inverted Polarity (IP).

Next, an external voltage source was used to test the functionality of the NP circuit. The outer contact (inverting input) was connected to the negative terminal of the source and the central contact (non-inverting input) to the positive terminal, which simulates the voltage across a disk when polarised with the negative charges on the circumference and positive in the centre. Upon connecting the cables to the relay contacts, it was observed that the picked up noise increased too, which resulted in an increased brightness of the LED. However, when the voltage supply of 2 mV DC from the source was switched on to test the circuit, it further raised the intensity of the LED. Supplying a negative voltage of -2 mV switched the LED off completely, as the In-Amp cannot output negative voltages due to the chosen design with the negative side of the batteries as the 0 V reference, so this result was expected. With these two tests the correct functionality of the amplifier circuit could be confirmed.

As the last control test, disk and PCB were rotated in absence of the magnet. The disk was spun first while the PCB was kept stationary and inversely the PCB was spun while the disk was kept stationary. Performing these checks with both amplifier polarities and spinning in CW and CCW directions, it was found that the LED remained switched off in absence of the magnet.

5.2.3 Results From Rotating Detector Experiments

With the functionality of the setup confirmed, the 8 configurations of unipolar induction, as given in Table 5.3 could now be tested. The first series of tests was performed with the NP amplifier and spinning the components in CW as well as in CCW direction. The second series of tests was conducted with the IP amplifier and again spinning CW and CCW, and the results for both test series are summarised in Table 5.5. It can be seen from these results that in CCW rotation and NP amplifier setting an induced voltage is observed in cases 2 and 4 only, where the disk (DA) is rotating on its own (case 2) and together with the magnet (case 4). No voltage could be detected for any of the other cases. For the IP amplifier in CCW rotation, a voltage is observed only in cases 5 (PCB (BC) spinning on its own) and 6 (PCB (BC) and magnets spinning), whereas the other

cases did not alight the LED. When the rotational direction is inverted to CW direction, it is now the IP amplifier showing a voltage in cases 2 and 4 and the NP amplifier showing a voltage in cases 5 and 6.

Table 5.5: Results for testing cases 1 to 8 in both rotational directions with both polarities of the amplifier. An ω indicates movement of the respective part and a 1 (true) represents an observed “on” state of the indicator light, meaning a voltage is observed.

Case				Observed State of LED			
	DA	BC	Magnet	CCW Rotation		CW Rotation	
				NP	IP	NP	IP
1	0	0	0	0	0	0	0
2	ω	0	0	1	0	0	1
3	ω	ω	0	0	0	0	0
4	ω	0	ω	1	0	0	1
5	0	ω	0	0	1	1	0
6	0	ω	ω	0	1	1	0
7	0	0	ω	0	0	0	0
8	ω	ω	ω	0	0	0	0

From the predictions in Table 5.3 one could have been led to expect cases 5 and 6 to show a voltage in CCW rotation and NP amplifier setting as well, but as this is not the case and they only show for IP operation, some deeper analysis of the results is in order. With the IP amplifier and CCW rotation, the disk (DA) will polarise as determined above, for all the cases where it is rotating, with the electrons on the perimeter and the positive charges in the centre. However, the amplifier remains off in these cases as it would need to output a negative voltage w.r.t. the zero volt reference, so consequently the LED will remain off as well. Intuitively, we would now expect that the closing wire (BC) polarises the same way as the disk (DA) due to the magnetic field and a voltage would be observable for CCW rotation and NP amplifier, but not for the IP amplifier.

However, this expectation is erroneous, as it is not the polarisation alone that needs to be examined, it is rather the electron flow in circuit ABCDA that needs to be considered in these results. When the PCB (BC) is spinning CCW in the magnetic field and polarises with the electrons on the perimeter and the positive charges in the centre, then the electrons will flow away from the inverting input, along the copper track to the periphery, into the relay contact, back through the disk (DA) and back up the copper track towards

the non-inverting input (see Fig. 5.9a). But this means for the NP amplifier that the electrons are flowing the wrong way, as it cannot output negative voltages. So it is precisely because the closing wire (BC) gets polarised in the same sense as the disk (DA) that the LED does not turn on in this case. If, however, we use the IP amplifier with CCW rotation, the electrons can flow into the inverting input (Fig. 5.9b) and the voltages in case 5 and 6 are observed. When the rotational direction is reversed to CW rotation, disk (DA) and closing wire (BC) will now polarise the opposite way (negative in centre, positive on perimeter), leading to exactly the opposite results of CCW rotation. That is, in cases 2 and 4 where the disk (DA) is rotating, electrons will flow away from the inverting input on the NP amplifier (LED remains off) but into the inverting input of the IP amplifier (LED turns on). For cases 5 and 6 where the closing wire (BC) rotates, electrons will flow into the inverting input in NP configuration, but away from the inverting input in IP configuration. The possible operational states in which the amplifiers can and cannot output a voltage are shown in Fig. 5.9.

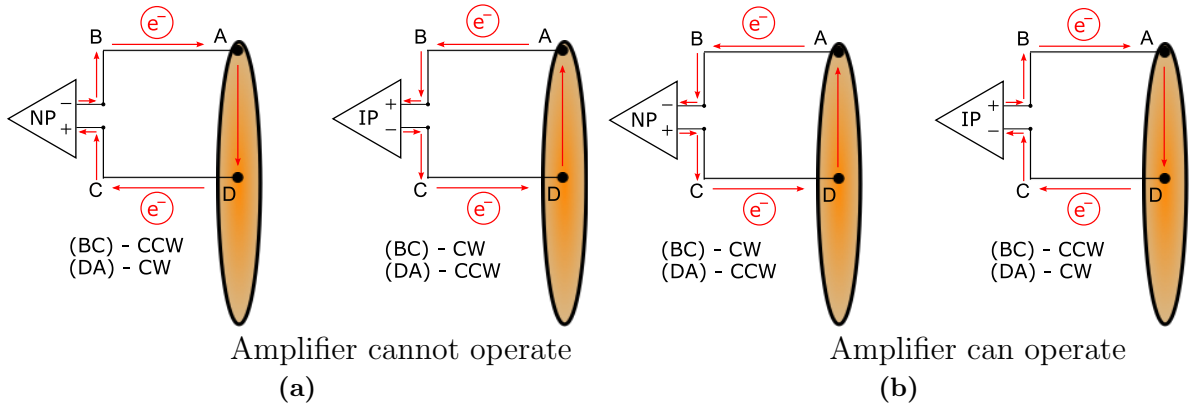


Figure 5.9: The electron flow in circuit ABCDA determines the operation of the amplifier, which in turn depends on the polarisation of the disk (DA) or closing wire (BC) due to the rotational direction in the magnetic field, a) states in which the amplifiers cannot operate in and no voltage can be observed; b) states the amplifiers can operate in and a voltage can be observed.

To further investigate the induced voltages in cases 5 and 6 and check that these are indeed caused by an EMF acting on the closing wire, two additional tests have been performed. i) It was considered that perhaps the magnetic field was too weak at the position of the closing wire, as it was further away from the magnet than the disk, hence the field strength was increased by adding two additional magnets to the setup. ii) The

intensity of the LED in case 5 was measured.

Two additional N42 neodymium magnets were added to the setup and set closely behind the closing wire, so that their distance would be approximately the same as the distance between disk and regular magnets and have the same polarity. They had larger radii (OD 40 mm, ID 25 mm) but similar field strength ($B_r = 0.34\text{ T}$) and were sitting on an extra bearing running on the sleeve the PCB is fixed to. Testing the PCB (BC) rotating in CCW direction with NP in the now significantly increased field revealed that the LED still remained switched off in both case 5 and 6. Further turning the additional magnets to have the opposite polarity to the regular magnets did not show any indication light, likely due to the fields resulting in opposite EMFs and cancelling their effects on the closing wire in the process. When the NP amplifier was rotated CW with the extra magnets in the same polarity as the regular ones to increase the field strength; in both case 5 and 6 the LEDs turned on again, this time with significantly increased brightness. Similarly for this rotation having the extra magnets in opposing polarity, reducing the field strength, the brightness of the LED was decreased in consequence, as the additional EMF counteracted the other.

The second additional test involved radiation intensity measurements of the LED to further investigate the induced voltage and confirm that it is indeed the result of an EMF acting on the closing wire. For this, only the regular magnets were used in the assembly and the whole setup was put into an enclosure to block surrounding light. Images were then taken for case 5 with a Thorlabs scientific camera D1024G13M at each rotational speed setting of the lathe. Intensity values were obtained by image analysis in *MATLAB* to gauge the intensity of the trace left by the LED in the camera image. The mean of the greyscale values of every image was calculated and scaled against a value of 255 (which would represent every pixel in the image being white) and so a relative intensity value was obtained for each speed setting. The relative intensities I_{rel} are plotted against the angular speed ω in Fig. 5.10, where a clear linear dependence between the two values can

be seen. A linear fit was found as

$$I_{rel} = \omega \cdot 2.04 \times 10^{-4} - 0.0193$$

with an R^2 of 0.969 with the intensity data. Further it was also observed that moving the magnets away from the disk (and thus the closing wire) would decrease the brightness of the LED, due to the field strength decreasing at greater distance. This was especially noticeable at higher rotational speeds where the LED is relatively bright and further confirms, additionally to the brightness measurements, that in case 5 it is indeed the closing wire that is experiencing an EMF and where the voltage is induced.

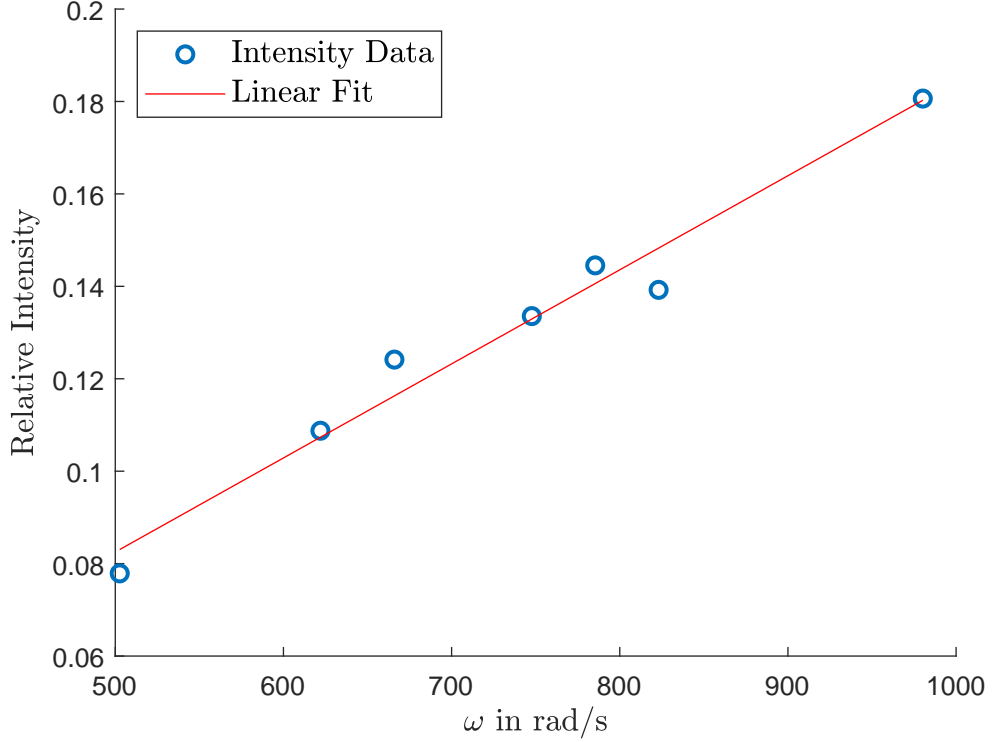


Figure 5.10: Relative Intensity of the LED in case 5 for different speeds of rotation. An intensity value of 1 represents an entirely white picture.

5.3 Discussion of Unipolar Induction Experiments

The experimental results of section 5.2.2 clearly show that the closing wire and measurement device have an influence on unipolar induction. This is especially evident from the

results of case 5 and the respective intensity measurements. Consequently, any analysis and description of the problem must consider the entire circuit ABCDA to avoid the creation of paradoxes and obscure physical causes and mechanisms responsible for the phenomenon. As these experiments show, it is the relative motion between disk (DA) and closing wire (BC) that determines the appearance of an induced voltage and not the motion of the magnet or the magnetic field *per se*, and it rather plays a secondary role. For the seat of induction it is found that in cases 2 and 5 it is clearly situated in the part of the circuit that moves through the magnetic field (case 2 the disk (DA) and case 5 the closing wire (BC)).

When analysing cases 4 and 6 however, it is found that a clear distinction of the induction's seat is not possible anymore. This is due to the fact that both SFH and MFH lead to the same prediction and the relative motions make it impossible to tell apart which portion of the circuit will be subjected to the EMF. For example, if we assumed SFH in case 4 where disk and magnet are spinning in CCW direction and observed with the NP amplifier, the result would be the disk polarising in the stationary field so that the electrons flow into the inverting input, thus operating the LED. If instead we assumed MFH, the field lines which are rotating CCW would cut the closing wire (which is stationary in the lab frame for this case), but relatively speaking, this motion is the same as the closing wire rotating CW through a stationary field. This means that, while the closing wire polarises due to the field motion, it polarises with the electrons flowing into the inverting input which results in an observed voltage. Figure 5.11 illustrates this relative equivalence of the co-rotating magnetic field motion for cases 4 and 6, both shown for CCW rotation.

We can find the same relative equivalence not only for case 6 in CCW rotation (where field and closing wire rotating CCW is the same as the disk spinning in a stationary field in CW direction), but also inversely for cases 4 and 6 when the field is first assumed moving CW. Consequently, because of this relative equivalence, it is not possible to distinguish the seat of induction between the moving and stationary portion of the circuit and similarly it is impossible to tell if the field is co-rotating with the magnet or stationary with the

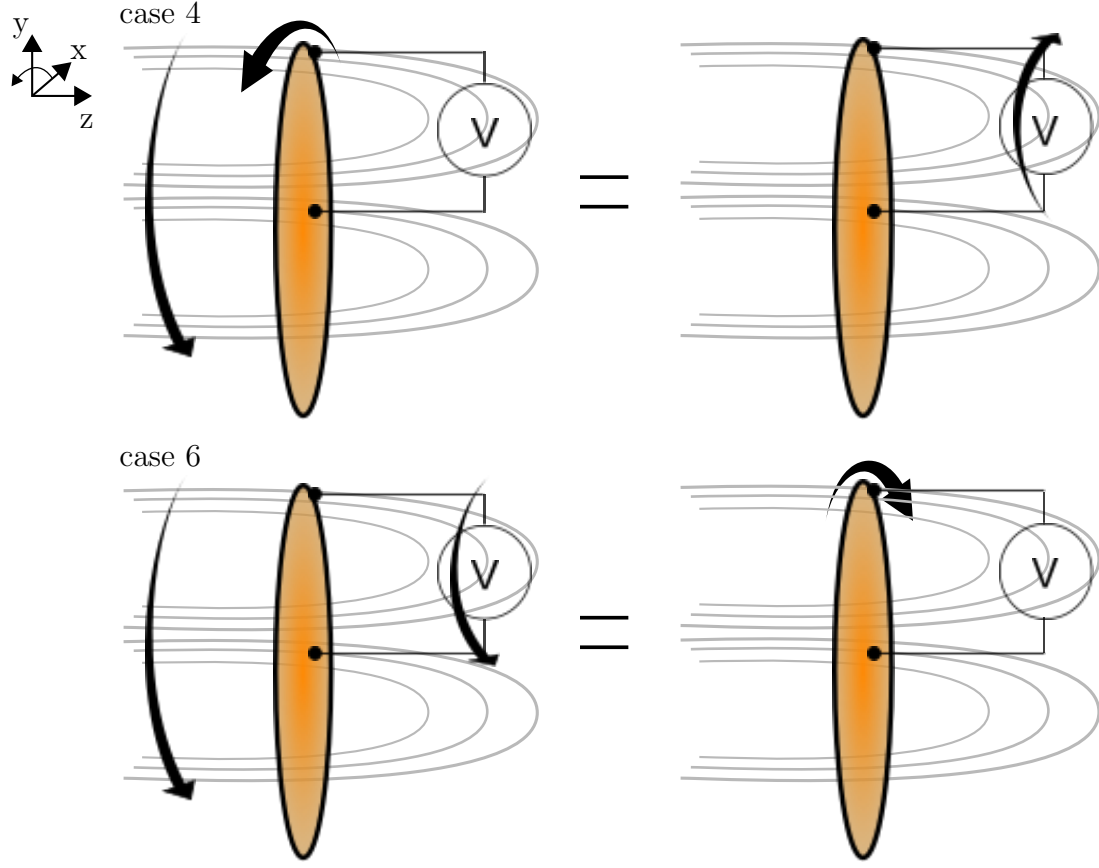


Figure 5.11: Relative motion of the magnetic field (which is assumed as co-rotating) compared to the circuit and disk for cases 4 and 6. The absolute motion in the lab frame is shown on the left for each case, whereas the relative equivalent motion for the respective stationary part is shown on the right.

current results. At least with this setup, the predictions and the outcome of both SFH and MFH assumptions is the same and it cannot be determined which hypothesis is the correct one. It appears that both theories are valid alternatives that can explain the results of the experiment, even though the question of the field's movement cannot be answered at this point, and it is unclear if the rotation around the field's symmetry axis can be detected in the future.

This means that the field's motion around the symmetry axis is ambiguous, and it is likely this ambiguity that is responsible for the ongoing debate in the literature where both views of SFH and MFH are argued and supported. Especially the one-piece Faraday generator [315] has been interpreted to be explainable with the field remaining stationary and the magnet cutting its own field lines upon rotation, which is used as an argument in favour of SFH. Another argument against the fields motion has been made on a theoretical

basis by Cramp *et al.* [367], who have argued that, if the field were to rotate with the magnet, its field lines would move faster than the speed of light at infinity, therefore it must remain stationary. However, we can find counterexamples where the field must clearly follow the magnets movement, such as rectilinear motion or magnets of different shapes (such as quadrupole or horseshoe magnets) or even a bar magnet spinning about a different axis than just the symmetry axis. If, for example, a bar magnet was spun so that its poles chased each other in succession (around its radial axis) there would be no doubt that the field lines would follow the position of the poles. This raises the question as to why rotation of a magnetic field around its symmetry axis should be an exception to the rule? What is the physical reason causing this peculiar behaviour?

In order to answer those questions it might be feasible to modify the experimental apparatus. A possible extension of the experiment presented here could include the modification to allow the permanent magnets to spin independently from disk and detector. If the magnets were seated on a separate shaft, it would be possible to rotate them in the opposite direction of the circuit components DA and BC, respectively. Especially in cases 4 and 6 investigating whether the magnet's rotational velocity would have an additional effect on the induced voltage could hint at the movement of the field and respectively the seat of induction. As the relative velocity between moving magnets and circuit component would increase for rotation in opposite directions, a proportional increase in induced voltage could be related to the field moving with the magnet.

Further experiments with one-piece Faraday generator setups could also show evidence about the field's movement and potentially elucidate the seat of induction in the future. Investigating, for example, how the measurement device behaves in the far field of the one-piece generator and how different wire routings effect it could be valuable. It is also conceivable that a non-contact detection method could grant further insight into the field's nature. If a rotating conducting magnet does indeed cut its own field lines, an electric field would be generated on the surface of the magnet regardless of the detection method, such that a non-contact electric field measurement could be employed to detect the charge separation. This is, however, not a trivial task as the movement of capacitive elements

is utilised in electric field meters, and the movement of these conductive elements in the magnetic field can cause parasitic induction in the detector and obscure the sought after radial field of the Faraday generator. Nonetheless, should these types of measurements be successful they might grant compelling evidence for or against the field's state of movement, field lines and even the physical reality of the field.

Astonishingly, it seems to be the ambiguity of the physical field model that leads to the creation of paradoxes and consequently sparks debates in the literature, but perhaps the better question to ask might be: "Is the field physically real or not?" Because if the field is not real it can neither co-rotate nor remain stationary and paradoxes are thus avoided. As of yet, no stand-alone proof exists that confirms the physical reality of a field directly, the action of a field cannot be measured independently of the associated force. But it is certain that the force acting between the charge carriers is real and instead of ascribing the action of the charges to a field that in turn gives rise to a force, it might be advantageous to regard the field as a book-keeping device. For example, Montgomery's approach [355] to unipolar induction considers first and foremost the motion of the conduction electrons and the conservation of energy. The field is still utilised for the calculations, but as a mathematical tool, like a vectorial map indicating how much interaction is possible in a certain direction and it does not necessarily need to be a physical entity to that end. It was further argued by Slepian [307] that field lines or "lines of force" do not have to be continuous, individual or closed curves and that only the knowledge of a local vector field is necessary to describe the observable phenomena. In his review about unipolar induction, Miller makes a similar argument [376], saying that "lines of force" are merely a tool for visualisation, but that does not necessarily make them a 'fruitful approach'. Instead their sources must be considered and Miller also questions 'whether lines of force have physical characteristics' at all. He states that shifting the focus away from the lines of force helps explain other forms of induction, where magnet and conductor are in relative motion as well, e.g. the Barnett experiment [341, 359, 364, 365]. It was commented by O'Rahilly [62, Vol. 2, p. 603], that saying the field is stationary only means that the vectorial field \vec{B} 'remains the same at every point of space round a rotating symmetrical

magnet’ and that stationary lines of force are ‘merely an out-of-date invention adopted for those who are supposed not to be able to grasp the mathematical idea of a vector field.’ In this sense, O’Rahilly is making the same argument as Miller, such that the lines of force can be a misleading approach, distracting from the actual cause of induction and the field.

But despite just the field approach, we have seen that the problem can also be analysed from the perspective of the Weber force. With the simulations of the Weber model (sec. 5.1.1.1) agreeing with both the experimental results of section 5.1.2 and the field model (sec. 5.1.1.2) we can find confirmation that a connection exists between Weber’s force and Faraday’s law. Additionally, Weber also correctly predicts for cases 1 to 8 the appearance of an induced voltage based on the relative motion between disk (DA) and closing wire (BC) and agrees with the experimental results of section 5.2.2. Weber’s force can readily explain unipolar induction without paradoxes as it is the microscopic circulating charges (i.e., Ampèrian currents) in the magnet that give rise to permanent magnetism and thus a magnetic force that is felt by the parts of the circuit in motion. With this concept of direct-action the field as an entity is absent in the explanation and the question of its movement does not arise naturally which avoids the conceptual problems of the field’s motion in this context. The EMF is instead a consequence of forces between electrical charges in relative motion, which is unambiguous for a given frame of reference and coordinate system. The typically conceived “field lines” or “lines of force” of the field are replaced with a Newtonian force acting along the line joining the particles interacting. Since the direct interaction with Weber’s force can equally well explain the unipolar induction phenomenon and leads to accurate predictions of the EMF, the question is raised whether the motion of the field lines and the magnetic field itself is important to the problem, further to the line of argument issued by Miller and Montgomery. If, at its core, it is first and foremost the relative motion of charges that is important, then the magnetic field can be thought of as a useful metaphor [62] and the principle of Ockham’s razor can be invoked. As a direct-action model avoids the field as a mediator, this principle favours direct-action as the theory with least assumptions and minimal complexity since entities

are not multiplied beyond necessity.

Related to a direct-action mechanism to explain unipolar induction is a discussion in the literature about the applicability of Ampère's force versus Grassmann's force to homopolar induction machines, in the generator as well as the motor configuration. Especially in connection with experiments performed by Guala-Valverde *et al.* [339, 377] investigating homopolar motor configurations, the associated authors have argued that only Ampère's force can explain the generation of torque in these machines and the Barnett experiment [159–161], accrediting field theory a failure to explain the mechanisms. In contrast to this opinion, it was argued that these experiments, as well as the experiments of Kennard and Bartlett, can very well be explained in a classical framework [378, 379]. In the opinion of the present author, it is likely that when these experiments are re-analysed with the full picture of the closing wire, both a direct-action/Weber force approach and field theory will correctly predict these experiments and similar to the unipolar induction experiments in this chapter, it will not be possible to distinguish between the two. Especially with the earlier review about the existence of longitudinal forces existing in the field model similar to the longitudinal forces of Ampère (sec. 2.2.1), it is likely that both theories can rather be regarded as complementary than exclusive. Nonetheless it can be said that Weber's theory, respectively a direct-action approach does present an elegant way to resolve associated paradoxes with unipolar induction. Furthermore, the magnetic field motion question is settled by the Weber approach which effectively sidesteps the field question completely.

6 Discussion

While some aspects of the results obtained from the electron beam deflection experiments (sec. 4) and unipolar induction experiments (sec. 5) have already been discussed in the associated chapters, a more general discussion will follow reflecting on the most important findings of this work. While the core of this work has focused on Maxwell's and Weber's theory specifically, this chapter will discuss these theories in relation to fundamental, conceptual and ontological aspects, but will not be limited to the two theories alone, as these aspects apply to the broader spectrum of field theories, direct-action and particle theories in general.

6.1 Similarities of Weber and Field Theory: Can They Be Distinguished?

From the experiments in section 4 with low velocity charged particle beams and in section 5 with unipolar induction and rotating magnetic fields, we have seen the similarity of both approaches and how they predict similar, if not the same results in these specific cases. This tendency is also demonstrated and emphasised in the literature review (sec. 2) where it was shown that Weber electrodynamics can account for phenomena usually explained with the Maxwellian theory of fields. This raises the question of where they differ from each other, and indeed we can ask: is there a so called “*experimentum crucis*” that can distinguish between the two theories?

This work has made an attempt to address this issue, as one of the key questions formulated in the introduction was whether experimental evidence can be found for or against any of the two theories or respectively if they can be proved or disproved. Other researches have attempted to find an answer, as shown by the works of Mikhailov or Tajmar *et al.*, and some comments will now be offered in regards to this question. Whether or not the theories can be distinguished has been asked indirectly before by Assis, discussing the direct-action transmission of force in Weber's theory and the transmission of force through a mediator in the field theory. Assis, who is arguably the world leader

with regards to Weber electrodynamics, eventually comments ‘we do not know and maybe we will never know’ [63, p. 228], which relates to the famous *ignoramus et ignorabimus* suggested by du Bois-Reymond, accepting that scientific knowledge will always be limited.

One might of course argue that it seems that the crucial evidence has already been found with recent work by Tajmar and Weikert on negative mass behaviour, the failure of Weber to predict radar equations correctly, the failure to predict mass change with velocity and the failure to predict certain behaviour in cold plasma and problems with fine structure splittings. But it must be re-iterated that, while these are admittedly current limitations of Weber’s theory, what we have seen from this work and the literature review shows once each theory is developed sufficiently and given the right treatment, they predict the same results. This is already true for the longitudinal forces which was originally thought to be in favour of Ampère’s and Weber’s forces but has since been shown to be present in field theory as well (see sec. 2.2.1). Limitations surrounding the radar equation and the cold plasma are partially due to the longitudinal forces in Weber’s theory and the absence thereof in the field model. However, since these forces can be found in the standard model as well, given the right treatment, it remains to be re-examined how these two situations would compare with both field and Weber’s theory under these circumstances. It is likely that, with further research and development of Weber’s electrodynamics, the current limitations surrounding the negative mass behaviour, high speed electrons, radar equation and cold plasma will yield the same outcome as the classic theory. For example, O’Rahilly [62, Vol. II, p. 622] argues with the help of Ritz’s theory that variable mass behaviour can be explained equally well with a variable force dependent on relative velocities. Also there exist other ideas to account for the observed results of mass change with velocity that involve the manipulation of mechanics [110, 260], treating it as a dynamical effect [380] or the idea that instead of variable mass variable charge can account for the observed effects [205]. These developments also hint at Weber’s force being an approximation up to second order of a more fundamental underlying force law.

To this date, there appears to be no single experiment that can decisively distinguish Weber and Maxwell electrodynamics and there might even be the possibility that we may

never be able to distinguish between them. When both theories are developed far enough and treated rigorously they might always give the same result, however, further research is needed. In that sense it must be said that both theories have the same goal, they are both aiming to describe the very same electromagnetic phenomena and it would not be surprising if, for that reason, both theories turn out to be (almost) exactly similar to each other, so similar that they cannot be distinguished from one another. To this end, both of these theories are just models, they are representations of physical reality and used for a common goal, which is the description and prediction of the observable effects of electricity and magnetism. As models, each might have its own benefits and drawbacks and one might be more effective or efficient to use in a certain situation than the other. But it would be inappropriate to say that one is better than the other. Considering that both theories can work equally well in most scenarios, it might be beneficial to use both theories in conjunction and apply whichever one is more appropriate for a given situation. From a pedagogical perspective we can then offer two alternative explanations which can advance the understanding of electricity and magnetism, as some might find the field more intuitive and some the direct particle interaction.

As these theories are just descriptive models of natural phenomena they can always be altered and adjusted with new experimental insight and evidence from observation which is the iterative process of research in general. The vast majority of research is conducted as incremental additions from a wide variety of contributors. As physics is concerned with not only the qualitative but also the quantitative scientific prediction of phenomena, this is a necessary process and every theory needs to be juxtaposed to relevant experimental data. This is also rooted in the original empirical nature of physical discoveries whose laws were derived from experiments, such as Ampère's force. One could say that there is a traditionalist view to regard physics as an empirical science that is solely dictated, informed and altered based on the experimental results it aspires to recreate, where the theory is a slave to the master of practice. In contrast, the modernist view is to construct a nearly perfect theoretical framework first which then dictates the experiments performed and makes predictions unknown to the experimentalist beforehand and the practice of

experimentation is slave to the master of theory. (This can be seen, for example, in the cosmology debate between MOND and the Λ -CDM model. MOND informs and alters the theory, in this case Newtonian gravitation, to explain the observations, whereas cold dark matter cosmology with dark energy is mostly derived from the theoretical framework of GRT and then set out to seek the existence of dark matter particles by designing suitable experiments.) At its core this discussion about which is more necessary, theory or experiment, and which of the two rules superior over the other, can seem like an argument of belief, where the theorist as well as the experimentalist will each promote their own agenda. While large collaborative experimental institutions like CERN have developed a tendency to receive guidance from theoretical physics to limit the range of feasible experiments based on predictions, it is evident that laws of nature can only be deduced from and confirmed by observable and repeatable results of experiments.

For an engineer it will always suffice to have a working tool that will give the desired results with a certain accuracy for a given application, whereas for a complete understanding of nature and the universe, as the physicist or philosopher is said to desire, a more contrived model might be necessary. This also relates to a discussion between Heisenberg and Dirac over whether physical theories should be “open” or “closed” theories [381]. While Heisenberg was of the opinion that theories are “closed” – meaning that a given theory is accurate and sufficient in its respective field and progress only happens in leaps that break with what was before. By contrast, Dirac was a proponent of “open” theories, meaning that every existing theory can be revised and adjusted at any point. With the arguments presented beforehand, it should be evident that the present author agrees with Dirac on this matter.

This is equally true for electromagnetics, where the theory should be adjusted to new insights, which is how scientists have originally derived the laws of electricity and magnetism. This duality of theory and experiment informing and influencing each other can already be found in both field and Weber electrodynamics, where each has constructed predictions from the theoretical framework that have then been investigated by experiments, and likewise adjustments have been suggested to the theory where they disagree with

observations. That means if, in the future, evidence is found for or against a fundamental concept these theories are based on, then the mathematical and physical descriptions should be adjusted accordingly to conform to the observations.

6.2 The Ether Concept

When we speak of these fundamental concepts, we usually think of two categories, theories based on direct-action and theories based on the ether concept or a similar form of mediator through which the interaction is transmitted. It is therefore of interest to discuss the ether concept itself and its relation with field theory in order to better understand the underlying premise. The ether concept has been debated by physicists at different stages in history and looking back we can roughly identify three distinct phases relating to the modern understanding of electromagnetic theory. That is: i) the historical role of ether (sec. 6.2.1) and how the views of Maxwell and Faraday have influenced the scientific consensus, ii) how the belief in the ether and the terminology changed among scientists in the post-Maxwellian era related to relativity (sec. 6.2.2) and lastly iii) the re-introduction of the ether with GRT and modern QFT (sec. 6.2.3).

6.2.1 Historical Role of Ether in Field Theories

Originally, field theory was based on the ether during the mid to late 19th century, when the theories describing electromagnetism were developed and scientists commonly believed in the existence of a fundamental substance permeating the universe. Even pre-Maxwellian, i.e. earlier than the mid-1800s, there was a general intuition among scientists and philosophers about a fundamental all-pervading substance, e.g. Newton seemed to believe in a form of ether himself [382]. But as this predates the birth of electromagnetic theory as we know it, our discussion will not be concerned with scientists' views preceding the middle of the 19th century, since Maxwell, Faraday, Lorentz and others largely adopted those views. O'Rahilly, in his discussion of the ether [62, Vol. II, Chap. XIII], specifically attributes Fresnel's work as responsible for replacing Newton's views about the emission of light with the nature of light as a wave instead. The ether was generally viewed

as a mechanical substance possessing a certain elasticity and density and the vibration thereof would be the propagation of light similar to that of sound in air, hence the term luminiferous ether was often used at the time, and the electron had not been discovered yet. Maxwell, of course, believed in the ether and was also largely influenced by Faraday's work and views about electric and magnetic fields and lines of force in conceiving his field theory [60]. These fields would act in space and matter, respectively the ether, to act as the mediator and transmit the action between the charges and also seen as displacements in the ether. How important the ether was and the use of its assumed mechanical properties can be seen in Maxwell's earlier work [383] and emphasised with the following quotation (original emphasis kept): 'The velocity of transverse undulations in our hypothetical medium, calculated from the electro-magnetic experiments of MM. Kohlrausch and Weber, agrees so exactly with the velocity of light calculated from the optical experiments of M. Fizeau, that we can scarcely avoid the inference that *light consists in the transverse undulations of the same medium which is the cause of electric and magnetic phenomena.*' The belief in the ether was similarly shared by Lorentz and there is reason to believe that the velocity in the associated force equation was viewed by Lorentz as relative to the ether as well [63] and O'Rahilly strongly argues that this is indeed the case. Even Weber also originally believed in the ether, and in a way his force formula attempted to model the interactions of particles within it, however the equation does not necessarily depend on it conceptually, since it contains only the relative velocity between interacting particles. Scientists also tried to detect the presence of the ether experimentally, as in the famous Michelson-Morley experiment or the Trouton-Noble experiment, which is the electric equivalent of the former. The Maxwellian phase of the ether with great emphasis on the experimental works of Michelson, Morley and colleagues between 1880 and 1930 is further reviewed in Swenson's book [384].

Even to this day, it seems to have not been possible to independently prove the ether or a similar fundamental substance, even though some authors claim some experiments as demonstrating its existence [70]. Since it is an important concept many of the theories are based on, we will need to briefly discuss the ether. If today the field has effectively replaced

the ether, it is still important to remind ourselves what the field and its associated theory is based on. As a general principle of physics, the ether appears intuitive and also necessary, since light clearly possesses the properties of a wave and wave propagation requires a medium. Hence, the medium which light travels through was historically conjectured as the luminiferous ether. But accepting a substance with the qualities of a medium for transmission, be that an ether or a field, will always raise the ontological question of what does it consist of, where did it come from and how did it come to be? (These philosophical questions of course also apply to particles and fields but we will discuss their ontological aspects later in section 6.3.2.) While these questions are not easily answered, we can, for now, accept the definition that it is the carrier substance in which all electric and magnetic interactions take place, and a concept which 19th century scientists generally believed in and largely based their theories on its existence. However, the general belief in the ether began to be doubted at the start of the 20th century with the lack of experimental evidence for its existence and of course the arrival of Einstein's SRT, where the ether concept was abandoned in favour of relativistic interactions with inertial reference frames all of equal importance.

6.2.2 Change of Ether Terminology and its Replacement by the Electromagnetic Field

O'Rahilly discusses the ether concept at length [62, Vol. II, Chap. XIII] and shows with many quotations how in the early 20th century more scientists were starting to question and abandon the idea of an ether, at least verbally. According to O'Rahilly, there were generally two factions among scientists at the time: the ones that abandoned the ether and still used Maxwell-Lorentz field theory regardless, and ones that believed in the ether but felt compelled to apologetically justify its existence and their use thereof. For example, he quotes Eddington who says that all physical properties of the ether that made it like a real fluid had to be abandoned. This shows how the lack of experimental evidence of the ether and its supposed properties led scientists to discard the concept and form the opinion that it is not needed for the Maxwell-Lorentz equations to work. However,

O’Rahilly strongly argues the other position, that the ether is intrinsic and necessary in those equations, because it is a required reference system with respect to which the velocity terms in the Lorentz force equation are defined. This necessity of an absolute reference frame is, of course, one of the reasons why in O’Rahilly’s opinion the field theory should be dismissed. He then discusses how the field has effectively replaced the ether, that the word ‘field’ was a compromise between the ether, attempting to describe the properties of space, and the void emptiness contained in the word “space” itself, and has thus been subsequently accepted by scientists as the new governing terminology. However, O’Rahilly emphasises that the underlying equations depending on the ether have not been altered and a re-naming has not changed the physical properties, as the equations depending upon that fundamental concept remained unchanged and a mere verbal adjustment is devoid of physical meaning. Therefore, the field is still the same as the ether from O’Rahilly’s perspective, which reinforces his dismissal of the field concept, containing absolute velocities. O’Rahilly in general promoted Ritz’s theory or that of Weber, as they contain relative velocities only and do not depend on the ether as part of their conception.

Even though this shows that O’Rahilly was an opponent of the ether, he provided a useful overview of what scientists thought in the early 20th century about the ether, and the discussion about the ether itself was still ongoing in the middle of the 20th century. We can generally see from this that the debate about the ether had at that point passed through two stages. The first stage is the original conception and belief in the all-pervading ether as a medium carrying all interactions up to and including 19th century science. The second stage was during the early 20th century, where the concept was largely dismissed in the scientific world due to lack of experimental evidence and a shift in terminology strongly influenced the opinions of scientists.

So at that point, the “field” replaced the ether in its terminology, however one must consequently ask what the “field” itself then is. O’Rahilly [62, chap. XIII], as well as Assis [225, chap. 3], [385], have discussed that there seems to be no clear definition of what the “field” as a scientific agency is, in particular O’Rahilly presents many quotations from

manuscripts and textbooks to illustrate this point. The most basic definition given is, that the field is a region of space in the vicinity of a magnet or electrified body, as this was the view Maxwell commonly utilised. But we also find statements about the field being just lines of force, the field being a real physical entity, the field existing without test bodies being present, the field only being introduced as a visual aid and not having physical meaning, the field being a change in the surrounding ether, the field being transformed space or properties of space, the field being a fundamental concept in its own right; to name a few. One must conclude that the definition of this important concept is indeed inconsistent, as there exist a multitude of associations of the field's nature. But regardless of this disparity, the field terminology has superseded the ether, and fields have become a central aspect widely used in physical sciences today.

6.2.3 Re-introducing Ether in Modern Theories

What followed after the change in terminology however, is a stage three, which we want to call the re-introduction of the ether, that in turn was tied to two important factors. Firstly, we have Einstein's GRT, which re-introduced the "new ether" as space-time properties into the theory after SRT had originally dispensed with it [386]. The increasing success of GRT has then led scientists to re-consider the ether and it has been discussed in that context how the ether concept is reconciled with the effects predicted by SRT and how they can be described as effects relative to the ether [387]. The second factor important for the re-introduction of the ether as a fundamental concept in physics is the development of QED and QFT, and especially Dirac has argued that in electrodynamics based on quantum mechanics, it is necessary to re-consider the ether as a medium in empty space [388]. Infeld [389] has argued against this in response to Dirac, making a mathematical argument by removing a coefficient in Dirac's equations that prevents the necessity to re-introduce the ether. However, Dirac replied in return that a full dynamical theory from his electrodynamics can only be obtained with the ether velocity included. The inclusion of quantum mechanics into electrodynamics has generally led to a shift in perspective and discussion away from the 19th and 20th century views and nowadays physicists are

more focused on the interaction of small fundamental particles in accelerators and the respective quantum fields and waveforms instead of the presence or absence of the ether as a whole.

When today we speak of fields that fill space and give empty space or the vacuum properties of a dielectric, that is in a way the same as having a medium with these properties, hence the thought of an ether-like field in which all charges interact does not appear as abstract. Although it could of course be argued that this is a misleading concept, if we think for example of the dielectric property of the vacuum, defined by the vacuum permittivity ε_0 and permeability μ_0 , one should also remember that these were originally introduced as a ratio between what was called electric and magnetic charges. It is thus only a factor that enters the equation, stating a property of how strongly charges interact electrically or magnetically. Therefore empty space is the reference or default value where the interaction is not changed, due to the absence of other charges in the interaction, if we suppose, for the sake of argument, that there are no other charges in empty space. One could argue that in this sense the ether would not be needed, when the charges interact directly and the interaction is then influenced by other charges (a material) present in the interaction. But the field remains a useful and successful tool to define properties of space and particles, such as spin or electric and magnetic field strength and describe the interactions occurring therein. So a modern discussion of the ether concept should be informed by the nature of quantum fields, as the ether has evolved beyond the original medium it was conceived as into a quantum physical entity with properties of fields and waves. This enables a more sophisticated analysis and discussion involving those properties that would not have been possible in the past.

Take for example, the principle of Ockham's razor. This logical principle has been invoked by the author of this work in section 5.3 to make an argument in favour of Weber's theory over field theory in explaining the behaviour of unipolar induction and rotating magnetic fields. The original point made was, that a direct particle interaction explanation of the phenomenon is favoured by Ockham's razor, as the additional entity of the field is avoided. However, once we try to apply this principle in the quantum

realm, will the same still be true? We are not dealing with “simple” particles and fields any more, a quantum physical object is also described by its wave-function due to the wave-particle dualism. In that sense, the most reduced model for an elementary particle – a point particle – would be disregarding the wave properties, and we cannot make a clear argument with Ockham’s razor any more in favour of just the reduced point particle, since the undulatory nature of the quantum object cannot be dismissed. So rather than thinking of the ether as a “classical” medium, we can find a modern interpretation within the quantum fields of different spin values that govern the interactions of particles and the properties of space-time. As another example, Cornille [70] interprets the ether as a type of neutrino sea.

6.3 The Fundamentality of Fields and Particles

This leads us to the remaining and fundamental key difference between the field theory approach and the direct-action approach: the conception of fundamental fields versus the conception of fundamental particles. It inevitably raises the question which of the two concepts is more fundamental and if charges give rise to the field or if the field gives rise to the charges. Einstein clearly viewed the field as the more fundamental concept, saying ‘the elementary particles of matter are in their essence nothing else than condensations of the electromagnetic field.’ But of course the question is not resolved as quickly and simply as this, we will need to consider several aspects of particles and QFT and modern particle-field theories in QED and QFT apply a hybrid model of both point particles and fields at a fundamental level. It should be mentioned though, that particle physicists imply quantum mechanical objects and waves when they speak of particles, rather than the conception of point particles underlying Weber’s force, for example. When it is spoken of particles in the following, it is implied that there is an underlying assumption of a materialistic entity that constitutes said particle, i.e. it consists of matter, rather than immaterial space which constitutes the field. It is not entirely clear yet if the particles in direct-action approaches are necessarily point particles or if they can also have quantum mechanical properties, e.g. Wheeler-Feynman direct-action theory has been developed for

quantum mechanics, whereas Weber's force has not.

6.3.1 The Size of the Electron

One aspect that should be considered in the debate about the fundamentality of fields and particles is the size of one of the fundamental particles we know: the electron. Since there is more than one way to deduce the electron's size, it will add to the discussion but not resolve it. So far, the electron has not been discovered to consist of smaller constituents (unlike the proton) and is still treated as an elementary particle in the standard model of physics. In many models and applications it is regarded as a point particle, meaning it is treated as an infinitesimal object in dimension 0. Its size and shape has been of interest to scientists, observations by Dehmelt of electrons in a Penning trap [390] find its radius to be smaller than 1×10^{-22} m. Hudson *et al.* [391] have investigated the electron's shape and deviation from a perfect sphere by measuring the electric dipole moment and found an upper boundary of its roundness of 1×10^{-30} e m, at which it is still perfectly spherical. This bound has been improved again by an order of magnitude a few years later [392] and was then independently confirmed [393], affirming that it is indeed a spherical particle within those bounds.

However, even with experimental limits determining electron size and shape, due to the wave-particle dualism we know that the electron exhibits both point-particle and wave-like behaviour, as shown by scattering experiments. If instead of a point particle we regard the electron from the quantum mechanical perspective, then we can use the Compton wavelength to find the size to which the wave-function of the electron can be confined (and thus effectively determine its quantum mechanical size). This leaves $\lambda_c = \hbar/m_e c$ for its wavelength and is on the order of 1×10^{-12} m, which means that the electron as a wave can probabilistically be located on the entire wavelength and only when the wave collapses (e.g. through collision) will it be at one specific point in space as a particle. The spin property of the electron is also an important factor to consider when trying to determine its size. The name stems from the original belief that the particle is indeed spinning around its axis, giving it angular and magnetic momentum. However, if the electron is

a dimensionless point then it cannot spin around its own axis, as it lacks the additional dimensions and degrees of freedom to do so. If instead it is a (tiny) sphere of finite size, its size will put limitations on its angular velocity. For example, the classical “Bohr”-electron radius originally derived from its energy content is on the order of 1×10^{-15} m, and for it to be actually spinning would mean its equator having to spin faster than the speed of light to obtain the right angular momentum. While this problem can theoretically be resolved by regarding the electron not as a single spherical particle but as a distribution of charge and mass in the Dirac field [394], it instead leads to a self-repulsion problem as the internal repulsive forces of the charge distribution inside the electron should cause it to explode. Furthermore, if the electron is treated as a point particle in a field theory then this will of course lead to the self-energy problem of the electron interacting with its own field.

6.3.2 Ontological and Philosophical Aspects of Models

So even to the seemingly simple question of “what is the size of the electron”, a straightforward answer cannot be readily found considering all these different aspects and properties of the electron. It follows from this that the discussion about the fundamentality of particles and fields incorporates quantum mechanical aspects and beyond the classical field and direct-action theories modern insights of QFT are perhaps essential in the debate. We can generally categorise the theories into three classes: pure field theories, pure particle theories and combined particle-field theories, both within the classical as well as the modern quantum mechanical framework. An academic discussion has emerged about which of these approaches is more fundamental and preferable over the others, as well as if fields (respectively quantum fields) are real physical entities [47, 71, 74, 395–399] and even further ontological aspects of QFT are discussed [400–404]. In a way, this discussion is an evolution of the debate about the ether concept, where in the late 19th and early 20th century scientists have argued for or against the all-pervading ether as a fundamental substance of the universe, and at the start of the 21st century scientists have now fully transitioned to argue about the fundamentality of the field which has replaced the ether.

Feynman was very aware of the importance of this discussion, as he said in his Nobel lecture that classic electromagnetism has problems that do not disappear when quantum mechanics is introduced into the problem. He is of course talking about the self-energy divergence here, and it is very true that this difficulty stems from classic field theory and the debate is now continued in the realm of QED and QFT as well as the philosophical aspects thereof. The self-energy divergence is only one of the aspects that the argument around the fundamentality of the different approaches is concerned with, it also entails free fields, the reality and existence of photons and their mechanism of interaction as waves or particles and similarly all fundamental particles and their existence as waves, particles and the respective quantum mechanical excitation states. The reader is encouraged to engage with the references [47, 71, 74, 395–404] if they are interested in the details of the debate. For this present discussion only a brief general overview is given and it shall suffice to say that the three categories, pure particles, pure fields and combined approach exist, and that each category has their respective proponents and arguments in favour of one and against the others. It can be concluded from this argument that an answer to the question of what the fundamental concept is, has not yet been found, and that the problems which each individual approach faces are still unresolved. At this point in time it seems unlikely that such problems can be solved solely from either a classical or quantum perspective and it will take significant advancements in all approaches and disciplines involved to find appropriate answers and solutions. To that end it may be possible to gain new insight if Weber electrodynamics or Ritz's electrodynamics, as examples of particle-based approaches, are successfully extended to incorporate quantum mechanics, which would allow for a deeper understanding of the underlying principles of particle theories. Of course, it is also possible that neither particle, field nor combined approach can be the answer to the fundamentality question, and an even more fundamental concept might underlie these approaches. Such a concept is suggested by string theory, where the vibrating strings comprise the smallest building blocks of the universe from which the rest emerges. Unfortunately it is not yet possible to test string theories experimentally. In addition, we are once more faced with the ontological question: where then did the

strings come from and how did they arise? Krause and Bueno [404, p. 4] even go as far as stating: ‘in the end, there does not seem to be a definitive answer to the question of the ultimate ontology of physics’.

6.4 Language, Philosophy of Science and Basic Assumptions in Specific Theories

There are several aspects to the philosophy of science and a wider discussion thereof can be found in [405], but for this discussion we will only focus on some relevant aspects that relate to the theories and their underlying concepts. First, it is important to note that these discussions about the ontology of the building blocks of the universe and the fundamentality of particles, fields and waves should not just be based on mathematical arguments and should always incorporate philosophical aspects because of both Gödel’s incompleteness theorem and Haag’s theorem. Due to these implications, no mathematical framework can ever be perfect or complete, and even if it was, it is just a tool that works on purely mathematical grounds and thereof multiple different working tools can be constructed. However, to resolve ontological questions, physical and philosophical arguments always need to be considered. It is likely that even the best physical theory will face some limitations due to its intrinsic incompleteness, and so it is possible that one theory might not be enough to describe all mechanisms and phenomena, and so another second approach is needed to make up for its shortcomings. This is also coupled to the very limitations of science itself and the instruments we have to observe what is before us. All these theories are models that try to describe our experiences, but this will always be limited by the context in which it is observed and the confined interpretation of reality by the observer. After all, the human mind cannot describe an objective reality, it can only perceive a filtered version of impressions of the outside, subject to its own physical senses, biases and previous experiences. Some might be inclined to argue that this is the reason that sophisticated instrumentation for scientific measurement is developed to observe in human’s stead, but the premise remains that the data and observations obtained need to be interpreted by a human that is trying to make sense of and translate the world into a

framework one can grasp, which in turn confines the observation to this very frame.

Next to the limited means of observation available to us, there is another boundary imposed onto our scientific knowledge and advancement by the limitations of language. For example, quantum mechanical objects exhibit very different behaviour from what was observed classically on the macro scale that the very discovery of quantum mechanics caused a drastic and radical shift in physics to what was before. However, because of this difference we struggle to describe the quantum object with the words available to us from the macroscopic world, we assign it wave-particle dualism, a probabilistic nature, different excitation states, colours and flavours, when these are all mere attempts to grasp the concept and describe its behaviour with the limited vocabulary we have, when in reality we do not know what the quantum mechanical object looks like and struggle to put it into words.

It is therefore of interest to examine the language terms used to describe electromagnetic phenomena. The essential feature is the interaction between electric charges which in the case of a Weber-type theory is concerned with the direct transmission of force, whereas in field theory the interaction is through a form of mediation between the charges. As Brown [103] has argued, especially when referring to light, our minds are conditioned by “thing-language” in the context that we feel intuitively that “*something*” (as in, some *thing*) is *travelling* between source and receiver to carry the action, such as a ray of light or a photon is said to travel through the ether or field. However, in reality ‘nothing has ever been found travelling’ [103, p. 33]. Even though Brown is mainly reasoning this for light, we would like to argue that the same concept applies to electromagnetic action, any test particle in the path between source and receiver will simply experience a force. This advises us to exercise linguistic care and be critical about scientific phrasing. The same is true with the use of mathematical terminology and Brown comments on the seemingly unavoidable use of the term energy in physics. Energy is not a causal agent, it is essentially a textbook definition in terms of force and distance. Moreover, “energy conservation” is no more than a book keeping operation.

In describing action-at-a-distance theories, not requiring the concepts of ether or fields

but constituting a direct interaction force, Brown introduces the term c , not as light velocity but as a retardation constant in the basic transmission process. One might conclude that what is fundamental is the word force. However, from the point of view of philosophy of science, Hertz in his ‘Principle of Mechanics’ refers to the mysterious concept of “force” as used in Newtonian physics. He suggested that the problem should be dealt with by re-stating Newtonian physics without using force as a basic concept. Newton, it appears, was certainly aware of the problem in his careful wording of the law of gravitation: ‘there are observed phenomena between two bodies in space which can be described by presuming that the bodies attract one another with a force directly proportional to the product of their masses and inversely proportional to the square of the distance separating them.’ In the popular formulation it simply reads: ‘two bodies attract one another [...]’ We must remind ourselves how the premise of the words we use to explain a mechanism shapes our understanding thereof and that some of the descriptive terms used are not necessarily physically real entities and can only be viewed as explanatory metaphors instead of attributing them a causal nature and that therein language itself can be biased and flawed.

It is also appropriate to comment briefly on the assumptions which underlie theories of electrodynamics. The field theory associated with Faraday, Maxwell and Einstein is characterised by the ether assumption. Maxwell himself is on record in remarking that without an ether the symbols in his equations have no physical significance, he states, [1, p. 158]: ‘If the action of the system E_2 on E_1 does in reality take place by direct action at a distance, without the intervention of any medium, we must consider the quantities [...] as mere abbreviated forms for certain symbolical expressions, and as having no physical significance.’ Then Einstein following Maxwell, has postulated the field as a fundamental entity rather than charges. By contrast action-at-a-distance theories, which do not assume an ether and associated fields, deal only with relative velocities and accelerations between charges. However, as Assis has commented [63, p. 236] ‘Despite these positive aspects it should be emphasized here that Weber’s electrodynamics is only a model of interaction between charges which describes certain classes of phenomena.’ In general, any theory

or model can be likened to attempting to fit a template to the behaviour of nature with limited success. Or as Cullwick has commented in a more poetic sense [79]: ‘the gap of ignorance which we now leave between charge and charge should not dismay us, for it is but a small part of the unfathomed mystery of experience which embraces all things, measurable or not, of which we are conscious.’

Therefore, a more general discussion about the role that assumptions play in the construction of theories of science appears adequate. It should be pointed out that this too is a limiting concept intrinsic to every theory. That is, the assumptions might sometimes be implicit in the pursuit of facts that scientists strive for, but we must remind ourselves of their nature and their importance as they define the premises a theory is built on from which so called facts are extracted. Brown [103] describes a fact as ‘an assertion that can be verified’ – and often we will find that this assertion has some underlying assumptions. We can generally distinguish assumptions into two categories. These are provable assumptions and unprovable assumptions, where respectively an assumption that can be disproven belongs to the category of provable assumptions. Further, we can say that an assumption, regardless of its category can be either a justifiable assumption or an unjustifiable assumption. For example, the assumption of quantum fields is a justifiable one, in that it works very well as a description of the universe, however, as of yet it is still an unprovable one as an independent proof of the field itself does not exist. And this leads us to the core limitation of an assumption, as every assumption that is made introduces either a simplification or an associated cost at the expense of something more complex or another assumption of equal quality. Any proof is only as good as its assumptions and they are sometimes made unconsciously, so it is important to be aware of what assumptions are made and what their associated cost is. Hossenfelder actively encourages to state and track those assumptions to evaluate if they later become justified or unjustified [406, p. 234]. The associated cost might be negligible for a given application, so that based on that assumption the desired outcome is achieved, however, this does not mean that the simplification and cost are non-existent. This will always put a limitation on knowledge and the knowability in science, as there could be an even more complex structure hidden

beyond these assumptions and theories. But of course we have to make some assumptions somewhere in order to know anything in the first place and the ontological question will always feed back into the problem of how did the even more complex thing arise? We must start (or stop) somewhere with an assumption and then use our limited means to try and prove or disprove this assumption in the pursuit of further knowledge.

Regardless of whether humans are equipped well enough in mind and observation to understand the world they live in, they will try anyway. And through this very act of trying they will be faced with all of these limitations. If eventually, the knowledge and discoveries within those limitations are still sufficient to arrive at a complete explanation, there will still be many iterations on the journey ultimately leading there, and it is, for that reason, crucial to be aware of and discuss those limitations on a philosophical basis. Only this way can it be judged whether the conclusion reached is a sufficient one or if further attempts at observation and interpretation need to be made and philosophy will have to decide at what point a sufficient degree of knowledge has been reached. Even though the fundamental questions have not yet been answered and at the present time it seems not possible to settle on any of the three categorical approaches between fields and particles and not decisively distinguish between Weber's and Maxwell's theories, we must remember that none of these theories and models are absolute and that for the limitations discussed herein, there might not be one single theory of everything and instead we can benefit from a hybrid approach incorporating the strengths of each individual approach. Further, it is easy to get lost in the discussion of the details over which theory is better than the other, but we must remind ourselves that they are just models and as long as they can deliver accurate results, regardless of the exact underlying premise, then that may be sufficient for the desired outcome. Moreover, it may well be advantageous to approach a problem from multiple perspectives and consider different viewpoints, as it would increase the generation of knowledge.

6.5 Additional Remarks

Finally, some general comments are offered about experimental research, the state of physics in general and the role of philosophy in physics. From the author’s perspective as an engineer, it is necessary to re-state the importance of experimental research, as partly emphasised by the overproduction crisis in cosmology mentioned by Hossenfelder [54]. Only experimental data can in the final instance decide about physical theories. After all, practical experiments deliver results that can actually be observed whereas theories can only attempt to describe what might be observed. To underline this statement, consider the words of Brown [103, p. 3]: ‘Thought-experiments can only produce conclusions from premises; genuine experiments yield conclusions from Nature.’

Modern physics, or perhaps it is more apt to say post-modern physics, is faced with some problems and some authors have accredited physics as being in a crisis [407–409]. Those problems partly stem from supersymmetry, naturalness and the pursuit of “mathematical beauty” and are addressed by particle physicist Hossenfelder in her book ‘Lost in Math: How Beauty Leads Physics Astray’ [406]. (For a brief reflection on the book the review by Butterfield is recommended [410].) Those aspirations to “beauty” present in the guiding principles of physical research nowadays is in turn shaping the experiments and their interpretation. Interestingly, Crowther [408] suggests some solutions to resolve the crisis with philosophical principles, and similarly, one can see Hossenfelder’s critique on using “mathematical beauty” as a methodology as a philosophical approach to address these problems. Field theory is the foundation that all subsequent theories (i.e. SRT, GRT, QFT) were developed from, but instead of re-examining the foundation on which the house is built, the trend tends to add more and more to it, and “new physics” are expected to emerge as a solution. This may or may not seem like a case of positivity bias, but maybe it is actually not “new physics” that is needed, maybe it is old physics in a new guise. Nowadays action-at-a-distance and Weber-type theories are often dismissed *a priori*, but they may offer solutions to some of those problems. We should remind ourselves that some of the significant advancements that led to “new physics” have happened in leaps, because the novel discoveries were so radically different that they did not fit the

existing template. In the case of SRT and quantum physics this was achieved by solving mathematical inconsistencies – so in a way it might not be a bad thing that Weber’s theory still has some mathematical inconsistencies with respect to experiments yet to be resolved. From the author’s perspective, joining Weber-type theories and particle physics would certainly be a welcome way forward in research and it might offer some new insight into the current puzzles surrounding supersymmetric expectations.

Further, the late Stephen Hawking had remarked ‘philosophy is dead’ because ‘philosophy has not kept up with modern developments in science, particularly physics.’ It was first expressed in his book ‘The Grand Design’ in 2010 [411], in the context that in Hawking’s opinion only physical data, such as from particle accelerators, can answer fundamental questions about the universe. Other physicists have expressed similar opinions, for example Steven Weinberg and Neil de Grasse Tyson. Further, this trend to dismiss philosophy seems to be not exclusive to physics, a similar notion has been observed and commented on among the life sciences [412].

While the dismissal of philosophy has, of course, instigated reactions by philosophers [413–415], it has similarly seen critique expressed in the physics community by Rovelli [416]. Most interestingly, Rovelli has pointed out that the dismissal of philosophy is an age old problem, dating back to ancient Greece, where Isocrates had argued against Plato’s Academy. Rovelli then presents several arguments why philosophy is needed in physics, refuting the claims about the morbid state of the discipline. Further, several historic examples of the influence of philosophy on scientific developments present in physics are invoked, showing the connectedness and influence between the two, eventually concluding that one needs the other. While the author does indeed share the belief that experimental data is of great importance to science in general, some more commentary seems adequate about the importance of philosophy to natural sciences. We have clearly seen in the literature review and the previous sections of this chapter that philosophers are discussing the fundamentality and other aspects of physical and quantum mechanical theories, and that these considerations are necessary to approach ontological questions. This means that either philosophy has caught up with physics nowadays or it is possible that it was

actually physics that has not kept up with philosophy. There seems to be generally a rift present between different disciplines of science, which is not unexpected, because scientists nowadays are much more specialised in a narrow field, which is a result of the great advancement in all scientific disciplines and the sheer amount of knowledge that is readily available in each respective discipline. So instead of the “universal genius” or scientists commonly researching multiple disciplines, as was the case up to and including the 19th century, it has become rare for scientists to deeply engage with disciplines outside of their own field. In and of itself this is not a bad thing, as the requirement for specialisation and expertise is to dedicate oneself to a narrow field. But the specific focus often entails a loss of broader perspective and so it is easy to overlook other perspectives or “the bigger picture”. This may also be linked to a general trend of the natural sciences and engineering not valuing the humanities to the same extent as they value other natural sciences.

7 Conclusion and Future Work

This work has investigated Weber electrodynamics with a special focus on experimental topics and also carried out tests to compare Weber's theory and field theory with observed experimental data. In the literature analysis both Maxwell's theory of fields and Weber's electrodynamics have been introduced, together with other alternative descriptions of electrodynamics. It was then reviewed how Weber is capable of explaining several electromagnetic phenomena, including Coulomb's force, Ampère's force, field equations, the telegraph equation and induction, and explored even beyond how Weber can further be related to concepts in general physics, such as the strong nuclear force, Newton's second law and Mach's principle. Moreover, Weber's theory has been applied to gravitational effects and relativistic phenomena such as the bending of light or frame dragging. On this basis it was suggested that Weber electrodynamics might well be a candidate for a unified theory and that it offers many explanations to known phenomena and can be considered as an alternative to the standard approach. But even with the several strengths of Weber's formula presented, the present limitations of the theory have also been explored and criticism of the theory addressed.

Several experimental tests have been performed and their results compared with both field theory and Weber's theory. In section 4 an electron beam was deflected using several current carrying solenoids, with the beam travelling across the solenoid as well as through the solenoid. The deflections were measured in each case and found to show good agreement with the predictions obtained from the simulations based on both Weber's force and field theory. In section 5 qualitative and quantitative unipolar induction experiments have been conducted. First, the quantitative measurements of an induced voltage across a spinning disk in the field of a bar magnet were obtained and compared with predictions from field and Weber theory. Again, both theories showed good agreement with the measured values. Following this, qualitative tests were carried out to resolve open questions about the phenomenon of unipolar induction and deduce its working mechanism. This involved a novel apparatus where each of the individual components, including magnet, disk and measurement circuit, were allowed to rotate independently from each other. It was found

that the relative motion of disk and measurement circuit is crucial for the observation of an induced voltage, and that this new experimental evidence allows “Faraday’s paradox” to be resolved. The paradox arises from considerations of the magnetic field’s movement and the apparent absence of a change in magnetic flux which would be necessary for the applicability of Faraday’s law. This is connected to an often present omission of the measurement circuit in the literature when analysing the problem. However, the results show that consideration of the entire circuit is required to restore the flux cutting for the applicability of Faraday’s law.

Finally, some aspects were discussed about the underlying fundamental premises of Weber and field theory and the limitations faced when trying to distinguish between them. The discussion focuses on the ether concept and the development thereof in the framework of modern physics, where the role of particles and quantum fields are discussed instead of the original ether with regard to philosophical and physical aspects. But the ontological questions in the debate, encompassing the fundamental concepts, are still to be answered and philosophers are in disagreement about which of the approaches between particles, fields and combined particle-fields is preferable in physics.

7.1 Review: Contrasting Weber and Field Approaches

From the literature review we have seen the capabilities of Weber’s electrodynamics, how it successfully models electromagnetic phenomena and that it has similar qualities to the Maxwellian field approach, in that it is consistent with field formulations and explains transmission through the telegraph and wave equations. For point particle interaction the Weber force can be used directly, whereas in field theory the Liénard-Wiechert-Schwarzschild force or Darwin Lagrangian needs to be utilised. When current elements are interacting, Weber’s force is transformed into Ampère’s force, while in field theory Grassmann’s force is commonly used. In this context we have also emphasised the importance of longitudinal forces and their role in Weber electrodynamics as well as their analogy in field theory, as they have been claimed to exist in both approaches. When regarding the conservation laws it is found that Weber’s force follows Newton’s third law

in the strong form, thus conserving linear momentum, and additionally conserves angular momentum as well as energy. In the field approach it is usually argued that conservation laws are not violated when the energy content of the field is taken into account, i.e. the field can obtain energy from a system and store it as well as release the same energy.

Further to just explaining electricity and magnetism, Weber's theory provides a basis for other physics disciplines and has a unifying character connecting several branches of physics. It has been shown how Weber's force connects to gravity and the strong force, however it is not yet known how the weak force relates to Weber's force. For standard field theory it is well known that strong force and weak force can be related to the electromagnetic force but it is still unknown how gravity can be unified with the other forces in that approach, although it is being researched (e.g. quantum gravity). Lastly, field theory is compatible with SRT as well as quantum mechanics, but there is no extensive research yet how Weber's theory can be related to these topics. We can see from this juxtaposition that both theories are similar, yet different, and a table is given below summarising some of the similarities and differences of both theories, giving an overview of their parallels (Tab. 7.1).

In the experimental sections we found that both Weber's force and field theory are in good agreement with experimental observations in the near field and low velocity limit. From both the literature review and conducted experiments it is found that, while both theories have some definitive conceptual differences, more than often they make the same predictions and arrive at the same results and are in fact very similar.

7.2 Revision: Can the Theories be Distinguished?

From the results of this work we cannot distinguish between the theories and it might be nigh impossible to distinguish between the two theories in the future, due to their similarities. In terms of philosophy of science, both theories are just models that represent nature only to a certain degree and attempt to describe observable phenomena, but neither of them is perfect and the theories themselves are subjective and limited. Field approach and direct-action approach are similar, yet different, and the discussion about which

Table 7.1: A comparison between field and Weber theory in selected categories

Category	Field theory	Weber electrodynamics
Point Particle Interaction	Liénard-Wiechert-Schwarzschild force	Weber force
Current Element Interaction	Grassmann's force	Ampère force
Longitudinal Forces	Can be obtained in various ways [165, 166, 182]	Intrinsic
Magnetic Force	Lorentz force	Weber-Ampère force
Conservation laws	Energy is stored or dissipated by the field to restore conservation laws	Follows linear momentum, angular momentum and energy conservation
Field Equations	Maxwell equations	Can be obtained in various ways [63, 127, 178–180]
Induction	Through changing electric and magnetic fields and flux	Through particle movement (velocity and acceleration)
Wave Equations	Arise from moving fields	Can be obtained through retarded time and also predicts telegraph equation
Compatibility with other forces of nature	Weak force, Strong force, Gravity not yet known	Gravity, Strong force, Weak force not yet known
Compatibility with SRT	Compatible through Lorentz transformation	Incompatible with Lorentz transformation, but may not be necessary
Extension to Quantum Mechanics	QED, QFT	Initial connections, but not yet fully known

of these is conceptually more fundamental is still ongoing, with an associated discussion about the fundamentality of particles and fields. Either theory has its respective problems, limitations, benefits and drawbacks and neither is necessarily better than the other on these grounds, it is rather a trade-off between these theories depending on the application for which they are intended. On this basis, the approaches can be seen as complementary rather than competing, and their utilisation depends on the boundary conditions, the desired outcome and which approach models a specific problem better than the other, or for that matter more effectively in terms of the explanation offered for the underlying mechanism of the application. In a practical sense and from an engineering perspective, this would tend to favour the approach that can enhance design capabilities. “Truth” or the origin of a certain phenomenon might lie somewhere in the middle of the theories in

question.

One can conclude that Weber's theory is not without limitations (but neither is field theory) and is only valid within the low velocity regime, with standing problems in relativistic physics (special as well as general), radiation and plasma applications as well as quantum electrodynamics. The direct-action approach still offers a viable alternative that can be considered for the explanation of electromagnetic and physical phenomena in general. Although Weber's theory still needs development and has not been developed to the same level as field theory (such as its extensions in relativity and quantum mechanics have), it might be a valuable asset for science to consider, as it can offer a different perspective but yields similar outcomes to the standard approach. Neither theory can exclude the other completely and they can in fact complement each other.

7.3 Reflection: Limitations and Advantages

We can now address the questions prompted in the introduction and try to find suitable answers, repeated here for convenience: can Weber electrodynamics be considered as a viable alternative to describe electromagnetic phenomena? What, if any, experimental evidence can be found for or against Weber's theory? Can the theory be proved or disproved? Can limits be put on the validity of the theory? Does the direct-action approach provide certain advantages or disadvantages? Could it even be beneficial to use both theories in conjunction within the right set of constraints?

With the results and arguments presented in this work, it is concluded that Weber electrodynamics should not only be considered as an alternative but also as a desirable addition to Maxwellian field theory. It offers from a particle perspective an equally valid explanation of observed phenomena, as well as the prediction thereof (albeit currently within limitations). In this sense Weber's theory can be regarded as an important component of electrodynamic theory. While experimental evidence has not been found that can wholly prove or disprove either of the theories, it has been demonstrated that Weber agrees with experiments in the near field and low velocity limit, and it is suggested that it will continue to do so with the right development, similar to field theory, in all cate-

gories of electromagnetism. While experimental evidence in relativistic electrodynamics and QED supports Maxwell's field theory, with the present state of affairs it seems that Weber's force in its standard form only agrees with experiments in the near field and low velocity limit. This suggests, along with recent studies, that Weber's force is a low velocity approximation up to second order in v/c of a more fundamental underlying force, and needs further development. Several modifications are conceivable, with possible generalisations of the Ritz-type or corrections to the Weber potential as suggested by Li [260] and it will be subject to future work to investigate the full capabilities and boundaries of the theory and its modifications.

A benefit of Weber's force is that it follows Newton's third law of motion, thus conserving linear momentum, and additionally conserving angular momentum as well as energy, so it does not violate conservation laws. In the field approach it is usually argued that conservation laws are not violated when the energy content of the field is taken into account, i.e. the field can obtain energy or momentum from a system and store it as well as release energy and momentum. Further, Weber's force accounts for longitudinal forces intrinsically, however, the absence of longitudinal forces seems to be desired in radar and plasma applications where the field approach benefits from this quality instead and Weber seems to fail to predict the expected results. But Weber's force can be calculated directly from the movement of the charges involved in an interaction and does not necessitate the calculation of one or more fields of those charges from which the force is calculated, which offers a clear force and particle-based approach, which avoids problems such as the self-energy divergence. Another benefit in Weber's theory is that charge velocities are clearly defined, whereas in field theory there may be some ambiguity left as to what velocities are to be used in the Lorentz force equation. This is correlated with the fact that Weber's force is completely relational and thus has the same value for any observer. Further to this, it can offer clear charge-based explanations for observable phenomena, as in the case of unipolar induction where the field can be ambiguous and terms like 'lines of force' or Faraday's 'tubes of force' can be unrewarding concepts offered to explain the working mechanism clearly (see sec. 5.3). Lastly, Weber's force offers the possibility to unify

gravitational forces with those of electromagnetism. It is thus considered constructive to use both theories in cooperation with each other, as each can compensate for the other's weakness and regarding a specific problem in question from both perspectives can lead to new insight. Examples for this can be found not only in the flux cutting analogy of unipolar induction, but also transformer induction where the particle perspective considers the acceleration of the current electrons whereas the field perspective links the magnetic flux of either side of the transformer. Similarly, the magnetic field of a solenoid deflecting an electron beam has been shown in this work from a particle perspective, where it is again the movement of the charges exerting an influence on the test body rather than the field mediating the force.

7.4 Future Work and Speculation

It will briefly be discussed in this last section what future research might be undertaken in relation to Weber electrodynamics, which may also relate directly to applications currently governed by field theory and thus could lead to new insights. After suggesting certain topics that could be worked on directly, it will be speculated what other capabilities Weber's theory might hold if given treatment in the right framework and with the necessary physical and mathematical rigour.

7.4.1 Future Work

On the basis of the present work, one can identify certain aspects of Weber's electrodynamics that would be especially interesting to research further. Firstly the importance of Ampère longitudinal forces and determining how they influence specific applications. While their existence has been reviewed and discussed in this work, it remains to be determined how relevant they are in specific experiments. For example, it was mentioned in the discussion that the present limitations surrounding the radar equation and cold plasmas are related to the longitudinal forces and that this is a topic for future investigation. As discussed in section 2.3, further development of Weber's force for signal transmission and radar applications would be of interest. Further, the general relevance of longitudinal

forces to nuclear fusion applications has been suggested [151, 166, 417], and based on this it remains to be determined how longitudinal forces could be applicable to plasma physics on a wider scale, especially as plasmas typically have a positive ion charge density and a negative electron charge density. But there is not yet extensive experimental work giving a quantitative estimate of the influence of the longitudinal forces on plasmas of which the present author is aware. It remains a task for the future to find if they influence the state of the plasma in any way or if their contribution is negligible, some recent experiments [170] suggest that the influence is frequency dependent but relatively small. Further research into longitudinal forces would certainly be of general interest to clarify their overall role in electrodynamics.

Another aspect that should be further investigated is charged particle optics based on Weber's electrodynamics, in particular the deflection of high-speed electrons as in the Bertozzi experiment and further exploring how Weber relates to mass change with velocity and SRT. With this work the modelling of electron beam deflection based on Weber's force has been advanced to a more rigorous three dimensional model in the low velocity regime and in the future this work may be extended to the high velocity limit as well to compare it with existing experimental data, as in the Bertozzi experiment or to obtain new experimental data. In order to advance the simulation in the high velocity regime, Weber's force will likely need modifications, such as suggested by Wesley, Assis, Montes and Li along with other types of modification and generalisation still to be explored. Further, it would be of interest to not just investigate modifications of Weber's force or Weber's potential for their compatibility with relativity and a speed limit, but also give them a more rigorous examination following the example of Bunchaft and Carneiro and investigate a given modification for energy conservation, the bending of light and perihelion precession, but also in relation to the negative mass and infinite acceleration behaviour to find the respective limitations of a chosen modification. Although the goal is not to just test the limitations of a given modification, the main interest lies in finding what predictions can be made and if new insights can be gained by modifying the force in a certain way.

It could be valuable to research further electrostatic induction and its connection to Weber's force, Assis notably mentions the experiments performed by Jefimenko and Edwards *et al.* [418–420]. Nowadays, there are more modern experiments that have been performed and extended the work of Edwards *et al.* with superconductors and electrostatic induction in general, but it seems like they have not yet been analysed from a Weber-perspective and similar experiments could help to further investigate the boundaries and validity of Weber's and field theory in these cases. Next to electrostatic induction, of course, investigating other induction experiments further and how Weber's force can predict them seems logical. We have seen in this thesis how Weber can successfully predict the working mechanism of unipolar induction, so it would be a rational next step to expand the research to other induction based experiments. For example those of Barnett, Kennard, Pegram or Bartlett and also relating this back to longitudinal forces which may be present in those cases as well, as they have been suggested to be present in the generator and motor configurations of unipolar machines by Guala-Valverde and Achilles. Some direct follow-up experiments on unipolar induction have also been suggested to further investigate the possibility of the magnetic field's movement, such as allowing the magnet to rotate opposite the circuit components and utilising a field detection instead of contact detection.

7.4.2 Speculation

These five aspects, longitudinal forces, a relativistic speed limit with Weber, the general modification of Weber's force and potential, electrostatic induction and induction effects in general, are clearly identifiable areas of research in which Weber electrodynamics can be advanced. But next to these relatively obvious categories, there might well be much more that Weber's force is capable of and where we do not yet realise its possibilities as a theory. For that reason, it is speculated how Weber's force might develop in the future, or what it should be able to predict in order to move beyond its framework of classical electrodynamics and incorporate quantum mechanical considerations, so that it may be on par with QFT, depending on the right development. This will also entail the suggestion of

some new possible modifications that could be applied to Weber's theory, which seem to have not been considered previously in the literature. But since the following remarks are speculative, they might not necessarily be successful in their nature, however, the author of the present thesis feels the need to mention and offer these ideas to the scientific community.

Given that Weber's theory seems to have at least some loose connections to quantum mechanics, it would be extremely interesting to investigate how it can be further related to other quantum mechanical effects, as this could resolve existing problems with Weber's force. For example, if it tries to emerge as a successful quantum mechanical theory, it should be able to explain the photoelectric effect, and it was mentioned in the literature review, section 2.2.2, how Weber and Zöllner speculated a connection between light and electricity, as well as spectral lines based on Weber's planetary model of the atom. So it does seem entirely plausible to also find a connection based on Weber's force with the photoelectric effect. It is also possible to speculate about other quantum mechanical effects as well, and it can be pointed out in this context, that intrinsically Weber does not seem able to account for the spin property of particles yet. So this might be an idea in and of itself, to find and research how or if Weber can account for spin of particles and what predictions it might make about the particles with a suitable extension to encapsulate spin. One possible idea in connection with spin and quantum mechanical phenomena in general could be to allow complex valued inputs in Weber's formula, or respectively allow particles to be represented by complex numbers. Or maybe it is somehow possible to use Weber's force with wave functions as well, which would come closer to actual quantum mechanical objects than the point-particle formulation of Weber's force. It could be conceivable that, if Weber can account for the dipole moment of particles, it would be able to predict the Stern-Gerlach experiment, for example.

By extension, Weber could then also be applied to semiconductor technologies and particle physics. Semiconductor technology has emerged in the second half of the last century and has seen great success and advancement since. So far the technology has only been viewed from a position of field theory (but also admittedly with quantum phys-

ical considerations) and it would be interesting to consider this field of study with Weber electrodynamics instead, or re-investigate effects such as the Quantum-Hall-effect from a Weber perspective. In terms of particle physics, it is straightforward to see a connection to Weber's force, since gluons are particles that model the transmission of a force, representing the interaction of fundamental particles, and it would be interesting to see how Weber treats the same interactions and how it could relate to gluons and respectively, what particles are predicted by Weber's theory in the quantum realm. And further connections can be conjectured based on a quantum mechanical version of Weber's force. We have discussed how the telegraph equation, which is a wave equation for the transmission of electromagnetic signals, can be derived from Weber's force. Similar to this, it might be possible to derive a Schrödinger-type equation with a quantum mechanical treatment of Weber's force, a recent study by Zhao [421] has derived a quantum mechanical wave equation that shows interesting similarities to Weber, in the sense that both theories can account for precessing electron orbits. But this might not only apply to quantum mechanics, the opposite may be possible on a macroscopic scale, if a Weber-type gravitational force is utilised, it might be possible to derive a wave equation for gravitational waves as well. Another topic that could further be investigated and is usually connected to quantum mechanical considerations is the AB-effect, but other than the brief work by Wesley mentioned in the literature analysis, no further exploration of the effect based on Weber's force has been undertaken. It seems useful to re-investigate the AB-effect based on Weber's electrodynamics, which could then also lead to insights about a possible connection to quantum physics.

It is also possible to imagine further novel modifications of Weber's force, next to the ones that have been discussed in the literature review and suggested earlier in this section. One idea could be to explore the capabilities of Weber's force in higher dimensions. In its standard form, it is restricted to three spatial dimensions and one temporal dimension, but we know from relativity theories, QFT or even string theory that sometimes higher dimensions are required. Thus it could be instructive to test the capabilities of Weber if it is treated in more dimensions or if it can merge spacetime similar to relativity, maybe

also in a quaternion representation, or other dimensional manifolds known from QFT or string theories. But there might be even more ways to extend, modify or generalise Weber's force and potential that have not yet been thought of.

Beyond the facets of modern physics however, there are older effects and other disciplines where Weber's force can be speculated to have a connection. Weber himself speculated about explaining thermoelectric effects based on his theory [63,204], although he was not able to explore the idea further before his death and to this day it does not seem like anyone has attempted to pursue this train of thought further. A possible approach to modelling thermoelectric effects with Weber could be done with the help of statistical treatments, e.g. considering the average thermal speed in a restricted volume of a conductor for a given volume charge density or individual charges within that volume, which would in turn lead to an electric potential in that volume element based on the speed of the charges. If that volume element is juxtaposed with another element of different velocity, a net electromotive force could be derived from Weber's force in that case. He also speculated further that his force law might be able to explain chemical catalytic forces [63,204] and related to these two ideas, one can also speculate that there may be a connection between Weber's force and the reaction energy of chemical reactions, maybe also based on the thermal speed and intermolecular forces of the constituents.

While on the subject, there might be a wider connection between Weber's force and intermolecular forces as well. The different types of intermolecular forces, e.g. London dispersion forces, the Keesom interaction giving rise to Van-der-Waals forces, dipole interaction, hydrogen bonding and ion interaction are at their core all based on electrodynamic attraction, so it appears straightforward to speculate that these could be modelled with the help of Weber's force. This could lead even further to the very origin of cohesion and adhesion forces, as all the fundamental attraction of atoms and particles is electromagnetic in nature. A general electromagnetic origin of capillary forces of water has been speculated by Pollack [422], and it would certainly fit the idea of Weber's force being able to explain intermolecular interaction. This can be further extended to related concepts that are known to be influenced by the presence of electric forces and potentials, such as

electrocapillarity, the surface energy of liquids and associated electrowetting, electroosmotic flow, electroviscosity or the ζ -Potential in electric double layers of electrolytes and liquids. It is conceivable that with quantum mechanical advancements in Weber's theory, it can be even further applied to other applications in chemistry, as for example density functional theory that is trying to predict the distribution of shared electrons in complex molecules, especially relevant in organic chemistry [423].

While at the moment the relation of these topics to Weber's force are speculative, we can generally appreciate the fundamental idea of the attraction of charged particles in all of these applications and it appears coherent to contemplate their connection on this basis. It also shows that there is still a lot of potential research to be pursued in Weber electrodynamics and that Weber's force might hold even greater value than currently known. Future research will hopefully show if and how Weber's force can offer more insight into what is currently known based on the classic interpretations of phenomena.

7.5 Closing Remarks

While it remains to be determined whether a field or a direct-action, particle based approach is philosophically more agreeable, one can conclude that the force law of Weber is comprehensive yet wonderfully simple and successful in explaining electromagnetic phenomena. It is thought that further developments of this theory and critical reasoning can open up new and exciting opportunities in physics, engineering and beyond. In relation to electromagnetic theories, philosophical considerations are and must remain a core aspect of scientific knowledge and the pursuit of fundamental questions. As Rovelli [416, p. 484] reminds us: 'philosophy can provide methods for producing new ideas, novel perspectives, and critical thinking. Philosophers have tools and skills that physics needs, but do not belong to the physicists training: conceptual analysis, attention to ambiguity, accuracy of expression, the ability to detect gaps in standard arguments, to devise radically new perspectives, to spot conceptual weak points, and to seek out alternative conceptual explanations.' Certainly, these tools are paramount if the fundamental questions in physics are to be resolved. One can argue that every scientific attempt to understand the world

better is, at its core, a philosophical one, and in order to do so, one must continue to ask scientific and philosophical questions. If one stops asking questions, one abandons the scientific method itself. Because after all, science is not about having the right answers. Science is about asking the right questions.

References

- [1] J. C. Maxwell, *A Treatise on Electricity and Magnetism Unabridged*. Dover, 1954.
- [2] J. Cresser, “Quantum physics notes,” *Department of Physics, Macquarie University, Australia*, 2011.
- [3] A. Einstein, “Zur elektrodynamik bewegter körper,” *Annalen der Physik*, vol. 354, pp. 769–822, 1905.
- [4] A. Einstein, “Die grundlage der allgemeinen relativitätstheorie,” *Annalen der physik*, vol. 4, 1916.
- [5] S. B. Giddings, “Black holes and other clues to the quantum structure of gravity,” *Galaxies*, vol. 9, no. 1, p. 16, 2021.
- [6] N. Jeffrey, M. Gatti, C. Chang, L. Whiteway, U. Demirbozan, A. Kovacs, G. Pollina, D. Bacon, N. Hamaus, T. Kacprzak, *et al.*, “Dark energy survey year 3 results: Curved-sky weak lensing mass map reconstruction,” *Monthly Notices of the Royal Astronomical Society*, 2021.
- [7] P. Ghosh, “New dark matter map reveals cosmic mystery,” *BBC News*. Retrieved June 01, 2021.
- [8] K.-H. Chae, F. Lelli, H. Desmond, S. S. McGaugh, P. Li, and J. M. Schombert, “Testing the strong equivalence principle: Detection of the external field effect in rotationally supported galaxies,” *The Astrophysical Journal*, vol. 904, no. 1, p. 51, 2020.
- [9] S. Hossenfelder and T. Mistele, “The redshift-dependence of radial acceleration: Modified gravity versus particle dark matter,” *International Journal of Modern Physics D*, vol. 27, no. 14, p. 1847010, 2018.
- [10] J. Felten, “Milgrom’s revision of Newton’s laws-dynamical and cosmological consequences,” *The Astrophysical Journal*, vol. 286, pp. 3–6, 1984.
- [11] W. Luo, J. Zhang, V. Halenka, X. Yang, S. More, C. J. Miller, L. Liu, and F. Shi, “Emergent gravity fails to explain color-dependent galaxy–galaxy lensing signal from sdss dr7,” *The Astrophysical Journal*, vol. 914, no. 2, p. 96, 2021.
- [12] P. Kroupa, H. Haghi, B. Javanmardi, A. H. Zonoozi, O. Müller, I. Banik, X. Wu, H. Zhao, and J. Dabringhausen, “Does the galaxy ngc1052–df2 falsify Milgromian dynamics?,” *Nature*, vol. 561, no. 7722, pp. E4–E5, 2018.
- [13] J. D. Bekenstein, “Relativistic gravitation theory for the modified Newtonian dynamics paradigm,” *Physical Review D*, vol. 70, no. 8, p. 083509, 2004.
- [14] C. Skordis and T. Złośnik, “New relativistic theory for modified Newtonian dynamics,” *Physical Review Letters*, vol. 127, no. 16, p. 161302, 2021.
- [15] P. E. M. Piña, F. Fraternali, T. Oosterloo, E. A. Adams, K. A. Oman, and L. Leisman, “No need for dark matter: resolved kinematics of the ultra-diffuse galaxy agc 114905,” *Monthly Notices of the Royal Astronomical Society*, 2021.

-
- [16] S. Das, “Mach principle and a new theory of gravitation,” *arXiv preprint arXiv:1206.6755*, 2012.
- [17] S. Devasia, “Ritz-type variable speed of light (vsl) cosmology,” *Physics Essays*, vol. 27, no. 4, pp. 523–536, 2014.
- [18] R. B. Driscoll, “The Hubble-Humason effect and general relativity need no cosmological expansion,” *Physics Essays*, vol. 23, no. 4, 2010.
- [19] B. G. Wallace, “Radar testing of the relative velocity of light in space,” *Spectroscopy Letters*, vol. 2, no. 12, pp. 361–367, 1969.
- [20] G. B. Brown, “What is wrong with relativity?,” *Physics Bulletin*, vol. 18, no. 3, p. 71, 1967.
- [21] H. Dingle, “The case against special relativity,” *Nature*, vol. 216, no. 5111, pp. 119–122, 1967.
- [22] L. Brillouin, *Relativity reexamined*. New York: Academic Press, 1970.
- [23] H. C. Hayden, “Special relativity: problems and alternatives,” *Physics Essays*, vol. 8, no. 3, pp. 366–375, 1995.
- [24] G. Galeczki, “Special relativity’s heel of Achilles: the units of measurements,” *JOURNAL OF NEW ENERGY*, vol. 5, pp. 16–21, 2001.
- [25] J. P. Hansen, “Verification of photon inertia by a laser light photon radiation experiment,” *Physics Essays*, vol. 15, no. 1, 2002.
- [26] W. Engelhardt, “Relativistic Doppler effect and the principle of relativity,” *Apeiron*, vol. 10, no. 4, pp. 29–49, 2003.
- [27] P. Graneau and N. Graneau, *In the grip of the distant universe: the science of inertia*. World Scientific, 2006.
- [28] R. J. Hannon, “Einstein’s enigmatic equation,” *Physics Essays*, vol. 20, no. 4, 2007.
- [29] G. Cao, “Some reflections on the special theory of relativity,” *Physics Essays*, vol. 23, no. 2, 2010.
- [30] S. Bryant, “The failure of the Einstein-Lorentz spherical wave proof,” *Proceedings of the NPA*, vol. 8, p. 64, 2010.
- [31] P. Hayes, “Popper’s response to Dingle on special relativity and the problem of the observer,” *Studies in History and Philosophy of Science Part B: Studies in History and Philosophy of Modern Physics*, vol. 41, no. 4, pp. 354–361, 2010.
- [32] V. Apollonov and Y. Voinov, “Experiments directly demonstrating that the speed of light is independent of the velocity of the source: An experimental fact or a misconception,” *International Journal of Research in Engineering and Science*, vol. 5, no. 8, pp. 49–55, 2017.
- [33] S. J. Gift, “Burst of trouble for relativity: New test of light speed constancy using electromagnetic signal pulses from a geostationary satellite,” *Physics Essays*, vol. 28, no. 1, pp. 20–23, 2015.
-

-
- [34] L. G. Sapogin, V. Dzhanibekov, M. Mokulsky, Y. A. Ryabov, Y. P. Savin, V. Utchastkin, *et al.*, “About the conflicts between the unitary quantum theory and the special and general relativity theories,” *Journal of Modern Physics*, vol. 6, no. 06, p. 780, 2015.
- [35] W. Engelhardt, “Relativity of time and instantaneous interaction of charged particles,” *American Journal of Modern Physics*, vol. 4, no. 2-1, pp. 15–18, 2015.
- [36] J. Hansen, “Experiments with light that challenge the current theories of relativity, quantum mechanics, and cosmology,” *Physics Essays*, vol. 29, no. 3, pp. 344–366, 2016.
- [37] R. G. Zieffle, “Failure of Einstein’s theory of relativity. i. refutation of the theory of special and general relativity by an empirical experiment and by an epistemological analysis,” *Physics Essays*, vol. 32, no. 2, pp. 216–227, 2019.
- [38] C. Master-Khodabakhsh, “An alternative to special relativity: How a flawed experiment and misunderstanding of the fundamental laws of physics diverted physicists from their logical path,” *Physics Essays*, vol. 33, no. 1, pp. 79–84, 2020.
- [39] R. G. Zieffle, “Refutation of Einstein’s relativity on the basis of the incorrect derivation of the inertial mass increase violating the principle of energy conservation. a paradigm shift in physics,” *Physics Essays*, vol. 33, no. 4, pp. 466–478, 2020.
- [40] S. Kühn, “General analytic solution of the telegrapher’s equations and the resulting consequences for electrically short transmission lines,” *Journal of Electromagnetic Analysis and Applications*, vol. 12, no. 6, pp. 71–87, 2020.
- [41] S. Kühn, “Analysis of a stochastic emission theory regarding its ability to explain the effects of special relativity,” *Journal of Electromagnetic Analysis and Applications*, vol. 12, no. 12, pp. 169–187, 2020.
- [42] K. T. McDonald, “The clock paradox and accelerometers1,” *Joseph Henry Laboratories, Princeton University, Princeton, NJ 08544*, 2020.
- [43] J. S. Reid, “Why we believe in special relativity: Experimental support for Einstein’s theory,” *Einstein 1905 Relativity*, 2005.
- [44] T. Roberts, S. Schleif, and J. Dlugosz, “What is the experimental basis of special relativity,” *Usenet Physics FAQ*, 2007.
- [45] S. Hossenfelder, “Bounds on an energy-dependent and observer-independent speed of light from violations of locality,” *Physical review letters*, vol. 104, no. 14, p. 140402, 2010.
- [46] W. Pietsch, “On conceptual issues in classical electrodynamics: Prospects and problems of an action-at-a-distance interpretation,” *Studies in History and Philosophy of Science Part B: Studies in History and Philosophy of Modern Physics*, vol. 41, no. 1, pp. 67–77, 2010.
- [47] D. Lazarovici, “Against fields,” *European Journal for Philosophy of Science*, vol. 8, no. 2, pp. 145–170, 2018.
-

-
- [48] W. E. Weber, *Wilhelm Weber's Werke*, vol. 3 (First part). Berlin: Julius Springer, 1893.
- [49] G. Lentze, "Dialogue concerning magnetic forces," *Studies in History and Philosophy of Science Part B: Studies in History and Philosophy of Modern Physics*, vol. 68, pp. 158–162, 2019.
- [50] M. Tajmar, "Propellantless propulsion with negative matter generated by electric charges," in *AIAA Joint Propulsion Conference, AIAA-2013*, vol. 3913, 2013.
- [51] M. Tajmar and A. K. T. Assis, "Particles with negative mass: production, properties and applications for nuclear fusion and self-acceleration," *Journal of Advanced Physics*, vol. 4, no. 1, pp. 77–82, 2015.
- [52] M. Tajmar, "Revolutionary propulsion research at TU dresden," in *Proceedings of the Advanced Propulsion Workshop, Estes Park*, pp. 20–22, 2016.
- [53] M. Tran, "Evidence for Maxwell's equations, fields, force laws and alternative theories of classical electrodynamics," *European Journal of Physics*, vol. 39, no. 6, p. 063001, 2018.
- [54] S. Hossenfelder, "Science needs reason to be trusted," *Nature Physics*, vol. 13, no. 4, pp. 316–317, 2017.
- [55] E. Whittaker, *A History of the Theories of Aether and Electricity: Vol. I: The Classical Theories; Vol. II: The Modern Theories, 1900-1926*, vol. 1. Courier Dover Publications, 1951.
- [56] O. Darrigol, "The electrodynamics of moving bodies from Faraday to Hertz," *Centaurus*, vol. 36, no. 3, pp. 245–360, 1993.
- [57] O. Darrigol, *Electrodynamics from Ampere to Einstein*. Oxford University Press, 2003.
- [58] A. K. T. Assis, *The experimental and historical foundations of electricity, Volume 1 & 2*. Apeiron Montreal, 2010.
- [59] P. Benjamin, *A history of electricity:(The intellectual rise in electricity) from antiquity to the days of Benjamin Franklin*. J. Wiley & Sons, 1895.
- [60] A. D. Yaghjian, "Reflections on Maxwell's treatise," *Progress In Electromagnetics Research*, vol. 149, pp. 217–249, 2014.
- [61] A. K. T. Assis and H. T. Silva, "Comparison between Weber's electrodynamics and classical electrodynamics," *Pramana*, vol. 55, no. 3, pp. 393–404, 2000.
- [62] A. O'Rahilly, *Electromagnetic Theory: A Critical Examination of Fundamentals*, vol. I and II. Dover Publications, 1965.
- [63] A. K. T. Assis, *Weber's electrodynamics*. Dordrecht: Springer, 1994.
- [64] J. D. Jackson, "Classical electrodynamics," 1999.
-

-
- [65] C. G. Darwin, “LI. the dynamical motions of charged particles,” *The London, Edinburgh, and Dublin Philosophical Magazine and Journal of Science*, vol. 39, no. 233, pp. 537–551, 1920.
- [66] L. Landau and E. Lifshitz, *Electrodynamics of Continuous Media*, vol. 2nd ed. Oxford: Pergamon, 1985.
- [67] L. Page and N. I. Adams Jr, “Action and reaction between moving charges,” *American Journal of Physics*, vol. 13, no. 3, pp. 141–147, 1945.
- [68] A. M. Steane, “Nonexistence of the self-accelerating dipole and related questions,” *Physical Review D*, vol. 89, no. 12, p. 125006, 2014.
- [69] P. Cornille, “The Lorentz force and Newton’s third principle,” *Canadian Journal of Physics*, vol. 73, no. 9-10, pp. 619–625, 1995.
- [70] P. Cornille, “Review of the application of Newton’s third law in physics,” *Progress in energy and combustion science*, vol. 25, no. 2, pp. 161–210, 1999.
- [71] C. T. Sebens, “Forces on fields,” *Studies in History and Philosophy of Science Part B: Studies in History and Philosophy of Modern Physics*, vol. 63, pp. 1–11, 2018.
- [72] A. Assis and F. Peixoto, “On the velocity in the Lorentz force law,” *The Physics Teacher*, vol. 30, no. 8, pp. 480–483, 1992.
- [73] F. A. Muller, “Inconsistency in classical electrodynamics?,” *Philosophy of Science*, vol. 74, no. 2, pp. 253–277, 2007.
- [74] M. Frisch, “Inconsistency, asymmetry, and non-locality: A philosophical investigation of classical electrodynamics,” 2005.
- [75] R. P. Feynman, “Space-time approach to quantum electrodynamics,” in *Selected Papers of Richard Feynman* (L. M. Brown, ed.), pp. 99–119, World Scientific, 2000.
- [76] P. A. M. Dirac, “The evolution of the physicist’s picture of nature,” *Scientific American*, vol. 208, no. 5, pp. 45–53, 1963.
- [77] R. E. Kastner, “Haag’s theorem as a reason to reconsider direct-action theories,” *arXiv preprint arXiv:1502.03814*, 2015.
- [78] D. J. Griffiths, “Introduction to electrodynamics,” 2005.
- [79] E. G. Cullwick, “Electromagnetism and relativity: with particular reference to moving media and electromagnetic induction,” 1959.
- [80] P. H. Moon and D. E. Spencer, *Foundations of electrodynamics*. Boston Technical Publishers, 1965.
- [81] P. Lorrain and D. R. Corson, “Electromagnetic fields and waves,” 1970.
- [82] J. C. Maxwell, “Xxv. on physical lines of force: Part i.—the theory of molecular vortices applied to magnetic phenomena,” *The London, Edinburgh, and Dublin Philosophical Magazine and Journal of Science*, vol. 21, no. 139, pp. 161–175, 1861.
-

-
- [83] W. E. Weber, *Wilhelm Weber's Werke*, vol. 4 (Second part). Berlin: Julius Springer, 1893.
- [84] W. Weber, *Determinations of electrodynamic measure: concerning a universal law of electrical action*. 21st Century Science and Technology, 2007.
- [85] W. Weber, *Electrodynamic measurements, especially measures of resistance*. 2021.
- [86] W. Weber, *Electrodynamic Measurements, Especially on Diamagnetism*. 2021.
- [87] R. Kohlrausch and W. Weber, *Electrodynamic measurements, especially attributing mechanical units to measures of current intensity*. 2021.
- [88] W. Weber, *Electrodynamic measurements, especially on electric oscillations*. 2021.
- [89] W. Weber, “Electrodynamic measurements – sixth memoir, relating specially to the principle of the conservation of energy,” *The London, Edinburgh and Dublin Philosophical Magazine and Journal of Science, Fourth Series*, vol. 43, no. 283, pp. 1–20, 1872.
- [90] W. Weber, *Electrodynamic measurements, especially on the energy of interaction*. 2021.
- [91] W. Weber, *Determinations of electrodynamic measure: particularly in respect to the connection of the fundamental laws of electricity with the law of gravitation*. 21st Century Science and Technology, 2021.
- [92] P. Davies, “A quantum theory of Wheeler–Feynman electrodynamics,” in *Mathematical Proceedings of the Cambridge Philosophical Society*, vol. 68, pp. 751–764, Cambridge University Press, 1970.
- [93] A. A. Martínez, “Ritz, Einstein, and the emission hypothesis,” *Physics in Perspective*, vol. 6, no. 1, pp. 4–28, 2004.
- [94] R. T. Smith and S. Maher, “Investigating electron beam deflections by a long straight wire carrying a constant current using direct action, emission-based and field theory approaches of electrodynamics,” *Progress In Electromagnetics Research*, vol. 75, pp. 79–89, 2017.
- [95] D. H. Frisch and J. H. Smith, “Measurement of the relativistic time dilation using μ -mesons,” *American Journal of Physics*, vol. 31, no. 5, pp. 342–355, 1963.
- [96] T. Alväger, A. Nilsson, and J. Kjellman, “On the independence of the velocity of light of the motion of the light source,” *Arkiv Fysik*, vol. 26, 1964.
- [97] T. Alväger, F. Farley, J. Kjellman, and L. Wallin, “Test of the second postulate of special relativity in the gev region,” *Physics Letters*, vol. 12, no. 3, pp. 260–262, 1964.
- [98] T. Filippas and J. Fox, “Velocity of gamma rays from a moving source,” *Physical Review*, vol. 135, no. 4B, p. B1071, 1964.
- [99] G. Babcock and T. Bergman, “Determination of the constancy of the speed of light,” *JOSA*, vol. 54, no. 2, pp. 147–151, 1964.
-

-
- [100] J. G. Fox, “Evidence against emission theories,” *American Journal of Physics*, vol. 33, no. 1, pp. 1–17, 1965.
- [101] K. Brecher, “Is the speed of light independent of the velocity of the source?,” *Physical Review Letters*, vol. 39, no. 17, p. 1051, 1977.
- [102] W. Ritz and R. Fritzius, “Critical researches on general electrodynamics,” *Critical Researches on General Electrodynamics: Introduction and First Part*, 1980. This is the 1980 Lucier-Fritzius-Toth English translation of Walter Ritz’s article, *Recherches critiques sur l’Électrodynamique Générale*, *Annales de Chimie et de Physique*, Vol. 13, p. 145, 1908.
- [103] G. B. Brown, *Retarded Action-at-a-distance: The Change of Force with Motion*. Cortney Publications, 1982.
- [104] G. Burniston Brown, “The effect of motion on optical phenomena,” *Revista de la real academia de ciencias físicas y naturales*, vol. LIV, no. 1, 1960.
- [105] G. Burniston Brown, “A new treatment of diffraction,” *Contemporary Physics*, vol. 5, no. 1, pp. 15–27, 1963.
- [106] P. Moon, D. E. Spencer, A. S. Mirchandaney, U. Y. Shama, and P. J. Mann, “The electrodynamics of Gauss, Neumann, and Hertz.,” *Physics Essays*, vol. 7, no. 1, pp. 28–33, 1994.
- [107] H. A. Lorentz, *La théorie électromagnétique de Maxwell et son application aux corps mouvants*, vol. 25. EJ Brill, 1892.
- [108] R. McCormach, “HA Lorentz and the electromagnetic view of nature,” *Isis*, vol. 61, no. 4, pp. 459–497, 1970.
- [109] A. E. Woodruff, “The contributions of Hermann von Helmholtz to electrodynamics,” *Isis*, vol. 59, no. 3, pp. 300–311, 1968.
- [110] J. P. Wesley, “Empirically correct electrodynamics,” *Foundations of Physics Letters*, vol. 10, no. 2, pp. 189–204, 1997.
- [111] T. E. Phipps, “Toward modernization of Weber’s force law,” *Physics Essays*, vol. 3, no. 4, p. 414, 1990.
- [112] J. Caluzi and A. K. T. Assis, “An analysis of Phipps’s potential energy,” *Journal of the Franklin Institute*, vol. 332, no. 6, pp. 747–753, 1995.
- [113] J. Montes, “On Limiting Velocity with Weber-like Potentials,” *Canadian Journal of Physics*, vol. 95, no. 8, pp. 770–776, 2017.
- [114] F. Tisserand, *Sur le mouvement des planètes autour du soleil, d’après la loi électrodynamique de Weber*. Gauthier-Villars, 1872.
- [115] P. Gerber, “Die räumliche und zeitliche ausbreitung der gravitation,” *Z Math Phys*, vol. 43, pp. 415–444, 1898.
- [116] E. Schrödinger, “Die erfüllbarkeit der relativitätsforderung in der klassischen mechanik,” *Annalen der Physik*, vol. 382, no. 11, pp. 325–336, 1925.
-

-
- [117] P. Moon and D. E. Spencer, “Electromagnetism without magnetism: an historical sketch,” *American Journal of Physics*, vol. 22, no. 3, pp. 120–124, 1954.
- [118] P. Moon and D. E. Spencer, “A new electrodynamics,” *Journal of the Franklin Institute*, vol. 257, no. 5, pp. 369–382, 1954.
- [119] P. Moon and D. E. Spencer, “On electromagnetic induction,” *Journal of the Franklin Institute*, vol. 260, no. 3, pp. 213–226, 1955.
- [120] P. Moon and D. E. Spencer, “Some electromagnetic paradoxes,” *Journal of the Franklin Institute*, vol. 260, no. 5, pp. 373–395, 1955.
- [121] P. Moon and D. E. Spencer, “A postulational approach to electromagnetism,” *Journal of the Franklin Institute*, vol. 259, no. 4, pp. 293–305, 1955.
- [122] J. A. Wheeler and R. P. Feynman, “Interaction with the absorber as the mechanism of radiation,” *Reviews of modern physics*, vol. 17, no. 2-3, p. 157, 1945.
- [123] J. A. Wheeler and R. P. Feynman, “Classical electrodynamics in terms of direct interparticle action,” *Reviews of modern physics*, vol. 21, no. 3, p. 425, 1949.
- [124] F. Hoyle and J. V. Narlikar, “Action at a distance in physics and cosmology,” *San Francisco*, 1974.
- [125] F. Hoyle and J. V. Narlikar, “Cosmology and action-at-a-distance electrodynamics,” *Reviews of Modern Physics*, vol. 67, no. 1, p. 113, 1995.
- [126] V. M. Canuto and J. V. Narlikar, “Cosmological tests of the Hoyle-Narlikar conformal gravity,” *The Astrophysical Journal*, vol. 236, pp. 6–23, 1980.
- [127] J. P. Wesley, “Weber electrodynamics, Part I. General theory, steady current effects,” *Foundations of Physics Letters*, vol. 3, no. 5, pp. 443–469, 1990.
- [128] J. Wesley, “Weber electrodynamics, part ii unipolar induction, z-antenna,” *Foundations of Physics Letters*, vol. 3, no. 5, pp. 471–490, 1990.
- [129] J. P. Wesley, “Weber electrodynamics: Part III. mechanics, gravitation,” *Foundations of Physics Letters*, vol. 3, no. 6, pp. 581–605, 1990.
- [130] A. K. T. Assis, “Deriving Ampere’s law from Weber’s law,” *Hadronic Journal*, vol. 13, pp. 441–451, 1990.
- [131] P. G. Moyssides, “Calculation of the sixfold integrals of the Ampere force law in a closed circuit,” *IEEE transactions on magnetics*, vol. 25, no. 5, pp. 4307–4312, 1989.
- [132] G. Cavalleri, G. Bettoni, E. Tonni, and G. Spavieri, “Experimental proof of standard electrodynamics by measuring the self-force on a part of a current loop,” *Physical Review E*, vol. 58, no. 2, p. 2505, 1998.
- [133] A. K. T. Assis, “Comment on “experimental proof of standard electrodynamics by measuring the self-force on a part of a current loop”,” *Physical Review E*, vol. 62, no. 5, p. 7544, 2000.
-

-
- [134] A. K. T. Assis and M. A. Bueno, “Equivalence between Ampere and Grassmann’s forces,” *IEEE transactions on magnetics*, vol. 32, no. 2, pp. 431–436, 1996.
- [135] M. Bueno and A. K. T. Assis, “Proof of the identity between Ampère and Grassmann’s forces,” *Physica Scripta*, vol. 56, no. 6, p. 554, 1997.
- [136] A. K. Assis and M. Bueno, “Bootstrap effect in classical electrodynamics,” *Revista Facultad de Ingenieria*, no. 7, pp. 49–55, 2000.
- [137] J. R. Hofmann, *André-Marie Ampère: Enlightenment and Electrodynamics*, vol. 7. Cambridge University Press, 1996.
- [138] A.-M. Ampère, “Mémoire présenté à l’académie royale des sciences, le 2 octobre 1820, où se trouve compris le résumé de ce qui avait été lu à la même académie les 18 et 25 septembre 1820, sur les effets des courans électriques,” in *Annales de Chimie et de Physique*, vol. 15, pp. 59–76, 1820.
- [139] A. Ampère, “The effects of electric currents,” *RAR Tricker, Early Electrodynamics—The First Law of Circulation*, pp. 140–154, 1965.
- [140] A. Assis, M. Souza Filho, J. Caluzi, and J. Chaib, “From electromagnetism to electrodynamics: Ampère’s demonstration of the interaction between current carrying wires,” pp. 9–16, 2007.
- [141] J. Chaib and F. Lima, “Resuming Ampère’s experimental investigation of the validity of Newton’s third law in electrodynamics,” in *Annales de la Fondation Louis de Broglie*, vol. 45, p. 19, 2020.
- [142] P. Graneau, “Electromagnetic jet-propulsion in the direction of current flow,” *Nature*, vol. 295, no. 5847, p. 311, 1982.
- [143] P. Graneau, “Application of Ampere’s force law to railgun accelerators,” *Journal of Applied Physics*, vol. 53, no. 10, pp. 6648–6654, 1982.
- [144] P. Graneau, “First indication of Ampere tension in solid electric conductors,” *Physics Letters A*, vol. 97, no. 6, pp. 253–255, 1983.
- [145] P. Graneau, “Ampere tension in electric conductors,” *IEEE transactions on magnetics*, vol. 20, no. 2, pp. 444–455, 1984.
- [146] P. Graneau, “Ampère-Neumann electrodynamics of metals,” 1985.
- [147] P. Graneau, “The Ampere-Neumann electrodynamics of metallic conductors,” *Fortschritte der Physik*, vol. 34, no. 7, pp. 457–501, 1986.
- [148] P. Graneau and N. Graneau, “The electromagnetic impulse pendulum and momentum conservation,” *Il Nuovo Cimento D*, vol. 7, no. 1, pp. 31–45, 1986.
- [149] P. Graneau, “Amperian recoil and the efficiency of railguns,” *Journal of applied physics*, vol. 62, no. 7, pp. 3006–3009, 1987.
- [150] P. Graneau, D. S. Thompson, and S. L. Morrill, “The motionally induced back-emf in railguns,” *Physics Letters A*, vol. 145, no. 8-9, pp. 396–400, 1990.
-

-
- [151] P. Graneau and N. Graneau, “The role of Ampere forces in nuclear fusion,” *Physics Letters A*, vol. 165, no. 1, pp. 1–13, 1992.
 - [152] A. K. T. Assis, “On the mechanism of railguns,” *Galilean Electrodynamics*, vol. 3, pp. 93–95, 1992.
 - [153] J. Nasilowski, “A note on longitudinal Ampere forces in gaseous conductors,” *Physics Letters A*, vol. 111, no. 6, pp. 315–316, 1985.
 - [154] P. Pappas, “The original Ampere force and Biot-Savart and Lorentz forces,” *Il Nuovo Cimento B (1971-1996)*, vol. 76, no. 2, pp. 189–197, 1983.
 - [155] T. Phipps and T. Phipps Jr, “Observation of Ampere forces in mercury,” *Physics Letters A*, vol. 146, no. 1-2, pp. 6–14, 1990.
 - [156] T. E. Phipps, “New evidence for Ampère longitudinal forces,” *Physics Essays*, vol. 3, no. 2, p. 198, 1990.
 - [157] J. Wesley, “Pinch effect and Ampere tension to drive Hering’s pump,” *Foundations of Physics Letters*, vol. 7, no. 1, pp. 95–104, 1994.
 - [158] V. Peoglos, “Measurement of the magnetostatic force of a current circuit on a part of itself,” *Journal of Physics D: Applied Physics*, vol. 21, no. 7, p. 1055, 1988.
 - [159] R. Achilles, “Again on the Guala-Valverde homopolar induction experiments,” *Spacetime & Substance*, vol. 3, no. 5, p. 235, 2002.
 - [160] R. Achilles and J. Guala-Valverde, “Action at a distance: A key to homopolar induction.,” *Apeiron: Studies in Infinite Nature*, vol. 14, no. 3, 2007.
 - [161] J. Guala-Valverde and R. Achilles, “A manifest failure of Grassmann’s force,” *Apeiron: Studies in Infinite Nature*, vol. 15, no. 2, 2008.
 - [162] C. Papageorgiou and T. Raptis, “Fragmentation of thin wires under high power pulses and bipolar fusion,”
 - [163] A. D. Alfaro, “Ampere’s longitudinal forces revisited,” tech. rep., NAVAL POST-GRADUATE SCHOOL MONTEREY CA MONTEREY United States, 2018.
 - [164] P. Pappas, L. Pappas, and T. Pappas, “Ampère cardinal forces—electrodynamics—proof and prediction of empirical Faraday induction,” *Physics Essays*, vol. 27, no. 4, pp. 570–579, 2014.
 - [165] M. Rambaut and J. Vigier, “The simultaneous existence of EM Grassmann-Lorentz forces (acting on charged particles) and Ampère forces (acting on charged conducting elements) does not contradict relativity theory,” *Physics Letters A*, vol. 142, no. 8-9, pp. 447–452, 1989.
 - [166] M. Rambaut and J. Vigier, “Ampere forces considered as collective non-relativistic limit of the sum of all Lorentz interactions acting on individual current elements: possible consequences for electromagnetic discharge stability and tokamak behaviour,” *Physics Letters A*, vol. 148, no. 5, pp. 229–238, 1990.
-

-
- [167] P. G. Moyssides, “The anticipated longitudinal forces by the Biot-Savart-Grassmann-Lorentz force law are in complete agreement with the longitudinal Ampère forces,” *The European Physical Journal Plus*, vol. 129, no. 2, pp. 1–17, 2014.
 - [168] R. Saumont, “Ampère force: Experimental tests,” in *Advanced Electromagnetism: Foundations, Theory And Applications*, pp. 620–635, World Scientific, 1995.
 - [169] N. Graneau, T. Phipps Jr, and D. Roscoe, “An experimental confirmation of longitudinal electrodynamic forces,” *The European Physical Journal D - Atomic, Molecular, Optical and Plasma Physics*, vol. 15, no. 1, pp. 87–97, 2001.
 - [170] S. Kühn, “Experimental investigation of an unusual induction effect and its interpretation as a necessary consequence of Weber electrodynamics,” *Journal of Electrical Engineering*, vol. 72, no. 6, pp. 366–373, 2021.
 - [171] A. Recknagel, *Physik, Elektrizität und Magnetismus*. VEB Verlag Technik, Berlin, 12th ed., 1980.
 - [172] D. H. Frisch and L. Wilets, “Development of the Maxwell-Lorentz equations from special relativity and Gauss’s law,” *American Journal of Physics*, vol. 24, no. 8, pp. 574–579, 1956.
 - [173] J. Field, “Derivation of the Lorentz force law, the magnetic field concept and the Faraday–Lenz and magnetic Gauss laws using an invariant formulation of the Lorentz transformation,” *Physica Scripta*, vol. 73, no. 6, p. 639, 2006.
 - [174] H. Dodig, “Direct derivation of Lienard–Wiechert potentials, Maxwell’s equations and Lorentz force from Coulomb’s law,” *Mathematics*, vol. 9, no. 3, p. 237, 2021.
 - [175] R. T. Smith, F. P. Jjunju, and S. Maher, “Evaluation of Electron Beam Deflections across a Solenoid Using Weber-Ritz and Maxwell-Lorentz Electrodynamics,” *Progress In Electromagnetics Research*, vol. 151, pp. 83–93, 2015.
 - [176] C. Baumgärtel, R. T. Smith, and S. Maher, “Accurately predicting electron beam deflections in fringing fields of a solenoid,” *Scientific reports*, vol. 10, no. 1, pp. 1–13, 2020.
 - [177] C. Baumgärtel and S. Maher, “A charged particle model based on Weber electrodynamics for electron beam trajectories in coil and solenoid elements,” *Progress In Electromagnetics Research C*, vol. 123, pp. 151–166, 2022.
 - [178] E. Kinzer and J. Fukai, “Weber’s force and Maxwell’s equations,” *Foundations of Physics Letters*, vol. 9, no. 5, pp. 457–461, 1996.
 - [179] Anonymous, *Advances in Weber and Maxwell Electrodynamics*. Amazon Fulfillment, 2018.
 - [180] Q. Li, “Electric field theory based on Weber’s electrodynamics,” *International Journal of Magnetism and Electromagnetism*, vol. 7:039, no. 2, pp. 1–6, 2021.
 - [181] S. Kühn, “The inhomogeneous wave equation, Liénard-Wiechert potentials, and Hertzian dipole in Weber electrodynamics,” *Preprint*, 2022.
-

-
- [182] M. Rambaut, “Macroscopic non-relativistic Ampère EM interactions between current elements reflect the conducting electron accelerations by the ion’s electric fields,” *Physics Letters A*, vol. 154, no. 5-6, pp. 210–214, 1991.
- [183] W. Weber and R. Kohlrausch, “Ueber die elektricitätsmenge, welche bei galvanischen strömen durch den querschnitt der kette fliesst,” *Annalen der Physik*, vol. 175, no. 9, pp. 10–25, 1856.
- [184] A. K. Assis, “On the first electromagnetic measurement of the velocity of light by Wilhelm Weber and Rudolf Kohlrausch,” *Volta and the History of Electricity*, pp. 267–286, 2003.
- [185] G. Kirchhoff, “Ueber die bewegung der elektricität in leitem,” *Annalen der Physik*, vol. 178, no. 12, pp. 529–544, 1857.
- [186] W. Weber, “Elektrodynamische maassbestimmungen insbesondere über elektrische schwingungen,” vol. 6, pp. 105–241, Teubner, Leipzig, 1864.
- [187] A. K. T. Assis and J. Hernandes, “Telegraphy equation from Weber’s electrodynamics,” *IEEE Transactions on Circuits and Systems II: Express Briefs*, vol. 52, no. 6, pp. 289–292, 2005.
- [188] J. Fukai, *A promenade along electrodynamics*. Vales Lake Publishing, 2003.
- [189] A. K. T. Assis, “Circuit theory in Weber electrodynamics,” *European Journal of Physics*, vol. 18, no. 3, p. 241, 1997.
- [190] M. Bueno and A. K. T. Assis, “Equivalence between the formulas for inductance calculation,” *Canadian journal of physics*, vol. 75, no. 6, pp. 357–362, 1997.
- [191] K. T. McDonald, “Weber’s electrodynamics and the Hall effect,”
- [192] R. T. Smith, S. Taylor, and S. Maher, “Modelling electromagnetic induction via accelerated electron motion,” *Canadian Journal of Physics*, vol. 93, no. 7, pp. 802–806, 2014.
- [193] R. T. Smith, F. P. Jjunju, I. S. Young, S. Taylor, and S. Maher, “A physical model for low-frequency electromagnetic induction in the near field based on direct interaction between transmitter and receiver electrons,” *Proceedings of the Royal Society A: Mathematical, Physical and Engineering Sciences*, vol. 472, no. 2191, p. 20160338, 2016.
- [194] A. K. Assis and D. S. Thober, “Unipolar induction and Weber’s electrodynamics,” in *Frontiers of Fundamental Physics*, pp. 409–414, Springer, 1994.
- [195] H. Härtel, “Unipolar induction-a messy corner of electromagnetism,” *European Journal of Physics Education*, vol. 11, no. 1, pp. 47–59, 2020.
- [196] A. K. T. Assis, J. Fukai, and H. Carvalho, “Weberian induction,” *Physics Letters A*, vol. 268, no. 4-6, pp. 274–278, 2000.
- [197] R. Feynman, *Lectures in Physics*, vol. II. California Institute of Technology, 1963. Chapter 17. The Laws of Induction.
-

-
- [198] T. C. E. Ma, “Field angular momentum in Feynman’s disk paradox,” *American Journal of Physics*, vol. 54, no. 10, pp. 949–950, 1986.
 - [199] K. A. Prytz, “Meissner effect in classical physics,” *Progress In Electromagnetics Research*, vol. 64, pp. 1–7, 2018.
 - [200] A. Assis and M. Tajmar, “Superconductivity with Weber’s electrodynamics: The London moment and the Meissner effect,” in *Annales de la Fondation Louis de Broglie*, vol. 42, p. 307, 2017.
 - [201] J. Wesley, “Induction produces Aharonov-Bohm effect,” *Apeiron*, vol. 5, no. 1-2, pp. 73–82, 1998.
 - [202] K. Prytz, “Antenna theory—the loop and the dipole,” in *Electrodynamics: The Field-Free Approach*, pp. 219–238, Springer, 2015.
 - [203] A. K. T. Assis, K. H. Wiederkehr, G. Wolfschmidt, *et al.*, “Weber’s planetary model of the atom,” 2011.
 - [204] W. E. Weber, *Electrodynamische Maassbestimmungen*, vol. 2. S. Hirzel, 1871.
 - [205] V. Bush, “The force between moving charges,” *Journal of Mathematics and Physics*, vol. 5, no. 1-4, pp. 129–157, 1926.
 - [206] R. Clemente and A. K. T. Assis, “Two-body problem for Weber-like interactions,” *International Journal of Theoretical Physics*, vol. 30, no. 4, pp. 537–545, 1991.
 - [207] E. Riecke, “Ueber molecularbewegung zweier theilchen, deren wechselwirkung durch das webersche gesetz der elektrischen kraft bestimmt wird,” *Nachrichten von der Königl. Gesellschaft der Wissenschaften und der Georg-Augusts-Universität zu Göttingen*, vol. 1874, pp. 665–2, 1874.
 - [208] G. Lolling, “Ueber bewegungen elektrischer theilchen nach dem Weber’schen grundgesetz der elektrodynamik,” *Verhandlungen der Kaiserlichen Leopoldinisch-Carolinischen Deutschen Akademie der Naturforscher*, vol. 44, no. 3, pp. 273–336, 1882.
 - [209] E. Ritter, “Ii. bewegung eines materiellen mit eletricität geladenen theilchens unter der einwirkung eines ruhenden centrum bei giltigkeit des Weber’schen gesetzes,” *Zeitschrift für Mathematik und Physik: Organ für angewandte Mathematik*, vol. 37, pp. 8–24, 1892.
 - [210] J. F. Zöllner, *Principien einer elektrodynamischen Theorie der Materie*, vol. 1. Engelmann, Leipzig, 1876.
 - [211] H. Torres-Silva, J. López-Bonilla, R. López-Vázquez, and J. Rivera-Rebolledo, “Weber’s electrodynamics for the hydrogen atom,” *Indonesian Journal of Applied Physics*, vol. 5, no. 01, pp. 39–46, 2015.
 - [212] U. Frauenfelder and J. Weber, “The fine structure of Weber’s hydrogen atom: Bohr–Sommerfeld approach,” *Zeitschrift für angewandte Mathematik und Physik*, vol. 70, no. 4, p. 105, 2019.
-

-
- [213] J. P. Wesley, “Evidence for Weber–Wesley electrodynamics,” in *Proceedings Conference on Foundations of Mathematics and Physics, Perugia, Italy*, pp. 27–29, 1989.
 - [214] E. J. Post, “A tale of fine structure coincidences,” in *Quantum Reprogramming*, pp. 151–168, Springer, 1995.
 - [215] J. Pearson and A. Kilambi, “Velocity-dependent nuclear forces and Weber’s electrodynamics,” *American Journal of Physics*, vol. 42, no. 11, pp. 971–975, 1974.
 - [216] A. K. T. Assis, “Deriving gravitation from electromagnetism,” *Canadian Journal of Physics*, vol. 70, no. 5, pp. 330–340, 1992.
 - [217] A. K. T. Assis, *Gravitation as a fourth order electromagnetic effect*, pp. 314–331. Singapore: World Scientific Publishers, 1995.
 - [218] M. Tajmar, “Derivation of the Planck and Fine-Structure Constant from Assis’s Gravity Model,” *Journal of Advanced Physics*, vol. 4, no. 3, pp. 219–221, 2015.
 - [219] C. Baumgärtel and M. Tajmar, “The Planck Constant and the Origin of Mass Due to a Higher Order Casimir Effect,” *Journal of Advanced Physics*, vol. 7, no. 1, pp. 135–140, 2018.
 - [220] A. K. T. Assis, “On Mach’s principle,” *Foundations of Physics Letters*, vol. 2, no. 4, pp. 301–318, 1989.
 - [221] M. Tajmar and A. K. T. Assis, “Influence of rotation on the weight of gyroscopes as an explanation for flyby anomalies,” *Journal of Advanced Physics*, vol. 5, no. 2, pp. 176–179, 2016.
 - [222] F. Bunchaft and S. Carneiro, “Weber-like interactions and energy conservation,” *Foundations of Physics Letters*, vol. 10, no. 4, pp. 393–401, 1997.
 - [223] R. Mendes, L. Malacarne, and A. Assis, *Virial Theorem For Weber’s Law*, pp. 67–70. Paramus: Rinton Press, 2004.
 - [224] R. A. Clemente and R. G. Cesar, “Cold plasma oscillations according to Weber’s law. an unphysical result,” *International journal of theoretical physics*, vol. 32, no. 7, pp. 1257–1260, 1993.
 - [225] A. K. T. Assis, *Relational Mechanics and Implementation of Mach’s Principle with Weber’s Gravitational Force*. C. Roy Keys Inc., Montreal, 2014.
 - [226] C. Seegers, *Über die Bewegung und die Störungen der Planeten, wenn dieselben sich nach dem weberschen elektrodynamischen Gesetz um die Sonne bewegen*. Springer-Verlag, 2013.
 - [227] H. Servus, *Untersuchungen über die Bahn und die Störungen der Himmelskörper mit Zugrundelegung des Weber’schen elektrodynamischen Gesetzes*. PhD thesis, 1885.
 - [228] J. K. F. Zöllner, *Über die Natur der Cometen: Beiträge zur Geschichte und Theorie der Erkenntniss*. Engelmann, 1872.
 - [229] P. Eby, “On the perihelion precession as a Machian effect.,” *Nuovo Cimento Lettere*, vol. 18, pp. 93–96, 1977.
-

-
- [230] S. Ragusa, “Gravitation with a modified Weber force,” *Foundations of Physics Letters*, vol. 5, no. 6, pp. 585–589, 1992.
 - [231] M. Lévy, “Sur l’application des lois électrodynamiques au mouvement des planètes,” *Compt. Rend. Acad. Sci*, vol. 110, p. 545, 1890.
 - [232] A. Sokolskii and A. Sadovnikov, “Lagrangian solutions for Weber’s law of attraction,” *Soviet Astronomy*, vol. 31, p. 90, 1987.
 - [233] J. Giné, “Is gravitational quantization another consequence of general relativity?,” *Chaos, Solitons & Fractals*, vol. 42, no. 3, pp. 1893–1899, 2009.
 - [234] A. Kholodenko, *Newtonian limit of Einsteinian gravity and dynamics of solar system*. 2015.
 - [235] Y. Tiandho, “Weber’s gravitational force as static weak field approximation,” in *AIP Conference Proceedings*, vol. 1708, p. 070012, AIP Publishing LLC, 2016.
 - [236] F. Lima, “Nonzero gravitational force exerted by a spherical shell on a body moving inside it, and cosmological implications,” *Gravitation and Cosmology*, vol. 26, no. 4, pp. 387–398, 2020.
 - [237] D. Roscoe, *Mach’s Principle And Instantaneous Action At a Distance*, pp. 175–188. Commack, New York: Nova Science Publishers, Inc., 1999.
 - [238] A. Assis, “A steady-state cosmology,” in *Progress in New Cosmologies*, pp. 153–167, Springer, 1993.
 - [239] A. K. Assis and P. Graneau, “Nonlocal forces of inertia in cosmology,” *Foundations of Physics*, vol. 26, no. 2, pp. 271–283, 1996.
 - [240] P. Graneau and N. Graneau, “Machian inertia and the isotropic universe,” *General Relativity and Gravitation*, vol. 35, no. 5, pp. 751–770, 2003.
 - [241] M. Tajmar and A. Assis, “Gravitational induction with Weber’s force,” *Canadian Journal of Physics*, vol. 93, no. 12, pp. 1571–1573, 2015.
 - [242] A. K. T. Assis, “Changing the inertial mass of a charged particle,” *Journal of the Physical Society of Japan*, vol. 62, no. 5, pp. 1418–1422, 1993.
 - [243] V. Mikhailov, “The action of an electrostatic potential on the electron mass,” in *Annales de la Fondation Louis de Broglie*, vol. 24, p. 161, 1999.
 - [244] V. F. Mikhailov, “Influence of an electrostatic potential on the inertial electron mass,” *Annales de la Fondation Louis de Broglie*, vol. 26, no. 4, pp. 633–638, 2001.
 - [245] V. Mikhailov, “Influence of a field-less electrostatic potential on the inertial electron mass,” in *Annales de la Fondation Louis de Broglie*, vol. 28, p. 231, Fondation Louis de Broglie, 2003.
 - [246] J. E. Junginger and Z. D. Popovic, “An experimental investigation of the influence of an electrostatic potential on electron mass as predicted by Weber’s force law,” *Canadian journal of physics*, vol. 82, no. 9, pp. 731–735, 2004.
-

-
- [247] I. Lőrincz and M. Tajmar, “Experimental Investigation of the Influence of Spatially Distributed Charges on the Inertial Mass of Moving Electrons as Predicted by Weber’s Electrodynamics,” *Canadian Journal of Physics*, vol. 95, no. 10, p. 1023, 2017.
 - [248] M. Weikert and M. Tajmar, “Investigation of the influence of a field-free electrostatic potential on the electron mass with Barkhausen-Kurz oscillation,” *arXiv preprint arXiv:1902.05419*, 2019.
 - [249] M. Tajmar and M. Weikert, “Evaluation of the influence of a field-less electrostatic potential on electron beam deflection as predicted by Weber electrodynamics,” *Progress In Electromagnetics Research M*, vol. 105, pp. 1–8, 2021.
 - [250] A. Assis, “On the unification of forces of nature,” *Annales de la Fondation Louis de Broglie*, vol. 27, no. 2, pp. 149–161, 2002.
 - [251] H. Fricke, *Two rival programmes in 19th. century classical electrodynamics action-at-a-distance versus field theories*. PhD thesis, The London School of Economics and Political Science (LSE), 1982.
 - [252] R. Clausius, “Ueber die ableitung eines neuen elektrodynamischen grundgesetzes.,” *Journal für die reine und angewandte Mathematik*, vol. 82, p. 85, 1877.
 - [253] A. E. Woodruff, “Action at a distance in nineteenth century electrodynamics,” *Isis*, vol. 53, no. 4, pp. 439–459, 1962.
 - [254] F. Zöllner, “Ueber die einwendungen von Clausius gegen das Weber’sche gesetz,” *Annalen der Physik*, vol. 236, no. 4, pp. 514–537, 1877.
 - [255] P. Erman, “Über die electroskopischen phänomene des gasapparats an der voltaischen säule,” *Annalen der Physik*, vol. 10, pp. 1–23, 1802.
 - [256] A. K. T. Assis and J. A. Hernandes, “The electric force of a current,” *Apeiron*, 2007.
 - [257] J. Hernandes and A. K. T. Assis, “Electric potential due to an infinite conducting cylinder with internal or external point charge,” *Journal of electrostatics*, vol. 63, no. 12, pp. 1115–1131, 2005.
 - [258] A. K. T. Assis, W. Rodrigues, and A. Mania, “The electric field outside a stationary resistive wire carrying a constant current,” *Foundations of Physics*, vol. 29, no. 5, pp. 729–753, 1999.
 - [259] J. Caluzi and A. K. T. Assis, “A critical analysis of Helmholtz’s argument against Weber’s electrodynamics,” *Foundations of physics*, vol. 27, no. 10, pp. 1445–1452, 1997.
 - [260] Q. Li, “Extending Weber’s electrodynamics to high velocity particles,” *International Journal of Magnetism and Electromagnetism*, vol. 8:040, pp. 1–9, 2022.
 - [261] A. K. T. Assis, *Arguments in favour of action at a distance*, pp. 45–56. Commack, New York: Nova Science Publishers, 1999.
-

-
- [262] E. G. Haug, “Demonstration that Newtonian gravity moves at the speed of light and not instantaneously (infinite speed) as thought!,” *Journal of Physics Communications*, vol. 5, no. 2, p. 025005, 2021.
 - [263] A. K. T. Assis, “Weber’s law and mass variation,” *Physics letters A*, vol. 136, no. 6, pp. 277–280, 1989.
 - [264] A. K. T. Assis and J. Caluzi, “A limitation of Weber’s law,” *Physics Letters A*, vol. 160, no. 1, pp. 25–30, 1991.
 - [265] A. K. T. Assis and R. Clemente, “The ultimate speed implied by theories of Weber’s type,” *International Journal of Theoretical Physics*, vol. 31, no. 6, pp. 1063–1073, 1992.
 - [266] C. W. Sherwin, “The Weber radar,” *Physics Essays*, vol. 4, no. 3, pp. 417–419, 1991.
 - [267] P. Barrett, H. Jones, and R. Franklin, “Dispersion of electron plasma waves,” *Plasma Physics*, vol. 10, no. 10, p. 911, 1968.
 - [268] J. Wesley, “Weber electrodynamics extended to include radiation,” *Speculations in Science and Technology*, vol. 10, no. 1, pp. 50–53, 1987.
 - [269] R. W. Gray, “Candid remarks on introductory classical electrodynamics and textbooks,” *preprint*, pp. 1–27, 2020.
 - [270] G. Holzmüller, *Üeber die Anwendung der Jacobi-Hamilton’schen Methode auf den Fall der Anziehung nach dem electrodynamischen Gesetze von Weber*. 1870.
 - [271] G. Schröder, “Fast pulsed magnet systems,” in *Handbook of Accelerator Physics and Engineering* (A. W. Chao and M. Tigner, eds.), no. CERN-SL-98-017-BT, ch. 3, pp. 460–466, Singapore: World Scientific, 1999.
 - [272] L. J. Wong, K.-H. Hong, S. Carbajo, A. Fallahi, P. Piot, M. Soljačić, J. D. Joannopoulos, F. X. Kärtner, and I. Kaminer, “Laser-induced linear-field particle acceleration in free space,” *Scientific reports*, vol. 7, no. 1, p. 11159, 2017.
 - [273] L. Arnaudon, P. Baudrenghien, C. Bertone, Y. Body, J. Broere, O. Brunner, M. Buzio, C. Carli, F. Caspers, J. Corso, J. Coupard, A. Dallochio, N. Dos Santos, R. Garoby, F. Gerigk, L. Hammouti, K. Hanke, M. Jones, I. Kozsar, J. Lettry, J. Lallement, A. Lombardi, L. Lopez-Hernandez, C. Maglioni, S. Mathot, S. Maury, B. Mikulec, D. Nisbet, C. Noels, M. Paoluzzi, B. Puccio, U. Raich, S. Ramberger, C. Rossi, N. Schwerg, R. Scrivens, G. Vandoni, S. Weisz, J. Vollaie, M. Vretenar, and T. Zickler, “The LINAC4 Project at CERN,” p. 4 p, Aug 2011.
 - [274] G. Dattoli, L. Mezi, and M. Migliorati, “Operational methods for integro-differential equations and applications to problems in particle accelerator physics,” *Taiwanese Journal of Mathematics*, pp. 407–413, 2007.
 - [275] O. Karamyshev, C. Welsch, and D. Newton, “Optimization of low energy electrostatic beam lines,” *Proceedings of IPAC2014*, 2014.
-

-
- [276] A. Papash, A. Smirnov, and C. Welsch, “Nonlinear and long-term beam dynamics in low energy storage rings,” *Physical Review Special Topics-Accelerators and Beams*, vol. 16, no. 6, p. 060101, 2013.
- [277] H. Fernández-Morán, “Electron microscopy with high-field superconducting solenoid lenses,” *Proceedings of the National Academy of Sciences of the United States of America*, vol. 53, no. 2, p. 445, 1965.
- [278] H. Fernández-Morán, “High-resolution electron microscopy with superconducting lenses at liquid helium temperatures,” *Proceedings of the National Academy of Sciences of the United States of America*, vol. 56, no. 3, p. 801, 1966.
- [279] V. Kasisomayajula, M. Booty, A. Fiory, and N. Ravindra, “Magnetic field assisted heterogeneous device assembly,” *Supplemental Proceedings: Materials Processing and Interfaces*, vol. 1, pp. 651–661, 2012.
- [280] L. Steinhauer and D. Quimby, “Advances in laser solenoid fusion reactor design,” in *The Technology of Controlled Nuclear Fusion: Proceedings of the Third Topical Meeting on the Technology of Controlled Nuclear Fusion, May 9-11, 1978, Santa Fe, New Mexico*, vol. 1, p. 121, National Technical Information Service, 1978.
- [281] K. Tobita, S. Nishio, M. Sato, S. Sakurai, T. Hayashi, Y. Shibama, T. Isono, M. Enoda, H. Nakamura, S. Sato, *et al.*, “SlimCS—compact low aspect ratio DEMO reactor with reduced-size central solenoid,” *Nuclear fusion*, vol. 47, no. 8, p. 892, 2007.
- [282] C. Engström, T. Berlind, J. Birch, L. Hultman, I. Ivanov, S. Kirkpatrick, and S. Rohde, “Design, plasma studies, and ion assisted thin film growth in an unbalanced dual target magnetron sputtering system with a solenoid coil,” *Vacuum*, vol. 56, no. 2, pp. 107–113, 2000.
- [283] X. Zhang, J. Xiao, Z. Pei, J. Gong, and C. Sun, “Influence of the external solenoid coil arrangement and excitation mode on plasma characteristics and target utilization in a dc-planar magnetron sputtering system,” *Journal of Vacuum Science & Technology A: Vacuum, Surfaces, and Films*, vol. 25, no. 2, pp. 209–214, 2007.
- [284] D. E. Bordelon, R. C. Goldstein, V. S. Nemkov, A. Kumar, J. K. Jackowski, T. L. DeWeese, and R. Ivkov, “Modified solenoid coil that efficiently produces high amplitude ac magnetic fields with enhanced uniformity for biomedical applications,” *IEEE transactions on magnetics*, vol. 48, no. 1, pp. 47–52, 2011.
- [285] J. Drees and H. Piel, “Particle beam treatment system with solenoid magnets,” Jan. 12 2017. US Patent App. 15/203,966.
- [286] S. Maher, F. P. Jjunju, and S. Taylor, “Colloquium: 100 years of mass spectrometry: Perspectives and future trends,” *Reviews of Modern Physics*, vol. 87, no. 1, p. 113, 2015.
- [287] K. M. Taminger, W. H. Hofmeister, and R. A. Halfey, “Use of beam deflection to control an electron beam wire deposition process,” Jan. 2013. US Patent 8,344,281.
-

-
- [288] E. Koleva, V. Dzharov, V. Gerasimov, K. Tsvetkov, and G. Mladenov, “Electron beam deflection control system of a welding and surface modification installation,” in *Journal of Physics: Conference Series*, vol. 992, p. 012013, IOP Publishing, 2018.
- [289] M. Berz, B. Erdélyi, and K. Makino, “Fringe field effects in small rings of large acceptance,” *Physical Review Special Topics-Accelerators and Beams*, vol. 3, no. 12, p. 124001, 2000.
- [290] B. Lencová, “Computation of electrostatic lenses and multipoles by the first order finite element method,” *Nuclear Instruments and Methods in Physics Research Section A: Accelerators, Spectrometers, Detectors and Associated Equipment*, vol. 363, no. 1-2, pp. 190–197, 1995.
- [291] J. Rouse and E. Munro, “Three-dimensional computer modeling of electrostatic and magnetic electron optical components,” *Journal of Vacuum Science & Technology B: Microelectronics Processing and Phenomena*, vol. 7, no. 6, pp. 1891–1897, 1989.
- [292] F. H. Read and N. J. Bowring, “The CPO programs and the BEM for charged particle optics,” *Nuclear Instruments and Methods in Physics Research Section A: Accelerators, Spectrometers, Detectors and Associated Equipment*, vol. 645, no. 1, pp. 273–277, 2011.
- [293] D. Cubric, B. Lencova, F. Read, and J. Zlamal, “Comparison of FDM, FEM and BEM for electrostatic charged particle optics,” *Nuclear Instruments and Methods in Physics Research Section A: Accelerators, Spectrometers, Detectors and Associated Equipment*, vol. 427, no. 1-2, pp. 357–362, 1999.
- [294] K. Makino and M. Berz, “Solenoid elements in COSY INFINITY,” *Institute of Physics CS*, vol. 175, pp. 219–228, 2004.
- [295] M. Aslaninejad, C. Bontoiu, J. Pasternak, J. Pozimski, and A. Bogacz, “Solenoid fringe field effects for the neutrino factory Linac-MAD-X investigation,” tech. rep., Thomas Jefferson National Accelerator Facility, Newport News, VA (United States), 2010.
- [296] T. Gorlov and J. Holmes, “Fringe field effect of solenoids,” in *9th International Particle Accelerator Conference (IPAC2018)*, (Vancouver, BC, Canada), pp. 3385–3387, IPAC, JaCoW Publishing, 2018.
- [297] M. Migliorati and G. Dattoli, “Transport matrix of a solenoid with linear fringe field,” *Il Nuovo Cimento della Società Italiana di Fisica-B: General Physics, Relativity, Astronomy and Mathematical Physics and Methods*, vol. 124, no. 4, p. 385, 2009.
- [298] D. Cebon, “Magnetic fields of solenoids and magnets.” <https://www.mathworks.com/matlabcentral/fileexchange/71881-magnetic-fields-of-solenoids-and-magnets>, 2019. Retrieved September 26, 2019.
- [299] N. Derby and S. Olbert, “Cylindrical magnets and ideal solenoids,” *American Journal of Physics*, vol. 78, no. 3, pp. 229–235, 2010.
-

-
- [300] E. E. Callaghan and S. H. Maslen, “The magnetic field of a finite solenoid,” tech. rep., NASA, 1960.
- [301] L. Lerner, “Magnetic field of a finite solenoid with a linear permeable core,” *American Journal of Physics*, vol. 79, no. 10, pp. 1030–1035, 2011.
- [302] S. R. Muniz, V. S. Bagnato, and M. Bhattacharya, “Analysis of off-axis solenoid fields using the magnetic scalar potential: An application to a Zeeman-slower for cold atoms,” *American Journal of Physics*, vol. 83, no. 6, pp. 513–517, 2015.
- [303] M. X. Lim and H. Greenside, “The external magnetic field created by the superposition of identical parallel finite solenoids,” *American Journal of Physics*, vol. 84, no. 8, pp. 606–615, 2016.
- [304] P. Arpaia, B. Celano, L. De Vito, A. Esposito, A. Parrella, and A. Vannozzi, “Measuring the magnetic axis alignment during solenoids working,” *Scientific reports*, vol. 8, no. 1, p. 11426, 2018.
- [305] P. Arpaia, L. De Vito, A. Esposito, A. Parrella, and A. Vannozzi, “On-field monitoring of the magnetic axis misalignment in multi-coils solenoids,” *Journal of Instrumentation*, vol. 13, no. 08, p. P08017, 2018.
- [306] P. Arpaia, B. Celano, L. De Vito, A. Esposito, N. Moccaldi, and A. Parrella, “Monitoring the magnetic axis misalignment in axially-symmetric magnets,” in *2018 IEEE International Instrumentation and Measurement Technology Conference (I2MTC)*, pp. 1–6, IEEE, 2018.
- [307] J. Slepian, “Lines of force in electric and magnetic fields,” *American Journal of Physics*, vol. 19, no. 2, pp. 87–90, 1951.
- [308] L. Tian, C. Tao, and M.-X. Tian, “Leakage flux analysis in toroidal core with circular cross section based on analytic calculation,” *WSEAS TRANSACTIONS on CIRCUITS and SYSTEMS*, vol. 15, pp. 1–8, 2016.
- [309] I. Hernández, F. De León, and P. Gómez, “Design formulas for the leakage inductance of toroidal distribution transformers,” *IEEE Transactions on Power Delivery*, vol. 26, no. 4, pp. 2197–2204, 2011.
- [310] J. Hernandez, A. Mania, F. Luna, and A. Assis, “The internal and external electric fields for a resistive toroidal conductor carrying a steady poloidal current,” *Physica Scripta*, vol. 78, no. 1, p. 015403, 2008.
- [311] M. R. A. Pahlavani and A. Shoulaie, “A novel approach for calculations of helical toroidal coil inductance usable in reactor plasmas,” *IEEE transactions on plasma science*, vol. 37, no. 8, pp. 1593–1603, 2009.
- [312] M. Faraday, “V. experimental researches in electricity,” *Philosophical transactions of the Royal Society of London*, no. 122, pp. 125–162, 1832.
- [313] M. Faraday, “On some new electro-magnetical motions, and on the theory of magnetism,” *Quarterly Journal of Science*, vol. 12, pp. 74–96, 1821.
-

-
- [314] W. Weber, “Unipolare induktion. resultate aus den beobachtungen des magnetischen vereins,” vol. III, pp. 63–90, 1839. Reprinted in Wilhelm Weber’s Werke, Vol. 2, E. Riecke.
 - [315] M. Crooks, D. B. Litvin, P. Matthews, R. Macaulay, and J. Shaw, “One-piece Faraday generator: A paradoxical experiment from 1851,” *American Journal of Physics*, vol. 46, no. 7, pp. 729–731, 1978.
 - [316] V. Leus and S. Taylor, “On the motion of the field of a permanent magnet,” *European journal of physics*, vol. 32, no. 5, p. 1179, 2011.
 - [317] C. Hering, “An imperfection in the usual statement of the fundamental law of electromagnetic induction,” *Proceedings of the American Institute of Electrical Engineers*, vol. 27, no. 3, pp. 339–349, 1908.
 - [318] C. Hering, “The laws of induction,” *Electrician*, vol. 73, p. 344, 1915.
 - [319] E. Cullwick, “An experiment on electromagnetic induction by linear motion,” *Journal of the Institution of Electrical Engineers*, vol. 85, no. 512, pp. 315–318, 1939.
 - [320] I. Tamm, “Fundamentals of the theory of electricity, 1976,” *Moscow: Mir Publ.*, [Translated from Russian: *Osnovy Teorii Elektrichestva (Moscow: Nauka, 1989)*].
 - [321] W. J. Duffin and W. J. Duffin, *Electricity and magnetism*. McGraw-Hill College, 1990.
 - [322] W. Panofsky and M. Phillips, *Classical Electricity and Magnetism*. Addison-Wesley, 1962.
 - [323] G. A. Bennet, “Electricity and modern physics: mks version,” tech. rep., Edward Arnold,, 1968.
 - [324] R. W. Pohl, *Elektrizitätslehre: Einführung in die Physik*. Springer, 1960.
 - [325] J. Vanderlinde, *Classical electromagnetic theory*, vol. 145. Springer Science & Business Media, 2006.
 - [326] A. Shadowitz, *Special relativity*. No. 6, Courier Corporation, 1988.
 - [327] E. M. Purcell and D. J. Morin, *Electricity and magnetism*. Cambridge University Press, 2013.
 - [328] E. Laureti, “Alcune osservationi sull induzione unipolare,” *Nova Astronautica*, vol. 12, no. 54, pp. 27–33, 1992.
 - [329] N. Zajev and V. Dokuchajev, “About the behaviour of force lines of the field of a rotating magnet,” *Electrotekhnika (Electrical Engineering)*, vol. 11, p. 64, 1964.
 - [330] A. Kelly, “Unipolar experiments,” *Annales de la Fondation Louis de Broglie*, vol. 29, no. 1-2, pp. 119–148, 2004.
 - [331] K. Rajaraman, “The field of a rotating cylindrical magnet,” *International Journal of Electrical Engineering Education*, vol. 45, no. 1, pp. 34–45, 2008.
-

-
- [332] V. N. Matveev and O. V. Matvejev, “Relativistic effects and emf localization in a unipolar generator,” in *Journal of Physics: Conference Series*, vol. 1251, p. 012036, IOP Publishing, 2019.
 - [333] G. I. Cohn, “Electromagnetic induction,” *Electrical Engineering*, vol. 68, no. 5, pp. 441–447, 1949.
 - [334] F. A. Kaempffer, *The elements of physics: a new approach*. Blaisdell Publishing Company, 1967.
 - [335] P. Scanlon, R. Henriksen, and J. Allen, “Approaches to electromagnetic induction,” *American Journal of Physics*, vol. 37, no. 7, pp. 698–708, 1969.
 - [336] N. Savage, “Electromagnetic induction,” *Elect. Eng.*, vol. 68, p. 645, 1949.
 - [337] M. Trocheris, “Civ. electrodynamics in a rotating frame of reference,” *The London, Edinburgh, and Dublin Philosophical Magazine and Journal of Science*, vol. 40, no. 310, pp. 1143–1154, 1949.
 - [338] J. G. Valverde and P. Mazzoni, “The principle of relativity as applied to motional electromagnetic induction,” *American Journal of Physics*, vol. 63, no. 3, pp. 228–229, 1995.
 - [339] J. Guala-Valverde, P. Mazzoni, and R. Achilles, “The homopolar motor: A true relativistic engine,” *American Journal of Physics*, vol. 70, no. 10, pp. 1052–1055, 2002.
 - [340] R. E. Berg and C. O. Alley, “The unipolar generator: A demonstration of special relativity,” *Department of Physics, University of Maryland, College Park, MD*, 2005.
 - [341] E. Kennard, “Xiii. on unipolar induction: Another experiment and its significance and evidence for the existence of the æther,” *The London, Edinburgh, and Dublin Philosophical Magazine and Journal of Science*, vol. 33, no. 194, pp. 179–190, 1917.
 - [342] L. Schiff, “A question in general relativity,” *Proceedings of the National Academy of Sciences of the United States of America*, vol. 25, no. 7, p. 391, 1939.
 - [343] H. Jehle, “Relationship of flux quantization to charge quantization and the electromagnetic coupling constant,” *Phys. Rev. D*, vol. 3, pp. 306–345, Jan 1971.
 - [344] H. Jehle, “Flux quantization and particle physics,” *Phys. Rev. D*, vol. 6, pp. 441–457, Jul 1972.
 - [345] H. Jehle, “Flux quantization and fractional charges of quarks,” *Phys. Rev. D*, vol. 11, pp. 2147–2177, Apr 1975.
 - [346] S. Bordoni, “Unipolar machines and the principle of relativity,” *Isonomia*, vol. 2037, p. 4348, 2017.
 - [347] H. A. Wilson, “Iii. on the electric effect of rotating a dielectric in a magnetic field,” *Philosophical Transactions of the Royal Society of London. Series A, Containing Papers of a Mathematical or Physical Character*, vol. 204, no. 372-386, pp. 121–137, 1904.
-

-
- [348] M. Wilson and H. A. Wilson, “On the electric effect of rotating a magnetic insulator in a magnetic field,” *Proceedings of the Royal Society of London. Series A, Containing Papers of a Mathematical and Physical Character*, vol. 89, no. 608, pp. 99–106, 1913.
 - [349] A. Einstein and J. Laub, “Über die elektromagnetischen grundgleichungen für bewegte körper,” *Annalen der Physik*, vol. 331, no. 8, pp. 532–540, 1908.
 - [350] F. Munley, “Challenges to Faraday’s flux rule,” *American journal of physics*, vol. 72, no. 12, pp. 1478–1483, 2004.
 - [351] G. Giuliani, “A general law for electromagnetic induction,” *EPL (Europhysics Letters)*, vol. 81, no. 6, p. 60002, 2008.
 - [352] M. B. Nezhad, *Study of Homopolar DC Generator*. The University of Manchester (United Kingdom), 2013.
 - [353] K. Zengel, “The history of the Faraday paradox of the unipolar generator,” *European Journal of Physics*, vol. 40, no. 5, p. 055202, 2019.
 - [354] K. T. McDonald, “Is Faraday’s disk dynamo a flux-rule exception?,” 2019.
 - [355] H. Montgomery, “Unipolar induction: a neglected topic in the teaching of electromagnetism,” *European journal of physics*, vol. 20, no. 4, p. 271, 1999.
 - [356] J. Guala-Valverde and S. de Energía, “Comments on Montgomery’s paper on electrodynamics,” *Apeiron*, vol. 11, no. 2, p. 327, 2004.
 - [357] A. Assis, “*Wilhelm Weber Main Works on Electrodynamics Translated into English*”, Volume 2: “*Weber’s Fundamental Force and the Unification of the Laws of Coulomb, Ampère and Faraday*”. 09 2021.
 - [358] C. Baumgärtel and S. Maher, “A novel model of unipolar induction phenomena based on direct interaction between conductor charges,” *Progress In Electromagnetics Research*, vol. 171, pp. 123–135, 2021.
 - [359] S. J. Barnett, “On electromagnetic induction and relative motion,” *Physical Review (Series I)*, vol. 35, no. 5, p. 323, 1912.
 - [360] S. J. Barnett, “Magnetization by rotation,” *Physical Review*, vol. 6, no. 4, p. 239, 1915.
 - [361] S. Barnett, “Xxviii. a new electron-inertia effect and the determination of m/e for the free electrons in copper,” *The London, Edinburgh, and Dublin Philosophical Magazine and Journal of Science*, vol. 12, no. 76, pp. 349–360, 1931.
 - [362] S. Barnett, “Gyromagnetic and electron-inertia effects,” *Reviews of Modern Physics*, vol. 7, no. 2, p. 129, 1935.
 - [363] A. Blondel, “The laws of induction,” *Electrician*, vol. 75, p. 344, 1915.
 - [364] E. Kennard, “Xciii. unipolar induction,” *The London, Edinburgh, and Dublin Philosophical Magazine and Journal of Science*, vol. 23, no. 138, pp. 937–941, 1912.
-

-
- [365] G. B. Pegram, “Unipolar induction and electron theory,” *Physical review*, vol. 10, no. 6, p. 591, 1917.
 - [366] L. Bewley, “Flux linkages and electromagnetic induction in closed circuits,” *Transactions of the American Institute of Electrical Engineers*, vol. 48, no. 2, pp. 327–337, 1929.
 - [367] W. Cramp and E. Norgrove, “Some investigations on the axial spin of a magnet and on the laws of electromagnetic induction,” *Journal of the Institution of Electrical Engineers*, vol. 78, no. 472, pp. 481–491, 1936.
 - [368] R. Stephenson, “Experiments with a unipolar generator and motor,” *American Journal of Physics*, vol. 5, no. 3, pp. 108–110, 1937.
 - [369] J. W. Then, “Experimental study of the motional electromotive force,” *American Journal of Physics*, vol. 30, no. 6, pp. 411–415, 1962.
 - [370] D. Bartlett, J. Monroy, and J. Reeves, “Spinning magnets and Jehle’s model of the electron,” *Physical Review D*, vol. 16, no. 12, p. 3459, 1977.
 - [371] N. Macleod, “Faraday’s disk revisited: Some new experiments concerning unipolar electromagnetic induction,” *Physics Essays*, vol. 25, no. 4, pp. 524–531, 2012.
 - [372] F. J. Müller, “Unipolar induction revisited: New experiments and the “edge effect” theory,” *IEEE transactions on magnetics*, vol. 50, no. 1, pp. 1–11, 2013.
 - [373] K. Chen, X. Li, and Y. Hui, “An experimental study on unipolar induction,” *Acta Physica Polonica A*, vol. 131, 2016.
 - [374] T. Valone, “The one-piece faraday generator,” in *Proceedings of the 26th intersociety energy conversion engineering conference*, pp. 473–478, 1991.
 - [375] C. Baumgärtel and S. Maher, “Resolving the paradox of unipolar induction - new experimental evidence on the influence of the test circuit,” *Scientific Reports*, 2022.
 - [376] A. I. Miller, “Unipolar induction: a case study of the interaction between science and technology,” *Annals of Science*, vol. 38, no. 2, pp. 155–189, 1981.
 - [377] J. Guala-Valverde and P. Mazzoni, “The unipolar dynamotor: a genuine relational engine,” *Apeiron*, vol. 8, no. 4, p. 41, 2001.
 - [378] A. Kholmetskii, “The Guala-Valverde and Barnett experiments both agree with the classical field theory,” *Physica Scripta*, vol. 77, no. 2, p. 025402, 2008.
 - [379] H. Montgomery, “Some comments on J. Guala-Valverde’s experiments on unipolar induction,” *Apeiron: Studies in Infinite Nature*, vol. 14, no. 1, 2007.
 - [380] P. Cornille and G. Galeczki, “Mass-increase with velocity is a dynamical effect,” *Journal of Theoretics Comprehensive Papers Section*.
 - [381] A. Bokulich, “Open or closed? Dirac, Heisenberg, and the relation between classical and quantum mechanics,” *Studies in History and Philosophy of Science Part B: Studies in History and Philosophy of Modern Physics*, vol. 35, no. 3, pp. 377–396, 2004.
-

-
- [382] P. E. Jourdain, “Newton’s hypotheses of ether and of gravitation from 1672 to 1679,” *The Monist*, pp. 79–106, 1915.
 - [383] J. C. Maxwell, “Iii. on physical lines of force: Part iii.—the theory of molecular vortices applied to statical electricity,” *The London, Edinburgh, and Dublin Philosophical Magazine and Journal of Science*, vol. 23, no. 151, pp. 12–24, 1862.
 - [384] L. S. Swenson, *The ethereal aether: a history of the Michelson-Morley-Miller aether-drift experiments, 1880-1930*. University of Texas Press, 2013.
 - [385] J. Ribeiro, A. Vannucci, and A. Assis, “The multiple definitions of ‘field’ in the context of electromagnetism,” *Proceedings of the VI Taller Internacional “ENFIQUI 2008”*, pp. 1–4, 2008.
 - [386] J. Stachel, “Why Einstein reinvented the ether,” *Physics World*, vol. 14, no. 6, p. 55, 2001.
 - [387] G. Builder, “Ether and relativity,” *Australian Journal of Physics*, vol. 11, no. 3, pp. 279–297, 1958.
 - [388] P. A. M. Dirac, “Is there an aether?,” *Nature*, vol. 168, no. 4282, pp. 906–907, 1951.
 - [389] L. Infeld, “Is there an aether?,” *Nature*, vol. 169, no. 4304, pp. 702–702, 1952.
 - [390] H. Dehmelt, “A single atomic particle forever floating at rest in free space: New value for electron radius,” *Physica Scripta*, vol. 1988, no. T22, p. 102, 1988.
 - [391] J. J. Hudson, D. M. Kara, I. Smallman, B. E. Sauer, M. R. Tarbutt, and E. A. Hinds, “Improved measurement of the shape of the electron,” *Nature*, vol. 473, no. 7348, pp. 493–496, 2011.
 - [392] J. Baron, W. C. Campbell, D. DeMille, J. M. Doyle, G. Gabrielse, Y. V. Gurevich, P. W. Hess, N. R. Hutzler, E. Kirilov, I. Kozyryev, *et al.*, “Order of magnitude smaller limit on the electric dipole moment of the electron,” *Science*, vol. 343, no. 6168, pp. 269–272, 2014.
 - [393] W. B. Cairncross, D. N. Gresh, M. Grau, K. C. Cossel, T. S. Roussy, Y. Ni, Y. Zhou, J. Ye, and E. A. Cornell, “Precision measurement of the electron’s electric dipole moment using trapped molecular ions,” *Physical review letters*, vol. 119, no. 15, p. 153001, 2017.
 - [394] C. T. Sebens, “Particles, fields, and the measurement of electron spin,” *Synthese*, vol. 198, no. 12, pp. 11943–11975, 2021.
 - [395] A. Hobson, “There are no particles, there are only fields,” *American Journal of Physics*, vol. 81, pp. 211–223, 2013.
 - [396] C. T. Sebens, “The fundamentality of fields,” preprint.
 - [397] M. Hubert and D. Romano, “The wave-function as a multi-field,” *European Journal for Philosophy of Science*, vol. 8, pp. 521–537, 2018.
 - [398] D. Romano, “Multi-field and Bohm’s theory,” *Synthese*, vol. 198, no. 11, pp. 10587–10609, 2021.
-

-
- [399] M. Fayngold, “On the only fields interpretation of quantum mechanics,” *arXiv preprint arXiv:2111.07242*, 2021.
 - [400] T. Y. Cao, “Structural realism and the interpretation of quantum field theory,” *Synthese*, vol. 136, no. 1, pp. 3–24, 2003.
 - [401] T. Y. Cao, “Ontological relativity and fundamentality: is qft the fundamental theory?,” *Synthese*, vol. 136, no. 1, pp. 25–30, 2003.
 - [402] S. French and J. Ladyman, “Remodelling structural realism: Quantum physics and the metaphysics of structure,” *Synthese*, vol. 136, no. 1, pp. 31–56, 2003.
 - [403] S. Saunders, “Structural realism, again,” *Synthese*, vol. 136, no. 1, pp. 127–133, 2003.
 - [404] D. Krause and O. Bueno, “Ontological issues in quantum theory,” September 2010. Forthcoming in *Manuscrito*.
 - [405] E. Agazzi, “The multiple aspects of the philosophy of science,” *Axiomathes*, vol. 31, no. 6, pp. 677–693, 2021.
 - [406] S. Hossenfelder, *Lost in math: How beauty leads physics astray*. Hachette UK, 2018.
 - [407] J. Lykken and M. Spiropulu, “Supersymmetry and the crisis in physics,” *Scientific American*, vol. 310, no. 5, pp. 34–39, 2014.
 - [408] K. Crowther, “Defining a crisis: The roles of principles in the search for a theory of quantum gravity,” *Synthese*, vol. 198, no. 14, pp. 3489–3516, 2021.
 - [409] S. Meucci, “Physics has evolved beyond the physical,” *Cosmos and History: The Journal of Natural and Social Philosophy*, vol. 16, no. 1, pp. 452–465, 2020.
 - [410] J. Butterfield, “Lost in math? a review of ‘lost in math: How beauty leads physics astray’, by Sabine Hossenfelder,” *arXiv preprint arXiv:1902.03480*, 2019.
 - [411] S. Hawking and L. Mlodinow, *The grand design*. Random House Digital, Inc., 2010.
 - [412] L. Laplane, P. Mantovani, R. Adolphs, H. Chang, A. Mantovani, M. McFall-Ngai, C. Rovelli, E. Sober, and T. Pradeu, “Opinion: Why science needs philosophy,” *Proceedings of the National Academy of Sciences*, vol. 116, no. 10, pp. 3948–3952, 2019.
 - [413] G. Harman, “Concerning Stephen Hawking’s claim that philosophy is dead,” *Filozofski vestnik*, vol. 32, no. 2, 2012.
 - [414] H. Hossieni, J. Fatah, S. Kaki, and A. Khalil, “Heisenberg uncertainty principle & Kant philosophy: Why Hawking thinks philosophy is dead,” *Journal of Consciousness Exploration & Research*, vol. 7, no. 10, 2016.
 - [415] E. Khaling, “Is philosophy dead?,” *Philosophy, Religion & Culture*, 2017.
 - [416] C. Rovelli, “Physics needs philosophy. philosophy needs physics,” *Foundations of Physics*, vol. 48, no. 5, pp. 481–491, 2018.
-

- [417] T. Phipps, “Electromagnetic force laws and hot fusion,” *Galilean Electrodynamics*, vol. 27, no. 4, pp. 79–80, 2016.
- [418] W. F. Edwards, C. Kenyon, and D. Lemon, “Continuing investigation into possible electric fields arising from steady conduction currents,” *Physical Review D*, vol. 14, no. 4, p. 922, 1976.
- [419] O. Jefimenko, “Demonstration of the electric fields of current-carrying conductors,” *American Journal of Physics*, vol. 30, no. 1, pp. 19–21, 1962.
- [420] O. D. Jefimenko, *Electricity and magnetism: an introduction to the theory of electric and magnetic fields*. Electret Scientific Company, 2 ed., 1989.
- [421] Y. Zhao, “A novel two-particle steady-state wave equation,” *Iranian Journal of Science and Technology, Transactions A: Science*, pp. 1–8, 2022.
- [422] G. H. Pollack, “The fourth phase of water,” *Ebner and Sons Publishers: Seattle, WA, USA*, 2013.
- [423] J. Kirkpatrick, B. McMorrow, D. H. Turban, A. L. Gaunt, J. S. Spencer, A. G. Matthews, A. Obika, L. Thiry, M. Fortunato, D. Pfau, *et al.*, “Pushing the frontiers of density functionals by solving the fractional electron problem,” *Science*, vol. 374, no. 6573, pp. 1385–1389, 2021.
- [424] G. Merziger, G. Mühlbach, D. Wille, and T. Wirth, *Formeln + Hilfen zur höheren Mathematik*. Binomi Verlag, 6th ed., 2010.

A Circular and Helical Motion

This Appendix will briefly show useful mathematical equations and diagrams to explain the circular and helical motions utilised in the modelling approaches of this work.

A.1 Circular Motion

An object moving on a circular trajectory is situated at a certain distance r from the centre of the circle described by the motion and moving along that path with a certain speed. The motion can be expressed in both Cartesian and polar coordinates [424] and a sketch can be seen in Fig. A.1

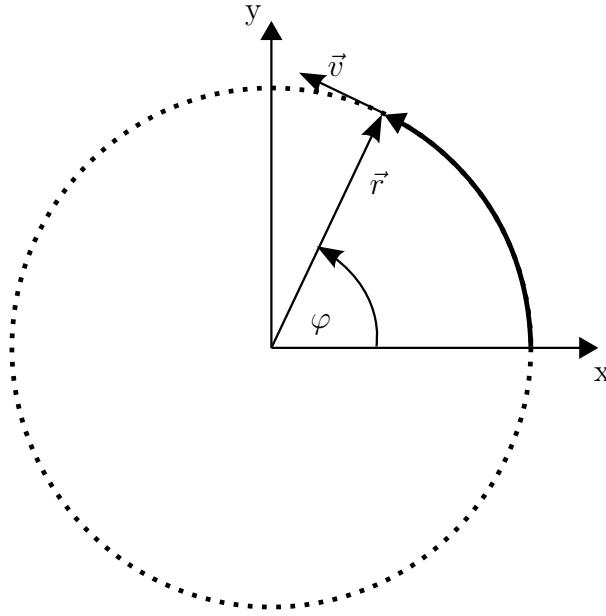


Figure A.1: Circular motion in a Cartesian coordinate system

The angle φ is the polar angle defining the angular distance travelled by a moving point in question. We can transform between the two systems of coordinates with the help of the following relations:

$$x = r \cos(\varphi) \quad (\text{A.1})$$

$$y = r \sin(\varphi) \quad (\text{A.2})$$

$$r = \sqrt{x^2 + y^2} \quad (\text{A.3})$$

$$\tan(\varphi) = \frac{y}{x} \quad (\text{A.4})$$

with the two dimensional plane as a special case where

$$\vec{r} = \begin{pmatrix} r \cos(\varphi) \\ r \sin(\varphi) \\ 0 \end{pmatrix} \quad (\text{A.5})$$

For circular motion of constant speed, so called uniform circular motion, we can further find the angular velocity as

$$\omega = \frac{d\varphi}{dt} \quad (\text{A.6})$$

and

$$\vec{v} = \vec{\omega} \times \vec{r} \quad (\text{A.7})$$

so that we can simply obtain the magnitude as

$$\omega = \frac{v}{r}. \quad (\text{A.8})$$

The angular acceleration can also be obtained as the time derivative of the angular velocity and due to the motion's confinement to a fixed radius it is subject to a certain centripetal acceleration, pointing towards the centre of the motion. For our examples however, the calculation of these quantities is not relevant and will be omitted in this short summary.

A.2 Helical Motion

Helical motion is similar to circular motion where a moving object is confined to a certain radius, but now it is also moving along a third axis. This can be seen as propagating in time or gradual spatial displacement, in our case the object also propagates in space parallel to the z-axis of a Cartesian coordinate system (Fig. A.2).

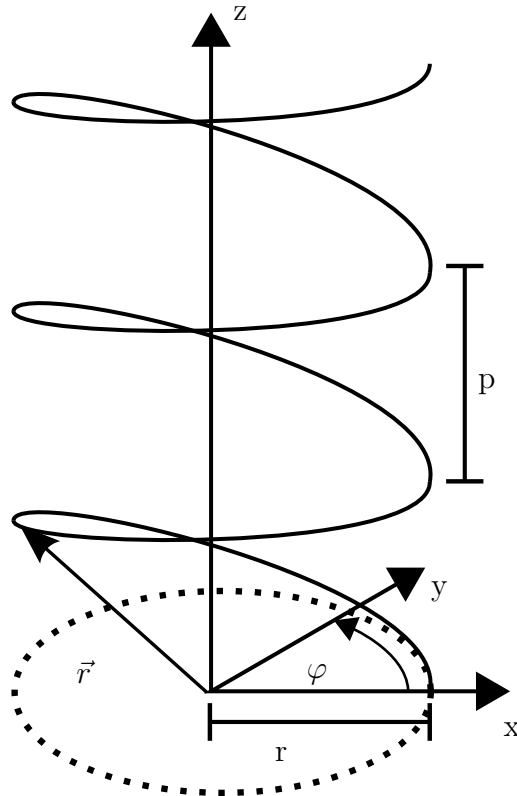


Figure A.2: Helical motion in a Cartesian coordinate system

We can define the position \vec{r} with the circular motion of the x- and y-components and add a motion along the third axis through the z component:

$$\vec{r} = \begin{pmatrix} r \cos(\varphi) \\ r \sin(\varphi) \\ dz \cdot \varphi \end{pmatrix} \quad (\text{A.9})$$

where dz is an infinitesimal element along the z-axis. The pitch of the helix is the distance taken along the z-axis to complete one full rotation, giving

$$p = dz \cdot 2\pi \quad (\text{A.10})$$

and if we assume a coil with a number of windings N and length l , like in section 4, we get for the length of the coil

$$l = N \cdot p, \quad (\text{A.11})$$

so that we can find the size of dz as

$$dz = \frac{l}{2\pi N} \quad (\text{A.12})$$

B Toroid Parametrisation

According to [424] a toroid is a body of rotation that is formed by rotating a circle around an axis that is in the same plane as the circle but reaches outside of it. Usually the circle being rotated has a smaller radius R_1 whereas the larger axis is of radius R_2 . Following the definition in [424], we have a toroid as shown in Fig. B.1 that can be parametrised as follows:

$$\vec{r} = \begin{pmatrix} (R_2 + R_1 \cos(\theta)) \cos(\varphi) \\ (R_2 + R_1 \cos(\theta)) \sin(\varphi) \\ R_1 \sin(\theta) \end{pmatrix}. \quad (\text{B.1})$$

Here φ is defined as the angle in the xy-plane and θ as the angle describing the smaller circle of size R_1 . In section 4 we utilised a slightly different definition, where the circle was rotated around a different axis in the right-handed coordinate system, so that it was parametrised as

$$\vec{r} = \begin{pmatrix} (R_2 + R_1 \cos(\theta)) \cos(\varphi) \\ R_1 \sin(\theta) \\ (R_2 + R_1 \cos(\theta)) \sin(\varphi) \end{pmatrix}. \quad (\text{B.2})$$

So we can see that in this parametrisation (B.2) the toroid has been rotated around a different axis from the parametrisation (B.1).

In [424] it is explicitly pointed out that we have the domains of definition for the angles φ and θ as

$$(\varphi, \theta) \in [0, 2\pi] \times [0, 2\pi], \quad (\text{B.3})$$

because the angle θ is locally defined inside the smaller circle of radius R_1 . This is unlike the common definitions of spherical coordinates, where for example

$$(\theta, \varphi) \in [0, \pi] \times [0, 2\pi], \quad (\text{B.4})$$

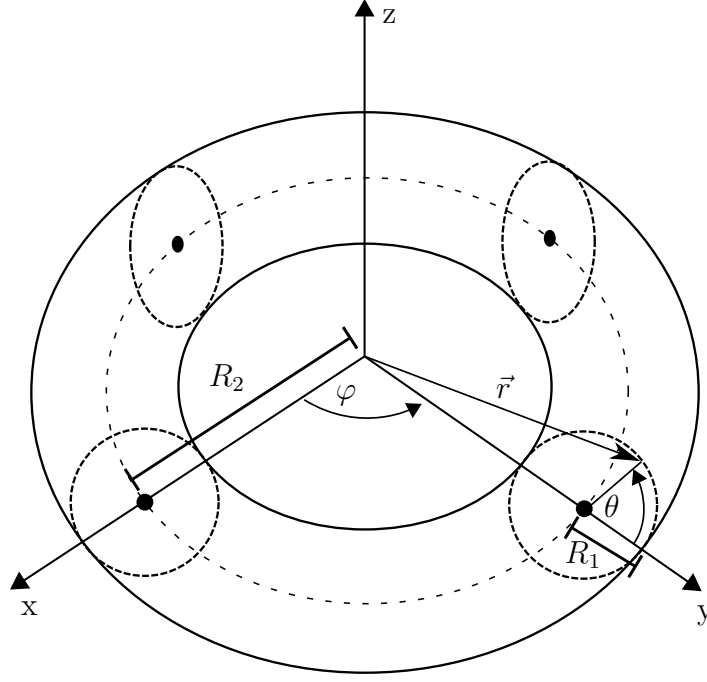


Figure B.1: Typical parametrisation of a Toroid in a right handed coordinate system

with θ defined as the distance from the pole and φ as the azimuthal angle on the xy -plane, leaving for a sphere

$$\vec{r} = \begin{pmatrix} \rho \sin(\theta) \cos(\varphi) \\ \rho \sin(\theta) \sin(\varphi) \\ \rho \cos(\theta) \end{pmatrix}. \quad (\text{B.5})$$

This distinction about the domains of definition is necessary to make in order to obtain the right bounds of integration, as well as the correct values for parametrisation.

C Matlab Codes and CPO Databuilder File

This appendix lists the *MATLAB* codes used to predict expected values from the Weber and field models in sections 4 and 5, as well as the databuilder file used with CPO in section 4.

Listing 1: Code for calculating the electron beam deflection based on Weber's force with a current element in helical motion and the beam travelling across the solenoid.

```

1 %Calculate deflection of electron beam across solenoid with
  helix motion approach
2
3 clearvars
4 clc
5
6 %% Set PARAMETERS %%
7 R_1 = 0.03; %m solenoid radius %0.05 originally 0.027; 0.03;
  0.020;
8 h = -(R_1 + 0.025); %m height of electron beam above solenoid
  which we assume remains constant

```

```

9 V = 2000; %V acceleration voltage
10 I = 1.0; %A
11 eps_0 = 8.854187817e-12; %vacuum permittivity
12 e = 1.60217662e-19; %elementary charge
13 m_e = 9.10938356e-31; %electron mass
14 c = 299792458; %lightspeed
15 v_e = sqrt(2*e*V/m_e); %m/s ~1200V acceleration voltage
16 const = (e*I)/(4*pi*eps_0*c*c); %constant outside integration
    , 2 from doublewound theory
17 N = 650; %Number of windings, in doublewound this is number
    of windings in one layer! 280; 650; 31;
18 l = 0.5; %m length of the solenoid, first test with 0.1
    0.255; 0.5; 0.025;
19 dz = l/(N*2*pi); % incremental increase with theta
20 p = l/N; % pitch of the coil
21
22 %% set z position of the coil and beam %%
23 z_1 = l*6/8; %beam position offset on z axis
24 z_2 = l/2; %start of the coil on the z axis it elongates only
    in one direction from there! (so it is end of the coil
    where current enters)
25 z_3 = -z_2;
26
27 %% Set beam path along x axis for loop %% Now x=b values!
28 b_start = -0.095;
29 b_last = +0.180;
30 b_step_size = 0.0001; %originally with 0.002
31 b = b_start : b_step_size : b_last;
32
33
34 v = ones(1,length(b))*v_e;
35 s = b_last + abs(b_start);
36 s_b = 0:b_step_size:s;
37 time = s_b./v_e;
38 t_end = time(find(time,1,'last'));
39
40 q_2 = e; %8.5e28*pi*0.000454545^2*
41
42 %%%% Helix approach %%%%
43 %% Integration steps for THETA in trapz %%
44 theta_start = 0;
45 theta_last = (N*2*pi);
46 theta_steps = N*72; %Look to increase (originally 72), 72 is
    enough!
47 % set the number of intervals of theta required between 0 and
    2pi
48 theta_step_size = theta_last / theta_steps; %check if this is
    off by one, seems like it is, but is okay in the context

```

```

    it is used.
49 theta = theta_start : theta_step_size : theta_last;
50
51 Fy_helix = zeros(1,length(b));
52 Fz_helix = zeros(1,length(b));
53 % dfi = zeros(length(theta),length(b));
54 % dfo = zeros(length(theta),length(b));
55 % This is POSITIVE ROTATION and positive z!!!
56 for j=1:length(b)
57
58     r_i = sqrt((R_1)^2 + (h)^2 + (b(j))^2 +(z_1-z_2+dz*theta)
59             .^2 + - 2*R_1*h*sin(theta) - 2*R_1*b(j)*cos(theta));
60 %y
61     i1i = sin(theta).^2.*(cos(theta))./r_i.^5;
62     i2i = sin(theta).^2./r_i.^5;
63     i3i = sin(theta).^2./r_i.^3;
64     i4i = sin(theta).*cos(theta).^2./r_i.^5;
65     i5i = theta.*sin(theta).*cos(theta)./r_i.^5;
66     i6i = sin(theta).*cos(theta)./r_i.^5;
67     i7i = theta.*sin(theta)./r_i.^5;
68     i8i = sin(theta)./r_i.^5;
69     i9i = sin(theta)./r_i.^3;
70     i10i = (cos(theta)).^2./r_i.^5;
71     i11i= theta.*cos(theta)./r_i.^5;
72     i12i = cos(theta)./r_i.^5;
73     i13i= theta./r_i.^5;
74     i14i= 1./r_i.^5;
75     i15i = sin(theta).*cos(theta)./r_i.^3;
76     i16i = cos(theta)./r_i.^3;
77     i17i = theta.*sin(theta)./r_i.^3;
78     i18i= theta.*cos(theta).^2./r_i.^5;
79     i19i= theta.^2.*cos(theta)./r_i.^5;
80     i20i= theta.^2./r_i.^5;
81     i21i = theta.*cos(theta)./r_i.^3;
82     i22i= theta./r_i.^3;
83     i23i= 1./r_i.^3;
84
85
86     i1o = sin(theta).^2.*(cos(theta))./r_o.^5;
87     i2o = sin(theta).^2./r_o.^5;
88     i3o = sin(theta).^2./r_o.^3;
89     i4o = sin(theta).*cos(theta).^2./r_o.^5;
90     i5o = theta.*sin(theta).*cos(theta)./r_o.^5;
91     i6o = sin(theta).*cos(theta)./r_o.^5;
92     i7o = theta.*sin(theta)./r_o.^5;
93     i8o = sin(theta)./r_o.^5;

```

```

94     i9o = sin(theta)./r_o.^3;
95     i10o = (cos(theta)).^2./r_o.^5;
96     i11o= theta.*cos(theta)./r_o.^5;
97     i12o = cos(theta)./r_o.^5;
98     i13o= theta./r_o.^5;
99     i14o= 1./r_o.^5;
100    i15o = sin(theta).*cos(theta)./r_o.^3;
101    i16o = cos(theta)./r_o.^3;
102    i17o = theta.*sin(theta)./r_o.^3;
103    i18o= theta.*cos(theta).^2./r_o.^5;
104    i19o= theta.^2.*cos(theta)./r_o.^5;
105    i20o= theta.^2./r_o.^5;
106    i21o = theta.*cos(theta)./r_o.^3;
107    i22o= theta./r_o.^3;
108    i23o= 1./r_o.^3;
109
110
111    Fi_y = v(j)*const*R_1*(-3*R_1^2*b(j)*i1i +3*R_1*(b(j))^2*
        i2i -2*R_1*i3i +3*R_1^2*h*i4i -3*R_1*dz^2*i5i +3*R_1*
        dz*z_2*i6i -3*R_1*dz*z_1*i6i +3*dz^2*b(j)*i7i -3*dz*(b
        (j))*z_2*i8i +3*dz*(b(j))*z_1*i8i -3*h*(b(j))^2*i8i
        +2*h*i9i -3*R_1*h^2*i10i +3*dz^2*h*i11i -3*dz*h*z_2*
        i12i +3*dz*h*z_1*i12i +3*h^2*b(j)*i12i -3*dz^2*b(j)*h/
        R_1*i13i +3*dz*h*b(j)*z_2/R_1*i14i -3*dz*h*b(j)*z_1/
        R_1*i14i) + R_1*e*q_2*a/(4*pi*eps_0*c*c) * (R_1^2*i15i
        -R_1*b(j)*i9i -R_1*h*i16i +h*b(j)*i14i);
112
113    Fo_y = v(j)*const*R_1*(-3*R_1^2*b(j)*i1o +3*R_1*(b(j))^2*
        i2o -2*R_1*i3o +3*R_1^2*h*i4o -3*R_1*dz^2*i5o -3*R_1*
        dz*z_3*i6o +3*R_1*dz*z_1*i6o +3*dz^2*b(j)*i7o +3*dz*(b
        (j))*z_3*i8o -3*dz*(b(j))*z_1*i8o -3*h*(b(j))^2*i8o
        +2*h*i9o -3*R_1*h^2*i10o +3*dz^2*h*i11o +3*dz*h*z_3*
        i12o -3*dz*h*z_1*i12o +3*h^2*b(j)*i12o -3*dz^2*b(j)*h/
        R_1*i13o -3*dz*h*b(j)*z_3/R_1*i14o +3*dz*h*b(j)*z_1/
        R_1*i14o) + R_1*e*q_2*a/(4*pi*eps_0*c*c) * (R_1^2*i15o
        -R_1*b(j)*i9o -R_1*h*i16o +h*b(j)*i14o);
114
115    Fy_helix(j) = trapz(theta,Fi_y+Fo_y);
116
117    Fi_z = v(j)*const*R_1*(3*R_1*dz*b(j)*i5i -3*R_1*b(j)*z_2*
        i6i +3*R_1*b(j)*z_1*i6i -3*dz*b(j)^2*i7i +2*dz*i17i
        +3*b(j)^2*z_2*i8i -2*z_2*i9i -3*b(j)^2*z_1*i8i +2*z_1*
        i9i -3*R_1*dz*h*i18i +3*R_1*h*z_2*i10i -3*R_1*h*z_1*
        i10i +3*dz^3*i19i -6*dz^2*z_2*i11i +6*dz^2*z_1*i11i
        +3*dz*h*b(j)*i11i +3*dz*z_2^2*i12i -6*dz*z_1*z_2*i12i
        -3*h*b(j)*z_2*i12i +3*dz*z_1^2*i12i +3*h*b(j)*z_1*i12i
        -3*dz^3*b(j)*i20i/(R_1) +6*dz^2*b(j)*z_2*i13i/(R_1)
        -6*dz^2*b(j)*z_1*i13i/(R_1) -(3*dz*b(j)*z_2^2*i14i)/(

```

```

118     R_1) +6*dz*b(j)*z_1*z_2*i14i/(R_1) -3*dz*b(j)*z_1^2*
119     i14i/(R_1)) + R_1*e*q_2*a/(4*pi*eps_0*c*c) * (-R_1*dz*
    i21i +R_1*z_2*i16i -R_1*z_1*i16i +dz*b(j)*i22i -b(j)*
    z_2*i23i +b(j)*z_1*i23i);

    Fo_z = v(j)*const*R_1*(-3*R_1*dz*b(j)*i5o -3*R_1*b(j)*z_3
    *i6o +3*R_1*b(j)*z_1*i6o +3*dz*b(j)^2*i7o -2*dz*i17o
    +3*b(j)^2*z_3*i8o -2*z_3*i9o -3*b(j)^2*z_1*i8o +2*z_1*
    i9o +3*R_1*dz*h*i18o +3*R_1*h*z_3*i10o -3*R_1*h*z_1*
    i10o -3*dz^3*i19o -6*dz^2*z_3*i11o +6*dz^2*z_1*i11o
    -3*dz*h*b(j)*i11o -3*dz*z_3^2*i12o +6*dz*z_1*z_3*i12o
    -3*h*b(j)*z_3*i12o -3*dz*z_1^2*i12o +3*h*b(j)*z_1*i12o
    +3*dz^3*b(j)*i20o/(R_1) +6*dz^2*b(j)*z_3*i13o/(R_1)
    -6*dz^2*b(j)*z_1*i13o/(R_1) +(3*dz*b(j)*z_3^2*i14o)/(
    R_1) -6*dz*b(j)*z_1*z_3*i14o/(R_1) +3*dz*b(j)*z_1^2*
    i14i/(R_1)) + R_1*e*q_2*a/(4*pi*eps_0*c*c) * (R_1*dz*
    i21o +R_1*z_3*i16o -R_1*z_1*i16o -dz*b(j)*i22o -b(j)*
    z_3*i23o +b(j)*z_1*i23o);

120
121     Fz_helix(j) = trapz(theta,Fi_z+Fo_z);
122 end
123
124
125 %% Impulse Calculation %%
126 Jy_helix_numeric = trapz(time,Fy_helix);
127 Jz_helix_numeric = trapz(time,Fz_helix);
128
129 y_helix_numeric = 0.5*Jy_helix_numeric*t_end/m_e
130 z_helix_numeric = 0.5*Jz_helix_numeric*t_end/m_e
131 beep
132 % end of code

```

Listing 2: Code for calculating the electron beam deflection based on field theory and the beam travelling across the solenoid.

```

1  %%%%%%%%%%%%%%%%%%%%%%%%%%%%%%%%%%%%%%%%%%%%%%%%%%%%%%%%%%%%%%%%%%%%%%%%%
2  % FieldSolenoid function authored by D. Cebon
3  %%%%%%%%%%%%%%%%%%%%%%%%%%%%%%%%%%%%%%%%%%%%%%%%%%%%%%%%%%%%%%%%%%%%%%%%%
4  %modified to experimental geometry by CB
5  %%%%%%%%%%%%%%%%%%%%%%%%%%%%%%%%%%%%%%%%%%%%%%%%%%%%%%%%%%%%%%%%%%%%%%%%%
6
7  %% 1 solenoid
8  clearvars; close all; clc;
9  a=0.03;           % Solenoid radius 0.027; 0.03; 0.02;
10 L=0.5;           % Solenoid length 0.255; 0.5; 0.025;
11 mu=pi*4e-7;
12 n=2600; % number of windings per unit length 2200; 2600; 2440
13 I=-1;
14 Br=mu*n*I;       % Residual field = field in infinite

```

```

    solenoid (mu*n*I)
15 h = -(a + 0.025); %m height of electron beam above solenoid
    which we assume remains constant
16 V = 2000; %V acceleration voltage
17 e = 1.60217662e-19; %elementary charge
18 m_e = 9.10938356e-31; %electron mass
19 c = 299792458; %lightspeed
20 v_e = sqrt(2*e*V/m_e); %m/s
21 z_1 = 6/8*L;
22 q = -e;
23
24
25 x_start = -0.095; % this is where electron is emitted
26 x_last = 0.180;
27 x_step = 0.0001;
28 x = x_start : x_step : x_last;
29 y_pos = h;
30 z = z_1;
31
32 t_start = 0;
33 t_last = abs(x_last-x_start)/v_e; % distance_on_x_axis/v_e
34 t_step_size = x_step/v_e;
35 t = t_start : t_step_size : t_last;
36
37 vel = [v_e;0;0];
38 %% impulse approach
39 Fx = zeros(1, length(x));
40 Fy = zeros(1, length(x));
41 Fz = zeros(1, length(x));
42
43 for j=1:length(x)
44     rho=sqrt(x(j)^2+y_pos^2);
45     BB=FieldSolenoid(a,L,Br,rho,z); % BB(1:2)=(Brho,Bz)
46     Brho=BB(1); Bz=BB(2);
47     B_abs=sqrt(BB(1)^2+BB(2)^2);
48
49     Bx=Brho*x(j)/rho; % because cos(phi) = x/rho for all
        quadrants!
50     By=Brho*y_pos/rho; % because sin(phi) = y/rho for all
        quadrants!
51
52     if rho == 0
53         Bx = 0; By = 0;
54     end
55
56     Bxyz = [Bx;By;Bz];
57 %     B_field(j) = Bz;
58

```

```

59         F = q*cross(vel,Bxyz);
60         Fx(j) = F(1);
61         Fy(j) = F(2);
62         Fz(j) = F(3);
63     end
64
65     Jy = trapz(t,Fy);
66     Jz = trapz(t,Fz);
67     y_imp = 0.5*Jy*t_last/m_e
68     z_imp = 0.5*Jz*t_last/m_e
69
70 % end of code

```

Listing 3: Code for calculating the electron beam deflection based on Weber’s force with a current element in helical motion and the beam travelling through the solenoid.

```

1  %This is a test of the Weber model for a beam travelling
   through a single
2  %wound solenoid. This version adds the acceleration for the
   electron beam
3  %in replacing v_1 with v_0 +a*t. The algorithm must be
   restructured to
4  %include the acceleration into the consecutive time steps and
   account for
5  %their changing.
6
7  clearvars; close all;
8  clc;
9  tic
10 %% Set PARAMETERS %%
11 R_1 = 0.1595/2; %m long solenoid radius 0.1595/2; short
   solenoid radius 0.052/2;
12 h = -(R_1 + 0.025); %m height of electron beam above solenoid
   which we assume remains constant
13 V = 2000; %V acceleration voltage
14 I = 1; %A
15 eps_0 = 8.854187817e-12; %vacuum permittivity
16 e = 1.60217662e-19; %elementary charge
17 m_e = 9.10938356e-31; %electron mass
18 c = 299792458; %lightspeed
19 n_copper = 8.49e28; %electrons per m^3
20 v_e = sqrt(2*e*V/m_e); %m/s ~1200V acceleration voltage
21 v_2 = I/(n_copper*e*pi*R_1^2); %drift velocity in solenoid.
22 const = (e*I)/(4*pi*eps_0*c*c); %constant outside integration
   , 2 from doublewound theory
23 N = 290; %Number of windings, in doublewound this is number
   of windings in one layer! 20; 290;
24 l = 0.17; %m length of the solenoid, first test with 0.1 %
   0.01; 0.17;

```

```

25 dz = 1/(N*2*pi); % incremental increase with theta
26 p = 1/N; % pitch of the coil
27
28 %% Integration steps for THETA in trapz %%
29 theta_start = 0;
30 theta_last = (N*2*pi);
31 theta_steps = N*72; %Look to increase (originally 72)
32 % set the number of intervals of theta required between 0 and
    2pi
33 theta_step_size = theta_last / theta_steps;
34 theta = theta_start : theta_step_size : theta_last;
35
36 %% set initial positions %%
37 v_1x = 0; a_1x = 0;
38 v_1y = 8*v_e/50; a_1y = 0;
39 v_1z = v_e; a_1z = 0;
40
41 x_1 = 0.0;
42 y_1 = 0.0;
43 z_1 = -0.165;%-0.165; -0.070
44 z_end = 0.085;%0.085; 0.175 %-z_1
45 z_2 = -1/2; %start of the coil on the z axis it elongates
    only in one direction from there! (so it is end of the
    coil where current enters)
46
47 %% Set z position of the coil and beam path along z axis for
    loop %% Now z=b values!
48 t_start = 0;
49 t_last = abs(z_end-z_1)/v_e; % basically distance_on_z_axis/
    v_e
50 z_step = 0.001;
51 t_step_size = z_step/v_e;
52 t = t_start : t_step_size : t_last;
53
54 x_pos = x_1*ones(1,(length(t)+1));
55 y_pos = y_1*ones(1,(length(t)+1));
56 z_pos = z_1*ones(1,(length(t)+1));
57
58 %% show initial position on 3D plot and plot solenoid %%
59 figure
60 plot3(R_1*cos(0:theta_step_size:2*pi),R_1*sin(0:
    theta_step_size:2*pi),z_2*ones(1,length(0:theta_step_size
    :2*pi)),'r');
61 hold on
62 plot3(R_1*cos(0:theta_step_size:2*pi),R_1*sin(0:
    theta_step_size:2*pi),-z_2*ones(1,length(0:theta_step_size
    :2*pi)),'r');
63 plot3(x_1,y_1,z_1,'o');

```

```

64 xlabel('x(t)')
65 ylabel('y(t)')
66 zlabel('z(t)')
67
68 cc=jet(length(t));
69 %% Set integration loop %%
70 F_y_helix = zeros(1,length(t));
71 F_x_helix = zeros(1,length(t));
72 F_z_helix = zeros(1,length(t));
73 for j=1:length(t)
74
75     r = sqrt( (x_pos(j)-R_1*cos(theta)).^2 +(y_pos(j)-R_1*sin
              (theta)).^2 +(z_pos(j)-z_2-dz*theta).^2 );
76
77     f_x = R_1*e*I./(4*pi*eps_0*c^2*r.^3).*(x_pos(j)-R_1*cos(
              theta)).*( -3./(2*r.^2).*( (2*v_1x*sin(theta).*(x_pos(
              j)-R_1*cos(theta)).^2) + (2*v_1y*sin(theta)-2*v_1x*cos
              (theta)).*(x_pos(j)-R_1*cos(theta)).*(y_pos(j)-R_1*sin
              (theta)) -2*v_1y*cos(theta).*(y_pos(j)-R_1*sin(theta))
              .^2 + (-2*v_1y*dz/R_1-2*v_1z*cos(theta)).*(y_pos(j)-
              R_1*sin(theta)).*(z_pos(j)-z_2-dz*theta) -2*v_1z*dz/
              R_1*(z_pos(j)-z_2-dz*theta).^2 +(2*v_1z*sin(theta)-2*
              v_1x*dz/R_1).*(x_pos(j)-R_1*cos(theta)).*(z_pos(j)-z_2
              -dz*theta)) +2*(v_1x*sin(theta) - v_1y*cos(theta) -
              v_1z*dz/R_1) +v_2/R_1*cos(theta).*(x_pos(j)-R_1*cos(
              theta)) +v_2/R_1*sin(theta).*(y_pos(j)-R_1*sin(theta))
              ); %+v_2/R_1*cos(theta).*(x_pos(j)-R_1*cos(theta)) +
              v_2/R_1*sin(theta).*(y_pos(j)-R_1*sin(theta))
78     f_y = R_1*e*I./(4*pi*eps_0*c^2*r.^3).*(y_pos(j)-R_1*sin(
              theta)).*( -3./(2*r.^2).*( (2*v_1x*sin(theta).*(x_pos(
              j)-R_1*cos(theta)).^2) + (2*v_1y*sin(theta)-2*v_1x*cos
              (theta)).*(x_pos(j)-R_1*cos(theta)).*(y_pos(j)-R_1*sin
              (theta)) -2*v_1y*cos(theta).*(y_pos(j)-R_1*sin(theta))
              .^2 + (-2*v_1y*dz/R_1-2*v_1z*cos(theta)).*(y_pos(j)-
              R_1*sin(theta)).*(z_pos(j)-z_2-dz*theta) -2*v_1z*dz/
              R_1*(z_pos(j)-z_2-dz*theta).^2 +(2*v_1z*sin(theta)-2*
              v_1x*dz/R_1).*(x_pos(j)-R_1*cos(theta)).*(z_pos(j)-z_2
              -dz*theta)) +2*(v_1x*sin(theta) - v_1y*cos(theta) -
              v_1z*dz/R_1) +v_2/R_1*cos(theta).*(x_pos(j)-R_1*cos(
              theta)) +v_2/R_1*sin(theta).*(y_pos(j)-R_1*sin(theta))
              ); %+v_2/R_1*cos(theta).*(x_pos(j)-R_1*cos(theta)) +
              v_2/R_1*sin(theta).*(y_pos(j)-R_1*sin(theta))
79     f_z = R_1*e*I./(4*pi*eps_0*c^2*r.^3).*(z_pos(j)-z_2-dz*
              theta).*( -3./(2*r.^2).*( (2*v_1x*sin(theta).*(x_pos(
              j)-R_1*cos(theta)).^2) + (2*v_1y*sin(theta)-2*v_1x*
              cos(theta)).*(x_pos(j)-R_1*cos(theta)).*(y_pos(j)-R_1*
              sin(theta)) -2*v_1y*cos(theta).*(y_pos(j)-R_1*sin(
              theta)).^2 + (-2*v_1y*dz/R_1-2*v_1z*cos(theta)).*(

```

```

y_pos(j)-R_1*sin(theta)).*(z_pos(j)-z_2-dz*theta) -2*
v_1z*dz/R_1*(z_pos(j)-z_2-dz*theta).^2 +(2*v_1z*sin(
theta)-2*v_1x*dz/R_1).*(x_pos(j)-R_1*cos(theta)).*(
z_pos(j)-z_2-dz*theta)) +2*(v_1x*sin(theta) - v_1y*cos
(theta) -v_1z*dz/R_1) +v_2/R_1*cos(theta).*(x_pos(j)-
R_1*cos(theta)) +v_2/R_1*sin(theta).*(y_pos(j)-R_1*sin
(theta)) ); %+v_2/R_1*cos(theta).*(x_pos(j)-R_1*cos(
theta)) +v_2/R_1*sin(theta).*(y_pos(j)-R_1*sin(theta))
80
81 F_x_helix(j) = trapz(theta,f_x);
82 F_y_helix(j) = trapz(theta,f_y);
83 F_z_helix(j) = trapz(theta,f_z);
84
85 a_1x = F_x_helix(j)/m_e;
86 a_1y = F_y_helix(j)/m_e;
87 a_1z = F_z_helix(j)/m_e;
88
89 x_pos(j+1) = x_pos(j) +v_1x*t_step_size + 0.5*a_1x*
t_step_size^2; % s = v_0*t +a/2*t^2
90 y_pos(j+1) = y_pos(j) +v_1y*t_step_size + 0.5*a_1y*
t_step_size^2;
91 z_pos(j+1) = z_pos(j) +v_1z*t_step_size + 0.5*a_1z*
t_step_size^2;
92
93 v_1x = v_1x + a_1x*t_step_size; % now set new v_0 for
next loop
94 v_1y = v_1y + a_1y*t_step_size;
95 v_1z = v_1z + a_1z*t_step_size;
96
97 plot3(x_pos(j+1),y_pos(j+1),z_pos(j+1),'o','color',cc(j
,:))
98 % drawnow
99 end
100
101 distance = z_pos(1,1:length(z_pos)-1);
102 figure
103 plot(distance,F_x_helix)
104 ylabel('Fx (N)');
105
106 figure
107 plot(distance,F_y_helix)
108 ylabel('Fy (N)');
109
110 figure
111 plot(distance,F_z_helix)
112 ylabel('Fz (N)');
113
114 %% position and times

```

```

115 % z_ind = find(abs(z_end-z_pos) < z_step/2);
116 [z_min, z_ind] = min(abs(z_end-z_pos));
117
118 z_last = z_pos(end)
119 z_dist = z_last-z_pos(1)
120
121
122 % z_ind = find(abs(z_end-z_pos) < z_step/2);
123 x_accel = x_pos(z_ind)-x_pos(1)
124 y_accel = y_pos(z_ind)-y_pos(1)
125 z_accel = z_pos(z_ind)-z_pos(1)
126 t_1 = t(z_ind)
127 delta_t = t_last-t_1
128 beep
129
130 toc
131 % end of code

```

Listing 4: Code for calculating the electron beam deflection based on field theory and the beam travelling through the solenoid.

```

1 %%%%%%%%%%%%%%%%%%%%%%%%%%%%%%%%%%%%%%%%%%%%%%%%%%%%%%%%%%%%%%%%%%%%%%%%%
2 % FieldSolenoid function authored by D. Cebon
3 %%%%%%%%%%%%%%%%%%%%%%%%%%%%%%%%%%%%%%%%%%%%%%%%%%%%%%%%%%%%%%%%%%%%%%%%%
4 %modified to experimental geometry by CB
5 %%%%%%%%%%%%%%%%%%%%%%%%%%%%%%%%%%%%%%%%%%%%%%%%%%%%%%%%%%%%%%%%%%%%%%%%%
6
7 %% 1 solenoid
8 clearvars; close all; clc;
9 a=0.052/2;          % Solenoid radius 0.1595/2; 0.052/2
10 L=0.010;           % Solenoid length
11 mu=pi*4e-7;
12 n=2000; %1706 for the 290 turn assumption. And 2000 for 340
    theoretical as well as short solenoid.
13 I=-5;
14 Br=mu*n*I;          % Residual field = field in infinite
    solenoid (mu*n*I)
15 h = -(a + 0.025); %m height of electron beam above solenoid
    which we assume remains constant
16 V = 2000; %V acceleration voltage
17 e = 1.60217662e-19; %elementary charge
18 m_e = 9.10938356e-31; %electron mass
19 c = 299792458; %lightspeed
20 v_e = sqrt(2*e*V/m_e); %m/s
21 q = -e;
22
23 %% set initial positions %%
24 v_1x = 0;
25 v_1y = 4*v_e/50;

```

```

26 v_1z = v_e;
27
28 x_1 = 0.0;
29 y_1 = 0.0;
30 z_1 = -0.070;
31 z_end = 0.175; %-z_1
32 z_2 = -L/2; %start of the coil on the z axis it elongates
    only in one direction from there! (so it is end of the
    coil where current enters)
33
34 %% Set z position of the coil and beam path along z axis for
    loop %% Now z=b values!
35 t_start = 0;
36 t_last = 1.01*(abs(z_end-z_1)/v_e); % basically
    distance_on_z_axis/v_e
37 t_step_size = 0.001/v_e; % basically z_step/v_e
38 t = t_start : t_step_size : t_last;
39
40 x_pos = x_1*ones(1,(length(t)+1));
41 y_pos = y_1*ones(1,(length(t)+1));
42 z_pos = z_1*ones(1,(length(t)+1));
43
44 %% show initial position on 3D plot and plot solenoid %%
45 figure
46 plot3(a*cos(0:0.02:2*pi),a*sin(0:0.02:2*pi),z_2*ones(1,length
    (0:0.02:2*pi)), 'r');
47 hold on
48 plot3(a*cos(0:0.02:2*pi),a*sin(0:0.02:2*pi),-z_2*ones(1,
    length(0:0.02:2*pi)), 'r');
49 plot3(x_1,y_1,z_1, 'o');
50 xlabel('x(t)')
51 ylabel('y(t)')
52 zlabel('z(t)')
53
54 cc=jet(length(t));
55 %% more efficient if field is only calculated locally.
56 Fy = zeros(1,length(t));
57 Fx = zeros(1,length(t));
58 Fz = zeros(1,length(t));
59 for j=1:length(t)
60     vel = [v_1x;v_1y;v_1z];
61     rho=sqrt(x_pos(j)^2+y_pos(j)^2); z=z_pos(j);
62     BB=FieldSolenoid(a,L,Br,rho,z); % BB(1:2)=(Brho,Bz)
63     Brho=BB(1); Bz=BB(2);
64     B_abs=sqrt(BB(1)^2+BB(2)^2);
65
66     Bx=Brho*x_pos(j)/rho; % because cos(phi) = x/rho for
        all quadrants!

```

```

67     By=Brho*y_pos(j)/rho; % because sin(phi) = y/rho for
        all quadrants!
68
69     if rho == 0
70         Bx = 0; By = 0;
71     end
72
73     Bxyz = [Bx;By;Bz];
74
75     F = q*cross(vel,Bxyz);
76     Fx(j) = F(1);
77     Fy(j) = F(2);
78     Fz(j) = F(3);
79
80     a_1x = Fx(j)/m_e;
81     a_1y = Fy(j)/m_e;
82     a_1z = Fz(j)/m_e;
83
84     x_pos(j+1) = x_pos(j) +v_1x*t_step_size + 0.5*a_1x*
        t_step_size^2; % s = v_0*t +a/2*t^2
85     y_pos(j+1) = y_pos(j) +v_1y*t_step_size + 0.5*a_1y*
        t_step_size^2;
86     z_pos(j+1) = z_pos(j) +v_1z*t_step_size + 0.5*a_1z*
        t_step_size^2;
87
88     v_1x = v_1x + a_1x*t_step_size; % now set new v_0 for
        next loop
89     v_1y = v_1y + a_1y*t_step_size;
90     v_1z = v_1z + a_1z*t_step_size;
91
92     plot3(x_pos(j+1),y_pos(j+1),z_pos(j+1),'o','color',cc(j
        ,:))
93 %     drawnow
94 end
95 % end of code

```

Listing 5: Code for calculating the induced voltage based on Weber electrodynamics with a spinning disk and stationary magnet.

```

1 % Trying to predict unipolar induction with Weber. Spinning
    disk,
2 % stationary magnet
3
4 clearvars; close all; clc;
5 %% Parameters %%
6 R_1= 0.068; % Solenoid radius 0.068
7 R_2= 0.04; % Disk radius
8 R_wire = 0.0005; % radius of coil wire
9 I = 3; % Ampere

```



```

10 mu = pi*4e-7; % magnetic permeability
11 eps_0 = 8.854187817e-12; %vacuum permittivity
12 e = 1.60217662e-19; %elementary charge
13 m_e = 9.10938356e-31; %electron mass
14 c = 299792458; %lightspeed
15 n_copper = 8.49e28; %electrons per m^3
16 v_1 = I/(n_copper*e*pi*R_wire^2); %speed of electrons in wire
17
18 N = 320; %Number of windings spinning coil 320
19 L = 0.020; %m length of spinning coil 0.02
20 p = L/N; % pitch of the coil
21 n_unit = N/L; % winding density
22 dz = L/(N*2*pi); % incremental increase with theta
23
24 rpm = 1100;
25 om = 2*pi*rpm/60;
26
27 z_1 = L/2; %
28 z_2 = 0.0;% position of disk, sits next to coil; L/2+0.005;
    0; L/2+0.01
29
30 %% Weber prediction %%
31
32 %make function handle for Weber force/EMF, apparently
    needs to be 1D
33 % theta_2 as fixed value
34 theta_2 = 2*pi/4;
35 f_x = @(theta_1,R_3) I*om*R_1*R_3/(4*pi*eps_0*c^2).*(R_1*
    cos(theta_1)-R_3.*cos(theta_2))./(sqrt((R_1*cos(
    theta_1)-R_3.*cos(theta_2)).^2 + (R_1*sin(theta_1)-R_3
    .*sin(theta_2)).^2+(z_1-z_2-dz*theta_1).^2)).^3
    .*(-3/2./(sqrt((R_1*cos(theta_1)-R_3.*cos(theta_2)).^2
    + (R_1*sin(theta_1)-R_3.*sin(theta_2)).^2+(z_1-z_2-dz
    *theta_1).^2)).^2 .*(-2*sin(theta_2).*sin(theta_1).*(
    R_1*cos(theta_1)-R_3.*cos(theta_2)).^2 + 2*(sin(
    theta_2).*cos(theta_1) + sin(theta_1).*cos(theta_2))
    .*(R_1*cos(theta_1)-R_3.*cos(theta_2)).*(R_1*sin(
    theta_1)-R_3.*sin(theta_2)) -2*cos(theta_2).*cos(
    theta_1).*(R_1*sin(theta_1)-R_3.*sin(theta_2)).^2 -2*
    sin(theta_2)*dz/R_1.*(R_1*cos(theta_1)-R_3.*cos(
    theta_2)).*(z_1-z_2-dz*theta_1) +2*cos(theta_2)*dz/R_1
    .*(R_1*sin(theta_1)-R_3.*sin(theta_2)).*(z_1-z_2-dz*
    theta_1) ) -2*sin(theta_2).*sin(theta_1) -2*cos(
    theta_2).*cos(theta_1) );
36 f_y = @(theta_1,R_3) I*om*R_1*R_3/(4*pi*eps_0*c^2).*(R_1*
    sin(theta_1)-R_3.*sin(theta_2))./(sqrt((R_1*cos(
    theta_1)-R_3.*cos(theta_2)).^2 + (R_1*sin(theta_1)-R_3
    .*sin(theta_2)).^2+(z_1-z_2-dz*theta_1).^2)).^3

```

```

.*(-3/2./(sqrt((R_1*cos(theta_1)-R_3.*cos(theta_2)).^2
+ (R_1*sin(theta_1)-R_3.*sin(theta_2)).^2+(z_1-z_2-dz
*theta_1).^2)).^2 .*(-2*sin(theta_2).*sin(theta_1).*(
R_1*cos(theta_1)-R_3.*cos(theta_2)).^2 + 2*(sin(
theta_2).*cos(theta_1) + sin(theta_1).*cos(theta_2))
.*(R_1*cos(theta_1)-R_3.*cos(theta_2)).*(R_1*sin(
theta_1)-R_3.*sin(theta_2)) -2*cos(theta_2).*cos(
theta_1).*(R_1*sin(theta_1)-R_3.*sin(theta_2)).^2 -2*
sin(theta_2)*dz/R_1.*(R_1*cos(theta_1)-R_3.*cos(
theta_2)).*(z_1-z_2-dz*theta_1) +2*cos(theta_2)*dz/R_1
.*(R_1*sin(theta_1)-R_3.*sin(theta_2)).*(z_1-z_2-dz*
theta_1) ) -2*sin(theta_2).*sin(theta_1) -2*cos(
theta_2).*cos(theta_1) );
37 f_z = @(theta_1,R_3) I*om*R_1*R_3/(4*pi*eps_0*c^2).*(
z_1-z_2-dz*theta_1
)./(sqrt((R_1*cos(
theta_1)-R_3.*cos(theta_2)).^2 + (R_1*sin(theta_1)-R_3
.*sin(theta_2)).^2+(z_1-z_2-dz*theta_1).^2)).^3
.*(-3/2./(sqrt((R_1*cos(theta_1)-R_3.*cos(theta_2)).^2
+ (R_1*sin(theta_1)-R_3.*sin(theta_2)).^2+(z_1-z_2-dz
*theta_1).^2)).^2 .*(-2*sin(theta_2).*sin(theta_1).*(
R_1*cos(theta_1)-R_3.*cos(theta_2)).^2 + 2*(sin(
theta_2).*cos(theta_1) + sin(theta_1).*cos(theta_2))
.*(R_1*cos(theta_1)-R_3.*cos(theta_2)).*(R_1*sin(
theta_1)-R_3.*sin(theta_2)) -2*cos(theta_2).*cos(
theta_1).*(R_1*sin(theta_1)-R_3.*sin(theta_2)).^2 -2*
sin(theta_2)*dz/R_1.*(R_1*cos(theta_1)-R_3.*cos(
theta_2)).*(z_1-z_2-dz*theta_1) +2*cos(theta_2)*dz/R_1
.*(R_1*sin(theta_1)-R_3.*sin(theta_2)).*(z_1-z_2-dz*
theta_1) ) -2*sin(theta_2).*sin(theta_1) -2*cos(
theta_2).*cos(theta_1) );
38
39 emf_x = integral2(f_x,0,N*2*pi,0,R_2,'method','iterated')
% , 'method','iterated' , 'AbsTol',1e-16, 'RelTol',1e
-16
40 emf_y = integral2(f_y,0,N*2*pi,0,R_2,'method','iterated')
% , 'method','iterated'
41
42 emf_r = 1000*sqrt(emf_x^2+emf_y^2)
43 emf_z = integral2(f_z,0,N*2*pi,0,R_2,'method','iterated')
% , 'method','iterated'
44 % end of code

```

Listing 6: Code for calculating the induced voltage based on field model with a spinning disk and stationary magnet.

```

1 % unipolar induction with the field model - first check
  general trend
2 % before applying B field from Cebtron model
3

```

```

4 clearvars; close all; clc;
5
6 %% Parameters %%
7 R_disk = 0.04; % m 0.005:0.04
8 R_mag = 0.068; % m
9 L_mag = 0.02; % m
10 N = 320;
11 n = N/L_mag;
12 I = 3; % A
13 mu = pi*4e-7; % magnetic permeability
14
15 rpm = 1100;
16 om = 2*pi*rpm/60; % angular velocity
17 f = rpm/60; % frequency.
18 Br = mu*I*n;
19 z = 0.01; % distance of disk from centre of coil 0.0; 0.01;
20 % now in next step use fieldbar code of ceborn to obtain Bz
    value and use for
21 % calcs. Only Bz because v x B dictates B_rho is irrelevant!
22
23
24 rho = 0:R_disk/1000:R_disk;
25
26 for j=1:length(rho)
27
28     BB=FieldSolenoid(R_mag,L_mag,Br,rho(j),z); % BB(1:2)
        =(Brho,Bz)
29     Brho=BB(1); Bz=BB(2);
30     B(j) = Bz;
31
32 end
33
34 %% calculate EMF in mV %%
35 emf_om = om*rho.*B;
36 EMF_om = 1000*trapz(rho,emf_om)
37 emf_Bz_om = 1000*0.5*om*Bz*R_disk^2

```

Listing 7: Databuilder file used with CPO to calculate deflections for a beam travelling across a solenoid.

```

1 CP03D -based on 4th test, relativistic cyclotron motion
2 tempa.dat name of hidden output file, for processed data
3 tempb.dat name of main ray output file, for ray data
4 n      v  n/p/m/a for print level, cumulative, colour
    electrodes
5 0 0 0 0 voltage reflection symmetries in x,y,z,x=y planes
6 1      number of different voltages (time-independent)
7 0.001 5    0 allowed consistency error, side/length ratio
    check, allow outside zs

```

```

8  n  apply inscribing correction (a/s/n=always/sometimes/never)
9  cylindrical electrode
10 27 0 0 -127.5  radius, centre of 1st end
11 0 0 127.5  centre of 2nd end
12 1 1  numbers of 2 applied voltages (can be same)
13 100 0      total nr of subdivs and 0,    or subdivs along
    and around axis
14 colour    1
15 end of electrode information
16 0      1  0.5      final nmbr segs, nmbr steps, weight
17 1e-07      charge inacc,non-0 total Q,improve matrix
    ,import,sp-ch
18 end of segment information
19 0.0000000E+00      rods at +/- x          applied
    voltages
20 s      solenoid, type 1
21 -1 30 30 1300      current, radii, nr of turns
22 0 0 250 0 0 -250      coordinates of 2 ends of solenoid
23 n      no more magnetic fields from menu
24 0 0 0 0 c  symmetries of rays in yz,zx,xy and x=y planes,
    compounded transformation
25 n n n      no more potentials and fields along a line
26 start of ray information
27 d      direct (d), or mesh (m) method and mesh spacing
28 p      'n/p/m/a' for 'nearlyzero/partial/most/all' printing
    level, rho/radius
29 -250 250      minimum and maximum x(mm) of screen 2D fields of
    view
30 -250 250      minimum and maximum y
31 -250 250      minimum and maximum z
32 -500 500      minimum and maximum x(mm) of rays
33 -500 500      minimum and maximum y
34 -500 500      minimum and maximum z
35 -1e+10 1e+10      minimum and maximum vx(m/s) of rays
36 -1e+10 1e+10      minimum and maximum vy
37 -1e+10 1e+10      minimum and maximum vz
38 + y      direction of time, stop when ray first hits an
    electrode
39 1e+10      final time (ms)
40 1          10          =max step length,interp pts
41 -0.0001 0.0001      fractional inaccuracies for (1) ray tracing
    and (2) potentials and fields
42 1          nr test planes,mult cross,iter foc,phase spc,
    scatt,quant,stp_tst
43 1 0 0 180      a,b,c,d of test plane defined by a*x+b*y+c*z=d
44 el          'el' for electron; or 'co' or 'va' for other
    particles
45 k kinetic energy (k); or total energy (t) and potential

```

```
46 set of single rays:
47 -95 -52 375 1 0 0 2000 0          x,y,z,vx,vy,vz,eV,I
48 last of this set of rays
49 n      calculate space-charges?
50 0 0 0 0      symmetries of rays in yz, zx, xy and x=y planes
```

I have, alas, studied philosophy,
Jurisprudence and medicine, too,
And, worst of all, theology
With keen endeavour, through and through –
And here I am, for all my lore,
The wretched fool I was before.
Called Master of Arts, and Doctor to boot,
For ten years almost I confute
And up and down, wherever it goes,
I drag my students by the nose –
And see that for all our science and art
We can know nothing. It burns my heart.

– *Goethe's Faust*
translated by Walter Kaufmann